DEVELOPMENT OF INNOVATIVE ANTIMICROBIALS FOR COSMECEUTICAL APPLICATIONS

Angela Cesaro

Dottorato in Biotecnologie – XXXIII ciclo

Università di Napoli Federico II

DEVELOPMENT OF INNOVATIVE ANTIMICROBIALS FOR COSMECEUTICAL APPLICATIONS

Angela Cesaro

Dottorato in Biotecnologie – XXXIII ciclo

Università di Napoli Federico II

Dottorando: Angela Cesaro

Relatore: Prof. Angela Arciello

Coordinatore: Prof. Marco Moracci

Settore Scientifico Disciplinare BIO-10

To my parents

“Every great
advance in science has issued from a new audacity of imagination”

(John Dewey)

INDICE

ABSTRACT

As a physical and chemical barrier, the skin arrests pathogens invasion, thus preventing harmless or even potentially lethal infections. When this barrier is damaged, the spread of infections is usually treated by using traditional antibiotics, which are often ineffective on Multi-Drug resistant bacteria. Antibiotic resistance is predicted to become the leading cause of death in our society, thus justifying the search for novel antimicrobials derived from previously underexplored sources. In this context, promising molecules as the antimicrobial peptides (AMPs) represent an innovative alternative, since the evolution of resistance against these compounds generally does not occur. Encrypted peptides deriving from human proteome represent a yet unexplored source of a novel class of antibiotics. In this Research project, we report that peptides hidden within human plasma display broad-spectrum antibiotic properties. Specifically, three peptides [r(P)ApoB$_L^{Pro}$, r(P)ApoB$_S^{Pro}$ and r(P)ApoB$_L^{Ala}$] derived from human apolipoprotein B (residues 887-922) exhibited potent antimicrobial activity against drug-resistant *Klebsiella pneumoniae*, *Acinetobacter baumannii*, *Pseudomonas aeruginosa* and *Staphylococci* both *in vitro* and in animal models. These peptides were found to target bacteria by depolarizing their cytoplasmic membranes and to inhibit biofilm. Importantly, the peptides were found to potentiate the activity of conventional antibiotics against bacteria and did not select for bacterial resistance even after a prolonged exposure of bacterial cells. In addition to their direct antimicrobial and antibiofilm activities, ApoB encrypted peptides displayed excellent toxicity profiles. To ensure translatability of these molecules, a retro-inverso variant [(ri)-r(P)ApoB$_S^{Pro}$] of the lead encrypted peptide was synthesized. The peptidomimetic here engineered was found to be resistant to proteases and demonstrated to preserve the bioactivities of the parental peptides with even stronger efficacy when tested in a pre-clinical mouse model. Finally, a hyaluronic acid-based hydrogel functionalized with (ri)-r(P)ApoB$_S^{Pro}$ was designed and characterized. The hydrogel system loaded with the retro-inverso variant of ApoB encrypted peptide was found to inhibit bacterial growth, to prevent pathogens migration and to stimulate cells viability. Altogether, obtained data open new avenues for the discovery of a novel generation of antibiotics from human blood and highlight the applicability of ApoB-derived peptides in the treatment of skin infections and diseases.

RIASSUNTO

Le infezioni della cute e dei tessuti molli, se non trattate in maniera adeguata, presentano una variabilità che va da innocue a potenzialmente letali. Esse rientrano tra i disturbi più diffusi riscontrati sia negli ambienti comuni che negli ambienti ospedalieri. Le cure e i trattamenti convenzionali, se protratti per un lungo periodo di tempo, concorrono in maniera significativa all'insorgenza di ceppi batterici antibiotico-resistenti. Infatti, malattie della cute e degli strati sub-cutanei, quali dermatiti, acne, psoriasi, piodermiti, rosacea e ulcere da decubito, sono causate principalmente dai cosiddetti "ESKAPE *pathogens*" (*Enterococcus faecium*, *Staphylococcus aureus*, *Klebsiella pneumoniae*, *Acinetobacter baumannii*, *Pseudomonas aeruginosa*, e specie *Enterobacter*), ovvero patogeni recalcitranti e resistenti alla maggior parte degli antibiotici tradizionali. L'agenzia federale adibita al controllo della sanità pubblica negli Stati Uniti d'America classifica tali ceppi batterici come vere e proprie minacce per la salute umana, essendo responsabili di oltre 2,8 milioni di infezioni antibiotico-resistenti e causando oltre 35.000 decessi nel solo 2019. Il trattamento delle infezioni cutanee risulta impegnativo anche perché la maggior parte degli agenti patogeni forma *biofilm* batterici, ovvero agglomerati di cellule microbiche immerse in una matrice polimerica, che funge da protezione per diversi fattori, incluse le terapie antibiotiche. È stato, inoltre, stimato che batteri immersi nella matrice del *biofilm* sono mille volte più resistenti agli antibiotici rispetto alle singole cellule batteriche in forma planctonica. Sebbene un tempo gli antibiotici fossero in grado di trattare la maggior parte delle infezioni batteriche, negli ultimi decenni il loro eccessivo e improprio utilizzo ha favorito il rapido sviluppo di ceppi patogeni resistenti. Secondo i dati diffusi dall'Organizzazione Mondiale della Sanità, si prospetta che da qui al 2050 i batteri resistenti agli antibiotici convenzionali saranno causa di almeno 10 milioni di decessi all'anno, ciò che ha portato a classificare il fenomeno della resistenza agli antibiotici come una delle principali minacce per la salute umana. Se si considera che, allo stesso tempo, la scoperta, lo sviluppo, la produzione e la commercializzazione di nuovi antibiotici sono notevolmente rallentati negli ultimi 20 anni, i dati risultano allarmanti. Pertanto, sono fortemente richieste efficaci strategie alternative.
In tale scenario, i peptidi antimicrobici (*Anti-Microbial Peptides*, *AMPs*), denominati anche peptidi adibiti alla difesa dell'ospite (*Host Defence Peptides, HDPs*), risultano essere una valida alternativa agli antibiotici convenzionali, dal momento che generalmente non determinano la

selezione di ceppi resistenti. Gli AMPs rappresentano un gruppo di molecole del sistema immunitario innato conservate durante l'evoluzione e presenti in tutti gli organismi viventi complessi. Tali molecole sono dotate di carica netta positiva e di un alto contenuto di residui idrofobici, proprietà alla base della loro abilità di interagire selettivamente con la membrana delle cellule batteriche e, in alcuni casi, di penetrarla legandosi a bersagli intracellulari. Nonostante gli sforzi sperimentali, ad oggi il meccanismo alla base della loro interazione con le membrane batteriche risulta ancora poco chiaro. Sono stati, però, proposti diversi modelli. Tra quelli più conosciuti, vi è il modello "*barrel-stave*", secondo cui le regioni idrofobiche del peptide interagiscano con le catene idrocarburiche dei fosfolipidi di membrana formando un poro rivestito internamente dalle regioni idrofiliche del peptide; vi è poi il modello "*toroidal*", che sembra descrivere il meccanismo di azione della maggior parte dei peptidi e prevede l'associazione di questi con i gruppi esposti dei fosfolipidi di membrana, ciò che provoca una curvatura del doppio strato lipidico a livello del poro; vi è infine il modello "*carpet*" per cui i peptidi si dispongono parallelamente alla superficie della membrana rivestendola come un "tappeto" e, quando la concentrazione dei peptidi supera un valore soglia, essi determinano la distruzione della membrana liberando micelle o piccoli aggregati peptidolipidici.
Gli agenti microbici sono presumibilmente esposti all'azione degli AMPs da milioni di anni e nessuna resistenza diffusa di questo tipo è stata mai segnalata. Poiché gli AMPs agiscono legandosi a composti idrofobici e/o polianionici della membrana, la selezione di un fenotipo resistente è molto poco probabile. Infatti, modificare l'architettura e/o la composizione dei lipidi di membrana è probabilmente una soluzione troppo "costosa" in termini energetici per la maggior parte delle specie microbiche. Gran parte dei peptidi antimicrobici sono in grado di determinare la morte diretta dei microrganismi patogeni, altri, invece, agiscono modulando i sistemi di difesa dell'ospite. Ciò li rende candidati eccellenti per lo sviluppo di una nuova generazione di antibiotici. Tali peptidi sono inoltre dotati di numerose altre proprietà biologiche, quali attività anti-biofilm, anti-infiammatoria, analgesica, antitumorale, antiossidante e di *wound healing* e sono in grado di agire in sinergia con differenti classi di antibiotici convenzionali e/o sostane naturali.
Nel 2006 è stato introdotto per la prima volta il termine "*criptoma*" per descrivere un sottoinsieme unico di proteine con la capacità di generare peptidi bioattivi, noti come "*criptidi*", i quali a loro volta possono avere proprietà correlate o migliorate rispetto al precursore proteico oppure possono esplicare funzioni biologiche completamente diverse. E' stato

riscontrato che, negli organismi pluricellulari, diverse proteine agiscono come fonti di peptidi antimicrobici "criptici". Queste proteine, le cui funzioni non sono necessariamente legate alla difesa dell'ospite, rilasciano peptidi bioattivi in seguito a scissioni proteolitiche da parte di proteasi batteriche e/o dell'ospite. Grazie al progresso scientifico e tecnologico, sono stati sviluppati diversi metodi in grado di ricercare e identificare nuovi peptidi criptici all'interno di proteine note.
Negli ultimi anni, il gruppo di ricerca presso cui è stato svolto il presente progetto di Dottorato, ha identificato mediante un *software* bioinformatico un nuovo peptide antimicrobico nell'apolipoproteina B umana (ApoB-100). Di tale peptide sono state prodotte tre diverse varianti, due più lunghe, qui denominate r(P)ApoB$_L^{Pro}$ e r(P)ApoB$_L^{Ala}$, che differiscono per la sostituzione di un residuo di prolina con un'alanina in posizione sette, e una versione più breve di tale sequenza, qui denominata r(P)ApoB$_S^{Pro}$. Tali peptidi sono stati prodotti efficientemente per via ricombinante in cellule di *Escherichia coli*, sotto forma di proteina chimerica. I peptidi derivanti dall'apolipoproteina B umana sono stati poi oggetto di caratterizzazione strutturale e funzionale. Il presente progetto di Dottorato ha interessato la valutazione dell'efficacia e dell'applicabilità di tali peptidi antimicrobici nel trattamento di infezioni cutanee multi-resistenti.
Gli obiettivi principali del presente lavoro di tesi possono essere schematizzati in quattro punti fondamentali:

1. Caratterizzazione delle proprietà antimicrobiche e anti-*biofilm* dei peptidi derivanti da ApoB su ceppi responsabili di infezioni cutanee, evidenziando la loro abilità di agire in sinergia con antibiotici tradizionali e di non selezionare fenotipi resistenti.

2. Valutazione della biocompatibilità dei peptidi in esame, analizzando possibili effetti tossici su cellule umane e sul microbioma della pelle. E' stato, inoltre, valutato il potenziale effetto anti-infiammatorio su co-culture di fibroblasti infettati con il batterio *S. aureus*.

3. Progettazione e caratterizzazione di una variante peptidomimetica dei peptidi derivanti da ApoB, dimostrandone l'aumento di stabilità e di efficacia *in vivo*.

4. Sviluppo di una formulazione topica a base di *hydrogel* in grado di incapsulare la variante peptidomimetica selezionata e di preservarne le bioattività.

Gli esperimenti volti alla valutazione dell'attività antimicrobica hanno dimostrato che i peptidi r(P)ApoB$_L^{Pro}$, r(P)ApoB$_S^{Pro}$ e r(P)ApoB$_L^{Ala}$ sono

in grado di inibire la crescita di ceppi del genere *Klebsiella*, *Acinetobacter* e Staphylococcus mediante depolarizzazione della membrana batterica. Inoltre, analisi per l'individuazione di "terapie combinate" hanno messo in luce la capacità dei peptidi in esame di agire in sinergia con antibiotici convenzionali. Esperimenti di microscopia elettronica e saggi cinetici hanno descritto il potenziale antimicrobico delle combinazioni peptide-antibiotico e la capacità dei peptidi derivanti da ApoB di non selezionare fenotipi resistenti. Ulteriori indagini volte alla valutazione delle proprietà anti-biofilm dei peptidi in esame hanno rivelato la capacità dei peptidi r(P)ApoB$_L^{Pro}$, r(P)ApoB$_S^{Pro}$ e r(P)ApoB$_L^{Ala}$ di destrutturare la matrice del biofilm batterico prodotto da ceppi microbici, quali *S. epidermidis* ATCC 35984 e *A. baumannii* ATCC 19606.

Le analisi di biocompatibilità e delle proprietà immunomodulanti dei peptidi derivanti da ApoB sono state approfondite durante il periodo di ricerca all'estero (6 mesi) presso il gruppo di ricerca diretto dal Professore Henk P. Haagsman dell'Università di Utrecht (Facoltà di Medicina Veterinaria, Università di Utrecht, Olanda). I risultati ottenuti hanno messo in luce gli ottimi profili di citotossicità dei peptidi in esame, escludendo possibili effetti tossici e immunogenici. Inoltre, è stato evidenziato il potenziale anti-infiammatorio del peptide r(P)ApoB$_S^{Pro}$ saggiato su co-culture di cellule eucariotiche infettate con *S. aureus*.

In collaborazione con il Professore César de la Fuente dell'Università della Pennsylvania (Dipartimento di Psichiatria e Microbiologia, Scuola di Medicina Perelman School of Medicine, Filadelfia, USA) è stata progettata una variante retro-inversa del peptide antimicrobico identificato nell'apolipoproteina B umana. Del nuovo peptidomimetico, qui denominato (ri)-r(P)ApoB$_S^{Pro}$, è stata dimostrata l'efficacia antimicrobica e l'aumentata stabilità sia *in vitro* che *in vivo*. Il peptide (ri)-r(P)ApoB$_S^{Pro}$, interamente composto da (D)-amminoacidi e con sequenza amminoacidica invertita rispetto al peptide naturale di partenza, ha mostrato significative attività antimicrobica e anti-biofilm su ceppi batterici antibiotico-resistenti, una maggiore resistenza alla degradazione proteolitica rispetto al peptide parentale e grande efficacia in modelli pre-clinici murini.

Al fine di fare un passo in avanti verso l'applicabilità delle molecole antimicrobiche qui selezionate, è stato progettato un sistema di *drug-delivery* basato su *hydrogel* presso i laboratori sperimentali e di produzione di AMP Biotec s.r.l. (6 mesi) diretti dalla Professoressa Rosanna Filosa e dal Dott. Alberto Di Crosta. A tale scopo, è stata messa a punto una formulazione ad uso topico basata su *hydrogel* di acido ialuronico funzionalizzato con il peptide (ri)-r(P)ApoB$_S^{Pro}$. Saggi

di attività antimicrobica hanno dimostrato l'efficacia del sistema *hydrogel*-peptide su ceppi batterici Gram-positivi e Gram-negativi, inclusi ceppi antibiotico-resistenti. Analisi di biocompatibilità hanno, inoltre, messo in luce la capacità del sistema di stimolare la vitalità di cheratinociti umani, dimostrando le enormi potenzialità del sistema *hydrogel* nei processi di rimarginazione delle ferite.
Nel complesso, i dati ottenuti supportano in maniera robusta la possibilità di impiego dei peptidi in esame quali nuovi agenti antimicrobici da impiegare nel trattamento di infezioni cutanee causate da batteri antibiotico-resistenti.

CHAPTER 1.

General Introduction

Angela Cesaro

Department of Chemical Sciences, PhD in Biotechnology

University of Naples Federico II

General introduction

1.1 The emerging problem of antibiotic resistance in skin infections

As the largest organ of the human body, the skin represents a physical barrier to prevent the invasion of pathogens [1]. In circumstances where the barrier is broken or when the balance between commensals (the beneficial microorganisms which colonize the skin) and pathogens is disturbed, skin diseases or even systemic diseases occur [1]. Skin and soft tissue infections (SSTIs) are among the most common disorders found in community and hospital environments [2]. These infections can appear in a variety of forms, ranging from superficial infections, which are controlled by treatment with topical antibiotics, to severe infections of deep tissues, which can lead to death if the patient is not appropriately treated [2]. Bacterial SSTIs, such as dermatitis, *acne vulgaris*, psoriasis, pyoderma, rosacea, cellulitis, and decubitus ulcers, are mainly caused by the ESKAPE pathogens (*Enterococcus faecium*, *Staphylococcus aureus*, *Klebsiella pneumoniae*, *Acinetobacter baumannii*, *Pseudomonas aeruginosa*, and *Enterobacter* species), which are bacteria recalcitrant and resistant to most of the common antibiotics. These bacterial strains are listed by the Centers for Disease Control and Prevention (CDC) as the biggest threats to human's health with more than 2.8 million antibiotic-resistant infections in the U.S. and more than 35,000 deaths in 2019 [3]. In atopic dermatitis, most *Staphylococcus aureus* isolates exhibited less susceptibility to methicillin, erythromycin, clindamycin, and oxacillin, and showed the highest resistance rate to benzylpenicillin followed by fusidic acid [4]. *S. epidermidis* strains, involved in such numerous skin diseases, as *acne vulgaris*, rosacea and ulcers [5][6][7], are often found resistant to antibiotics as rifamycin, fluoroquinolones, gentamicin, tetracycline, methicillin, clindamycin, and sulfonamides [8]. Others pathogens known to colonize wounds, thus causing skin infections, present often a multi-drug-resistant (MDR) profile [9][10][11]. For example, the clinical isolates of *Acinetobacter* spp., which were usually susceptible to gentamicin, minocycline, nalidixic acid, ampicillin, or carbenicillin in the early 1970s, developed resistance to almost all groups of drugs including the first and second generation of cephalosporins already since 1975 [12]. Similarly, there is an increasing prevalence of carbapenems-resistant *K. pneumoniae* and *P. aeruginosa* strains resistant to β-lactams and the fluoroquinolones [13][14]. The development of cellular resistance is generally the result of endogenous genes mutations, or is due to the transfer of resistance determinants

from other microorganisms [15][16][17][18]. Involved genes, collectively known as the *resistome* [19], act through different molecular mechanisms, such as inactivation of drugs *via* hydrolysis (*e.g.*, via β-lactamase) or modification (*e.g.*, aminoglycoside resistance), alteration of cellular targets (*e.g.*, by DNA gyrase mutation in fluoroquinolone resistance), development of permeation barriers, thus preventing drug access to the target (*e.g.*, the Gram-negative outer membrane) or activation of membrane-pumps specialized in drug efflux [20][21] **(Figure 1)**. Moreover, on human skin, 1×10^{21} microbial cells are estimated to live in biofilm, in which microbes produce a matrix of extracellular polymers that confer many advantages on their inhabitants [22]. The treatment of SSTIs and wounds is challenging because most of the pathogens form microbial biofilms [22]. As a mechanical shield, the components of the biofilm matrix are able to inhibit the effect of the antimicrobials [23] and make the pathogenic agents 1,000 times more resistant to conventional drugs than the corresponding planktonic cells [24]. Microorganisms growing in a biofilm state cause at least 65% of all human infections, and are particularly prevalent in infections on body surfaces (skin and soft tissue, lung, bladder, endocarditis, etc.), and in chronic infections [22]. Although antibiotics were once capable of treating most bacterial infections, in the last decades their excessive and improper use have favored the fast development of resistant bacterial strains [25]. Since the discovery, development, manufacture, and marketing of novel antibiotics have significantly slowed down, estimates claim that by 2050 worldwide 10 million people *per* year will die from infections caused by drug-resistant bacteria and the World Health Organization classifies the phenomenon of antibiotic resistance as one of the biggest threats to human health [26].

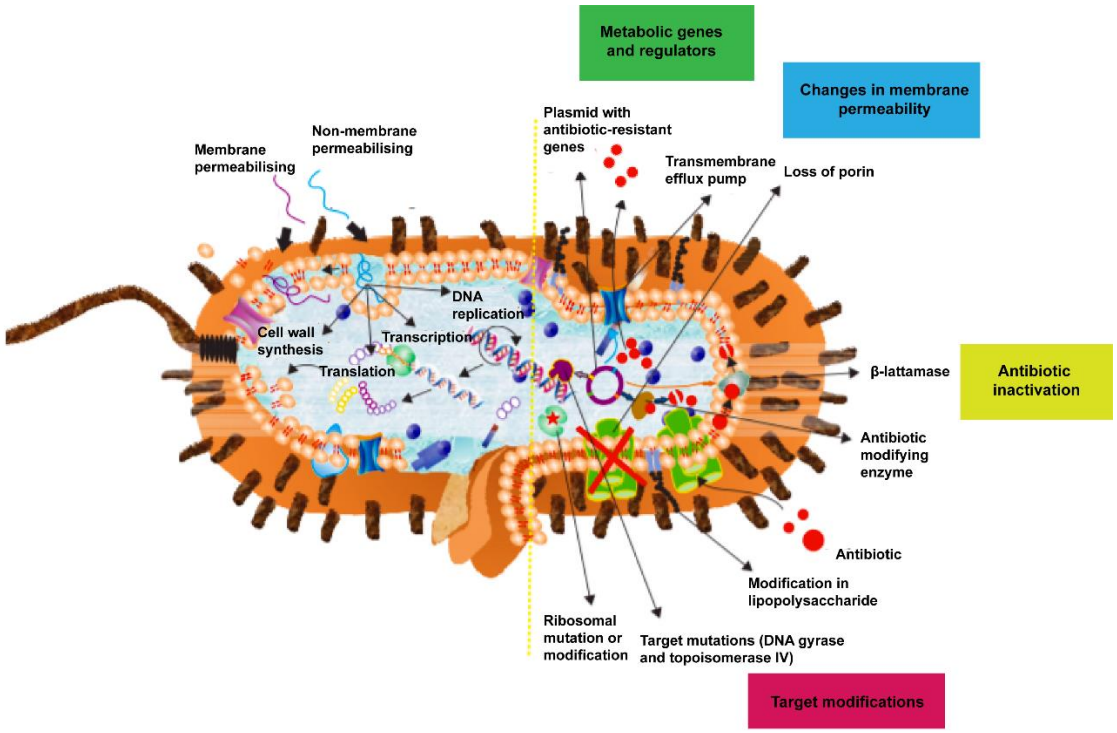

Figure 1. Mechanisms of antimicrobial action and resistance development. Mechanisms of antimicrobials are described in left section (indicated by the dashed yellow line) of the bacterial cell. Right section of the bacterial cell shows resistance mechanisms [25].

1.2 Antimicrobial peptides (AMPs)

The emergence of antibiotic resistance is leading to the design of novel antimicrobials less susceptible to resistance mechanisms than conventional antibiotics. In this context, innovative molecules as antimicrobial peptides (AMPs) represent a promising alternative to the old generations of antibiotics, since the evolution of resistance against these compounds is demonstrated to be less probable with respect to other antimicrobials [27][28][25]. AMPs are a group of evolutionarily conserved small proteins of the innate immune system, present in all complex living organisms. They work by disrupting bacterial cell membranes, modulating the immune response, and regulating inflammation [25] [29]. Natural AMPs have a size ranging from 12 to 50 amino acids, are mostly cationic owing to the presence of a high content

in lysine and arginine residues, and contain over 50% hydrophobic amino acids [30][31][32]. Despite the huge diversity in amino acid composition and cellular targets, AMPs are unified by their affinity for negatively charged prokaryotic membranes with strong electrical potential gradients [30]. Indeed, AMPs interaction with prokaryotic membranes represent a prerequisites for their entry into the cells or to direct disruption of the bacterial cell membrane [25][33][34]. The mechanism at the basis of their interaction with membranes has been extensively studied by experimental efforts. In the classical models, the peptides disintegrate the membrane after reaching a threshold concentration and inserting themselves across the phospholipids bilayer to form either peptide-lined pores in the **barrel-stave model**, solubilize the membrane into micellar structures in the **carpet model**, or form peptide-and-lipid-lined pores in the **toroidal pore model**. In the revised **disordered toroidal pore model**, pore formation is more stochastic and involves fewer peptides [35]. Other studies explained that the peptides can act by thickening the membrane or forming non-bilayer intermediates, or the membrane itself can be remodeled by clusters of anionic lipids surrounding the peptides. In others models, the peptides can dissipate the membrane potential without others damages, adsorb to the membrane by targeting oxidized phospholipids or, in the molecular electroporation model, they can increase the membrane potential, thus making the membrane transiently permeable [35]. Although membrane permeabilization is widely accepted as one of the possible mechanisms, interference with cell wall biogenesis, protein synthesis, protein folding, enzymatic activity and targeting intracellular components including DNA have also been proposed [25][35] **(Figure 2)**. Recent structure to function relationship studies classified the AMPs in three major classes: α-helical peptides, β-sheet peptides and extended peptides [35]. The **α-helical AMPs**, such as LL-37, magainins, mellitin, temporin L and B, are among the most studied. The lengths and properties of the α-helical influence the depth of membrane insertion and the thickness of the bilayer. Interestingly, the α-helical AMPs temporin B and L intercalate more efficiently into membrane containing an oxidized phosphatidylcholine lipid [35]. The **β-sheet AMPs**, as human α and β defensins, can also include several β-hairpin often stabilized by disulfide bridges between Cys residues. Many of these peptides seem to act by toroidal pore formation, others, instead, form oligomeric transmembrane barrels in anionic membranes [35]. **Extended AMPs**, as indolicidin, are peptides which do not fold into regular secondary structure elements and often contain high content of certain amino acids, specifically Arg, Trp or Pro residues. Many of these

peptides are not membrane active, but they exert antimicrobial activity by interacting with intracellular targets, such as heat-shock proteins or DNA [35].

Pathogenic agents have been exposed to antimicrobial peptides presumably for millions of years and no widespread resistance has been reported [36]. Since they act by targeting hydrophobic and/or polyanionic compounds of the membrane, the development of resistance against AMPs has occurred to a much lesser degree than the traditional antibiotics, whose targets, often essential bacterial proteins, are subjected to severe and growing resistance problems [36]. Thus, changing the architecture and/or compositions of membrane lipids is probably a “costly” solution for most microbial species [30].

To date, numerous natural and synthetic AMPs have been investigated because of their versatility, and many therapeutic fields have focused on them [37][38]. They display antimicrobial and anti-biofilm activity against both Gram-negative and Gram-positive bacterial strains, and can be used in combination with traditional antibiotics to improve the therapeutic effects, and even to broaden antibacterial spectrum [39][40]. Renalexin peptide, for example, was reported to potentiate the activity of polymyxin E, doxycycline, and clarithromycin. Magainin 2 also elicit synergistic effects when combined with ceftriaxone, amoxicillin–clavulanate and piperacillin, and the proline-rich antibacterial peptide A3-APO in combination with imipenem was found to increase survival in a murine model [25]. AMPs have also been found to display activity against fungi and yeasts, and to exert inhibitory effects on various DNA and RNA viruses including HIV, influenza virus, and hepatitis B virus [37][40]. Moreover, many AMPs are able to modulate host immunity by activating immunocytes, and modulating inflammation, alternatively by promoting or suppressing it. To emphasize their pleiotropic nature, they are often referred to as Host Defence Peptides (HDPs), or, more specifically, as Innate Defense Regulatory (IDR) peptides, since reports on their immunomodulatory activities have mostly been confirmed at the level of innate immunity [41]. Human α- and β-defensins, for example, can recruit leukocytes by direct chemotaxis or induce the expression of chemokines or cytokines including interleukin 8 (IL-8), monocyte chemoattractant protein (MCP-1) and interferon α (IFN-α) by indirect chemotaxis [42][43][44]. Furthermore, several AMPs act as anti-inflammatory agents protecting the host by bacterial endotoxins, such as lipopolysaccharide (LPS) and lipoteichoic acid (LTA) of Gram-negative and Gram-positive bacteria, respectively [42][45]. Indeed, many well-known AMPs, as LL-37 and protegrin-39, display their anti-inflammatories properties by neutralizing endotoxins [46].

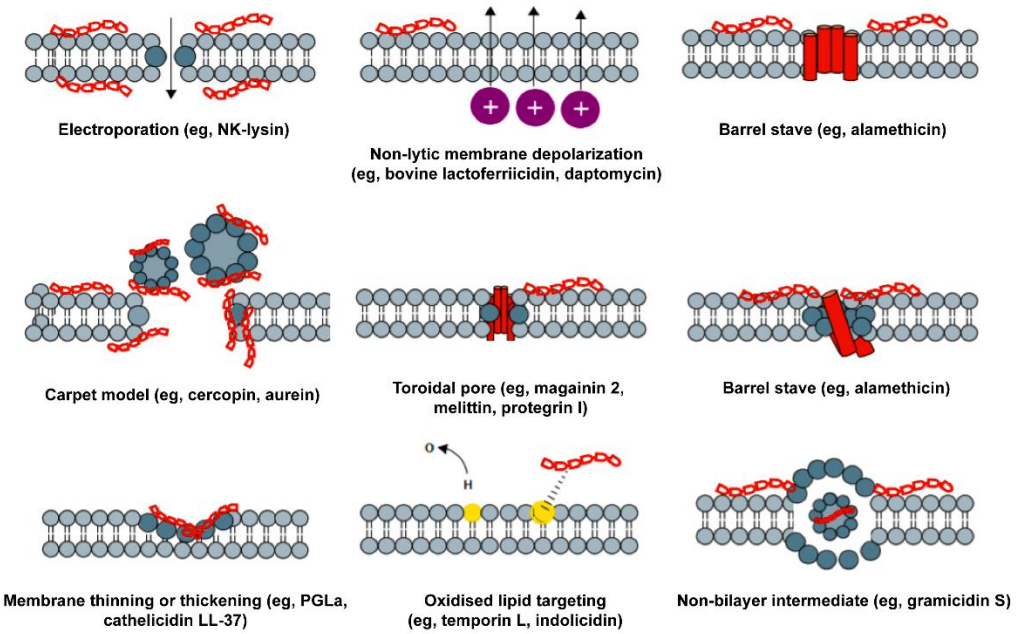

Figure 2. Mechanisms for interaction of AMPs with bacterial cell membranes. Schematic representation of events that occur at the bacterial cell membrane following interaction with AMPs [25].

1.3 Cryptic antimicrobial peptides

Many well-known proteins were found to hide multiple and unpredicted functions, that come out only following proteolytic cleavage. Peptides derived from hemoglobin, lactoferrin, lysozyme, collagen, histone-like proteins and ribonucleases were demonstrated to be involved in the regulation of several cellular processes as neuronal signaling, inflammatory response, adaptive immune response, differentiation, cell proliferation, wound healing and angiogenesis [47][48][49][50]. The presence of these activities, buried within a protein sequence, could reflect an evolutionary mechanism to increase the functionality of macromolecules [51]. In 2006, the term “cryptome” was introduced to describe a unique subset of proteins with the ability to generate bioactive peptides and proteins, known respectively as “cryptides” and “crypteins”, which may have related or increased properties with respect to precursor proteins or possess completely unrelated biological functions [52]. For these reasons, the cryptic peptides were classified in type 1 or 2 when the protein fragments have *in vivo* novel or the same bioactivity of the parent molecule, respectively, and in type

3 when they are generated *in vitro* and display novel biological properties [52]. The first cryptides were reported in 1960-70 when proteolytic products with antibacterial and antiviral activities were identified in human and mammals milk [53][54]. Since then, the number of putative cryptic peptides enormously expanded with the development of modern high throughput proteomic platforms [55][56]. In multicellular eukaryotes, several proteins were found to act as sources of “cryptic” antimicrobial peptides. These proteins, whose functions are not necessarily related to host defense, release bioactive peptides after proteolytic processing by bacterial and/or host proteases [57].

Several approaches were developed to discover novel cryptides, such as high-throughput diagnostic screening, mass spectrometry-based proteomic analyses, and computational biology techniques [58]. Many cryptic antimicrobial peptides were identified in a mixture of peptides generated by the digestion of the parent protein with one or more proteases, as the AMP released by neuthrophil elastase at the C-terminus of human thrombin [59]. Instead, other cryptic AMPs were discovered by homology to already known antimicrobial peptides, as the AMP from the C-terminus of S1 proteinases [60], or on the basis of structural and functional hypotheses, as in the case of COG133 peptide found in the receptor binding region of human apolipoprotein E [ApoE-(133–149)] [61][62]. Recently, *in silico* methods were also set up to localize AMP-like regions inside protein sequences performing the screening of protein databases [63][64][65][66]. Pane and co-workers have developed a scoring method, which allows to localize cryptic antimicrobial peptides within protein sequences by estimating their theoretical antimicrobial potency [67]. The algorithm is based on the finding that the antimicrobial potency of AMPs is directly proportional to a score – named “absolute score” (AS) – depending on the net charge (C), hydrophobicity (H) and length (L) of the peptide sequence. Indeed, $AS = L \times [(Cm \times Hn)/S_{max}]$ where S_{max} is the maximum value of product $(Cm \times Hn)$ and “m” and “n” are strain dependent variables, which define the relative contribution of charge and hydrophobicity to antimicrobial activity [67]. A simple sliding window strategy, using windows of any desired protein and sequence length, can be easily performed by this method [58]. Thus, the interesting evidence is that these “hidden” peptides can offer new opportunities for protein-based therapies because of their unexpected biological activities [51][47].

1.4 Antimicrobial peptidomimetics

Over the last decades, peptides emerged as an extraordinary class of molecules in drug development, as they combine versatility and potency [68]. Moreover, advances in peptides chemical synthesis allow to decrease manufacturing costs, making them more attractive in the industrial field [68]. Despite their bioactivity and biocompatibility, most of the bioactive peptides discovered present limitations. For example, they can be degraded into fragments, thereby losing any function imparted by the sequence and their structure [69]. The design of more stable molecules which mimic structurally and functionally the bioactive peptides has become an established methodology to improve the pharmacokinetic drawbacks of these innovative drugs [70]. Thus, the so-called peptidomimetics, which arise from the modulation or chemical modification of peptides by using non-canonical amino acids or non-peptide scaffolds, emerge as potential therapeutic agents able to overcome the limitations of the natural peptides [70]. Peptidomimetic drug research has progressed to become a multidisciplinary research field engaging synthetic, computational, and biophysical chemists, biochemists, pharmacologists, and drug development scientists worldwide [71]. The evolution of peptidomimetic drug discovery has been led by countless academic, industrial, and government companies to achieve the rational transformation of the first-generation peptide compounds to highly modified analogs [71].

The peptidomimetics are generally divided into three categories: i) type I mimetics are defined as short peptides with the same secondary structure of the lead peptide but minor alterations of the sequence; ii) type II mimetics are non-peptide molecules based on a scaffold that does not mimic the peptide secondary structure; iii) type III mimetics are also defined as non-peptide molecules that match the spatial topology of key interaction motifs of the lead peptide. However, these categories were recently subdivided into four different classes: classes A–D, where class A mimetics are the most identical to the lead peptide and class D mimetics display the least similarities [72] **(Figure 3)**.

Many antimicrobial peptidomimetics were demonstrated to be effective towards several pathogenic agents including drug resistant bacteria and are currently in Phase II clinical trials [73]. The pharmaceutical company Lytix Biopharma AS (Tromsø, Norway) has commenced Phase I/IIa clinical trials with an antimicrobial peptidomimetic known as Lytixar TM (also known as LTX-109) displaying a combination of high antibacterial activity against methicillin-resistant *Staphylococci* and *Staphylococcal* biofilms [73]. Another antimicrobial peptidomimetic,

known as POL7080, was developed by the company Polyphor, and was found to be highly active on a panel of clinical isolates, including drug resistant *Pseudomonas* bacteria, and with a potent bactericidal activity in a mouse septicemia infection model [74]. At present, Phase I clinical studies of POL7080 have been completed in healthy individuals in Europe, demonstrating the clinical safety and tolerability of this peptidomimetic [74]. Antimicrobial peptidomimetics hold vast potentialities as excellent anti-infective drugs due to their wide range of biological activities, low costs of production when compared with those of proteins and antibodies, ease of structural modifications and stability improvements, and promising pharmacokinetic profiles [75].

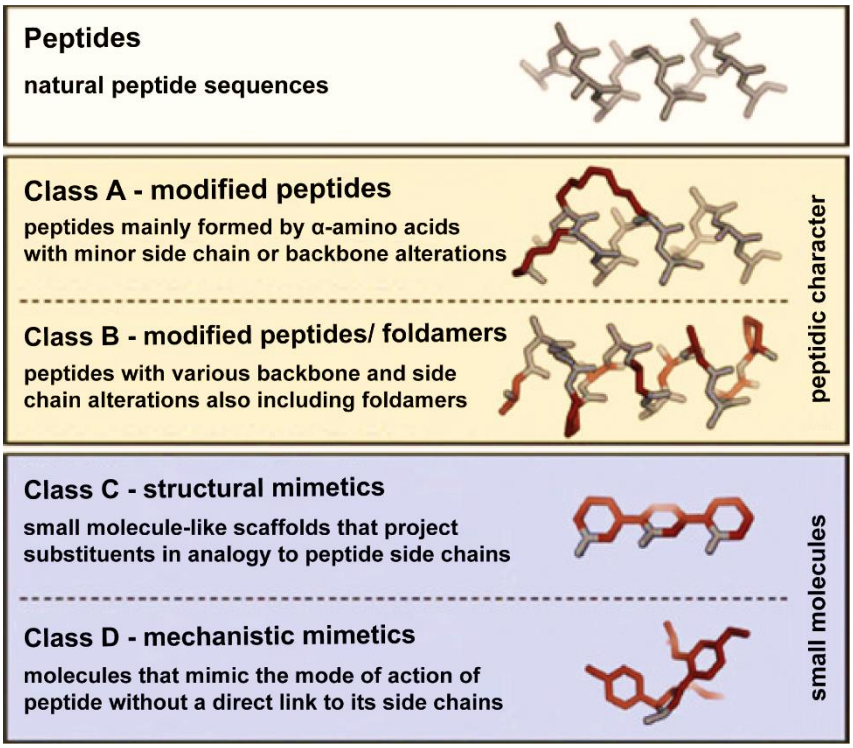

Figure 3. Classification of peptidomimetics. Classes A–D, where class A mimetics share much of the lead peptide and class D mimetics display the least similarities.

1.5 Topical dermatological formulations

Topical formulations are a class of compounds used to deliver a therapeutically effective concentration of a specific drug at the target site [76]. Many types of formulations are available and are specifically designed to exert a local effect on the skin or into the deeper cutaneous layers [76]. Advantages related to these products include the possibility to increase the dose of drug where it is needed and the reduction of side effects to other organs compared to systemic therapeutics [77]. Topical formulations contain an active ingredient and a vehicle, which usually consists of water, oil, alcohol, or propylene glycol mixed with preservatives, emulsifiers, absorption promoters, and fragrances [77].
There are three major categories of topical dosage forms (liquid, semi-solid, and solid), and different formulations can classified as solutions, lotions, creams, ointments, gels, pastes, aerosol foams or spray, powders, and transdermal patches [78]. The appropriate formulation depends on many factors, including the sites involved, the action desired, the nature, bioavailability and stability of the drug to be incorporated, the required shelf-life of the final product, the disease severity, and the host profile [79].
Bacterial skin and soft tissue infections, as dermatitis, *acne vulgaris*, psoriasis, decubitus ulcers and chronic wounds, pose a great clinical challenge for the topical administration of antimicrobial peptides. Several studies have been carried out to develop different AMPs formulations, which include nanoparticles, hydrogels, creams, ointments, and patches [80]. Nanoparticles improve the peptides stability and activity. In some cases, they can even enhance the peptides solubility. However, the major disadvantage of nanoparticle-based formulations is their residence time at the site of application. A potentially effective formulation for AMPs topical delivery is also represented by the hydrogels. They are able to control drug release by various mechanisms, *e.g.*, electrostatic, covalent conjugation, and degradation profiles, and provide moisture at the target site **(Figure 4)**. However, it has to be highlighted that it is necessary to modify and to optimize the hydrogel network to avoid possible negative effects on peptide efficacy. Recent advances are focused on AMPs loaded nanoparticles and hydrogels based on natural polymers (*e.g.*, collagen and hyaluronic acid), which prevent peptides degradation and enhance their residence time in wound sites. On the other hand, creams and ointments are topical formulations widely used and approved for their safety and suitability, but they present the limit to be easily removed from the site, with consequent negative effects on the amount of AMP

reaching the wound. Other strategies are represented by patches, which provide an interesting approach to deliver AMPs. However, it is necessary that the peptides are sufficiently flexible to preserve their antimicrobial activity [80]. Although, by using these delivery systems, the peptides are less subjected to be degraded and/or neutralized with respect to oral or systemic administration, different factors arising from the wound microenvironment or the skin spots might destabilize them. Therefore, the optimization of opical formulations suitable for AMPs is a requirement to overcome the stability issues and to promote the wound-healing processes [80].

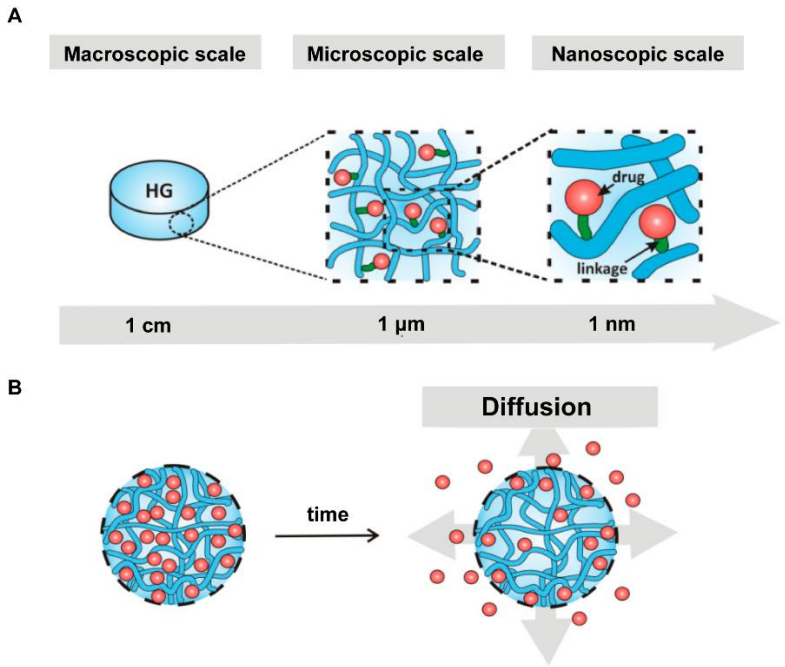

Figure 4. Schematic representation of a hydrogel-based formulation. (A) Size and porous structure of the hydrogel loaded with the bioactive drug. (B) Drug release from the polymeric matrix of the hydrogel [81].

1.6 Aims of the Thesis

The overall aim of the present Thesis project is the characterization of three cryptic peptides identified in human apolipoprotein B by using an algorithmic approach [82], in order to evaluate their applicability in the treatment of skin and soft tissue infections. Following this Chapter 1 comprising a general introduction to the experimental part, Chapters 2-6 will report a detailed experimental characterization of peptides structures, bioactivities *in vitro* and *in vivo*, and applicability. A summary of the main chapters is reported below:

- **Chapter 2** describes the antimicrobial activity of ApoB-derived encrypted peptides towards common skin pathogens by highlighting their ability to act in synergism with conventional antibiotics while not determining the insurance of resistance phenotype even after a prolonged incubation with bacterial cells; peptides' anti-biofilm effects on the main three stages of biofilm development are described.;
- **Chapter 3** describes the biocompatibility of ApoB-derived encrypted peptides on eukaryotic cell cultures and on skin microbiome as well as their anti-inflammatory effects on co-cultures of human fibroblasts infected with *S. aureus*;
- **Chapter 4** mainly focuses on the design and characterization of a retro-inverso variant of the leads encrypted peptide by demonstrating increased stability and anti-infective properties *in vivo*;
- **Chapter 5** depicts the development of a hydrogel-based formulation loaded with the selected antimicrobial peptidomimetics as well as the analysis of its chemical and biological properties;
- **Chapter 6** comprises a general discussion on the main findings and conclusions derived from the present research.

1.7 References

[1] A. L. Byrd, Y. Belkaid, and J. A. Segre, “The human skin microbiome.,” *Nat. Rev. Microbiol.*, vol. 16, no. 3, pp. 143–155, Mar. 2018, doi: 10.1038/nrmicro.2017.157.

[2] J. S. Lim, H. Park, S. Cho, and H.-S. Yoon, “Antibiotic Susceptibility and Treatment Response in Bacterial Skin Infection,” *Ann. Dermatol.*, vol. 30, no. 2, p. 186, 2018, doi: 10.5021/ad.2018.30.2.186.

[3] S. Santajit and N. Indrawattana, “Mechanisms of Antimicrobial Resistance in ESKAPE Pathogens,” *Biomed Res. Int.*, vol. 2016, pp. 1–8, 2016, doi: 10.1155/2016/2475067.

[4] M.-Y. Jung, J.-Y. Chung, H.-Y. Lee, J. Park, D.-Y. Lee, and J.-M. Yang, “Antibiotic Susceptibility of Staphylococcus aureus in Atopic Dermatitis: Current Prevalence of Methicillin-Resistant Staphylococcus aureus in Korea and Treatment Strategies,” *Ann. Dermatol.*, vol. 27, no. 4, p. 398, 2015, doi: 10.5021/ad.2015.27.4.398.

[5] B. Kumar, R. Pathak, P. B. Mary, D. Jha, K. Sardana, and H. K. Gautam, “New insights into acne pathogenesis: Exploring the role of acne-associated microbial populations,” *Dermatologica Sin.*, vol. 34, no. 2, pp. 67–73, Jun. 2016, doi: 10.1016/j.dsi.2015.12.004.

[6] D. M. E. Bowdish, D. J. Davidson, and R. E. W. Hancock, “Immunomodulatory Properties of Defensins and Cathelicidins,” in *Journal of the American Academy of Dermatology*, vol. 306, 2006, pp. 27–66.

[7] N. Malanovic and K. Lohner, “Gram-positive bacterial cell envelopes: The impact on the activity of antimicrobial peptides.,” *Biochim. Biophys. Acta*, vol. 1858, no. 5, pp. 936–46, May 2016, doi: 10.1016/j.bbamem.2015.11.004.

[8] M. Otto, “Staphylococcus epidermidis — the ‘accidental’ pathogen,” *Nat. Rev. Microbiol.*, vol. 7, no. 8, pp. 555–567, Aug. 2009, doi: 10.1038/nrmicro2182.

[9] D. M. Guerrero *et al.*, “Acinetobacter baumannii -Associated Skin and Soft Tissue Infections: Recognizing a Broadening Spectrum of Disease,” *Surg. Infect. (Larchmt).*, vol. 11, no. 1, pp. 49–57,

Feb. 2010, doi: 10.1089/sur.2009.022.

[10] C.-M. Chang *et al.*, “Community-Acquired Klebsiella pneumoniae Complicated Skin and Soft-Tissue Infections of Extremities: Emphasis on Cirrhotic Patients and Gas Formation,” *Infection*, vol. 36, no. 4, pp. 328–334, Aug. 2008, doi: 10.1007/s15010-008-7272-3.

[11] R. Serra *et al.*, “Chronic wound infections: the role of Pseudomonas aeruginosa and Staphylococcus aureus,” *Expert Rev. Anti. Infect. Ther.*, vol. 13, no. 5, pp. 605–613, May 2015, doi: 10.1586/14787210.2015.1023291.

[12] A. Mizuno, K. Matsui, and S. Shuto, “From Peptides to Peptidomimetics: A Strategy Based on the Structural Features of Cyclopropane.,” *Chemistry*, vol. 23, no. 58, pp. 14394–14409, Oct. 2017, doi: 10.1002/chem.201702119.

[13] J. Reyes, A. C. Aguilar, and A. Caicedo, “Carbapenem-Resistant Klebsiella pneumoniae: Microbiology Key Points for Clinical Practice,” *Int. J. Gen. Med.*, vol. Volume 12, pp. 437–446, Nov. 2019, doi: 10.2147/IJGM.S214305.

[14] P. D. Lister, D. J. Wolter, and N. D. Hanson, “Antibacterial-Resistant Pseudomonas aeruginosa: Clinical Impact and Complex Regulation of Chromosomally Encoded Resistance Mechanisms,” *Clin. Microbiol. Rev.*, vol. 22, no. 4, pp. 582–610, Oct. 2009, doi: 10.1128/CMR.00040-09.

[15] J. L. Martínez, T. M. Coque, and F. Baquero, “What is a resistance gene? Ranking risk in resistomes.,” *Nat. Rev. Microbiol.*, vol. 13, no. 2, pp. 116–23, 2015, doi: 10.1038/nrmicro3399.

[16] J. A. Perry and G. D. Wright, “Forces shaping the antibiotic resistome,” *BioEssays*, vol. 36, no. 12, pp. 1179–1184, Dec. 2014, doi: 10.1002/bies.201400128.

[17] H. Ceri, M. E. Olson, C. Stremick, R. R. Read, D. Morck, and A. Buret, “The Calgary Biofilm Device: New Technology for Rapid Determination of Antibiotic Susceptibilities of Bacterial Biofilms,” *J. Clin. Microbiol.*, vol. 37, no. 6, pp. 1771–1776, Jun. 1999, doi: 10.1128/JCM.37.6.1771-1776.1999.

[18] M. O. A. Sommer, G. Dantas, and G. M. Church, “Functional Characterization of the Antibiotic Resistance Reservoir in the

Human Microflora," *Science (80-.).*, vol. 325, no. 5944, pp. 1128–1131, Aug. 2009, doi: 10.1126/science.1176950.

[19] G. D. Wright, "The antibiotic resistome: the nexus of chemical and genetic diversity," *Nat. Rev. Microbiol.*, vol. 5, no. 3, pp. 175–186, Mar. 2007, doi: 10.1038/nrmicro1614.

[20] H. Nikaido, "Multiple antibiotic resistance and efflux.," *Curr. Opin. Microbiol.*, vol. 1, no. 5, pp. 516–23, Oct. 1998, doi: 10.1016/s1369-5274(98)80083-0.

[21] I. T. Paulsen, "Multidrug efflux pumps and resistance: regulation and evolution.," *Curr. Opin. Microbiol.*, vol. 6, no. 5, pp. 446–51, Oct. 2003, doi: 10.1016/j.mib.2003.08.005.

[22] H.-C. Flemming and S. Wuertz, "Bacteria and archaea on Earth and their abundance in biofilms," *Nat. Rev. Microbiol.*, vol. 17, no. 4, pp. 247–260, Apr. 2019, doi: 10.1038/s41579-019-0158-9.

[23] C. de la Fuente-Núñez *et al.*, "Anti-Biofilm and Immunomodulatory Activities of Peptides That Inhibit Biofilms Formed by Pathogens Isolated from Cystic Fibrosis Patients," *Antibiotics*, vol. 3, no. 4, pp. 509–526, Oct. 2014, doi: 10.3390/antibiotics3040509.

[24] H. Ceri, M. E. Olson, C. Stremick, R. R. Read, D. Morck, and A. Buret, "The Calgary Biofilm Device: New Technology for Rapid Determination of Antibiotic Susceptibilities of Bacterial Biofilms," *J. Clin. Microbiol.*, vol. 37, no. 6, pp. 1771–1776, 1999, doi: 10.1128/JCM.37.6.1771-1776.1999.

[25] M. Magana *et al.*, "The value of antimicrobial peptides in the age of resistance," *Lancet Infect. Dis.*, vol. 20, no. 9, pp. e216–e230, Sep. 2020, doi: 10.1016/S1473-3099(20)30327-3.

[26] A. Pfalzgraff, K. Brandenburg, and G. Weindl, "Antimicrobial Peptides and Their Therapeutic Potential for Bacterial Skin Infections and Wounds," *Front. Pharmacol.*, vol. 9, Mar. 2018, doi: 10.3389/fphar.2018.00281.

[27] C. D. Fjell, J. A. Hiss, R. E. W. Hancock, and G. Schneider, "Designing antimicrobial peptides: form follows function.," *Nat. Rev. Drug Discov.*, vol. 11, no. 1, pp. 37–51, Dec. 2011, doi: 10.1038/nrd3591.

[28] R. Spohn *et al.*, "Integrated evolutionary analysis reveals

antimicrobial peptides with limited resistance," *Nat. Commun.*, vol. 10, no. 1, p. 4538, Dec. 2019, doi: 10.1038/s41467-019-12364-6.

[29] T. Ganz, "The role of antimicrobial peptides in innate immunity.," *Integr. Comp. Biol.*, vol. 43, no. 2, pp. 300–4, Apr. 2003, doi: 10.1093/icb/43.2.300.

[30] M. Zasloff, "Antimicrobial peptides of multicellular organisms," *Nature*, vol. 415, no. 6870, pp. 389–395, Jan. 2002, doi: 10.1038/415389a.

[31] R. E. W. Hancock and R. Lehrer, "Cationic peptides: a new source of antibiotics.," *Trends Biotechnol.*, vol. 16, no. 2, pp. 82–8, Feb. 1998, doi: 10.1016/s0167-7799(97)01156-6.

[32] H. G. Boman, "Antibacterial peptides: basic facts and emerging concepts.," *J. Intern. Med.*, vol. 254, no. 3, pp. 197–215, Sep. 2003, doi: 10.1046/j.1365-2796.2003.01228.x.

[33] E. Glukhov, M. Stark, L. L. Burrows, and C. M. Deber, "Basis for selectivity of cationic antimicrobial peptides for bacterial versus mammalian membranes.," *J. Biol. Chem.*, vol. 280, no. 40, pp. 33960–7, Oct. 2005, doi: 10.1074/jbc.M507042200.

[34] M. Umeyama, A. Kira, K. Nishimura, and A. Naito, "Interactions of bovine lactoferricin with acidic phospholipid bilayers and its antimicrobial activity as studied by solid-state NMR," *Biochim. Biophys. Acta - Biomembr.*, vol. 1758, no. 9, pp. 1523–1528, Sep. 2006, doi: 10.1016/j.bbamem.2006.06.014.

[35] L. T. Nguyen, E. F. Haney, and H. J. Vogel, "The expanding scope of antimicrobial peptide structures and their modes of action.," *Trends Biotechnol.*, vol. 29, no. 9, pp. 464–72, Sep. 2011, doi: 10.1016/j.tibtech.2011.05.001.

[36] F. C.D., H. J.A., H. R.E.W., and S. G., "Designing antimicrobial peptides: Form follows function," *Nature Reviews Drug Discovery*. 2012.

[37] N. Mookherjee, M. A. Anderson, H. P. Haagsman, and D. J. Davidson, "Antimicrobial host defence peptides: functions and clinical potential.," *Nat. Rev. Drug Discov.*, vol. 19, no. 5, pp. 311–332, May 2020, doi: 10.1038/s41573-019-0058-8.

[38] R. I. Lehrer and T. Ganz, "Cathelicidins: a family of endogenous

antimicrobial peptides," *Curr. Opin. Hematol.*, vol. 9, no. 1, pp. 18–22, Jan. 2002, doi: 10.1097/00062752-200201000-00004.

[39] D. Pletzer, S. R. Coleman, and R. E. W. Hancock, "Anti-biofilm peptides as a new weapon in antimicrobial warfare.," *Curr. Opin. Microbiol.*, vol. 33, pp. 35–40, Oct. 2016, doi: 10.1016/j.mib.2016.05.016.

[40] J. Lei *et al.*, "The antimicrobial peptides and their potential clinical applications.," *Am. J. Transl. Res.*, vol. 11, no. 7, pp. 3919–3931, 2019, [Online]. Available: http://www.ncbi.nlm.nih.gov/pubmed/31396309.

[41] T. Rončević, J. Puizina, and A. Tossi, "Antimicrobial Peptides as Anti-Infective Agents in Pre-Post-Antibiotic Era?," *Int. J. Mol. Sci.*, vol. 20, no. 22, p. 5713, Nov. 2019, doi: 10.3390/ijms20225713.

[42] D. M. E. Bowdish, D. J. Davidson, and R. E. W. Hancock, "Immunomodulatory Properties of Defensins and Cathelicidins," in *Current Topics in Microbiology and Immunology*, 2006, pp. 27–66.

[43] W. K. K. Wu, C. C. M. Wong, Z. J. Li, L. Zhang, S. X. Ren, and C. H. Cho, "Cathelicidins in inflammation and tissue repair: Potential therapeutic applications for gastrointestinal disorders," *Acta Pharmacol. Sin.*, vol. 31, no. 9, pp. 1118–1122, Sep. 2010, doi: 10.1038/aps.2010.117.

[44] A. L. Hilchie, K. Wuerth, and R. E. Hancock, "Immune modulation by multifaceted cationic host," *Nat Chem Biol*, 2013.

[45] L. Martin, A. van Meegern, S. Doemming, and T. Schuerholz, "Antimicrobial Peptides in Human Sepsis," *Front. Immunol.*, vol. 6, Aug. 2015, doi: 10.3389/fimmu.2015.00404.

[46] R. Ramos *et al.*, "Wound healing activity of the human antimicrobial peptide LL37.," *Peptides*, vol. 32, no. 7, pp. 1469–76, Jul. 2011, doi: 10.1016/j.peptides.2011.06.005.

[47] N. Ueki, K. Someya, Y. Matsuo, K. Wakamatsu, and H. Mukai, "Cryptides: Functional cryptic peptides hidden in protein structures," *Biopolymers*, vol. 88, no. 2, pp. 190–198, 2007, doi: 10.1002/bip.20687.

[48] D. C. Pimenta and I. Lebrun, "Cryptides: buried secrets in proteins.," *Peptides*, vol. 28, no. 12, pp. 2403–10, Dec. 2007, doi:

10.1016/j.peptides.2007.10.005.

[49] I. Gomes *et al.*, “Hemoglobin-derived peptides as novel type of bioactive signaling molecules.,” *AAPS J.*, vol. 12, no. 4, pp. 658–69, Dec. 2010, doi: 10.1208/s12248-010-9217-x.

[50] J. S. Gelman, J. Sironi, L. M. Castro, E. S. Ferro, and L. D. Fricker, “Hemopressins and other hemoglobin-derived peptides in mouse brain: comparison between brain, blood, and heart peptidome and regulation in Cpefat/fat mice.,” *J. Neurochem.*, vol. 113, no. 4, pp. 871–80, May 2010, doi: 10.1111/j.1471-4159.2010.06653.x.

[51] D. J. Autelitano, A. Rajic, A. I. Smith, M. C. Berndt, L. L. Ilag, and M. Vadas, “The cryptome: a subset of the proteome, comprising cryptic peptides with distinct bioactivities,” *Drug Discov. Today*, vol. 11, no. 7–8, pp. 306–314, Apr. 2006, doi: 10.1016/j.drudis.2006.02.003.

[52] A. D.J., R. A., S. A.I., B. M.C., I. L.L., and V. M., “The cryptome: a subset of the proteome, comprising cryptic peptides with distinct bioactivities,” *Drug Discov. Today*, 2006.

[53] C. Liepke, H. D. Zucht, W. G. Forssmann, and L. Ständker, “Purification of novel peptide antibiotics from human milk.,” *J. Chromatogr. B. Biomed. Sci. Appl.*, vol. 752, no. 2, pp. 369–77, Mar. 2001, doi: 10.1016/s0378-4347(00)00516-8.

[54] H. J. Hosea Blewett, M. C. Cicalo, C. D. Holland, and C. J. Field, “The Immunological Components of Human Milk,” in *Advances in Food and Nutrition Research*, 2008, pp. 45–80.

[55] I. Messana *et al.*, “Trafficking and Postsecretory Events Responsible for the Formation of Secreted Human Salivary Peptides,” *Mol. Cell. Proteomics*, vol. 7, no. 5, pp. 911–926, May 2008, doi: 10.1074/mcp.M700501-MCP200.

[56] I. Messana, T. Cabras, F. Iavarone, F. Vincenzoni, A. Urbani, and M. Castagnola, “Unraveling the different proteomic platforms.,” *J. Sep. Sci.*, vol. 36, no. 1, pp. 128–39, Jan. 2013, doi: 10.1002/jssc.201200830.

[57] K. Pane *et al.*, “A new cryptic cationic antimicrobial peptide from human apolipoprotein E with antibacterial activity and immunomodulatory effects on human cells,” *FEBS J.*, vol. 283, no. 11, pp. 2115–2131, Jun. 2016, doi: 10.1111/febs.13725.

[58] R. Gaglione, E. Pizzo, E. Notomista, C. de la Fuente-Nunez, and A. Arciello, “Host Defence Cryptides from Human Apolipoproteins: Applications in Medicinal Chemistry,” *Curr. Top. Med. Chem.*, vol. 20, no. 14, pp. 1324–1337, Jun. 2020, doi: 10.2174/1568026620666200427091454.

[59] P. P. *et al.*, “Proteolysis of human thrombin generates novel host defense peptides,” *PLoS Pathog.*, 2010.

[60] G. Kasetty *et al.*, “The C-terminal sequence of several human serine proteases encodes host defense functions.,” *J. Innate Immun.*, vol. 3, no. 5, pp. 471–82, 2011, doi: 10.1159/000327016.

[61] U. K. Misra, C. L. Adlakha, G. Gawdi, M. K. McMillian, S. V Pizzo, and D. T. Laskowitz, “Apolipoprotein E and mimetic peptide initiate a calcium-dependent signaling response in macrophages.,” *J. Leukoc. Biol.*, vol. 70, no. 4, pp. 677–83, Oct. 2001, doi: 10.1189/jlb.70.4.677.

[62] J. R. Lynch *et al.*, “APOE Genotype and an ApoE-mimetic Peptide Modify the Systemic and Central Nervous System Inflammatory Response,” *J. Biol. Chem.*, vol. 278, no. 49, pp. 48529–48533, Dec. 2003, doi: 10.1074/jbc.M306923200.

[63] M. Torrent *et al.*, “AMPA: an automated web server for prediction of protein antimicrobial regions,” *Bioinformatics*, vol. 28, no. 1, pp. 130–131, Jan. 2012, doi: 10.1093/bioinformatics/btr604.

[64] A. Niarchou, A. Alexandridou, E. Athanasiadis, and G. Spyrou, “C-PAmP: Large Scale Analysis and Database Construction Containing High Scoring Computationally Predicted Antimicrobial Peptides for All the Available Plant Species,” *PLoS One*, vol. 8, no. 11, p. e79728, Nov. 2013, doi: 10.1371/journal.pone.0079728.

[65] G. D. Brand *et al.*, “Probing Protein Sequences as Sources for Encrypted Antimicrobial Peptides,” *PLoS One*, vol. 7, no. 9, p. e45848, Sep. 2012, doi: 10.1371/journal.pone.0045848.

[66] M. H. S. Ramada *et al.*, “Encrypted Antimicrobial Peptides from Plant Proteins,” *Sci. Rep.*, vol. 7, no. 1, p. 13263, Dec. 2017, doi: 10.1038/s41598-017-13685-6.

[67] K. Pane *et al.*, “Antimicrobial potency of cationic antimicrobial peptides can be predicted from their amino acid composition: Application to the detection of ‘cryptic’ antimicrobial peptides,” *J.*

Theor. Biol., vol. 419, pp. 254–265, Apr. 2017, doi: 10.1016/j.jtbi.2017.02.012.

[68] A. Lobo-Ruiz and J. Tulla-Puche, “Synthetic approaches of naturally and rationally designed peptides and peptidomimetics,” in *Peptide Applications in Biomedicine, Biotechnology and Bioengineering*, Elsevier, 2018, pp. 23–49.

[69] H. R. Reese, C. C. Shanahan, C. Proulx, and S. Menegatti, “Peptide science: A ‘rule model’ for new generations of peptidomimetics.,” *Acta Biomater.*, vol. 102, pp. 35–74, Jan. 2020, doi: 10.1016/j.actbio.2019.10.045.

[70] A. Mizuno, K. Matsui, and S. Shuto, “From Peptides to Peptidomimetics: A Strategy Based on the Structural Features of Cyclopropane,” *Chem. - A Eur. J.*, vol. 23, no. 58, pp. 14394–14409, Oct. 2017, doi: 10.1002/chem.201702119.

[71] J. B. Taylor and D. J. Triggle, “Comprehensive Medicinal Chemistry,” *Quant. Struct. Relationships*, vol. 10, no. 4, pp. 372–373, 1991, doi: 10.1002/qsar.19910100410.

[72] L. Mabonga and A. P. Kappo, “Peptidomimetics: A Synthetic Tool for Inhibiting Protein–Protein Interactions in Cancer,” *Int. J. Pept. Res. Ther.*, vol. 26, no. 1, pp. 225–241, Mar. 2020, doi: 10.1007/s10989-019-09831-5.

[73] I. Wiegand, K. Hilpert, and R. E. W. Hancock, “Agar and broth dilution methods to determine the minimal inhibitory concentration (MIC) of antimicrobial substances.,” *Nat. Protoc.*, vol. 3, no. 2, pp. 163–75, 2008, doi: 10.1038/nprot.2007.521.

[74] N. Srinivas *et al.*, “Peptidomimetic Antibiotics Target Outer-Membrane Biogenesis in Pseudomonas aeruginosa,” *Science (80-.).*, vol. 327, no. 5968, pp. 1010–1013, Feb. 2010, doi: 10.1126/science.1182749.

[75] B. Mojsoska and H. Jenssen, “Peptides and Peptidomimetics for Antimicrobial Drug Design,” *Pharmaceuticals*, vol. 8, no. 3, pp. 366–415, Jul. 2015, doi: 10.3390/ph8030366.

[76] A. Nair, S. Jacob, B. Al-Dhubiab, M. Attimarad, and S. Harsha, “Basic considerations in the dermatokinetics of topical formulations,” *Brazilian J. Pharm. Sci.*, vol. 49, no. 3, pp. 423–434, Sep. 2013, doi: 10.1590/S1984-82502013000300004.

[77] F. Lyons and L. Ousley, *Dermatology for the Advanced Practice Nurse*. New York, NY: Springer Publishing Company, 2014.

[78] T. Garg, G. Rath, and A. K. Goyal, “Comprehensive review on additives of topical dosage forms for drug delivery,” *Drug Deliv.*, vol. 22, no. 8, pp. 969–987, Nov. 2015, doi: 10.3109/10717544.2013.879355.

[79] C. T. Ueda *et al.*, “Topical and Transdermal Drug Products,” *Dissolution Technol.*, vol. 17, no. 4, pp. 12–25, 2010, doi: 10.14227/DT170410P12.

[80] R. K. Thapa, D. B. Diep, and H. H. Tønnesen, “Topical antimicrobial peptide formulations for wound healing: Current developments and future prospects,” *Acta Biomater.*, vol. 103, pp. 52–67, Feb. 2020, doi: 10.1016/j.actbio.2019.12.025.

[81] A. Chyzy, M. Tomczykowa, and M. E. Plonska-Brzezinska, “Hydrogels as Potential Nano-, Micro- and Macro-Scale Systems for Controlled Drug Delivery,” *Materials (Basel).*, vol. 13, no. 1, p. 188, Jan. 2020, doi: 10.3390/ma13010188.

[82] R. Gaglione *et al.*, “Novel human bioactive peptides identified in Apolipoprotein B: Evaluation of their therapeutic potential.,” *Biochem. Pharmacol.*, vol. 130, pp. 34–50, Apr. 2017, doi: 10.1016/j.bcp.2017.01.009.

CHAPTER 2.

ApoB encrypted peptides as novel antimicrobial and anti-biofilm agents against common skin pathogens

Angela Cesaro

Department of Chemical Sciences, PhD in Biotechnology

University of Naples Federico II

ApoB encrypted peptides as novel antimicrobial and anti-biofilm agents against common skin pathogens

1. Introduction

In 2019, more than 2.8 million people suffered from antibiotic-resistant infections and over 35,000 individuals died in the U.S. [1] ESKAPE pathogens (*Enterococcus faecium*, *Staphylococcus aureus*, *Klebsiella pneumoniae*, *Acinetobacter baumannii*, *Pseudomonas aeruginosa*, and *Enterobacter* species) are of particular concern as they are resistant to most available antibiotics [2]. Further, it has been recently estimated that, at the current rate of antibiotic resistance coupled with the lack of antibiotic discovery, by 2050 worldwide 10 million people will die annually from infections caused by drug-resistant bacteria. The World Health Organization has described this global problem as one of the biggest threats to human health [3].

Therefore, alternatives to conventional antibiotics are urgently needed to treat such drug-resistant infections. Recently our research group has developed and used an algorithmic approach to systematically explore the human proteome searching for encrypted peptides with antibiotic properties, an effort that yielded thousands of previously unexplored molecules [4][5]. This innovative algorithm is able to highlight cryptic bioactive peptides inside a protein sequence and to provide a prediction of their antimicrobial activity by a quantitative score [4]. These proteins, whose biological function is not necessarily related to host innate immune defense, contain within their sequence encrypted peptides that may be released upon proteolytic cleavage by bacterial or host proteases [6]. The presence of these peptide fragments, hidden within proteins, may reflect an evolutionary mechanism to increase the range of functionalities of proteins [7]. By this innovative bioinformatic approach, three encrypted peptides have been identified in plasma protein human apolipoprotein B [5]. Plasma lipoproteins, such as high-density, low-density and very low-density lipoproteins (HDL, LDH and VLDH), play a key role in lipid transport among tissues and organs [4][5][8]. Indeed, Apolipoprotein B is responsible for carrying lipids, including cholesterol, around the body to cells within all tissues, and high levels of apolipoprotein B are related to heart disease [9]. The encrypted peptides identified represent a novel and previously untapped class of potential antibiotics and may be fascinatingly seen as a great opportunity to develop protein-based therapies to be employed in the treatment of skin infections [7][10].

2. Methods

Materials. All the reagents were purchase from Sigma-Merck (Milan, Italy), unless specified otherwise.

Bacterial strains and growth conditions. Five bacterial strains were used in the present study, *i.e. S. epidermidis* ATCC 35984, *S. aureus* ATCC 12600, *S. aureus* ATCC 29213, *A. baumannii* ATCC 19606, *K. pneumoniae* ATCC 70603 and *Pseudomonas aeruginosa* PAO1. All bacterial strains were grown in Muller Hinton Broth (MHB, Becton Dickinson Difco, Franklin Lakes, NJ) and on Tryptic Soy Agar (TSA; Oxoid Ltd., Hampshire, UK). In all the experiments, bacteria were inoculated and grown overnight in MHB at 37 °C. The next day, bacteria were transferred to a fresh MHB tube and grown to mid-logarithmic phase.

Peptides. Expression and isolation of recombinant peptides was carried out as previously described [5] with the only exception of a final gel-filtration step, that was added in order to remove salts used along the purification process and that tend to attach to the peptides, as previously reported [11]. CATH-2 and (ri)-r(P)ApoB$_S^{Pro}$ peptides were obtained from CPC Scientific Inc. (Sunnyvale, USA) and CASLO ApS (Kongens Lyngby, Denmark), respectively.

Antimicrobial activity. The antimicrobial activity of ApoB-derived peptides was assayed on a panel of skin pathogens, such as *S. epidermidis* ATCC 35984, *S. aureus* ATCC 12600, *S. aureus* ATCC 29213, *A. baumannii* ATCC 19606, *K. pneumoniae* ATCC 70603 and *P. aeruginosa* PAO1 by using broth microdilution method [12]. Bacteria were grown to mid-logarithmic phase in MHB at 37 °C. Then, cells have been diluted to 4×10^6 CFU/mL in Difco 0.5X Nutrient Broth (Becton-Dickenson, Franklin Lakes, NJ) and mixed 1:1 v/v with two-fold serial dilutions peptides (0-40 µmol L^{-1}). Following over-night incubation, each sample was diluted, plated on TSA and incubated at 37 °C for 24 h to count the number of colonies. All the experiments were carried out in three independent replicates.

DiSC$_3$(5) assay. A cytoplasmic membrane depolarization assay was performed on *S. epidermidis* ATCC 35984, *S. aureus* ATCC 12600, *S. aureus* ATCC 29213, *A. baumannii* ATCC 19606 and *K. pneumoniae* ATCC 70603 using the membrane potential-sensitive dye 3,3'-dipropylthiadicarbocyanine iodide (diSC$_3$-5 - TCI America) [13].

Bacterial cells in the mid-logarithmic phase were washed and resuspended in 5 mmol L^{-1} HEPES buffer (pH 7.2) containing 20 mmol L^{-1} glucose and 0.1 mol L^{-1} KCl at a density corresponding to an optical value at 600 nm of 0.06-0.03. Cell suspension was incubated with 1 µmol L^{-1} $DiSC_3(5)$ for 45 min to stabilize the fluorescence, and then the peptides were added to bacterial suspensions at concentrations corresponding to their MIC_{100} values. Changes in fluorescence intensity were continuously recorded by using GloMax® Discover System (Promega, Madison, Wisconsin, USA), with excitation and emission wavelengths of 620 nm and 670 nm, respectively. Cytoplasmic membrane depolarization assays were independently performed three times.

Checkerboard assay and definition of fractional inhibitory concentration (FIC) index. Combinations of ApoB-derived peptides and antimicrobial agents were tested on *S. epidermidis* ATCC 35984, *S. aureus* ATCC 12600, *A. baumannii* ATCC 19606, *K. pneumoniae* ATCC 70603 by the so-called "checkboard" assay to determine Fractional Inhibitory Concentration (FIC) indexes. To this purpose, two-fold serial dilutions of each peptide were tested in combination with two-fold serial dilutions of EDTA or antibiotics widely used in topical formulations, *i.e* vancomycin, erythromycin, colistin, polymyxin B, fusidic acid, clindamycin, gentamicin, and benzoyl peroxide. The FIC indexes were calculated as follows: $FIC_A + FIC_B$, where $FIC_A = \frac{MIC_{100} \text{ of drug A in combination}}{MIC_{100} \text{ of drug A alone}}$, and $FIC_B = \frac{MIC_{100} \text{ of drug B in combination}}{MIC_{100} \text{ of drug B alone}}$. FIC indexes ≤ 0.5 were classified as synergism, FIC indexes between 0.5 and 1 or 1 and 4 were associated with additive and indifferent effects, respectively [5].

Scanning electron microscopy analyses. To perform scanning electron microscopy (SEM) analyses, *K. pneumoniae* ATCC 70603 (2×10^8 CFU/mL) was incubated with 0.58 µmol L^{-1} $r(P)ApoB_S^{Pro}$ in combination with 0.36 µmol mL^{-1} colistin for 3 h at 37 °C. Following incubation, bacterial cells were centrifuged at 10,000 rpm at 4 °C and fixed in 2.5% glutaraldehyde. Following over-night incubation, the samples were washed three times in distilled water (dH_2O) and dehydrated with a graded ethanol series: 25% ethanol (1 × 10 min); 50% ethanol (1 × 10 min); 75% ethanol (1 × 10 min); 95% ethanol (1 × 10 min); 100% anhydrous ethanol (3 × 30 min). Bacterial cells deposited into glass substrate were first sputter-coated with a thin layer of Au-Pd (Sputter Coater Denton Vacuum DeskV) to allow subsequent

morphological characterization using a FEI Nova NanoSEM 450 at an accelerating voltage of 5 kV with Everhart Thornley Detector (ETD) and Through Lens Detector (TLD) at high magnification.

Killing kinetic studies. To kinetically analyze bacterial killing by combinations of ApoB-derived peptides and conventional antibiotics, as colistin and polymyxin B, experiments were performed on *K. pneumoniae* ATCC 70603 treated with a combination of both antimicrobials or with the single agents at concentrations corresponding to their MIC_{100} values. Bacterial cells were diluted to 4×10^6 CFU/mL in Difco 0.5X Nutrient Broth and mixed 1:1 v/v with the peptide, the antibiotic or both. At defined time intervals, samples were serially diluted, and each dilution was plated on tryptic soy agar. Following an incubation of 20 h at 37°C, colonies were counted.

Bacterial resistance development assay. *S. epidermidis* ATCC 35984 and *A. baumannii* ATCC 19606 bacterial strains were subjected to a prolonged exposure to colistin, gentamicin, $r(P)ApoB_L^{Pro}$, $r(P)ApoB_L^{Ala}$ or $r(P)ApoB_S^{Pro}$. Antimicrobial assays were then performed as previously described [12]. Following treatment with peptide or antibiotic, bacterial cells, corresponding to treatment with sub-MIC concentrations of peptide or antibiotic, were collected and subjected to a further treatment over time. Strains that developed resistance to antibiotics were isolated and stored to be characterized.

Anti-biofilm activity assays. Anti-biofilm activity assays were performed on *S. epidermidis* ATCC 35984, *S. aureus* ATCC 12600, *A. baumannii* ATCC 19606, and *K. pneumoniae* ATCC 70603. Bacteria were grown over-night at 37 °C and then diluted to 4×10^8 CFU/mL in 0.5x MHB medium. Incubations with increasing concentrations of each peptide (0-40 µmol L^{-1}) were carried out either for 4 h, in order to test peptide effects on cells attachment, or for 24 h, in order to test peptide effects on biofilm formation, as previously described [5]. When the effects of peptides on preformed biofilm were evaluated, bacterial biofilm was formed for 24 h at 37 °C, and then treated with peptides under test. In the case of crystal violet assays, bacterial biofilm was washed with phosphate buffer (PBS 1X) and then incubated with the dye (0.04%) for 20 min at room temperature. At the end of the incubation, samples were washed with PBS and then the dye bound to cells was dissolved in acetic acid 33%. Spectrophotometric analyses were then carried out at a wavelength of 600 nm. Confocal laser scanning microscopy analyses in static conditions were performed by

using Thermo Scientific™ Nunc™ Lab-Tek™ Chambered Coverglass systems (Thermo Fisher Scientific, Waltham, MA, USA). The viability of the cells embedded into biofilm structure was evaluated by sample staining with LIVE/DEAD® Bacterial Viability kit (Molecular Probes Thermo Fisher Scientific, Waltham, MA, USA). Staining was performed accordingly to manufacturer instructions. Biofilm images were captured by using a confocal laser scanning microscope (Zeiss LSM 710, Zeiss, Germany) and a 63X objective oil-immersion system. Biofilm architecture was analyzed by using the Zen Lite 2.3 software package. Each experiment was performed in triplicate. All images were taken under identical conditions.

3. Results

Antimicrobial properties of ApoB-derived peptides

Plasma lipoproteins or apolipoproteins, such as human apolipoprotein B (ApoB-100), are water-soluble complexes composed of lipids and one or more proteins [14]. The concentration of ApoB in normal plasma is approximately 1.1 mg mL^{-1} [15]. Plasma ApoB, in addition to its physiological role, seems to play an important role in bacterial neutralization [16]. By an algorithmic approach using physicochemical features as a scoring function [17], encrypted peptides within the sequence of ApoB (amino acids 882-929) were identified **(Figure 1A)**. According to the amino acid composition of two ApoB-100 isoforms and their corresponding computational scores associated to the protein sequence, we recombinantly produced in *Escherichia coli* cells three versions of the encrypted peptide identified in human ApoB-100 [r(P)$ApoB_L^{Pro}$, r(P)$ApoB_S^{Pro}$ and r(P)$ApoB_L^{Ala}$]. The sequences present a Pro residue at the N-terminal extremity because of the excision method used where peptides were released after the acidic cleavage of an Asp-Pro bond [5][8][18][11][6]. The ApoB peptide variants were labeled with Pro and Ala indicating the amino acid residue in position 7, which is the mutation that differentiates the two isoforms. The labels L and S indicate a longer or a shorter version of the same amino acid sequence identified and corresponding to the relative and absolute scores, respectively, generated by the algorithm [5].

Firstly, we assessed the antimicrobial activity of ApoB-derived peptides against the following bacterial pathogens: *S. epidermidis* ATCC 35984, *S. aureus* ATCC 12600, *A. baumannii* ATCC 17878, and *K. pneumoniae* ATCC 70603, using broth microdilution assays [12] to determine the minimal inhibitory concentration (MIC) values. The peptides were found to exert significant antibacterial effects (MIC_{100}

values ranging from 2.5 to 20 μmol L^{-1}) against all the bacterial strains tested. In particular, *S. epidermidis* ATCC 35984, and *S. aureus* ATCC 12600 were found to be susceptible to the encrypted peptides at 10 - 20 μmol L^{-1}. The peptides were even more active against *A. baumannii* ATCC 17878 and *K. pneumoniae* ATCC 70603 with MIC_{100} values ranging from 2.5 to 5 μmol L^{-1}, thus indicating the increased ability of the peptides to target Gram-negative bacteria **(Figure 1B)**.

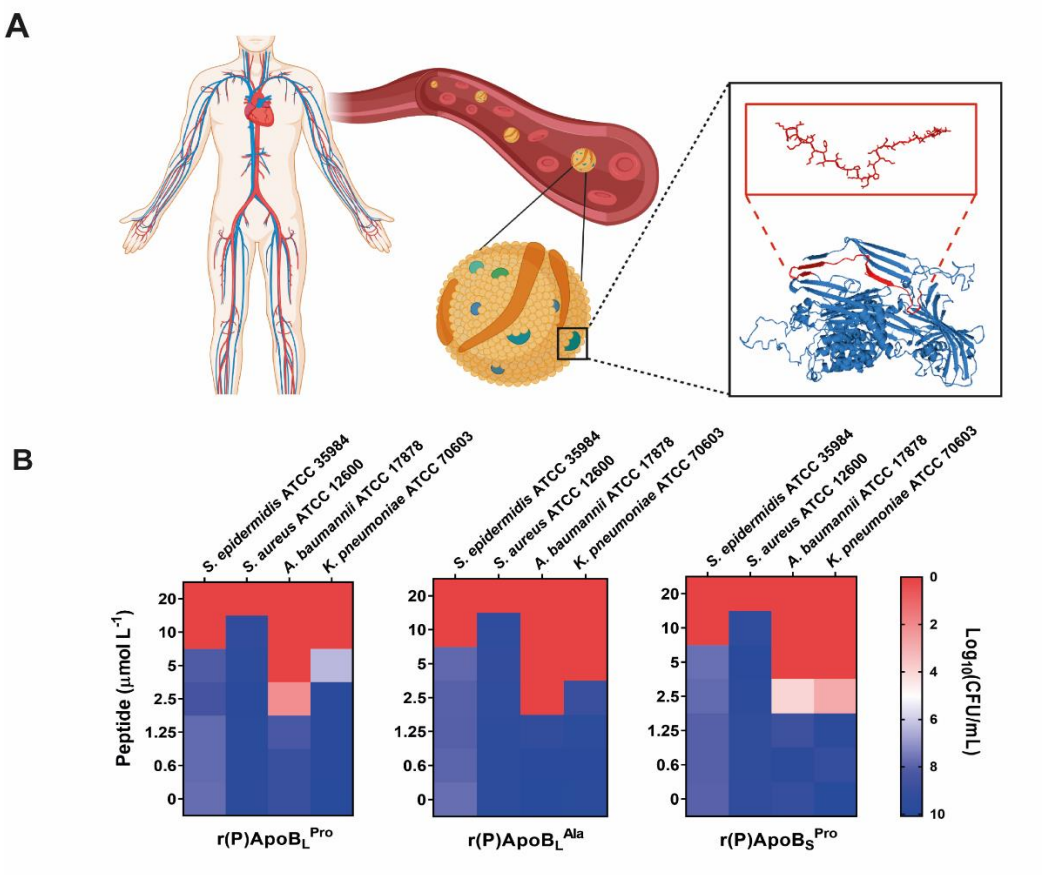

Figure 1. Antimicrobial activity of ApoB-derived peptides. (A) Schematic representation of the proteolytic release of ApoB-derived peptides from precursor human plasma apolipoprotein B. **(B)** Antimicrobial activity of ApoB-derived peptides against four bacterial strains; reported data refer to assays performed in triplicate and heat maps show averaged log (CFU mL^{-1}) values.

To gain insights into the antibacterial mechanism of action of ApoB-derived peptides, we evaluated their ability to depolarize bacterial membranes by using the voltage-sensitive dye $DiSC_3(5)$ in the presence of live bacterial cells. $DiSC_3(5)$ is a cationic membrane-

permeable fluorescent dye that penetrates lipid bilayers and accumulates in polarized cells [19]. The aggregation of $DiSC_3(5)$ molecules led to a fluorescence quenching effect, lasting about 45 min in our experiments. Upon membrane depolarization, the dye molecules are rapidly released because of their cationic nature, leading to increased fluorescence intensity [13]. CATH-2 peptide was used as a positive control, since it is known to exert antimicrobial activity by depolarizing bacterial cytoplasmic membranes [20][21]. We demonstrated that, upon treatment of bacteria with ApoB-derived peptides in the presence of the voltage-sensitive dye $DiSC_3(5)$, an increase in fluorescence intensity indicating depolarization of the bacterial membrane was observed for all the pathogens tested **(Figure 2)**. Hence, our data demonstrate that the peptides induced membrane depolarization, thus leading to variations in electrochemical potential and eventually to cell death.

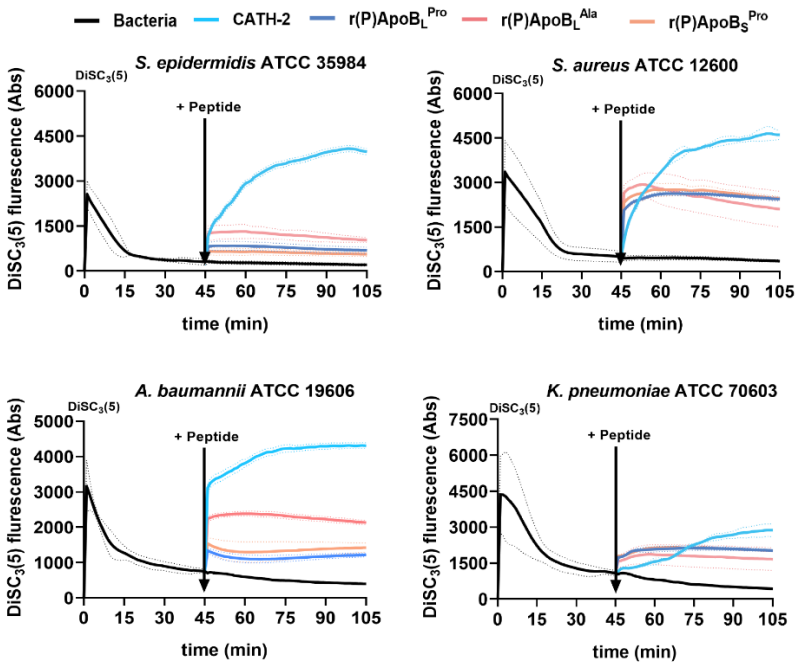

Figure 2. Mechanism of action. Analysis of fluorescence intensity variation upon bacterial treatment with ApoB-derived peptides and CATH-2 peptide (positive control) in the presence of $DiSC_3(5)$ dye.

We also assessed the ability of ApoB-derived peptides to potentiate the activity of conventional antibiotics *via* synergistic interactions. Indeed, through synergistic or additive interactions, it is possible to significantly reduce the therapeutic doses of antimicrobial agents, thus minimizing

undesired side effects, such as the selection of resistance phenotypes [22][23]. To assess this phenomenon, we performed checkerboard assays and determined the Fractional Inhibitory Concentration (FIC) index in each case [24]. Firstly, we determined the antimicrobial activity of each peptide when used as a monotherapy **(Figure 3A)**. Checkerboard assays revealed widespread additive or partial synergistic effects (0.5>FIC index>1; light purple color in **Figure 3B**) when peptides were combined with conventional antimicrobials, such as vancomycin, erythromycin, gentamicin, clindamycin and EDTA. Importantly, peptides r(P)ApoB$_L^{Pro}$ and r(P)ApoB$_S^{Pro}$ synergized with the LPS binders polymyxin B and colistin against the Gram-negative pathogen *K. pneumoniae* ATCC 70603 (FIC index ≤0.5; purple signals in **Figure 3C**), thus significantly reducing the doses of both peptide and antibiotic needed to eradicate infections associated with this bacterium. Interestingly, synergistic effects were detected when ApoB-derived peptides were tested in combination with antibiotics active on bacterial membranes (*e.g.*, polymyxin B and colistin), whereas additive interactions were observed for combinations with antibiotics inhibiting protein synthesis (*e.g.*, erythromycin, clindamycin and gentamicin) and targeting the bacterial cell wall (*e.g.*, vancomycin). r(P)ApoB$_S^{Pro}$ was found to potentiate the activity of almost every antibiotic selected, thus highlighting its potentiality for the future development of therapeutic options .

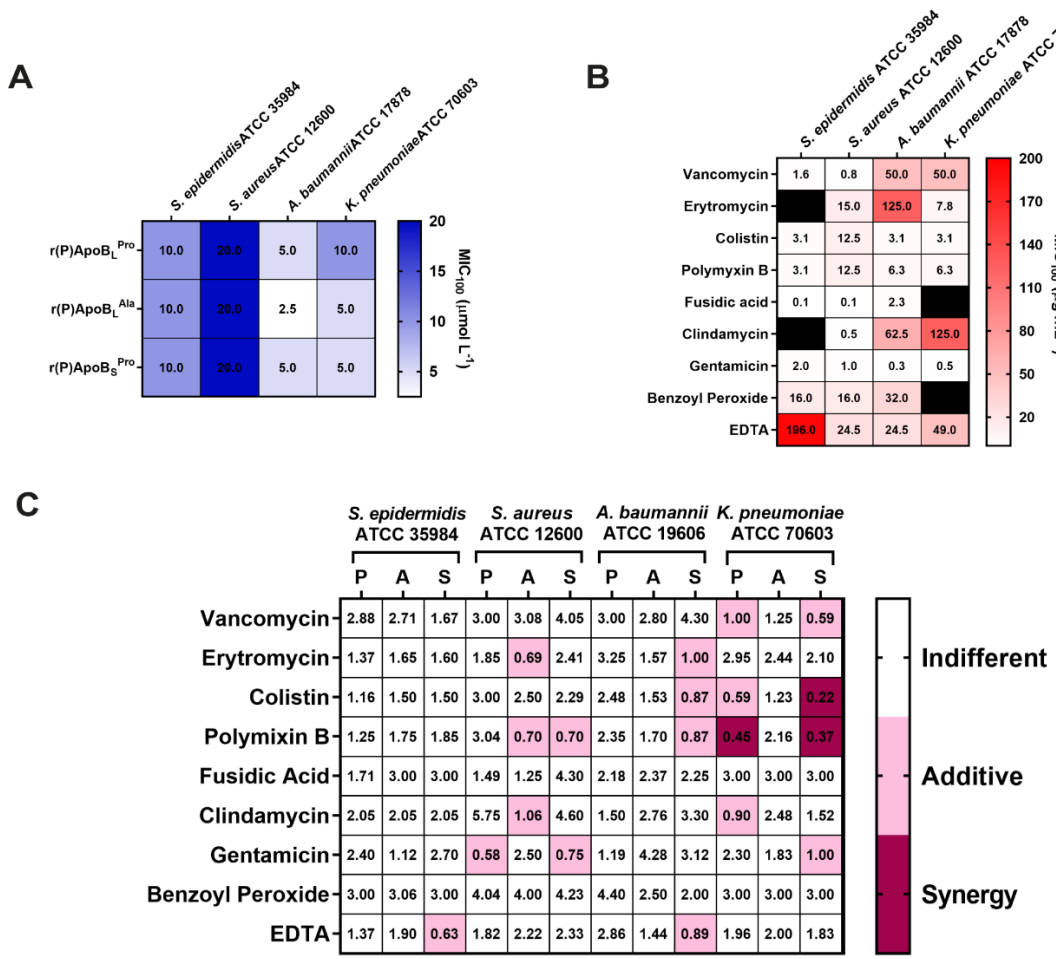

Figure 3. Antimicrobial effects of ApoB-derived peptides alone or in combinations. Antimicrobial activity of **(A)** ApoB-derived peptides and **(B)** conventional antimicrobial agents against *S. epidermidis* ATCC 35984, *S. aureus* ATCC 12600, *A. baumannii* ATCC 17878 and *K. pneumoniae* ATCC 70603 strains. Black cells indicate bacterial resistance. **(C)** Synergistic interactions (expressed as FIC values) of each peptide in combination with conventional antimicrobials against four bacterial strains. In the heat map, synergistic effects are reported in purple, additive effects in light purple and indifferent interactions in white.

The synergistic effects between ApoB-derived peptides and conventional antibiotics were further confirmed by changes in cell morphology observed by scanning electron microscopy (SEM) assays

(Figure 4). Combinations of r(P)ApoB$_S^{Pro}$ (0.093xMIC$_{100}$ = 0.46 µmol L^{-1}) and colistin (0.127xMIC$_{100}$ = 0.34 µmol L^{-1}) altered the morphology of *K. pneumoniae* ATCC 70603 and substantially decreased bacterial viability **(Figure 4)** when tested at concentrations found to be ineffective when each agent was administered alone **(Figure 4)**.

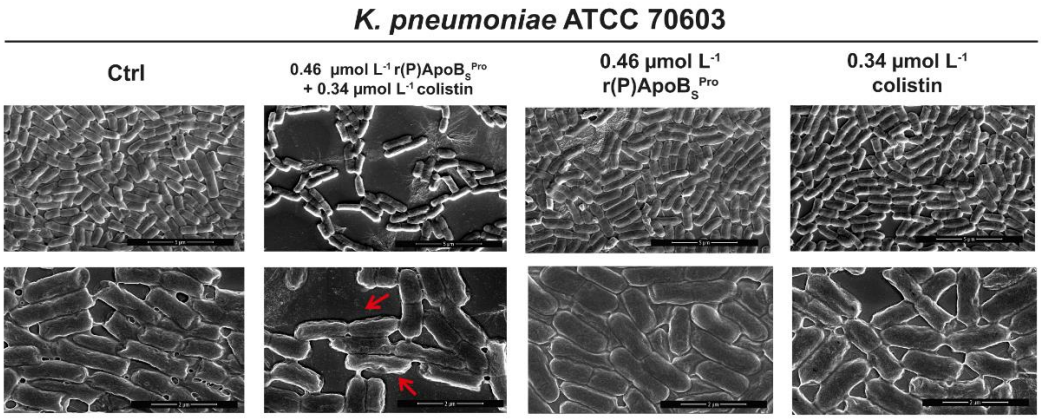

Figure 4. Morphological analyses by SEM. Antimicrobial effects of r(P)ApoB$_S^{Pro}$ peptide in combinations with colistin on *K. pneumoniae* ATCC70603. Red arrows indicate morphological alterations of bacterial membranes caused by peptide treatment.

We also performed kinetic analyses to evaluate the efficacy over time of the most promising combinations of antimicrobials. A longer exposure to antimicrobials is generally associated with an increased likelihood of selecting for bacterial resistance [25]. Kinetic killing curves were obtained by concomitantly treating bacteria with combinations of ApoB-derived peptides and colistin or polymyxin B. Again, significant antimicrobial effects were observed at concentrations much lower than those required when these agents were administered alone **(Figure 5)**. In addition, combination therapy killed bacteria much more rapidly (10 min) than in monotherapy (60 or 180 min) **(Figure 5)**.

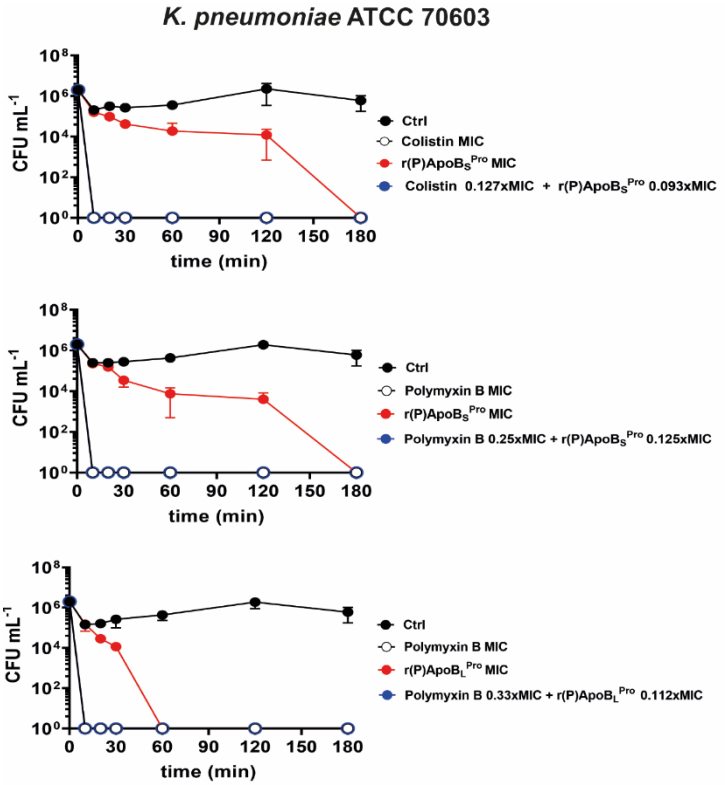

Figure 5. Time killing curves obtained by incubating *K. pneumoniae* ATCC 70603 with the lead combinations of ApoB-derived peptides and antibiotics; curves have been compared with those obtained by incubating cells with single agents at bactericidal concentrations. Data represent the mean (±standard deviation, SD) of three independent experiments.

We also performed experiments to assess whether prolonged exposure to ApoB-derived peptides led to the evolution of resistance phenotypes, since it is known that classical AMPs are less likely to trigger bacterial resistance than standard antibiotics [26]. *A. baumannii* ATCC 17878 and *S. epidermidis* ATCC 35984 were selected as representatives of Gram-negative and Gram-positive organisms, respectively. They were longitudinally treated with r(P)ApoB$_L^{Pro}$, r(P)ApoB$_L^{Ala}$ and r(P)ApoB$_S^{Pro}$. Control sample groups were treated with the antibiotics colistin and gentamicin, selected on the basis of their distinct mechanisms of action, the former destabilizing the bacterial extracellular membrane and the latter acting on intracellular targets. *A. baumannii* cells acquired resistance to colistin after one day of treatment. After seven days of treatment with colistin, the MIC_{100} of this antibiotic against *A. baumannii*

increased from 3.12 to 25 μg mL^{-1} (2.7 to 21.6 μmol mL^{-1}). On the other hand, the MIC_{100} of gentamicin and ApoB-derived peptides did not change over the seven-day-long experiment, thus indicating that *A. baumannii* did not develop resistance mechanisms against these agents. Conversely, when *S. epidermidis* cells were exposed to gentamicin, MIC_{100} values increased from 2 to 8 μg mL^{-1} (1.3 to 5.2 μmol mL^{-1}). No resistance development was observed for *S. epidermidis* throughout the experiment when treated with ApoB-derived peptides or colistin **(Figure 6A)**. *A. baumannii* resistance towards colistin increased by up to 10-fold, whereas *S. epidermidis* resistance to gentamicin increased by up to 4-fold **(Figure 6A)**. Importantly, neither *A. baumannii* nor *S. epidermidis* developed resistance to the encrypted peptides, thus underlining their promise. SEM results also revealed that those strains that evolved resistance during the experiment displayed different morphologies than the original antibiotic-susceptible bacteria. For example, both colistin-resistant *A. baumannii* ATCC 17878 and gentamicin-resistant *S. epidermidis* ATCC 35984 presented wrinkled borders as opposed to the smooth colonies of bacteria at the beginning of the experiment **(Figure 6B)**.

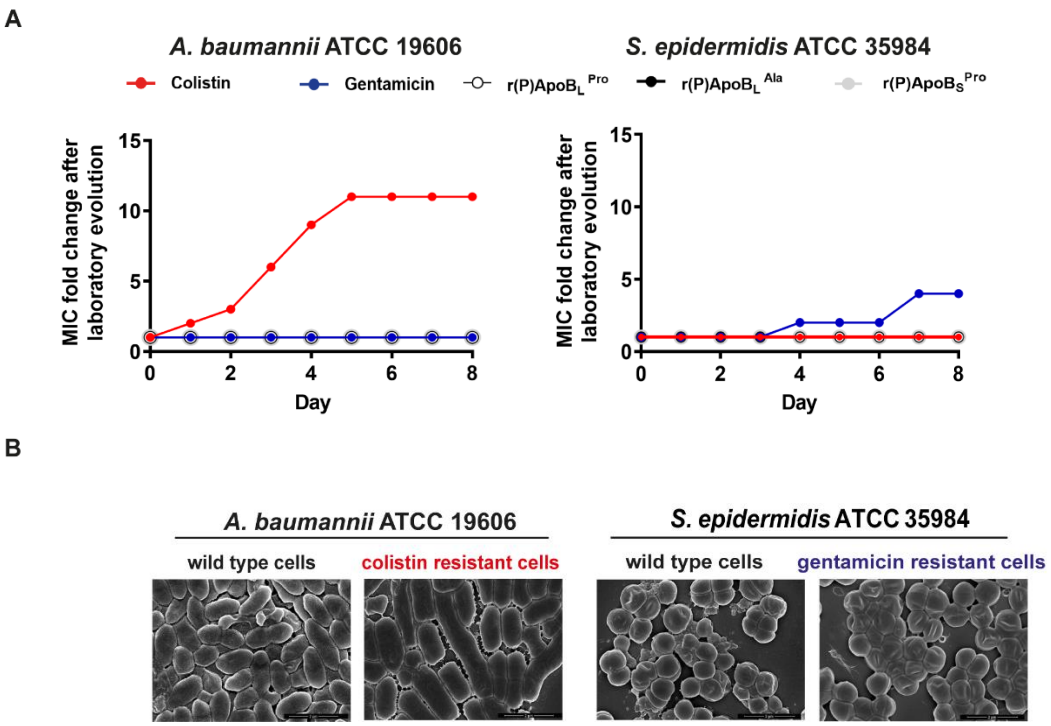

Figure 6. Resistance development studies. (A) Evaluation of resistance phenotype development upon prolonged treatment of *A. baumannii* ATCC 17878 and *S. epidermidis* ATCC 35984 with colistin, gentamicin, r(P)ApoB$_L^{Pro}$, r(P)ApoB$_L^{Ala}$ and r(P)ApoB$_S^{Pro}$. **(B)** Morphological analyses of wild-type and selected resistant *A. baumannii* ATCC 17878 and *S. epidermidis* ATCC 35984 strains by SEM.

Effects of ApoB-derived peptides on biofilm adhesion and formation

To verify whether ApoB-derived peptides aree able to prevent biofilm formation of common skin bacterial pathogens, such as *S. epidermidis* ATCC 35984, *S. aureus* ATCC 12600, *A. baumannii* ATCC 17878 and *K. pneumoniae* ATCC 70603, we firstly performed crystal violet assays. By this way, the effects of peptides on the three main stages of biofilm development, *i.e*. adhesion, formation and detachment [27], were analyzed. Sub-MIC$_{100}$ peptide concentrations, ranging from 1.25 to 5 μmol mL^{-1}, led to significant inhibition (30-40%) of biofilm adhesion and formation of Gram-negative strains *A. baumannii* ATCC 17878 and *K. pneumoniae* ATCC 70603, and of Gram-positive bacterium *S. epidermidis* ATCC 35984. Conversely, no significant effects were detected against *S. aureus* ATCC 12600 **(Figure 7)**.

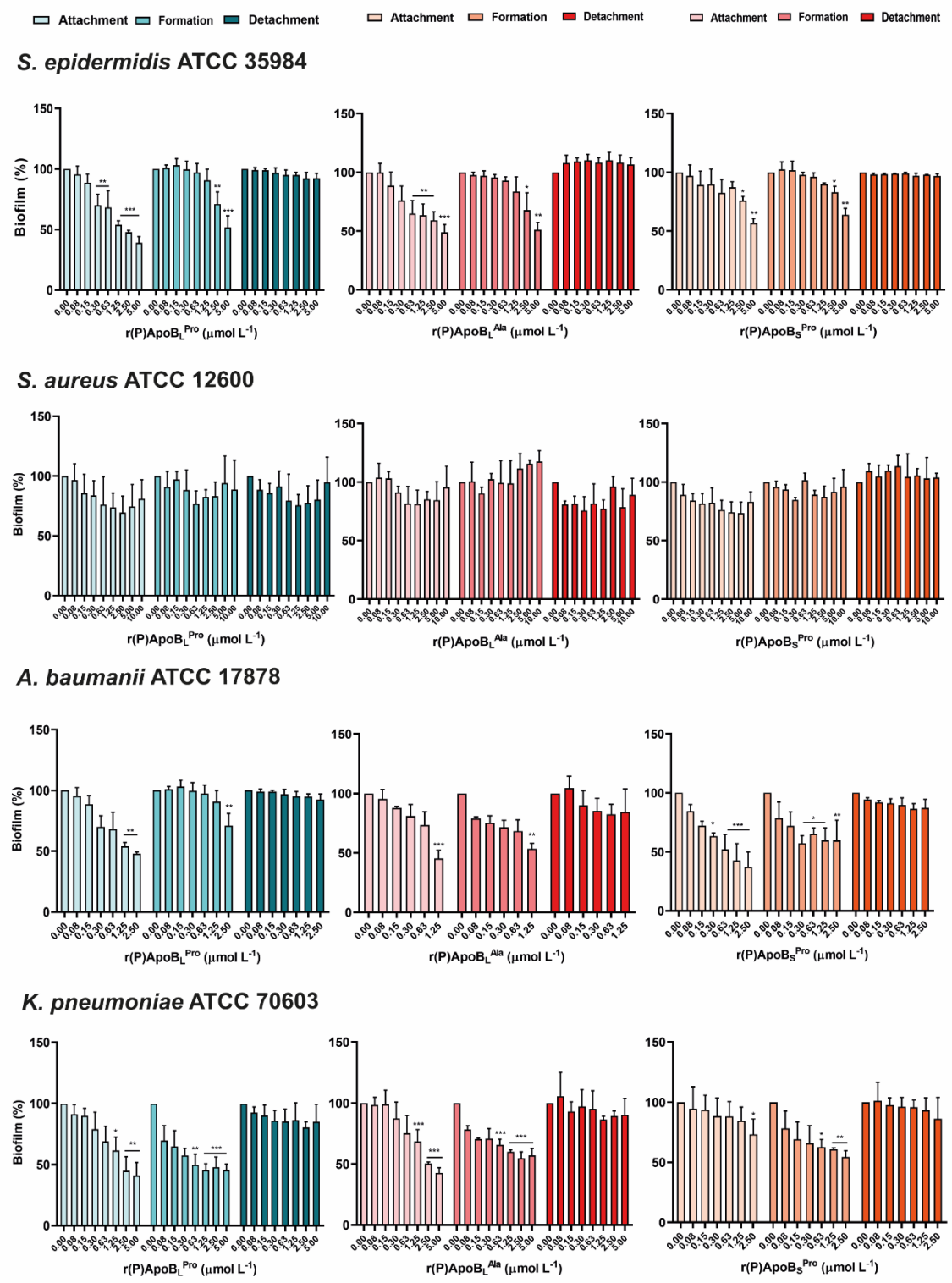
Attachment
Formation
Detachment
S. epidermidis ATCC 35984
S. aureus ATCC 12600
A. baumanii ATCC 17878
K. pneumoniae ATCC 70603
Biofilm (%)
r(P)ApoB_L^Pro (μmol L^-1)
r(P)ApoB_L^Ala (μmol L^-1)
r(P)ApoB_S^Pro (μmol L^-1)

Figure 7. Antibiofilm activity of ApoB-derived peptides. Anti-biofilm activity of ApoB-derived peptides on *S. epidermidis* ATCC 35984, *S. aureus* ATCC 12600, *A. baumannii* ATCC 17878 and *K. pneumoniae* ATCC 70603 strains. The effects of increasing concentrations of r(P)ApoB$_L^{Pro}$ (blue), r(P)ApoB$_L^{Ala}$ (pink), and r(P)ApoB$_S^{Pro}$ (orange) peptides were evaluated on cells attachment, biofilm formation, or on preformed biofilm. Biofilm was stained with crystal violet and measured at 600 nm. Data represent the mean (±standard deviation, SD) of at least three independent experiments, each one carried out with triplicate determinations. Significant differences were indicated as *(P<0.05), **(P<0.01), ***(P<0.001) for treated *versus* control samples.

Afterwards, we performed confocal laser scanning microscopy (CLSM) analyses to assess the effects of each peptide against *A. baumannii* ATCC 17878 and *S. epidermidis* ATCC 35984. The peptides significantly altered biofilm architecture and reduced biofilm biovolume in the case of both strains. Peptide r(P)ApoB$_L^{Pro}$ was found to exert the strongest effect (biovolume reduced by 3-fold compared to the untreated control) on *A. baumannii* ATCC 17878 biofilm attachment, whereas r(P)ApoB$_L^{Ala}$ and r(P)ApoB$_S^{Pro}$ triggered cell filamentation in *A. baumannii*, thus suggesting they might interfere with cell division mechanisms by blocking septation [8], in agreement with the high percentage of dead cells observed **(Figure 8A)**. No significant anti-biofilm effects for any of the peptides were observed on *A. baumannii* biofilm formation **(Figure 8A)**. The three ApoB-derived peptides disrupted the biofilm matrix and reduced biofilm biovolume of *S. epidermidis* ATCC 35984 at sub-MIC$_{100}$ concentrations (5 μmol mL^{-1}). Peptides r(P)ApoB$_L^{Pro}$ and r(P)ApoB$_L^{Ala}$ further affected biofilm formation by inducing cell death (*i.e.*, red cell aggregates in **Figure 8B**). Overall, our data suggest that ApoB-derived peptides exert their anti-biofilm activity against *S. epidermidis* ATCC 35984 through multiple mechanisms **(Figure 8B)**.

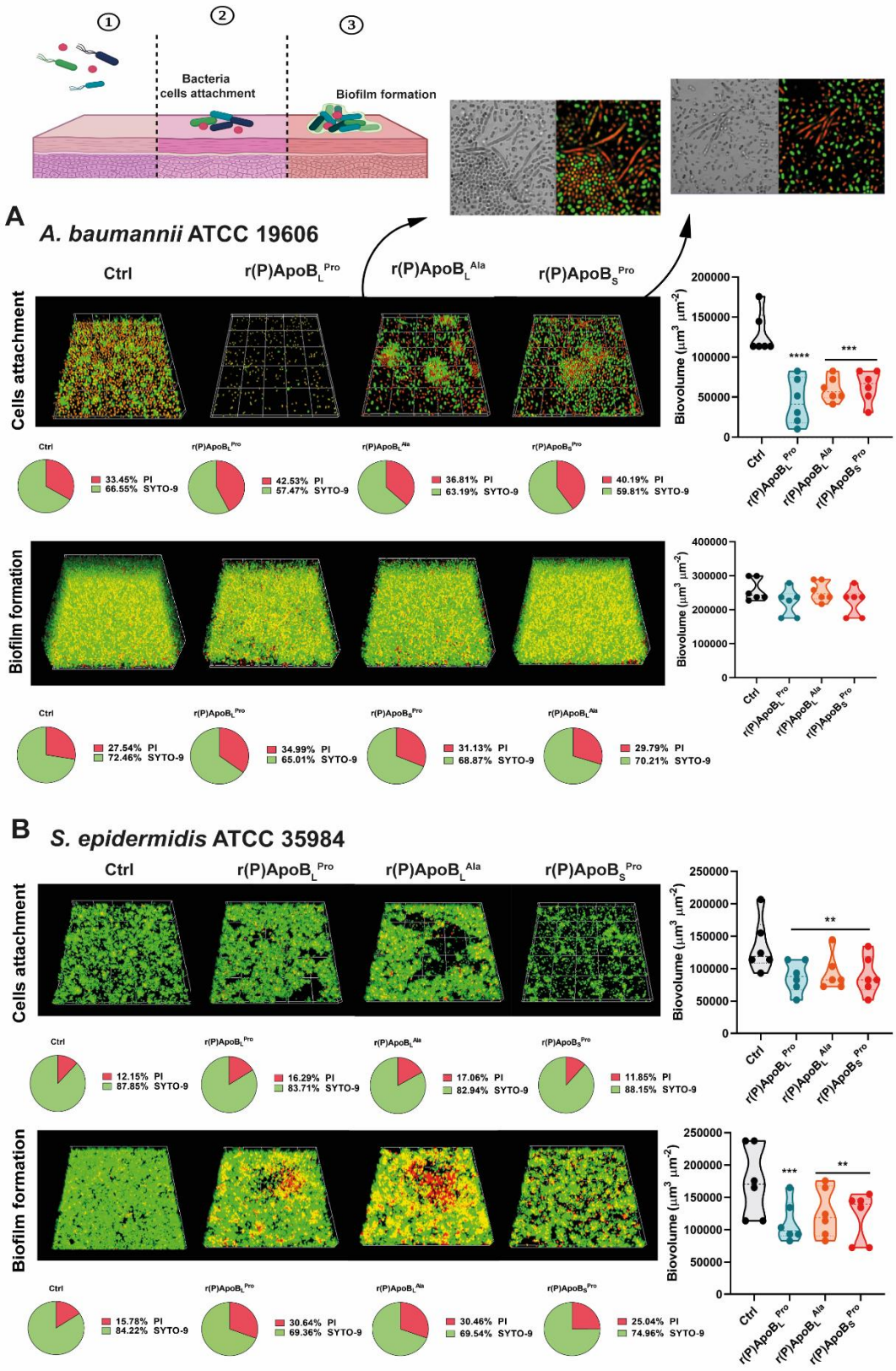
1
2
3
Bacteria cells attachment
Biofilm formation
A
A. baumannii ATCC 19606
Ctrl
r(P)ApoB$_L^{Pro}$
r(P)ApoB$_L^{Ala}$
r(P)ApoB$_S^{Pro}$
Cells attachment
Biofilm formation
33.45% PI
66.55% SYTO-9
42.53% PI
57.47% SYTO-9
36.81% PI
63.19% SYTO-9
40.19% PI
59.81% SYTO-9
27.54% PI
72.46% SYTO-9
34.99% PI
65.01% SYTO-9
31.13% PI
68.87% SYTO-9
29.79% PI
70.21% SYTO-9
Biovolume (µm^3 µm^{-2})
****
***
B
S. epidermidis ATCC 35984
12.15% PI
87.85% SYTO-9
16.29% PI
83.71% SYTO-9
17.06% PI
82.94% SYTO-9
11.85% PI
88.15% SYTO-9
15.78% PI
84.22% SYTO-9
30.64% PI
69.36% SYTO-9
30.46% PI
69.54% SYTO-9
25.04% PI
74.96% SYTO-9
**

Fig. 3. Antibiofilm activity of ApoB-derived peptides. Schematic representation of two stages of bacterial biofilm development. Effects of ApoB-derived peptides on cells attachment and biofilm formation in the case of **(A)** *A. baumannii* ATCC17878 and **(B)** *S. epidermidis* ATCC35984 by CLSM imaging. Biofilm cells were stained by LIVE/DEAD BacLight bacterial viability kit (Molecular Probes, Eugene, OR) containing a 1:1 ratio of SYTO-9 (green fluorescence, all cells) and propidium iodide (PI; red fluorescence, dead cells). Two dimensional structures of the biofilms were obtained by confocal z-stack using Zen Lite 2.3 software. All the images were taken under identical conditions. Biovolume (μm^3 μm^{-2}) and fluorescence intensity were calculated by using Zen Lite 2.3 software. Significant differences were indicated as (*P<0.05), (***P<0.001) or (****P<0.0001) for treated *versus* control samples, each experiment was carried out in triplicate.

4. Discussion

Numerous proteins encoding encrypted peptides with biological functions that are unrelated to those of the parent protein have been recently found throughout the human body, thus opening new avenues for antibiotic discovery [7]. Encrypted peptides represent an underexplored source of novel antimicrobials [3]. Here, we characterized in detail the antimicrobial, antibiofilm, and the resistance development of encrypted peptides identified *via* an algorithmic approach, in the human apolipoprotein B-100 (residues 887–922) [5]. The antimicrobial activity of these peptides (2.5-20 µmol L^{-1}) is similar to that of another peptide identified in human apolipoprotein E [4] and other antimicrobial peptides, such as TsAP-2, HM2 & HM5, ranalexin and stylisin 2 [28].

We demonstrate that ApoB-derived peptides target bacteria by rapidly depolarizing the cytoplasmic membrane, a mechanism that is shared with other peptides including several cathelicidins, melittin and the ion channel-forming gramicidin D [29][30][31]. We also show that the peptides potentiate the activity of conventional antibiotics against bacteria [23], thus revealing a role for these agents as adjuvants in conjunction with classical therapies. Importantly, contrary to existing antibiotics, the encrypted peptides did not readily select for bacterial resistance in the experimental conditions tested.

The encrypted peptides displayed significant anti-biofilm activity against a range of pathogenic strains, including those responsible for numerous skin infections [32][33]. The peptides reduced biofilm biovolume, altered biofilm architecture, and induced cell death. Hence, the anti-

biofilm activity of these molecules is comparable to that of human hepcidin 20, an AMP secreted by hepatocytes that, at concentrations ranging from 3.15 to 25 µmol L^{-1}, is capable of reducing the extracellular matrix mass, altering biofilm architecture, and targeting polysaccharide intercellular adhesin in *S. epidermidis* [34]. These results are significant as biofilms display increased resistance to antibiotic treatment and are associated with numerous human infections [35][36]. We provide experimental evidence that these peptides exhibit antimicrobial and anti-biofilm properties, target bacteria by depolarizing their cytoplasmic membrane, and potentiate the activity of conventional antibiotics. Importantly, these peptides do not select for bacterial resistance mechanisms, which traditionally hinder antibiotic efficacy.

5. References

[1] S. Santajit and N. Indrawattana, “Mechanisms of Antimicrobial Resistance in ESKAPE Pathogens,” *Biomed Res. Int.*, vol. 2016, pp. 1–8, 2016, doi: 10.1155/2016/2475067.

[2] M. S. Mulani, E. E. Kamble, S. N. Kumkar, M. S. Tawre, and K. R. Pardesi, “Emerging Strategies to Combat ESKAPE Pathogens in the Era of Antimicrobial Resistance: A Review.,” *Front. Microbiol.*, vol. 10, p. 539, Apr. 2019, doi: 10.3389/fmicb.2019.00539.

[3] A. Pfalzgraff, K. Brandenburg, and G. Weindl, “Antimicrobial Peptides and Their Therapeutic Potential for Bacterial Skin Infections and Wounds,” *Front. Pharmacol.*, vol. 9, Mar. 2018, doi: 10.3389/fphar.2018.00281.

[4] K. Pane *et al.*, “A new cryptic cationic antimicrobial peptide from human apolipoprotein E with antibacterial activity and immunomodulatory effects on human cells,” *FEBS J.*, vol. 283, no. 11, pp. 2115–2131, Jun. 2016, doi: 10.1111/febs.13725.

[5] R. Gaglione *et al.*, “Novel human bioactive peptides identified in Apolipoprotein B: Evaluation of their therapeutic potential,” *Biochem. Pharmacol.*, vol. 130, pp. 34–50, Apr. 2017, doi: 10.1016/j.bcp.2017.01.009.

[6] R. Gaglione, E. Pizzo, E. Notomista, C. de la Fuente-Nunez, and A. Arciello, “Host Defence Cryptides from Human Apolipoproteins: Applications in Medicinal Chemistry,” *Curr. Top. Med. Chem.*, vol. 20, no. 14, pp. 1324–1337, Jun. 2020, doi: 10.2174/1568026620666200427091454.

[7] D. J. Autelitano, A. Rajic, A. I. Smith, M. C. Berndt, L. L. Ilag, and M. Vadas, “The cryptome: a subset of the proteome, comprising cryptic peptides with distinct bioactivities,” *Drug Discov. Today*, vol. 11, no. 7–8, pp. 306–314, Apr. 2006, doi: 10.1016/j.drudis.2006.02.003.

[8] R. Gaglione *et al.*, “Effects of human antimicrobial cryptides identified in apolipoprotein B depend on specific features of bacterial strains,” *Sci. Rep.*, vol. 9, no. 1, p. 6728, Dec. 2019, doi: 10.1038/s41598-019-43063-3.

[9] M. D. Shapiro and S. Fazio, “Apolipoprotein B-containing lipoproteins and atherosclerotic cardiovascular disease,”

F1000Research, vol. 6, p. 134, Feb. 2017, doi: 10.12688/f1000research.9845.1.

[10] N. Ueki, K. Someya, Y. Matsuo, K. Wakamatsu, and H. Mukai, “Cryptides: Functional cryptic peptides hidden in protein structures,” *Biopolymers*, vol. 88, no. 2, pp. 190–198, 2007, doi: 10.1002/bip.20687.

[11] R. Gaglione *et al.*, “Cost-effective production of recombinant peptides in Escherichia coli,” *N. Biotechnol.*, vol. 51, pp. 39–48, Jul. 2019, doi: 10.1016/j.nbt.2019.02.004.

[12] I. Wiegand, K. Hilpert, and R. E. W. Hancock, “Agar and broth dilution methods to determine the minimal inhibitory concentration (MIC) of antimicrobial substances,” *Nat. Protoc.*, vol. 3, no. 2, pp. 163–175, Feb. 2008, doi: 10.1038/nprot.2007.521.

[13] J. D. te Winkel, D. A. Gray, K. H. Seistrup, L. W. Hamoen, and H. Strahl, “Analysis of Antimicrobial-Triggered Membrane Depolarization Using Voltage Sensitive Dyes,” *Front. Cell Dev. Biol.*, vol. 4, Apr. 2016, doi: 10.3389/fcell.2016.00029.

[14] P. D. Lister, D. J. Wolter, and N. D. Hanson, “Antibacterial-resistant Pseudomonas aeruginosa: clinical impact and complex regulation of chromosomally encoded resistance mechanisms.,” *Clin. Microbiol. Rev.*, vol. 22, no. 4, pp. 582–610, Oct. 2009, doi: 10.1128/CMR.00040-09.

[15] F. K. Welty, A. H. Lichtenstein, P. H. R. Barrett, G. G. Dolnikowski, and E. J. Schaefer, “Human Apolipoprotein (Apo) B-48 and ApoB-100 Kinetics With Stable Isotopes,” *Arterioscler. Thromb. Vasc. Biol.*, vol. 19, no. 12, pp. 2966–2974, Dec. 1999, doi: 10.1161/01.ATV.19.12.2966.

[16] R. Han, “Plasma lipoproteins are important components of the immune system,” *Microbiol. Immunol.*, vol. 54, no. 4, pp. 246–253, Apr. 2010, doi: 10.1111/j.1348-0421.2010.00203.x.

[17] K. Pane *et al.*, “Antimicrobial potency of cationic antimicrobial peptides can be predicted from their amino acid composition: Application to the detection of ‘cryptic’ antimicrobial peptides,” *J. Theor. Biol.*, vol. 419, pp. 254–265, Apr. 2017, doi: 10.1016/j.jtbi.2017.02.012.

[18] R. Gaglione *et al.*, “Cryptides Identified in Human Apolipoprotein

B as New Weapons to Fight Antibiotic Resistance in Cystic Fibrosis Disease," *Int. J. Mol. Sci.*, vol. 21, no. 6, p. 2049, Mar. 2020, doi: 10.3390/ijms21062049.

[19] X. Wu and J. G. Hurdle, "Screening for a Diamond in the Rough," *Chem. Biol.*, vol. 20, no. 9, pp. 1091–1092, Sep. 2013, doi: 10.1016/j.chembiol.2013.09.002.

[20] A. van Dijk *et al.*, "Immunomodulatory and Anti-Inflammatory Activities of Chicken Cathelicidin-2 Derived Peptides," *PLoS One*, vol. 11, no. 2, p. e0147919, Feb. 2016, doi: 10.1371/journal.pone.0147919.

[21] A. van Dijk *et al.*, "Identification of chicken cathelicidin-2 core elements involved in antibacterial and immunomodulatory activities," *Mol. Immunol.*, vol. 46, no. 13, pp. 2465–2473, Aug. 2009, doi: 10.1016/j.molimm.2009.05.019.

[22] M. Berditsch, T. Jäger, N. Strempel, T. Schwartz, J. Overhage, and A. S. Ulrich, "Synergistic Effect of Membrane-Active Peptides Polymyxin B and Gramicidin S on Multidrug-Resistant Strains and Biofilms of Pseudomonas aeruginosa," *Antimicrob. Agents Chemother.*, vol. 59, no. 9, pp. 5288–5296, Sep. 2015, doi: 10.1128/AAC.00682-15.

[23] F. Reffuveille, C. de la Fuente-Núñez, S. Mansour, and R. E. W. Hancock, "A Broad-Spectrum Antibiofilm Peptide Enhances Antibiotic Action against Bacterial Biofilms," *Antimicrob. Agents Chemother.*, vol. 58, no. 9, pp. 5363–5371, Sep. 2014, doi: 10.1128/AAC.03163-14.

[24] K. R. V. Thappeta, Y. S. Vikhe, A. M. H. Yong, M. B. Chan-Park, and K. A. Kline, "Combined Efficacy of an Antimicrobial Cationic Peptide Polymer with Conventional Antibiotics to Combat Multidrug-Resistant Pathogens," *ACS Infect. Dis.*, vol. 6, no. 5, pp. 1228–1237, May 2020, doi: 10.1021/acsinfecdis.0c00016.

[25] H. L. Wilson, K. Daveson, and C. B. Del Mar, "Optimal antimicrobial duration for common bacterial infections," *Aust. Prescr.*, vol. 42, no. 1, p. 5, Feb. 2019, doi: 10.18773/austprescr.2019.001.

[26] B. El Shazely, G. Yu, P. R. Johnston, and J. Rolff, "Resistance Evolution Against Antimicrobial Peptides in Staphylococcus aureus Alters Pharmacodynamics Beyond the MIC," *Front.*

Microbiol., vol. 11, Feb. 2020, doi: 10.3389/fmicb.2020.00103.

[27] M. Crouzet *et al.*, “Exploring early steps in biofilm formation: set-up of an experimental system for molecular studies,” *BMC Microbiol.*, vol. 14, no. 1, p. 253, Dec. 2014, doi: 10.1186/s12866-014-0253-z.

[28] M. Rahnamaeian and A. Vilcinskas, “Short antimicrobial peptides as cosmetic ingredients to deter dermatological pathogens,” *Appl. Microbiol. Biotechnol.*, vol. 99, no. 21, pp. 8847–8855, Nov. 2015, doi: 10.1007/s00253-015-6926-1.

[29] G. Boix-Lemonche, M. Lekka, and B. Skerlavaj, “A Rapid Fluorescence-Based Microplate Assay to Investigate the Interaction of Membrane Active Antimicrobial Peptides with Whole Gram-Positive Bacteria,” *Antibiotics*, vol. 9, no. 2, p. 92, Feb. 2020, doi: 10.3390/antibiotics9020092.

[30] R. N. Murugan *et al.*, “De Novo Design and Synthesis of Ultra-Short Peptidomimetic Antibiotics Having Dual Antimicrobial and Anti-Inflammatory Activities,” *PLoS One*, vol. 8, no. 11, p. e80025, Nov. 2013, doi: 10.1371/journal.pone.0080025.

[31] W. Gao *et al.*, “Identification of a novel cathelicidin antimicrobial peptide from ducks and determination of its functional activity and antibacterial mechanism,” *Sci. Rep.*, vol. 5, no. 1, p. 17260, Dec. 2015, doi: 10.1038/srep17260.

[32] F. Longo, C. Vuotto, and G. Donelli, “Biofilm formation in Acinetobacter baumannii.,” *New Microbiol.*, vol. 37, no. 2, pp. 119–27, Apr. 2014, [Online]. Available: http://www.ncbi.nlm.nih.gov/pubmed/24858639.

[33] C. Calà, E. Amodio, E. Di Carlo, R. Virruso, T. Fasciana, and A. Giammanco, “Biofilm production in Staphylococcus epidermidis strains, isolated from the skin of hospitalized patients: genetic and phenotypic characteristics.,” *New Microbiol.*, vol. 38, no. 4, pp. 521–9, Oct. 2015, [Online]. Available: http://www.ncbi.nlm.nih.gov/pubmed/26485010.

[34] J. A. Perry and G. D. Wright, “Forces shaping the antibiotic resistome.,” *Bioessays*, vol. 36, no. 12, pp. 1179–84, Dec. 2014, doi: 10.1002/bies.201400128.

[35] C. de la Fuente-Núñez, F. Reffuveille, L. Fernández, and R. E. Hancock, “Bacterial biofilm development as a multicellular

adaptation: antibiotic resistance and new therapeutic strategies," *Curr. Opin. Microbiol.*, vol. 16, no. 5, pp. 580–589, Oct. 2013, doi: 10.1016/j.mib.2013.06.013.

[36] C. de la Fuente-Núñez, M. H. Cardoso, E. de Souza Cândido, O. L. Franco, and R. E. W. Hancock, "Synthetic antibiofilm peptides," *Biochim. Biophys. Acta - Biomembr.*, vol. 1858, no. 5, pp. 1061–1069, May 2016, doi: 10.1016/j.bbamem.2015.12.015.

CHAPTER 3.

Biocompatibility assessment of ApoB-derived peptides

Angela Cesaro

Department of Chemical Sciences, PhD in Biotechnology

University of Naples Federico II

Biocompatibility assessment of ApoB-derived peptides

1. Introduction

The adverse drug reactions associated with antimicrobials have become an important and concern topic to be considered. Although the role of an antimicrobial is to kill or prevent the growth of pathogenic agents, these drugs may also impact the host in an injurious manner [1]. Antimicrobial toxicity is induced by different factors and range from transient to life-threatening events, such as seizures or cardiac arrhythmias [2]. Generally, the toxicity occurs when the drug interacts with specific tissues, thus altering physiological pathways, as the aplastic anemia due to the chloramphenicol, the neuromuscular blockade or the nephrotoxicity related to aminoglycoside and the hepatitis caused by the isoniazid. Many of these side effects are based on damage to host mitochondria, which share homology with prokaryote [1]. Instead, other side effects are associated with toxic compounds released upon microbial lysis, as components inducing inflammatory responses [3]. For example, the Jarisch-Herxheimer reaction (JHR) occurs in patients with syphilis treated with penicillin. Causes of inflammation in the JHR are related to spirochetal inflammatory substances including lipoproteins and pyrogens, which promote the release of cytokines [4]. Moreover, peptide-based therapies can induce immune responses and cause allergies, although the peptides are less immunogenic than recombinant proteins and antibodies. Indeed, patients often describe a response as an allergy or hypersensitivity, as adverse drug reactions. In general, the subcutaneous route of administration has the highest risk to induce an immune response, followed by intramuscular, intranasal, and intravenous routes. Immunogenicity of peptides or proteins can potentially affect their efficacy and lead to adverse reactions by inducing secretion of pro-inflammatory cytokines [5]. The effects of peptides on the immune system depend on the physicochemical properties and amino-acid sequence, but their immunogenicity and risk of inducing allergy are difficult to predict without appropriate tests [5].

Topical antimicrobial treatments, particularly of broad-spectrum agents, can also alter resident skin bacterial communities. In fact, cutaneous microbial populations display changes for multiple days post antibiotics treatment [6]. This effect makes the host more susceptible to the risk of colonization by other pathogens, since commensal microorganisms exert essential roles in the host protection and in the immune system stimulation [7]. Several studies have demonstrated correlations between psoriasis and alterations in skin microbial communities.

Similarly, dysbiosis of the skin microbiome has been found to be related to diseases as atopic dermatitis and vitiligo [8]. A high biocompatibility index towards both host and commensals is a fundamental prerequisite in the development and marketing of novel antimicrobials. For these reasons, the biocompatibility of ApoB-derived peptides under study has been evaluated by using multiple experimental approaches.

2. Methods

Materials. All the reagents were purchase from Sigma-Merck (Milan, Italy), unless specified otherwise.

Peptides. Expression and isolation of recombinant peptides was carried out as previously described [9] with the only exception of a final gel-filtration step, that was added in order to remove salts used along the purification process and that tend to attach to the peptides, as previously reported [10]. CATH-2 peptide was obtained from CPC Scientific Inc. (Sunnyvale, USA).

Eukaryotic cell culture and cytotoxicity assays. Immortalized human keratinocytes (HaCaT), human epidermoid carcinoma cells (A431), human dermal fibroblasts (HDF) were cultured in high-glucose Dulbecco's modified Eagle's medium (DMEM) supplemented with 10% fetal bovine serum (FBS), 1% antibiotics (Pen/strep) and 1% L-glutamine. THP-1 cells were obtained from ATCC (American Type Culture Collection: TIB-202) and cultured in suspension in RPMI containing Glutamax supplemented with 10% (v/v) FBS. All the cell lines have been grown at 37 °C in a humidified atmosphere containing 5% CO_2. Cells have been seeded into 96-well plates at a density of 3×10^3 cells/well in 100 µL of complete DMEM 24 h prior to the treatment. They were then incubated in the presence of increasing peptide concentrations (0-20 µmol L^{-1}) for 24, 48 and 72 h. Following treatment with peptides, MTT assays were performed as previously described [9][11]. Briefly, cell culture supernatants were replaced with 0.5 mg/mL MTT (3-(4,5-dimethylthiazol-2-yl)-2,5-diphenyltetrazolium bromide) reagent dissolved in DMEM medium without red phenol (100 µL/well). After 4 h of incubation at 37 °C, the resulting insoluble formazan salts were solubilized in 0.04 M HCl in anhydrous isopropanol and quantified by measuring the absorbance at λ = 570 nm using an automatic plate reader spectrophotometer (Synergy™ H4 Hybrid Microplate Reader, BioTek Instruments, Inc., Winooski, Vermont,

USA). Cell survival was expressed as means of the percentage values compared to control untreated cells.
Lactate dehydrogenase secretion in culture medium was measured by using Lactate Dehydrogenase Activity Assay Kit (MAK066; Sigma) according to the manufacturer's instructions. At the end of cell treatment, aliquots of supernatants were collected and added to a reaction mix containing Lactate Assay Buffer, Lactate Enzyme Mix, and Lactate Substrate Mix. Absorbance at 490 nm was determined for each sample using an automatic plate reader spectrophotometer. The positive control was obtained by treating cells with lysis buffer provided by the manufacturer.

Gene expression studies. Human dermal fibroblasts were seeded into 24-well plates at a density of 1.5×10^4 cells *per* well. After 24 h, culture medium was replaced by fresh DMEM (negative control) or by *S. aureus* culture at multiplicity of infection (MOI) of 0.01 and the samples were treated with 10 µmol L^{-1} of each ApoB-derived cryptide or with 2.5 µmol L^{-1} of CATH-2. Total RNA was extracted by using Trizol (Ambion, Carlsbad, CA) reagent according to the manufacturer's instructions. RNA was reverse transcribed by using the iScript cDNA synthesis kit (Bio-Rad, Veenendaal, the Netherlands) according to the manufacturer's instructions. Quantitative real-time PCR (qRT-PCR) was then performed to evaluate mRNA expression by using manufacturer's protocol (iQ SYBR Green Supermix - Bio-Rad). Reactions were performed by using the following primer sequences: for IL-8, 5'- CTGGCCGTGGCTCTCTTG' (sense) and 5'-CCTTGGCAAAACTGCACCTT-3' (antisense); for IL-6, 5'-TGCAATAACCACCCCTGACC-3' (sense) and 5'-TGCGCAGAATGAGATGAGTTG-3' (antisense); and for β-actin, 5'-ATGTGGATCAGCAAGCAGGAGTA-3' (sense) and 5'-GCATTTGCGGTGGACGAT-3' (antisense). Quantification of target gene expression was normalized using β-actin mRNA as an internal control gene.

Enzyme-Linked Immunosorbent Assay (ELISA). In order to evaluate possible pro-inflammatory effects exerted by ApoB-derived peptides, THP-1 cells, upon treatment with 100 µmol L^{-1} phorbol 12-myristate 13-acetate (PMA) for 3 days, were plated into 96-well plates at a density of 3×10^3 cells in 100 µL of medium *per* well. Following incubation with peptide under test, medium was collected to quantify cytokines levels. IL-8, TNF-α and MCP-1 levels in collected supernatants were determined by using human immunoassay kits (DuoSet ELISA kits,

R&D Systems, Minneapolis, MN) according to the manufacturer's instructions. Samples optical density was measured by using an ELISA reader set to 450 nm with a wavelength correction set to 540 nm. All the experiments were performed in triplicate.

Histone deacetylase enzyme (HDAC) assay. Human keratinocytes were treated with 20 µmol L^{-1} of each ApoB-derived cryptide or with 50 nmol L^{-1} of Tricostatin A for 30 min. Effects on Histone DeAcetylase enzyme (HDAC) activity were then evaluated by using HDAC-Glo™ I/II Assays and Screening System (Promega) according to the manufacturer's instructions.

Bacterial strains and growth conditions. Five bacterial strains were used in the present study, *i.e. S. epidermidis, S. capitis, S. hominis, S. warneri, S. haemolyticus, M. luteus, C. auricosum, and C. xenosis*. All bacterial strains were grown in Tryptic Soy Broth (TSB; Oxoid Ltd., Hampshire, UK) and on Tryptic Soy Agar (TSA; Oxoid Ltd., Hampshire, UK). In all the experiments, bacteria were inoculated and grown overnight in TSB at 37 °C. The next day, bacteria were transferred to a fresh TSB tube and grown to mid-logarithmic phase.

Antimicrobial activity. The antimicrobial activity of ApoB-derived peptides was assayed on a panel of skin pathogens, such as *S. epidermidis, S. capitis, S. hominis, S. warneri, S. haemolyticus, M. luteus, C. auricosum, and C. xenosis* by using broth microdilution method [12]. Bacteria were grown to mid-logarithmic phase in TSB at 37 °C. Then, cells have been diluted to 4×10^6 CFU/mL in Difco 0.5X Nutrient Broth (Becton-Dickenson, Franklin Lakes, NJ) and mixed 1:1 v/v with two-fold serial dilutions peptides (0-40 µmol L^{-1}). Following over-night incubation, each sample was diluted, plated on TSA and incubated at 37 °C for 24 h to count the number of colonies. All the experiments were carried out in three independent replicates.

3. Results

Biocompatibility and anti-inflammatory effects of encrypted peptides

To determine whether the peptides exerted toxic effects against eukaryotic cells and verify their biocompatibility towards skin cell cultures, we performed dose-response and time-course 3-(4, 5-dimethylthiazolyl-2)-2,5-diphenyltetrazolium bromide (MTT) and lactate dehydrogenase (LDH) cytotoxicity assays against both human dermal fibroblasts (HDF) and human epidermoid carcinoma cell (A431) lines.

Due to their cationic nature, most AMPs preferentially interact with negatively charged membranes, such as those of bacteria. The presence of cholesterol and the absence of acidic phospholipids on the external surface of normal human cell membranes are at the basis of AMPs selective toxicity towards prokaryotic cells [13]. Conversely, the net negative charge of tumor cell membranes conferred by modifications in phospholipid composition promotes the anticancer activity of several AMPs [14]. When incubated with normal human fibroblasts, ApoB-derived peptides exhibited only slight toxicity after 72 h of treatment at the highest peptide concentrations tested (20 μmol L^{-1}). Instead, peptides led to 30-40% decrease of cell viability in the case of carcinoma cells at 10-20 μmol L^{-1} after 48-72 h **(Figure 1)**.

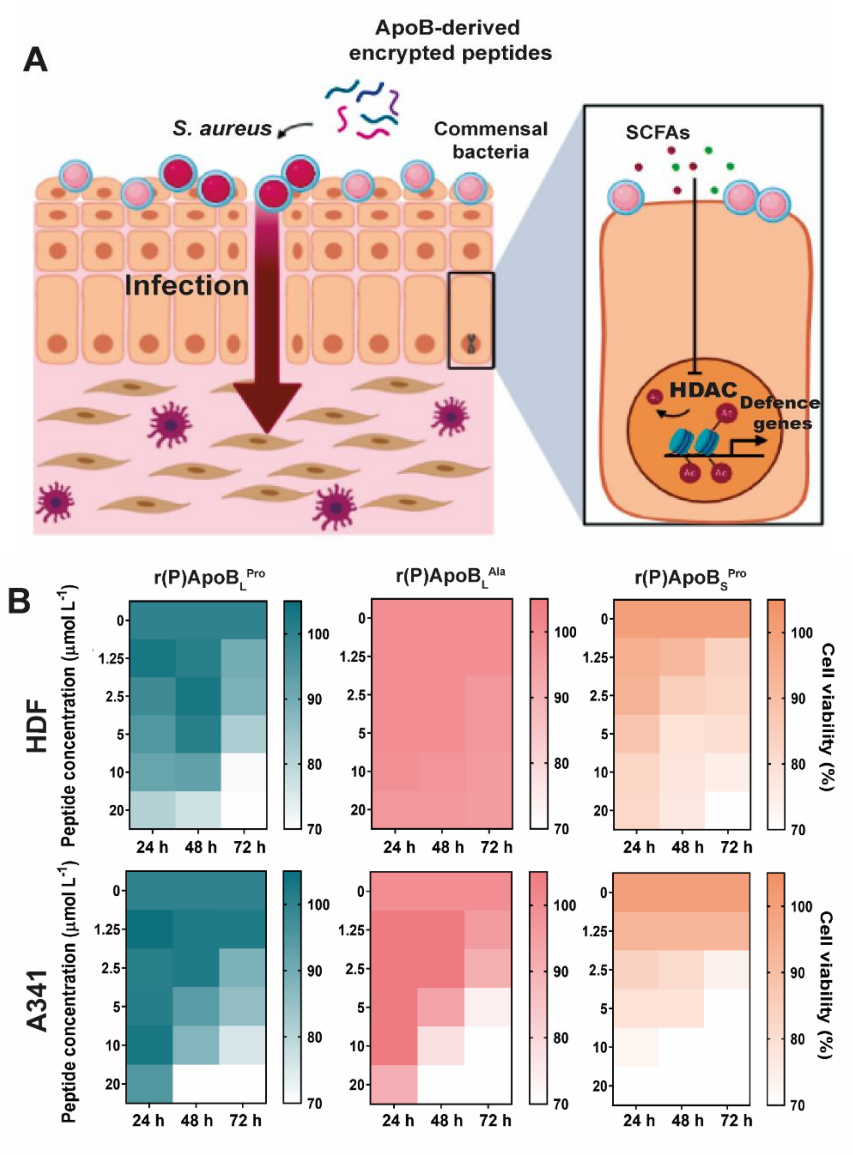

Figure 1. Biocompatibility of ApoB-derived peptides. (A) Schematic representation of the skin barrier. **(B)** Cytotoxic effects of increasing concentrations of r(P)ApoB$_L^{Pro}$ (blue), r(P)ApoB$_S^{Pro}$ (orange) and r(P)ApoB$_L^{Ala}$ (pink) on HDF (human dermal fibroblasts) and A431 (human epidermoid carcinoma cells) cell lines over time. Cell viability was assessed by MTT assays and expressed as the percentage of viable cells compared to untreated cells (control).

To evaluate whether peptides exert cytostatic or cytotoxic effects through membrane damage, LDH release in culture medium was detected as a biomarker of membrane damage [15]. Human dermal fibroblasts (HDF) and human epidermoid carcinoma cells (A431) were treated with each peptide at a concentration of 10 and 20 µmol L^{-1} for 72 h prior to analyze the presence of released LDH. No significant LDH release was detected, thus indicating no damage to eukaryotic cell membranes caused by cell exposure to peptides under the experimental conditions tested **(Figure 2)**.

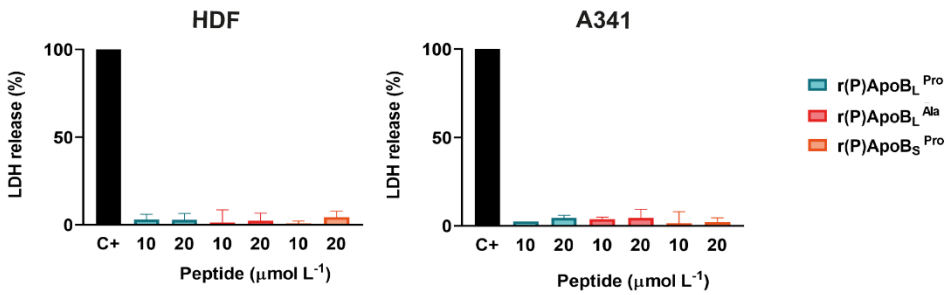

Figure 2. Biocompatibility of ApoB-derived peptides. LDH release upon treatment of HDF and A431 cells with ApoB-derived peptides. The positive control was obtained by treating cells with lysis buffer.

Enzyme-linked immunosorbent (ELISA) assays were also performed to exclude any potential inflammatory response induced by the treatment of human differentiated monocytes (THP-1) with ApoB-derived peptides. We evaluated the levels of interleukin 8 (IL-8), tumor necrosis factor (TNFα) and monocyte chemoattractant protein-1 (MCP-1) in differentiated THP-1 cells upon treatment with each peptide tested at 5 or 20 µmol L^{-1} for 24 h. No significant release of the pro-inflammatory cytokines IL-8, of TNFα and of the chemokine involved in the leukocyte activation and migration MCP-1was detected in peptide treated groups compared to positive control samples incubated with 10 ng mL^{-1} of lipopolysaccharide (LPS from *P. aeruginosa* PAO1) [16] **(Figure 3)**.

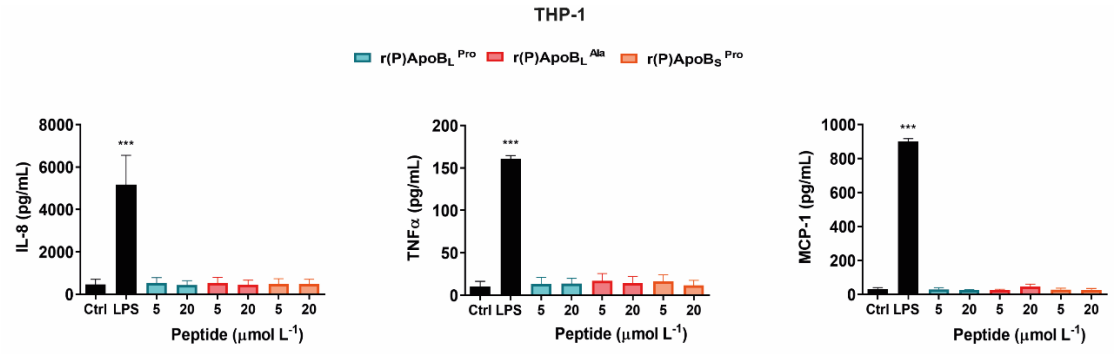

Figure 3. Immunomodulatory effects induced on THP-1. Induction of IL-8, TNFα and MCP-1 in THP-1 cells treated with ApoB-derived peptides with respect to the control group stimulated with LPS from *P. aeruginosa* PAO1.

We also evaluated the effects of ApoB-derived peptides on HDFs infected with *S. aureus* ATCC 29213, the primary pathogen infecting skin and soft tissues [17]. In particular, we assessed the effects of ApoB-derived peptides (10 μmol L^{-1}) and of the positive control peptide CATH-2 (2.5 μmol L^{-1}) on the expression of pro-inflammatory cytokines IL-8 and IL-6 by RT-qPCR **(Figure 4)**. Peptide r(P)ApoB$_S^{Pro}$ was found to reduce the inflammatory response triggered by *S. aureus* ATCC 29213 infection in HDFs **(Figure 4)**.

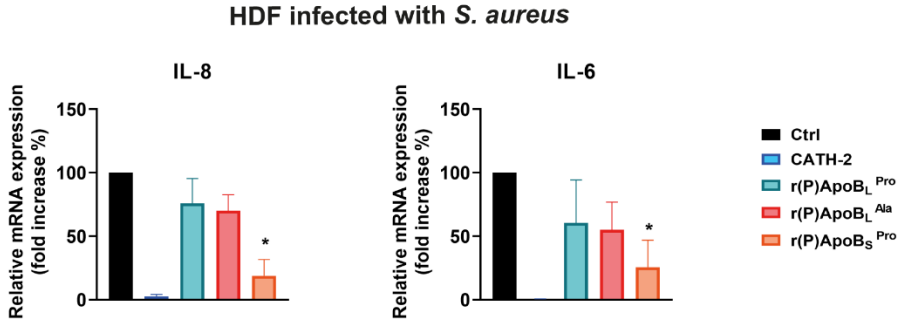

Figure 4. Anti-inflammatory properties of ApoB-derived peptides. ApoB-derived peptides effects on IL-8 and IL-6 expression in HDF cells infected with *S. aureus* ATCC 29213 by RT-qPCR. In all the cases, data represent the average (±standard deviation, SD) of at least three independent experiments, each one carried out in triplicate. Significant differences were indicated as (*P<0.05) for treated *versus* control samples.

Effects of ApoB-derived peptides on skin microbiome

Histone deacetylase enzymes, encoded by the HDAC genes, play a key role in integrating commensal bacteria-derived signals to calibrate epithelial cell responses [18]. As a consequence, a decrease in HDAC activity in skin keratinocytes correlates with imbalances in physiological host-commensal interactions. Thus, in order to rule out any potential side effects of the peptides against skin cells, we assessed whether r(P)ApoB$_L^{Pro}$, r(P)ApoB$_L^{Ala}$, and r(P)ApoB$_S^{Pro}$ affected the activity of HDAC enzymes. Briefly, HaCaT human keratinocytes were treated for 30 min with 20 µmol L^{-1} of each peptide and 50 nmol L^{-1} of the selective HDAC inhibitor trichostatin A, which was used as a positive control. ApoB-derived peptides did not affect HDAC activity, indicating that they might not influence the balance between skin microbiota and epithelial cells **(Figure 5)**. We also assessed the antimicrobial activity of ApoB encrypted peptides on common skin commensals, *i.e. S. epidermidis*, *S. capitis*, *S. hominis*, *S. warneri*, *S. haemolyticus*, *M. luteus*, *C. auricosum*, and *C. xenosis*. In 70% of the cases, peptides were found to be not active or active only at the highest concentrations tested (10 - 20 µmol L^{-1}), what is indicative of a weak antimicrobial activity against these bacterial strains **(Figure 5)**.

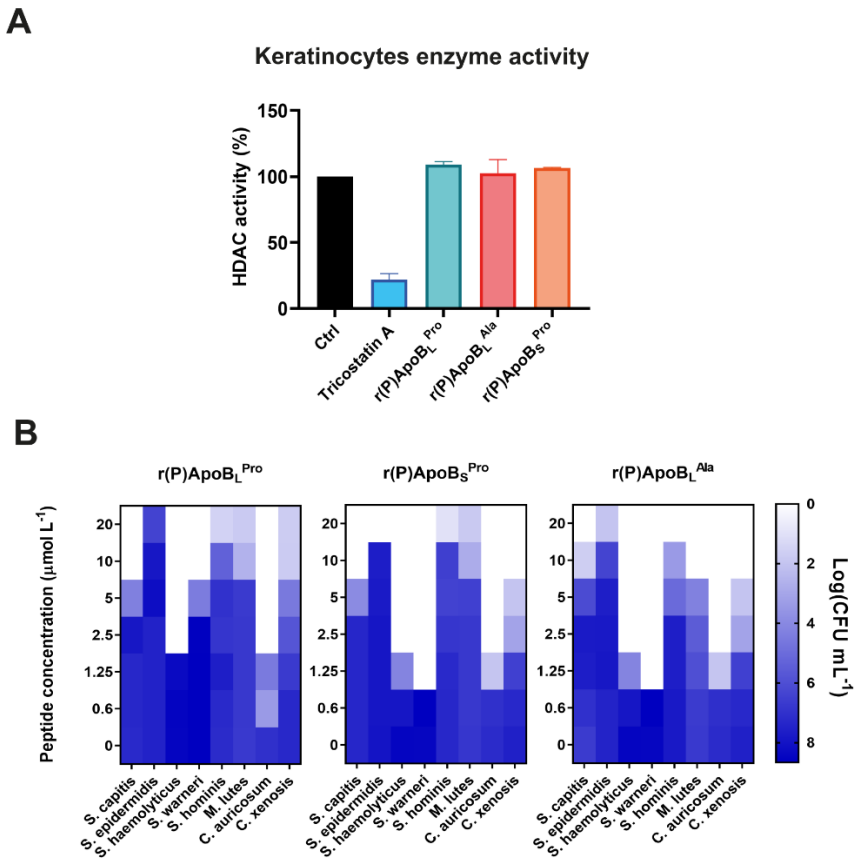

Figure 5. Skin microbiome biocompatibility. (A) Effects of ApoB-derived peptides on HDAC activity in HaCaT cells. HDAC activity is expressed as a percentage of the activity determined in untreated control cells. **(B)** Antimicrobial activity (µmol L^{-1}) of ApoB encrypted peptides against eight bacterial strains. Assays were performed in three independent replicates and heat map Log(CFUmL^{-1}) values are the arithmetic mean of the replicates in each experimental condition.

4. Discussion

Cytokine-mediated immunogenicity is one of the potential side effects of peptide-based therapeutic approaches as it can lead to cytotoxic effects and allergic responses [19][20]. Human ApoB-derived peptides did not exert toxicity against normal human skin cells and did not induce inflammatory responses in human monocytes. A slight toxicity was observed in human fibroblasts only 72 h post-treatment at the highest concentrations tested of r(P)ApoB$_L^{Pro}$ and r(P)ApoB$_S^{Pro}$ (20 µmol L^{-1}), thus indicating a higher degree of biocompatibility in the case of r(P)ApoB$_L^{Ala}$ compared to r(P)ApoB$_L^{Pro}$. Interestingly, the peptides were more toxic against cancer cells, consistent with data reported in the literature for several antimicrobial peptides endowed with anticancer properties [14]. Clinical studies have revealed that several skin diseases are associated with an increased inflammatory response induced by endogenous AMPs. This is the case of defensins and of cathelicidin LL-37, both of which trigger secretion of several cytokines at the injury site [21]. ApoB-derived peptides operate differently, as they don't induce an increase of cytokine release.

Skin infections caused by opportunistic bacteria, such as *Staphylococci*, *Pseudomonas*, and *Acinetobacter* strains are accompanied by the activation of a significant immune response in the underlying skin cells [22]. In particular, recent studies demonstrated that *S. aureus* contributes to long-lasting cutaneous inflammation and local immunosuppression [23]. The ability of peptides to modulate the immune response makes them promising and innovative alternatives for the treatment of SSTIs. Peptide r(P)ApoB$_S^{Pro}$ was found to be able to repress the expression of pro-inflammatory cytokines IL-8 and IL-6 in a co-culture model of infected skin wounds containing human cells and bacteria. Our results are in line with previous studies describing the role of ApoB in controlling *S. aureus* virulence [24]. It is worth noting that patients with psoriasis, a skin disorder associated with infections by *streptococci* and *Staphylococcus* species, tend to have reduced ApoB plasma levels, thus indicating an interesting and complex role of this lipoprotein in host defense [25]. However, ApoB-derived peptides did not inhibit histone-acetylation activity, which plays a key role in the calibration of host-commensal balance [18][26][27], thus underscoring the potential of these peptides for treating topical infections. Alterations in skin commensals composition are responsible for pathologic states of numerous dermatological diseases, including atopic dermatitis, psoriasis, and acne [8]. Environmental factors and, in particular, the common antimicrobial therapies are the main causes of this issue [6].

ApoB encrypted peptides demonstrated slight antimicrobial effects towards skin commensal population, thus representing a promising strategy to treat skin and soft tissue infections without significantly affecting commensal bacterial strains.

5. References

[1] A. E. Barnhill, M. T. Brewer, and S. A. Carlson, “Adverse effects of antimicrobials via predictable or idiosyncratic inhibition of host mitochondrial components.,” *Antimicrob. Agents Chemother.*, vol. 56, no. 8, pp. 4046–51, Aug. 2012, doi: 10.1128/AAC.00678-12.

[2] L. A. Mandell, P. Ball, and G. Tillotson, “Antimicrobial Safety and Tolerability: Differences and Dilemmas,” *Clin. Infect. Dis.*, vol. 32, no. Supplement 1, pp. S72–S79, Mar. 2001, doi: 10.1086/319379.

[3] R. Nau and H. Eiffert, “Modulation of release of proinflammatory bacterial compounds by antibacterials: potential impact on course of inflammation and outcome in sepsis and meningitis.,” *Clin. Microbiol. Rev.*, vol. 15, no. 1, pp. 95–110, Jan. 2002, doi: 10.1128/cmr.15.1.95-110.2002.

[4] T. Butler, “The Jarisch-Herxheimer Reaction After Antibiotic Treatment of Spirochetal Infections: A Review of Recent Cases and Our Understanding of Pathogenesis.,” *Am. J. Trop. Med. Hyg.*, vol. 96, no. 1, pp. 46–52, Jan. 2017, doi: 10.4269/ajtmh.16-0434.

[5] M. Deptuła, A. Wardowska, M. Dzierżyńska, S. Rodziewicz-Motowidło, and M. Pikuła, “Antibacterial Peptides in Dermatology–Strategies for Evaluation of Allergic Potential,” *Molecules*, vol. 23, no. 2, p. 414, Feb. 2018, doi: 10.3390/molecules23020414.

[6] A. J. SanMiguel, J. S. Meisel, J. Horwinski, Q. Zheng, and E. A. Grice, “Topical Antimicrobial Treatments Can Elicit Shifts to Resident Skin Bacterial Communities and Reduce Colonization by Staphylococcus aureus Competitors.,” *Antimicrob. Agents Chemother.*, vol. 61, no. 9, Sep. 2017, doi: 10.1128/AAC.00774-17.

[7] A. L. Byrd, Y. Belkaid, and J. A. Segre, “The human skin microbiome.,” *Nat. Rev. Microbiol.*, vol. 16, no. 3, pp. 143–155, Mar. 2018, doi: 10.1038/nrmicro.2017.157.

[8] H.-W. Chang *et al.*, “Alteration of the cutaneous microbiome in psoriasis and potential role in Th17 polarization,” *Microbiome*, vol. 6, no. 1, p. 154, Dec. 2018, doi: 10.1186/s40168-018-0533-1.

[9] R. Gaglione *et al.*, “Novel human bioactive peptides identified in Apolipoprotein B: Evaluation of their therapeutic potential,” *Biochem. Pharmacol.*, vol. 130, pp. 34–50, Apr. 2017, doi: 10.1016/j.bcp.2017.01.009.

[10] R. Gaglione *et al.*, “Cost-effective production of recombinant peptides in Escherichia coli,” *N. Biotechnol.*, vol. 51, pp. 39–48, Jul. 2019, doi: 10.1016/j.nbt.2019.02.004.

[11] R. Gaglione *et al.*, “Insights into the anticancer properties of the first antimicrobial peptide from Archaea,” *Biochim. Biophys. Acta - Gen. Subj.*, vol. 1861, no. 9, pp. 2155–2164, Sep. 2017, doi: 10.1016/j.bbagen.2017.06.009.

[12] I. Wiegand, K. Hilpert, and R. E. W. Hancock, “Agar and broth dilution methods to determine the minimal inhibitory concentration (MIC) of antimicrobial substances,” *Nat. Protoc.*, vol. 3, no. 2, pp. 163–175, Feb. 2008, doi: 10.1038/nprot.2007.521.

[13] F. Veas and G. Dubois, “IL-22 Induces an Acute-Phase Response Associated to a Cohort of Acute Phase Proteins and Antimicrobial Peptides as Players of Homeostasis,” in *Acute Phase Proteins - Regulation and Functions of Acute Phase Proteins*, InTech, 2011.

[14] C. Wang *et al.*, “Rapid Cytotoxicity of Antimicrobial Peptide Tempoprin-1CEa in Breast Cancer Cells through Membrane Destruction and Intracellular Calcium Mechanism,” *PLoS One*, vol. 8, no. 4, p. e60462, Apr. 2013, doi: 10.1371/journal.pone.0060462.

[15] Y. Lu *et al.*, “PFR peptide, one of the antimicrobial peptides identified from the derivatives of lactoferrin, induces necrosis in leukemia cells,” *Sci. Rep.*, vol. 6, no. 1, p. 20823, Aug. 2016, doi: 10.1038/srep20823.

[16] K. Pane *et al.*, “A new cryptic cationic antimicrobial peptide from human apolipoprotein E with antibacterial activity and immunomodulatory effects on human cells,” *FEBS J.*, vol. 283, no. 11, pp. 2115–2131, Jun. 2016, doi: 10.1111/febs.13725.

[17] J. P. Hoffmann *et al.*, “In situ Treatment With Novel Microbiocide Inhibits Methicillin Resistant Staphylococcus aureus in a Murine Wound Infection Model,” *Front. Microbiol.*, vol. 10, Jan. 2020, doi:

10.3389/fmicb.2019.03106.

[18] M. Pernot, R. Vanderesse, C. Frochot, F. Guillemin, and M. Barberi-Heyob, “Stability of peptides and therapeutic success in cancer.,” *Expert Opin. Drug Metab. Toxicol.*, vol. 7, no. 7, pp. 793–802, Jul. 2011, doi: 10.1517/17425255.2011.574126.

[19] M. Rahnamaeian and A. Vilcinskas, “Short antimicrobial peptides as cosmetic ingredients to deter dermatological pathogens,” *Appl. Microbiol. Biotechnol.*, vol. 99, no. 21, pp. 8847–8855, Nov. 2015, doi: 10.1007/s00253-015-6926-1.

[20] Y. Fujita and H. Taguchi, “Current status of multiple antigen-presenting peptide vaccine systems: Application of organic and inorganic nanoparticles,” *Chem. Cent. J.*, vol. 5, no. 1, p. 48, Dec. 2011, doi: 10.1186/1752-153X-5-48.

[21] P. Méndez-Samperio, “Recent advances in the field of antimicrobial peptides in inflammatory diseases,” *Adv. Biomed. Res.*, vol. 2, no. 1, p. 50, 2013, doi: 10.4103/2277-9175.114192.

[22] E. M. Haisma, M. H. Rietveld, A. de Breij, J. T. van Dissel, A. El Ghalbzouri, and P. H. Nibbering, “Inflammatory and Antimicrobial Responses to Methicillin-Resistant Staphylococcus aureus in an In Vitro Wound Infection Model,” *PLoS One*, vol. 8, no. 12, p. e82800, Dec. 2013, doi: 10.1371/journal.pone.0082800.

[23] J. E. E. Totté, W. T. van der Feltz, L. G. M. Bode, A. van Belkum, E. J. van Zuuren, and S. G. M. A. Pasmans, “A systematic review and meta-analysis on Staphylococcus aureus carriage in psoriasis, acne and rosacea,” *Eur. J. Clin. Microbiol. Infect. Dis.*, vol. 35, no. 7, pp. 1069–1077, Jul. 2016, doi: 10.1007/s10096-016-2647-3.

[24] P. R. Hall *et al.*, “Nox2 Modification of LDL Is Essential for Optimal Apolipoprotein B-mediated Control of agr Type III Staphylococcus aureus Quorum-sensing,” *PLoS Pathog.*, vol. 9, no. 2, p. e1003166, Feb. 2013, doi: 10.1371/journal.ppat.1003166.

[25] A. Pietrzak *et al.*, “Serum lipid metabolism in psoriasis and psoriatic arthritis - an update.,” *Arch. Med. Sci.*, vol. 15, no. 2, pp. 369–375, Mar. 2019, doi: 10.5114/aoms.2018.74021.

[26] A. Schwarz, A. Bruhs, and T. Schwarz, “The Short-Chain Fatty Acid Sodium Butyrate Functions as a Regulator of the Skin

Immune System," *J. Invest. Dermatol.*, vol. 137, no. 4, pp. 855–864, Apr. 2017, doi: 10.1016/j.jid.2016.11.014.

[27] P. Sittipo, J. Shim, and Y. Lee, "Microbial Metabolites Determine Host Health and the Status of Some Diseases," *Int. J. Mol. Sci.*, vol. 20, no. 21, p. 5296, Oct. 2019, doi: 10.3390/ijms20215296.

CHAPTER 4.

Design and characterization of a novel peptidomimetic with improved properties with respect to encrypted peptide identified in human ApoB

Angela Cesaro

Department of Chemical Sciences, PhD in Biotechnology

University of Naples Federico II

Design and characterization of a novel peptidomimetic with improved properties with respect to encrypted peptide identified in human ApoB

1. Introduction

Despite their numerous properties, antimicrobial peptides have a natural structural conformation, which makes them extremely sensitive to endo- and exopeptidases present in biological systems [1]. A powerful tool to transform proteolytically unstable peptides into compounds with improved bioactivities and pharmacokinetic profiles is represented by the development of peptidomimetics. Peptidomimetics are defined as "*compounds whose essential elements mimic a natural peptide and that retain the ability to interact with the biological target by producing the same biological effect* " [2]. Many different approaches are used to generate peptidomimetics and the selection of the right design strategy depends on what is known about the parental peptide in terms of structure, sequence and function [2].

Several synthetic tools have been developed to improve peptide stability, including chemical alteration and modification, use of non-natural amino acids and addition of stabilizing agents [3]. Chemical modifications, such as C-terminal amidation, N-terminal acetylation, cyclization *via* disulfide bonds or conjugation of agents, such as PEG, to the N- or C-termini was found to improve peptide proteolytic profiles. Similarly, the incorporation of non-natural amino acids or phosphorylated amino acids were demonstrated to increase peptide stability both *in vitro* and *in vivo* [3]. Other promising approaches involve the synthesis of new molecules without any apparent structural analogies with the lead peptide, but that interact with the same target or that display the interacting elements in the same spatial orientation [2]. However, obtained modified peptides need to be retested for their binding affinity and activities. Indeed, since every modification might alter the lead peptide efficacy, further changes might be required to restore original biological properties [3].

To ensure peptide translatability, we modified the primary structure of the naturally occurring ApoB-derived peptide by designing a retro-inverso sequence composed entirely of D-enantiomeric amino acids. In this **Chapter**, we investigate and characterize the biological activities, biocompatibility and proteolytic stability of a peptidomimetic designed from the encrypted antimicrobial sequence identified in human Apolipoprotein B.

2. Methods

Materials. All the reagents were purchase from Sigma-Merck (Milan, Italy), unless specified otherwise.

Peptides. Expression and isolation of recombinant peptides was carried out as previously described [4] with the only exception of a final gel-filtration step, that was added in order to remove salts used along the purification process and that tend to attach to the peptides, as previously reported [5]. CATH-2 and (ri)-r(P)ApoB$_S^{Pro}$ peptides were obtained from CPC Scientific Inc. (Sunnyvale, USA) and CASLO ApS (Kongens Lyngby, Denmark), respectively.

Bacterial strains and growth conditions. Five bacterial strains were used in the present study, *i.e. S. epidermidis* ATCC 35984, *S. aureus* ATCC 12600, *A. baumannii* ATCC 19606, *K. pneumoniae* ATCC 70603, *P. aeruginosa* PAO1, *P. aeruginosa* ATCC 27853, methicillin-resistant *S. aureus* (MRSA WKZ-2) and *E. coli* ATCC 25922. All bacterial strains were grown in Muller Hinton Broth (MHB, Becton Dickinson Difco, Franklin Lakes, NJ) and on Tryptic Soy Agar (TSA; Oxoid Ltd., Hampshire, UK). In all the experiments, bacteria were inoculated and grown overnight in MHB at 37 °C. The next day, bacteria were transferred to a fresh MHB tube and grown to mid-logarithmic phase.

Antimicrobial activity. The antimicrobial activity of (ri)-r(P)ApoB$_S^{Pro}$ was assayed on a panel of pathogens, such as *S. epidermidis* ATCC 35984, *S. aureus* ATCC 12600, *A. baumannii* ATCC 19606, *K. pneumoniae* ATCC 70603, *P. aeruginosa* PAO1, *P. aeruginosa* ATCC 27853, methicillin-resistant *S. aureus* (MRSA WKZ-2) and *E. coli* ATCC 25922 by using broth microdilution method [6]. Bacteria were grown to mid-logarithmic phase in MHB at 37 °C. Then, cells have been diluted to 4×10^6 CFU/mL in Difco 0.5X Nutrient Broth (Becton-Dickenson, Franklin Lakes, NJ) and mixed 1:1 v/v with two-fold serial dilutions peptides (0-40 µmol L^{-1}). Following over-night incubation, each sample was diluted, plated on TSA and incubated at 37 °C for 24 h to count the number of colonies. All the experiments were carried out in three independent replicates.

Antimicrobial activity of peptides upon pre-incubation in 10% serum. The antimicrobial activity of r(P)ApoB$_S^{Pro}$ and (ri)-r(P)ApoB$_S^{Pro}$ was evaluated against four bacterial strains upon pre-incubation in 10%

FBS (fetal bovine serum, Microgem Lab, Cat. S1860, Italy). According to Oliva et al. [7], all the peptides were incubated in serum for 1 h or 16 h at 37 °C (water bath) prior to MIC_{100} values determination by standard protocols. Experiments were performed in triplicate for each peptide.

Stability assay. The resistance to enzymatic degradation was evaluated accordingly to the method described by Powell et al. [8]. Briefly, peptides at a concentration of 2 mg mL^{-1} were exposed to a solution of 25% fetal bovine serum in water. Aliquots were collected after 0.5, 1, 2, and 4 h. Upon collection, 10 µL of trifluoroacetic acid were added to samples that were kept on ice for 10 min. Enzymatic degradation of peptides was followed by reverse-phase high performance liquid chromatography coupled to mass spectrometry (RP-HPLC/ESI-MS). The percentage of remaining intact peptide was calculated by integrating the area under the curve related to the peptide at time point zero. Experiments were performed on a Model 6130 Infinity mass spectrometer coupled to a Model 1260 HPLC system (Agilent), using a Phenomenex Gemini C_{18} column (2.0 mm × 150 mm, 3.0 µm particles, 110 Å pores). Solvent A was 0.1 % TFA in water, and solvent B was 90 % acetonitrile in solvent A. Elution was obtained with a 5–95 % solvent B gradient performed over 20 min at 0.2 mL min^{-1} flow. Peptides elution was monitored at 220 nm. Mass measurements were performed in a positive mode with the following conditions: mass range between 100 to 2500 *m/z*, ion energy of 5.0 V, nitrogen gas flow of 12 L min^{-1}, solvent heater of 250 °C, multiplier of 1.0, capillary of 3.0 kV and cone voltage of 35 V. All the experiments were done in three independent replicates.

Anti-biofilm activity assays. Anti-biofilm activity assays were performed on *S. epidermidis* ATCC 35984 and *A. baumannii* ATCC 19606. Bacteria were grown over-night at 37 °C and then diluted to 4×10^8 CFU/mL in 0.5x MHB medium. Incubations with increasing concentrations of each peptide (0-40 µmol L^{-1}) were carried out either for 4 h, in order to test peptide effects on cells attachment, or for 24 h, in order to test peptide effects on biofilm formation, as previously described [4]. In the case of crystal violet assays, bacterial biofilm was washed with phosphate buffer (PBS 1X) and then incubated with the dye (0.04%) for 20 min at room temperature. At the end of the incubation, samples were washed with PBS and then the dye bound to cells was dissolved in acetic acid 33%. Spectrophotometric analyses were then carried out at a wavelength of 600 nm.

Circular dichroism spectroscopy. CD experiments were performed on a Jasco J-815 circular dichroism spectropolarimeter. The cell path length was 0.1 cm or 1 cm in the case of more diluted titration points. CD spectra were collected at 25 °C in the 190-260 nm (far-UV) at 0.2 nm intervals, with a 50 nm/min scan rate, 1.0 nm bandwidth and a 4 sec response. Either 4 or 16 accumulations were performed during titration experiments. Each spectrum was corrected by subtracting the background, and reported with a FFT filter. Lyophilized peptides were dissolved in ultra-pure water (Romil, Waterbeach, Cambridge, GB) at a concentration of 1,600 µmol L^{-1}, determined on the basis of peptide dry weight and BCA assay (ThermoFisher Scientific, Waltham, MA). CD spectra of the peptides were collected in buffer alone (2.5 mM phosphate buffer, pH 7.4) or in the presence of 50% v/v trifluoroethanol (TFE, Sigma-Merck, Milan, Italy), lipopolysaccharide (LPS) from *E.coli* 0111:B4 strain (Sigma-Merck, Milan, Italy), or lipoteichoic acid (LTA) from *S. aureus* (Sigma-Merck, Milan, Italy). Inverse titration experiments were performed by addition known amounts of peptide in either 0.2 mg/mL LPS or LTA. After addition, samples were equilibrated with a magnetic stirrer for 3 min prior to acquisition. CD spectra were corrected by subtracting every time the contribution of the compound under test at any given concentration. CD spectra deconvolution was performed by using a Microsoft Excel-ported version of the PEPFIT program that is based on peptide-derived reference spectra, in order to estimate secondary structure contents after specular inversion of the raw data [9].

Eukaryotic cell culture and cytotoxicity assays. Immortalized human keratinocytes (HaCaT) and human dermal fibroblasts (HDF) were cultured in high-glucose Dulbecco's modified Eagle's medium (DMEM) supplemented with 10% fetal bovine serum (FBS), 1% antibiotics (Pen/strep) and 1% L-glutamine. All the cell lines have been grown at 37 °C in a humidified atmosphere containing 5% CO_2. Cells have been seeded into 96-well plates at a density of 3×10^3 cells/well in 100 µL of complete DMEM 24 h prior to the treatment. They were then incubated in the presence of increasing peptide concentrations (0-20 µmol L^{-1}) for 24, 48 and 72 hours. Following treatment with peptides, MTT assays were performed as previously described [4][10]. Briefly, cell culture supernatants were replaced with 0.5 mg/mL MTT (3-(4,5-dimethylthiazol-2-yl)-2,5-diphenyltetrazolium bromide) reagent dissolved in DMEM medium without red phenol (100 µL/well). After 4 h of incubation at 37 °C, the resulting insoluble formazan salts were

solubilized in 0.04 M HCl in anhydrous isopropanol and quantified by measuring the absorbance at λ = 570 nm using an automatic plate reader spectrophotometer (Synergy™ H4 Hybrid Microplate Reader, BioTek Instruments, Inc., Winooski, Vermont, USA). Cell survival was expressed as mean of the percentage values compared to control untreated cells.

Hemolytic activity. The release of hemoglobin from human erythrocytes was used as a measure for the hemolytic activity of (ri)-r(P)ApoB$_S^{Pro}$. Briefly, human red blood cells (RBCs) were collected from EDTA anti-coagulated blood, washed three times by centrifugation at 800 g for 10 minutes and 200-fold diluted in PBS pH 7.4. Aliquots of diluted erythrocytes (75 µL) were added to peptide solution (0-40 µmol L^{-1}; 75 µL) in 96-well microtiter plates, and the mixture was incubated for 1 h at room temperature. Following the incubation, the plate was centrifuged for 10 min at 1,300g, and 100 µL of supernatant from each well were transferred to a new 96-well plate. Absorbance values were determined at 405 nm by using an automatic plate reader (Synergy™ H4 Hybrid Microplate Reader, BioTek Instruments, Inc., Winooski, Vermont, USA). The percentage of hemolysis was determined by comparison with the control samples containing PBS (negative control) or 1% (v/v) SDS in PBS solution (positive control, complete lysis).

$$\text{Hemolysis (\%)} = \frac{(\text{Abs405 nm peptide} - \text{Abs405 nm negative control})}{(\text{Abs405 nm positive control} - \text{Abs405 nm negative control})} \times 100.$$

Cell infection assay. Immortalized human keratinocytes (HaCaT) were seeded into 24-well plates at a density of $3x10^5$ cells/well, and allowed to attach for 24 h at 37 °C in a humidified atmosphere containing 5% CO_2.

Following incubation, cells were washed three time with PBS and infected with *E. coli* ATCC 25922 at multiplicity of infection (MOI) of 2 in the presence or not of (ri)-r(P)ApoB$_S^{Pro}$ 10 µmol L^{-1}. To measure the number of bacteria in the wells, keratinocytes were washed three times with PBS and 500 µl of 1% Triton X-100 were added, in order to detach and lyse the cells. Samples containing the detached keratinocytes were serially diluted, plated onto TSA agar plates, and incubated over-night at 37°C to count the number of colonies. The number of bacteria present in the samples was followed over time (0-2-4 h).

Scarification skin infection mouse model. The anti-infective activity of ApoB-derived peptides against *P. aeruginosa* strain PAO1 in a mouse model was assessed accordingly to Pane et al. [11]. Briefly, *P. aeruginosa* strain PAO1 was grown in tryptic soy broth medium

overnight at 37 °C (250 rpm). The next day, bacteria were grown to mid-logarithmic phase, subsequently washed twice with sterile PBS (pH 7.4, 13,000 rpm for 1 min) and resuspended to a final concentration of 5.5 × 10^6 CFU/20 µL. To generate skin infection, female CD-1 mice (5−6 weeks old) were anesthetized with isoflurane and their backs shaved. To damage the stratum corneum and the upper layer of the epidermis, a superficial linear skin abrasion was made with a needle. Five minutes after wounding, an aliquot of 20 µL containing 5.5 × 10^6 CFU of bacteria in PBS was inoculated over each defined area containing the scratch. Peptide solutions (20 or 200 µmol L^{-1}/20 µL) were administered to the infected area 1 h after the infection. Animals were euthanized at day 2 or 4 and the area of scarified skin was excised 2-4 days post-infection, homogenized using a bead beater for 20 min (25 Hz), and serially diluted for CFU quantification. Two independent experiments were performed with 4 mice *per* group. Statistical significance was assessed using a one-way ANOVA test.

3. Results

In vitro antimicrobial and anti-biofilm activity of synthetic retro-inverso r(P)ApoB$_S^{Pro}$

An approach to overcome proteolytic degradation of peptides involves the use of the enantiomeric form [12]. The engineering of retro-derivatives is an alternative strategy able to guarantee high topochemical similarities with their precursors. It is performed by reversing the (D)-peptide sequence while flipping its termini, thus restoring the (L)-amino side chain angles [13][14][15]. The peptide r(P)ApoB$_S^{Pro}$ was selected as our lead peptide derived from ApoB100 because of its shorter length and excellent anti-infective and cytotoxic profiles. We proceeded to synthesize the retro-inverso version of r(P)ApoB$_S^{Pro}$, here named (ri)-r(P)ApoBs^{Pro}, by reversing its peptide sequence and replacing all (L) amino acids with their (D) counterparts **(Figure 1A)**.

Firstly, we evaluated the antimicrobial activity of (ri)-r(P)ApoB$_S^{Pro}$, that was found to display a higher activity against Gram-negative rather than Gram-positive bacterial strains, as previously reported for its parental peptide r(P)ApoB$_S^{Pro}$ **(Figure 1B)**. MIC_{100} values determined for (ri)-r(P)ApoB$_S^{Pro}$ were found to range from 2.5 to 5 µmol L^{-1} against *A. baumannii* ATCC 17878, *K. pneumoniae* ATCC 70603, *P. aeruginosa* PAO1, *P. aeruginosa* ATCC 27853, and *E. coli* ATCC 25922, whereas the peptide was found to be active at 10 µmol L^{-1} and 20 µmol L^{-1} against *S. epidermidis* ATCC 35984, *S. aureus* ATCC 12600 and methicillin-resistant *S. aureus* (MRSA WKZ-2), respectively, thus

demonstrating that introduced modifications did not alter the antimicrobial profile of the peptide **(Figure 1B)**. Furthermore, similarly to the lead peptide, (ri)-r(P)ApoB$_S^{Pro}$ was found to significantly inhibit (40-50%) the biofilm in preliminary stages of biofilm growth when assayed on the Gram-negative strain *A. baumannii* ATCC 17878 and the Gram-positive bacterium *S. epidermidis* ATCC 35984 **(Figure 1C)**.

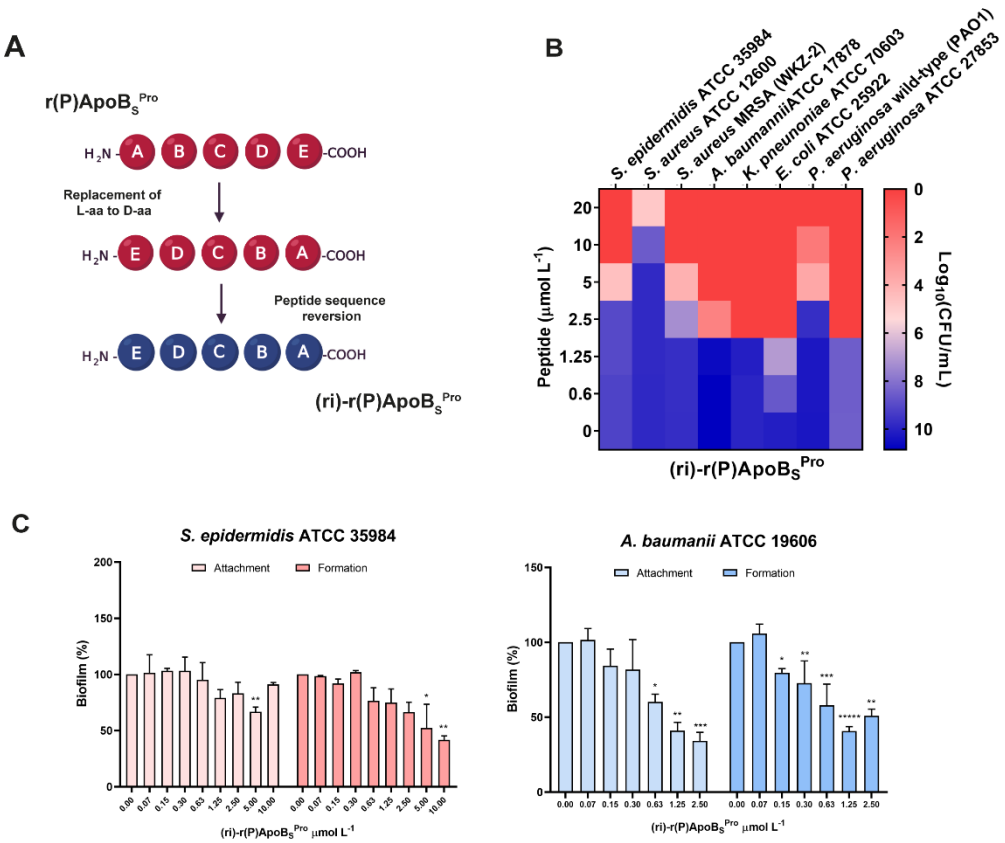

Figure 1. Antimicrobial and anti-biofilm activities of retro-inverso synthetic peptide. (A) Schematic representation of retro-inverso peptide design leading to (ri)-r(P)ApoB$_S^{Pro}$. **(B)** Antimicrobial activity of (ri)-r(P)ApoB$_S^{Pro}$ (µmol L^{-1}) against four bacterial strains; reported data refer to assays performed in triplicate and heat maps show averaged log$_{10}$(CFU mL^{-1}) values. **(C)** Anti-biofilm activity of (ri)-r(P)ApoB$_S^{Pro}$ on *S. epidermidis* ATCC 35984 and *A. baumannii* ATCC 17878 strains. The effects of increasing concentrations of (ri)-r(P)ApoB$_S^{Pro}$ peptide were evaluated on cells attachment and biofilm formation. Data represent the mean (±standard deviation, SD) of at least three independent experiments, each one carried out with triplicate determinations. Significant differences were indicated as *($P < 0.05$), **($P < 0.01$), ***($P<0.001$), ****($P<0.0001$) for treated *versus* control samples.

Conformational analyses of (ri)-r(P)ApoB$_S^{Pro}$ peptide by Far-UV circular dichroism

Far-UV CD spectroscopy has been used to analyze peptides antimicrobial activity from a structural point of view. The retro-inverso peptide appeared largely unstructured in buffer (2.5 mM phosphate buffer, pH 7.4) with a broad maximum centered at 199 nm **(Figure 2A)**. Nevertheless, molar residue ellipticity was found to be significantly lower in absolute values with respect to that of its (L)-amino acid variant [9] (~ 13 kdeg cm^2 dmol^{-1} res^{-1} versus –30 kdeg cm^2 dmol^{-1} res^{-1} for (ri)-r(P)ApoB$_S^{Pro}$ and r(P)ApoB$_S^{Pro}$, respectively), thus suggesting the presence of some secondary structure elements.

Indeed, best deconvolution of the spectrum in buffer resulted in approximately 34% of β secondary structure content, whereas previously characterized r(P)ApoB$_S^{Pro}$ was found to assume a fully random conformation [9]. We also found that, upon exposure to 50% TFE, a widely-adopted secondary structure inducer [16][17], (ri)-r(P)ApoB$_S^{Pro}$ assumed partial (~10%) helical conformation **(Figure 2A)**, as evidenced by the presence of two broad minima at around 208 and 222 nm, and a maximum at <200 nm. This behavior was found to be similar to that previously described for r(P)ApoB$_S^{Pro}$ peptide [9].

More interestingly, contrarily to its parental (L)-peptide, the retro-inverso variant secondary structure was found to be significantly altered by incubation with lipopolysaccharide (LPS), the predominant glycolipid in the outer membrane of Gram-negative bacteria. When increasing amounts of peptide were incubated with 0.2 mg/mL LPS endotoxin, the maximum wavelength shifted from 220 to 200 nm **(Figure 2B)**, suggesting a major switch towards β-strand conformation at higher LPS:peptide ratios.

Considering the lower peptide antimicrobial activity towards Gram-positive bacteria, we hypothesized a less pronounced effect induced by lipoteichoic acid (LTA), an anionic glycerol phosphate polymer of cell wall [18][19], on peptide conformation. When increasing amounts of peptide were incubated with 0.2 mg/mL LTA from *S. aureus*, slighter variations of peptide spectrum were observed **(Figure 2C)**. In particular, band maximum wavelength shifted only from 215 to 200 nm with a far lower effect on the molar residue ellipticity, most probably due to only minimal β-strand formation. CD spectra deconvolution are summarized in **Figure 2D**.

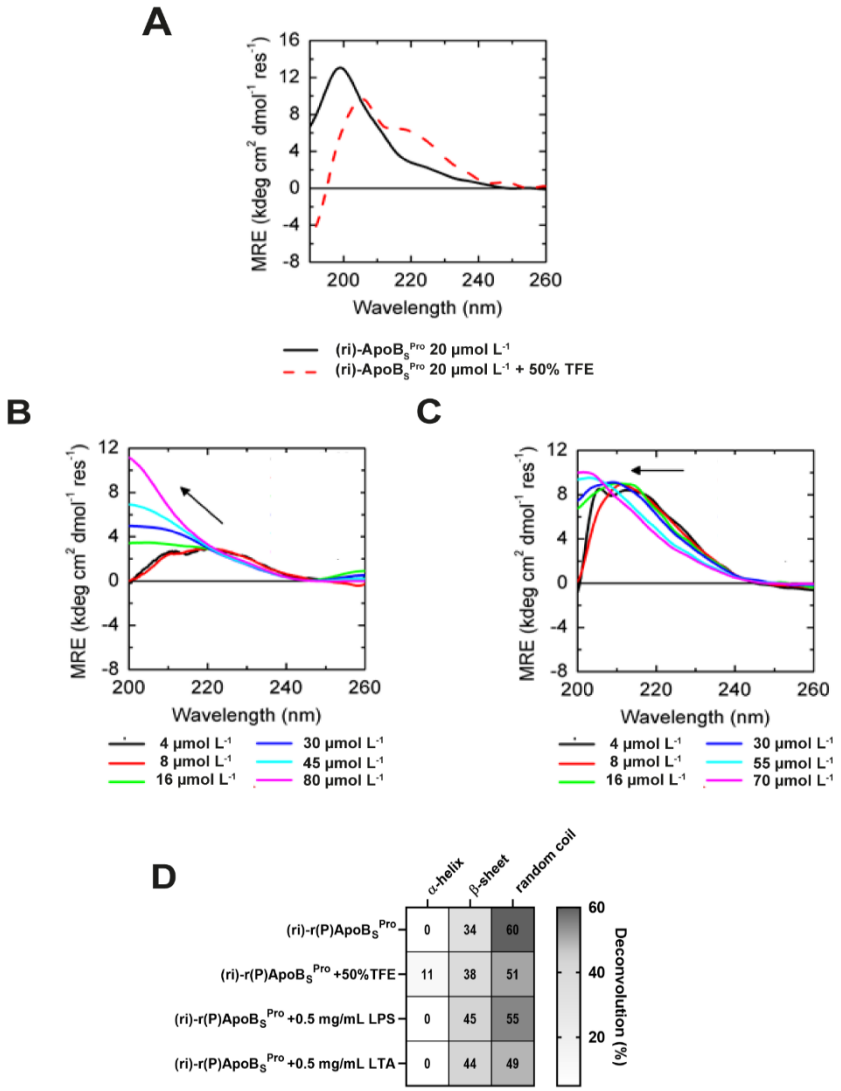

Figure 2. Conformational analyses of (ri)-r(P)ApoB$_S^{Pro}$ peptide by Far-UV circular dichroism. (A) CD spectra of peptide (ri)-r(P)ApoB$_S^{Pro}$ 20 µmol L^{-1} in the absence (black line) or in the presence (red dashed line) of 50% (v/v) TFE. CD spectra at different concentrations of (ri)-r(P)ApoB$_S^{Pro}$ in the presence of constant amounts (0.2 mg/mL) of either LPS **(B)** or LTA **(C)**. CD spectra deconvolution percentages of (ri)-r(P)ApoB$_S^{Pro}$ peptide in 2.5 mM sodium phosphate pH 7.4 buffer and in the presence of 50% TFE, 0.5 mg mL^{-1} LPS or LTA. Secondary structure percentages were calculated using CDPRO software.

Stability profile of (ri)-r(P)ApoB$_S^{Pro}$

To determine synthetic peptide proteolytic stability, we verified (ri)-r(P)ApoB$_S^{Pro}$ susceptibility to serum proteases compared to parental peptide r(P)ApoB$_S^{Pro}$. Peptides' MIC$_{100}$ values were measured upon incubation in 10% fetal bovine serum for 1 and 16 h. While natural r(P)ApoB$_S^{Pro}$ peptide completely lost its activity upon incubation in serum showing MIC$_{100}$ values against *S. aureus* ATCC 12600, *A. baumannii* ATCC 17878 and *K. pneumoniae* ATCC 70603 higher than 80 µmol L^{-1}, as opposed to 5-20 µmol L^{-1}, the antimicrobial activity of (ri)-r(P)ApoB$_S^{Pro}$ retro-inverso peptide remained unvaried even after 16 h pre-incubation in serum **(Figure 3A)**. Obtained results are in line with degradation profile data **(Figure 3B)**. Indeed, parental peptide was found to be degraded in a few minutes after exposure to serum proteases, whereas (ri)-r(P)ApoB$_S^{Pro}$ demonstrated higher stability by persisting (~50% of initial concentration added) even 4 h post-exposure to proteases in serum **(Figure 3B)**.

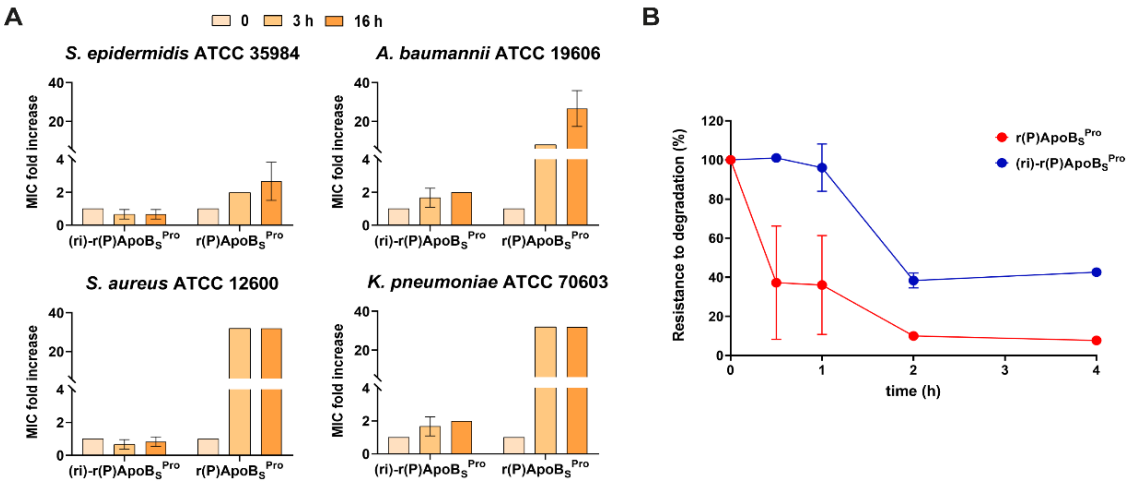

Figure 3. Stability profile of retro-inverso synthetic peptide. (A) Antibacterial activity of (ri)-r(P)ApoB$_S^{Pro}$ peptide after preincubation in 10% serum with proteases. Reported data refer to assays performed in triplicate and the fold changes in antimicrobial activity are calculated as ratio between peptide MIC values obtained after and before incubation for 1 h and 16 h in the presence of 10% serum at 37 °C. **(B)** Resistance to degradation of (ri)-r(P)ApoB$_S^{Pro}$ exposed to fetal bovine serum (FBS) proteases for 4 h.

Biocompatibility of (ri)-r(P)ApoB$_S^{Pro}$ towards human skin cells

We performed additional experiments to verify the biocompatibility of (ri)-r(P)ApoB$_S^{Pro}$ towards skin cell cultures and to exclude hemolytic effects, since it has been reported that incorporation of D-amino acids into peptide sequences might lead to toxic effects [20]. Peptide (ri)-r(P)ApoB$_S^{Pro}$ did not significantly affect cell viability when analysed by MTT assays. Indeed, viability of immortalized human keratinocytes (HaCaT) and normal human fibroblasts (HDFs) was not found to significantly change upon exposure to increasing concentrations of the peptide for different time intervals **(Figure 4A).** Moreover, when we tested (ri)-r(P)ApoB$_S^{Pro}$ on human red blood cells (RBCs), the peptide showed a slight lytic effect only at the highest concentrations tested, thus indicating a good profile of biocompatibility **(Figure 4B)**. Skin and soft tissue infections occur when bacteria adhere to host cells. The ability of the peptide to prevent the adhesion of pathogens to skin cells is an interesting aspect to be considered. Hence, we assessed the effects of (ri)-r(P)ApoB$_S^{Pro}$ on human keratinocytes infected with *E. coli* ATCC 25922 cells. After 4 h of incubation, the synthetic retro-inverso peptide was found to be able to reduce by 50% the number of bacterial cells infecting keratinocytes with respect to control untreated cells **(Figure 4C)**.

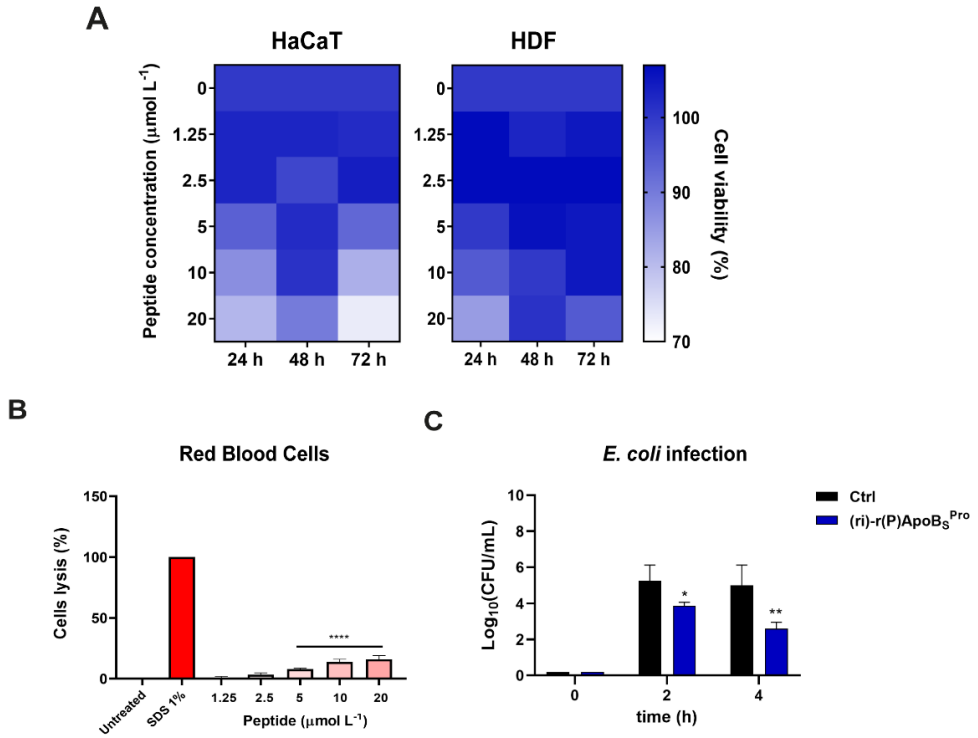

Figure 4. Effects of retro-inverso synthetic peptide on human eukaryotic cell lines (A) Cytotoxic effects of increasing concentrations of (ri)-r(P)ApoB$_S^{Pro}$ on HaCaT (Immortalized human keratinocytes) and HDF (human dermal fibroblasts) cells. Cell viability was assessed by MTT assays and expressed as the percentage of viable cells compared to untreated cells (control). **(B)** Hemolytic activity of (ri)-r(P)ApoB$_S^{Pro}$ towards human red blood cells (RBCs) after 1 h of incubation at 37 °C. Data represent the mean (±standard deviation, SD) of at least three independent experiments, each one carried out with triplicate determinations. **(C)** *E. coli* bacterial cells adhesion on HaCaT cells in the presence of (ri)-r(P)ApoB$_S^{Pro}$ peptide. Experiments were performed three times in duplicate. Error bars represent the standard deviation of the mean. Significant differences were indicated as *($P < 0.05$) or **($P < 0.01$) for treated *versus* control samples.

In vivo antimicrobial activity of synthetic retro-inverso r(P)ApoB$_S^{Pro}$

To assess peptides applicability, we tested ApoB-derived peptides in a murine abscess infection model **(Figure 5A)**. The Gram-negative bacterium *P. aeruginosa* PAO1, responsible for dangerous skin wounds [21] and found to be susceptible to ApoB encrypted peptides, was used to induce the infection in mice **(Figure 5B)**. Upon induction of skin infections in mice, a single dose of either (ri)-r(P)ApoB$_S^{Pro}$ (20 and 200 µmol L^{-1}) or of each of the three natural ApoB-derived peptides (200 µmol L^{-1}) was administered. Treatment with r(P)ApoB$_L^{Pro}$, r(P)ApoB$_L^{Ala}$, or r(P)ApoB$_S^{Pro}$ significantly reduced *P. aeruginosa* CFU/mL counts by ~3 to 4 orders of magnitude after four days of treatment. Similar results were obtained with our control peptide CATH-2. It has to be highlithed that treatment with (ri)-r(P)ApoB$_S^{Pro}$ at a significantly lower dose (20 µmol L^{-1}) reduced bacterial load by ~3 orders of magnitude, while treatment with a higher peptide concentration (200 µmol L^{-1}) completely sterilized the infection four days post-treatment **(Figure 5C)**. No significant weight changes or any obvious inflammation event were detected during the treatment period, thus confirming the lack of toxicity of these peptides in the murine model **(Figure 5D).** Altogether, our data demonstrate the promising anti-infective activity of (ri)-r(P)ApoB$_S^{Pro}$ in a pre-clinical mouse model.

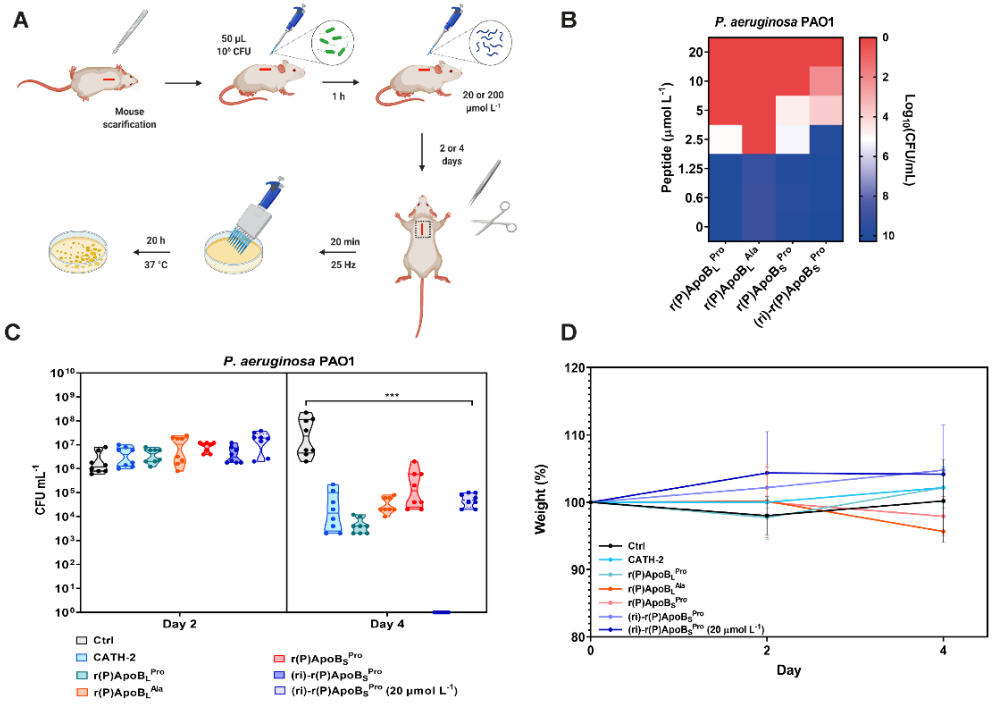

Figure 5. *In vivo* activity of natural and synthetic encrypted peptides derived from human ApoB. (A) Schematic representation of the *in vivo* experimental design. The back of mice was shaved, and an abrasion was generated to damage the stratum corneum and the upper layer of the epidermis. Subsequently, an aliquot of 50 µL containing 106 CFU of *P. aeruginosa* PAO1 in phosphate buffer was inoculated over each defined area. One hour after the infection, peptides at 20 or 200 µmol L^{-1} were administered to the infected area. Four animals *per* group were euthanized at day 2 or 4 post-infection and the area of scarified skin was excised and homogenized for 20 min (25 Hz). **(B)** Effects of natural and synthetic encrypted peptides derived from human ApoB on *P. aeruginosa* PAO1. **(C)** Homogenized samples were serially diluted for CFU quantification (statistical significance was determined using two-way ANOVA followed by Dunnett's test, *** $P < 0.001$). **(D)** Mouse body weight measurements were performed throughout the experiment and normalized by the body weight at the beginning of the experiment.

4. Discussion

One of the main limitations to the development of peptide therapeutics is their low stability in complex biological environments that contain proteolytic enzymes [12]. Linear peptides are sensitive to proteolysis, drastically reducing their biological activity and their application as antimicrobial agents [22]. By rational design and molecular modeling, it is possible to introduce many structural modifications to improve stability profiles and pharmacokinetic properties of antimicrobial peptides [23].

An approach to overcome proteolytic degradation of peptides involves the use of the enantiomeric form [12]. Many studies demonstrated that (D)-amino acids AMP analogues present improvements in the degradation profiles and have activities similar to their parental (L)-peptides found in nature. Due to their resistance to enzymatic degradation, (D)-amino-acid-containing peptides are molecules functionally attractive to be applied in medical devices and in the development of inhalants, oral or systemic drugs [13]. Simple replacement of (L) with (D)-amino acids is generally ineffective, since side-chain orientation is completely altered with respect to the target [14]. To guarantee structural stability, spatial orientation, side-chain topology, and overall peptide bioactivity, an alternative approach is represented by the design of retro-inverso derivatives obtained by reversing the peptide sequence [13][14][15]. Retro-inverso variants are known to present high topochemical similarities with their precursors and equivalent bioactivities [13]. The synthetic retro-inverso peptide r(P)ApoB$_S^{Pro}$, here designed and characterized, has been found to share many of the features of the parental (L)-peptide. Indeed, no significant changes in antimicrobial activity were observed. Moreover, the presence of serum proteases was found not to alter peptide antimicrobial efficacy, thus indicating that the introduced modifications were responsible for a significant improvement in peptide stability. This was confirmed by the analysis of degradation profiles that indicated a longer half-life of (ri)-r(P)ApoB$_S^{Pro}$ peptide compared to r(P)ApoB$_S^{Pro}$.

From a structural point of view, the retro-inverso peptide showed some differences with respect to the parental (L)-peptide, as indicated by Far UV-CD analyses. Indeed, while r(P)ApoB$_S^{Pro}$ was found to be unstructured in aqueous buffer [9], (ri)-r(P)ApoB$_S^{Pro}$ peptide showed approximately 34% of β secondary structure content. Furthermore, in the presence of LPS or LTA, the β-strand content of the retro-inverso derivative increased, even if the effect was found to be more pronounced in the presence of LPS, in agreement with peptide higher

antimicrobial activity towards Gram-negative bacteria. These effects were not observed in the case of the natural (L)-peptide characterized by a higher susceptibility to proteases.
We also evaluated the effects of the synthetic retro-inverso peptide on a panel of human eukaryotic cells. Peptide biocompatibility and its ability to protect human keratinocytes from infections make (ri)-r(P)ApoB$_S^{Pro}$ an excellent candidate to be employed in the future development of antimicrobial therapies. ApoB-derived peptides were also found to exert significant anti-infective properties in a pre-clinical mouse model. It has to be highlithed that the retro-inverso variant showed anti-infective activity at concentrations ten times lower than those required to have the same effect with natural peptides. Altogether, obtained data demonstrate that the synthetic version of the lead peptide is characterized by higher stability and effectiveness both *in vitro* and *in vivo*.

5. References

[1] M. Pernot, R. Vanderesse, C. Frochot, F. Guillemin, and M. Barberi-Heyob, “Stability of peptides and therapeutic success in cancer,” *Expert Opin. Drug Metab. Toxicol.*, vol. 7, no. 7, pp. 793–802, Jul. 2011, doi: 10.1517/17425255.2011.574126.

[2] E. Lenci and A. Trabocchi, “Peptidomimetic toolbox for drug discovery.,” *Chem. Soc. Rev.*, vol. 49, no. 11, pp. 3262–3277, Jun. 2020, doi: 10.1039/d0cs00102c.

[3] Y. A. Haggag, “Peptides as Drug Candidates: Limitations and Recent Development Perspectives,” *Biomed. J. Sci. Tech. Res.*, vol. 8, no. 4, Sep. 2018, doi: 10.26717/BJSTR.2018.08.001694.

[4] R. Gaglione *et al.*, “Novel human bioactive peptides identified in Apolipoprotein B: Evaluation of their therapeutic potential,” *Biochem. Pharmacol.*, vol. 130, pp. 34–50, Apr. 2017, doi: 10.1016/j.bcp.2017.01.009.

[5] R. Gaglione *et al.*, “Cost-effective production of recombinant peptides in Escherichia coli,” *N. Biotechnol.*, vol. 51, pp. 39–48, Jul. 2019, doi: 10.1016/j.nbt.2019.02.004.

[6] I. Wiegand, K. Hilpert, and R. E. W. Hancock, “Agar and broth dilution methods to determine the minimal inhibitory concentration (MIC) of antimicrobial substances,” *Nat. Protoc.*, vol. 3, no. 2, pp. 163–175, Feb. 2008, doi: 10.1038/nprot.2007.521.

[7] R. Oliva *et al.*, “Exploring the role of unnatural amino acids in antimicrobial peptides,” *Sci. Rep.*, vol. 8, no. 1, p. 8888, Dec. 2018, doi: 10.1038/s41598-018-27231-5.

[8] M. F. Powell *et al.*, “Peptide stability in drug development. II. Effect of single amino acid substitution and glycosylation on peptide reactivity in human serum.,” *Pharm. Res.*, vol. 10, no. 9, pp. 1268–73, Sep. 1993, doi: 10.1023/a:1018953309913.

[9] R. Gaglione *et al.*, “Novel human bioactive peptides identified in Apolipoprotein B: Evaluation of their therapeutic potential.,” *Biochem. Pharmacol.*, vol. 130, pp. 34–50, Apr. 2017, doi: 10.1016/j.bcp.2017.01.009.

[10] R. Gaglione *et al.*, “Insights into the anticancer properties of the first antimicrobial peptide from Archaea,” *Biochim. Biophys. Acta*

- *Gen. Subj.*, vol. 1861, no. 9, pp. 2155–2164, Sep. 2017, doi: 10.1016/j.bbagen.2017.06.009.

[11] K. Pane *et al.*, “Identification of Novel Cryptic Multifunctional Antimicrobial Peptides from the Human Stomach Enabled by a Computational–Experimental Platform,” *ACS Synth. Biol.*, vol. 7, no. 9, pp. 2105–2115, Sep. 2018, doi: 10.1021/acssynbio.8b00084.

[12] C. G. Starr and W. C. Wimley, “Antimicrobial peptides are degraded by the cytosolic proteases of human erythrocytes,” *Biochim. Biophys. Acta - Biomembr.*, vol. 1859, no. 12, pp. 2319–2326, Dec. 2017, doi: 10.1016/j.bbamem.2017.09.008.

[13] M. H. Cardoso, E. S. Cândido, K. G. N. Oshiro, S. B. Rezende, and O. L. Franco, “Peptides containing d -amino acids and retro-inverso peptides,” in *Peptide Applications in Biomedicine, Biotechnology and Bioengineering*, Elsevier, 2018, pp. 131–155.

[14] M. Garton, S. Nim, T. A. Stone, K. E. Wang, C. M. Deber, and P. M. Kim, “Method to generate highly stable D-amino acid analogs of bioactive helical peptides using a mirror image of the entire PDB,” *Proc. Natl. Acad. Sci.*, vol. 115, no. 7, pp. 1505–1510, Feb. 2018, doi: 10.1073/pnas.1711837115.

[15] C. de la Fuente-Núñez *et al.*, “D-Enantiomeric Peptides that Eradicate Wild-Type and Multidrug-Resistant Biofilms and Protect against Lethal Pseudomonas aeruginosa Infections,” *Chem. Biol.*, vol. 22, no. 2, pp. 196–205, Feb. 2015, doi: 10.1016/j.chembiol.2015.01.002.

[16] R. E. W. Hancock and H.-G. Sahl, “Antimicrobial and host-defense peptides as new anti-infective therapeutic strategies.,” *Nat. Biotechnol.*, vol. 24, no. 12, pp. 1551–7, Dec. 2006, doi: 10.1038/nbt1267.

[17] J. M. Le, G. Alachouzos, M. Chino, A. J. Frontier, A. Lombardi, and K. L. Bren, “Tuning Mechanism through Buffer Dependence of Hydrogen Evolution Catalyzed by a Cobalt Mini-enzyme.,” *Biochemistry*, vol. 59, no. 12, pp. 1289–1297, Mar. 2020, doi: 10.1021/acs.biochem.0c00060.

[18] N. Malanovic and K. Lohner, “Gram-positive bacterial cell envelopes: The impact on the activity of antimicrobial peptides,” *Biochim. Biophys. Acta - Biomembr.*, vol. 1858, no. 5, pp. 936–

946, May 2016, doi: 10.1016/j.bbamem.2015.11.004.

[19] R. Oliva *et al.*, “Similarities and differences for membranotropic action of three unnatural antimicrobial peptides,” *J. Pept. Sci.*, vol. 26, no. 8, Aug. 2020, doi: 10.1002/psc.3270.

[20] D. V. Grishin, D. D. Zhdanov, M. V. Pokrovskaya, and N. N. Sokolov, “D-amino acids in nature, agriculture and biomedicine,” *All Life*, vol. 13, no. 1, pp. 11–22, Jan. 2020, doi: 10.1080/21553769.2019.1622596.

[21] M. S. Dryden, “Complicated skin and soft tissue infection.,” *J. Antimicrob. Chemother.*, vol. 65 Suppl 3, no. Supplement 3, pp. iii35-44, Nov. 2010, doi: 10.1093/jac/dkq302.

[22] R. Böttger, R. Hoffmann, and D. Knappe, “Differential stability of therapeutic peptides with different proteolytic cleavage sites in blood, plasma and serum,” *PLoS One*, vol. 12, no. 6, p. e0178943, Jun. 2017, doi: 10.1371/journal.pone.0178943.

[23] J. Vagner, H. Qu, and V. J. Hruby, “Peptidomimetics, a synthetic tool of drug discovery,” *Curr. Opin. Chem. Biol.*, vol. 12, no. 3, pp. 292–296, Jun. 2008, doi: 10.1016/j.cbpa.2008.03.009.

CHAPTER 5.

Development of an innovative cosmeceutical formulations to encapsulate ApoB-derived peptidomimetic

Angela Cesaro

Department of Chemical Sciences, PhD in Biotechnology

University of Naples Federico II

Development of an innovative cosmeceutical formulations to encapsulate ApoB-derived peptidomimetic

1. Introduction

Several formulations, including suspensions, micro/nanoparticles, patches, and hydrogels have been proposed to control topical drug delivery. Among different alternatives, hydrogel-based systems have been found to offer many advantages in the treatment of skin wounds and infections [1]. According to the definition, hydrogel-based systems are networks of natural or synthetic crosslinked polymers with a three-dimensional configuration able to imbibe high amounts of water [2]. The hydrogel swelling ability is the result of the hydrophilic moieties in the structure, which is resistant to water dissolution thanks to the presence of cross-linkers between polymeric chains [3]. The presence of water has the ability to provide a shooting effect by cooling the wound surface, whereas the presence of natural polymers improves the biocompatibility profile of the formulation [4]. Several polymers have been chemically modified to develop synthetic hydrogels with improved properties [3]. These delivery systems are classified on the basis of their origin, physical properties, nature of swelling, method of preparation, ionic charges, rate of biodegradation and kind of crosslinking [5]. Recently, hydrogels based on hyaluronic acid (HA) confirmed their interesting properties not only as scaffolds, but also as suitable carriers of biologically active substances [2]. HA is an essential component of the natural extracellular matrix where it plays an important role in many biological processes, including wound healing. HA is biocompatible, biodegradable, non-immunogenic and has unique viscoelastic and rheological properties that make it an excellent polymer to build hydrogel systems with desired morphology and bioactivity [6]. Here, we developed and characterized a HA-based hydrogel system loaded with the peptidomimetic (ri)-r(P)ApoB$_S^{Pro}$ with the main aim to specifically deliver this antimicrobial peptide to the site of infection. The combination of hyaluronic acid biological properties, of hydrogel systems swelling and hydrating capabilities, and of the efficacy of the selected antimicrobial peptide represents a promising starting point to develop a strategy able to target skin disorders and infections, thus opening interesting perspectives to the future applicability of ApoB-derived peptides in the dermatological field.

2. Methods

Materials. All the reagents were purchase from Sigma-Merck (Milan, Italy), unless specified otherwise. HA crosslinked with 2.5% 1,4-butanediol diglycidyl ether (BDDE) was provided from Altergon Italia s.r.l.

Peptides. (ri)-r(P)ApoB$_S^{Pro}$ peptide was obtained from CASLO ApS (Kongens Lyngby, Denmark).

Preparation of HA-BDDE hydrogel loaded with (ri)-r(P)ApoB$_S^{Pro}$ peptide. Peptide (ri)-r(P)ApoB$_S^{Pro}$ was added to hyaluronic acid hydrogel crosslinked with 2.5% 1,4-butanediol diglycidyl ether (HA-BDDE) at a ratio of 4:1 (v/v). A solution of peptide at a concentration of 80 or 320 µmol L^{-1} was stirred with HA-BDDE and then lyophilized for 24 h, in order to obtain white spongy samples. Control samples were prepared under the same experimental conditions, but in the absence of the peptide. Prior to all the characterizations, dried hydrogels were rehydrated and sterilized by exposure to UV light for 20 min.

Swelling properties characterization. Hydrogels swelling properties were characterized by measuring the gravimetric change over time as described by Jie Zhu et al. [7]. Briefly, the freeze-dried hydrogels were weighed (S_0) and then immersed into distillated water. To obtain the swelling ratio, hydrogels samples were weighed (S_1) at different time intervals until swelling equilibrium was reached. Each sample was measured in three replicates. Hydrogels swelling ratio was calculated as follows:

$$\text{Swelling ratio (\%)} = \frac{S_1 - S_0}{S_0} \times 100$$

Degradation analyses. Swollen hydrogels were weighed (W_0) and degradation performances were evaluated by incubating the samples with 300 U mL^{-1} of hyaluronidase (ref. H3506, Sigma-Merck) solubilized in 0.02 M sodium phosphate pH 7.4 containing 0.01 % bovine serum albumin and 77 mM NaCl, as described by Wanxu Cao et al. [8]. The mixtures were placed at 37 °C (water bath) and the weight loss percentage was calculated by weighing samples (W_1) at defined time intervals. Every sample was measured in three replicates. Degradation behavior was expressed as the percentage of weight loss and was calculated as follows:

$$\text{Weight change (\%)} = \frac{W_1}{W_0} \times 100$$

***In vitro* peptide release from hydrogel system**

To determine peptide release, HA-BDDE hydrogels loaded with 80 or 320 µmol L^{-1} (ri)-r(P)ApoB$_S^{Pro}$ were immersed in distilled water and incubated at 37 °C over time. At defined time points, aliquots of 100 µL were collected and 100 µL of water were added, in order to maintain volume constant. The amounts of released (ri)-r(P)ApoB$_S^{Pro}$ were measured by HPLC analyses on a Shimadzu LC-20 Prominence (Shimadzu Corporation, Japan), mounted with a thermostated PDA detector (SPD-M20A). Samples were eluted on a Phenomenex Aeris Peptide XB-C18 3.6 µm column (150x4.6 mm), with a linear gradient of ultra-pure water (A) and acetonitrile (B) (UpS solvent, Romil) from 15% to 95% of solvent B over 20 minutes. TFA was added to both eluents (0.1% v/v). A five-points calibration curve was used. Each calibration standard solution was prepared by dilution in the working buffer (ultra-pure water) of the primary standard (1600 µmol L^{-1} in ultra-pure water sample, determined on the basis of peptide dry weight), in order to obtain the following concentrations: 2.5, 5, 10, 20, and 40 µmol L^{-1}. Linear regression was used to fit the peak areas as integrated from the 220 nm chromatogram (R^2=0.997). In each calibration curve, a blank sample was included. Two separate analyses of peptide release were performed on a blind and randomized basis, by injecting all the collected solutions at different time intervals (0, 0.5, 1, 2, 3, 24, 48, 72 h). For quality controls, blank, zero and spiked samples (5, 10 and 40 µmol L^{-1}) were injected, the latter being found within 10% deviation of the nominal concentration.

Bacterial strains and growth conditions. Two bacterial strains were used in the present study, *i.e.* methicillin-resistant *S. aureus* (MRSA WKZ-2) and *E. coli* ATCC 25922. Both bacterial strains were grown in Muller Hinton Broth (MHB, Becton Dickinson Difco, Franklin Lakes, NJ) and on Tryptic Soy Agar (TSA; Oxoid Ltd., Hampshire, UK). In all the experiments, bacteria were inoculated and grown over-night in MHB at 37 °C. The next day, bacteria were transferred to a fresh MHB tube and grown to mid-logarithmic phase.

Antimicrobial activity. The antimicrobial activity of HA-BDDE hydrogel loaded with (ri)-r(P)ApoB$_S^{Pro}$ was assayed on methicillin-resistant *S. aureus* (MRSA WKZ-2) and *E. coli* ATCC 25922. Bacteria were grown to mid-logarithmic phase in MHB at 37 °C. Then, cells were diluted to 4×10^6 CFU/mL in Difco 0.5X Nutrient Broth (Becton-Dickenson, Franklin Lakes, NJ) and mixed 1:1 v/v with HA-BDDE hydrogel loaded with peptide at a final concentration of 80 or 320 µmol L^{-1}. Following

over-night incubation, each sample was diluted, plated on TSA and incubated at 37 °C for 24 h to count the number of colonies. All the experiments were carried out in three independent replicates.

Migration assay

To examine bacteria migration across the hydrogel, the upper chambers of a transwell plate (Costar 3422®, Corning Corporation, USA) were coated with control saline solution, HA-BDDE hydrogel or HA-BDDE hydrogel loaded with (ri)-r(P)ApoB$_S^{Pro}$, as described by Xiaojuan Li et al. [9]. Following coating, methicillin-resistant *S. aureus* (MRSA WKZ-2) and *E. coli* ATCC 25922 bacterial cells were diluted to 4×10^6 CFU/mL in Difco 0.5X Nutrient Broth (Becton-Dickenson, Franklin Lakes, NJ), and added to previously coated upper chambers. Medium in the lower wells was then analyzed at defined time intervals to monitor bacterial cells migration from upper to lower wells. Migrated bacteria were quantified by diluting and plating each sample on TSA. Following incubation at 37 °C for 24 h, the number of colonies was counted. The experiment was performed in three independent replicates.

Eukaryotic cell cultures and cytotoxicity assays. Immortalized human keratinocytes (HaCaT) and human dermal fibroblasts (HDF) were cultured in high-glucose Dulbecco's modified Eagle's medium (DMEM) supplemented with 10% fetal bovine serum (FBS), 1% antibiotics (Pen/strep) and 1% L-glutamine. All the cell lines were grown at 37 °C in a humidified atmosphere containing 5% CO_2. Cells were seeded into 96-well plates at a density of 6×10^3 cells/well in 100 µL of complete DMEM 24 h prior to the treatment. They were then incubated for 24 h in the presence of HA-BDDE hydrogel hydrated with cell culture medium and previously loaded with the peptide at a final concentration of 80 or 320 µmol L^{-1}. Following treatment, cells were washed three times with PBS to remove hydrogel residues and cell supernatants were replaced with 0.5 mg/mL MTT (3-(4,5-dimethylthiazol-2-yl)-2,5-diphenyltetrazolium bromide) reagent dissolved in DMEM medium without red phenol (100 µL/well). After 4 h of incubation at 37 °C, the resulting insoluble formazan salts were solubilized in 0.04 M HCl in anhydrous isopropanol and quantified by measuring the absorbance at λ = 570 nm using an automatic plate reader spectrophotometer (Synergy™ H4 Hybrid Microplate Reader, BioTek Instruments, Inc., Winooski, Vermont, USA). Cell survival was expressed as means of the percentage values compared to control untreated cells.

3. Results

Swelling and degradation profiles of HA hydrogel systems

The ability to retain a high amount of water is one of the key properties of hydrogel-based systems. Indeed, they can swell in water under physiological conditions without dissolving. Swelling capability plays a key role in keeping the injured site moist and in controlling bleeding. Moreover, this mechanical characteristic is fundamental to allow molecules to diffuse into or to be released from the hydrogels [7]. In order to verify whether the presence of the peptide could affect swelling and degradation profiles of HA-BDDE hydrogels under test, analyses were performed. As shown in **Figure 1 A**, HA-BDDE hydrogels loaded with peptide under test at different concentrations retained a swelling behavior similar to that of control sample, thus indicating that the presence of the peptide doesn't affect the ability of the system to absorb water and to expand. Similarly, the degradation profile was found not to be affected by the presence of the peptide, since the activity of hyaluronidase enzyme that acts by cleaving the (1→4)-linkages between N-acetylglucosamine and glucuronate was found to be unchanged **(Figure 1B)**.

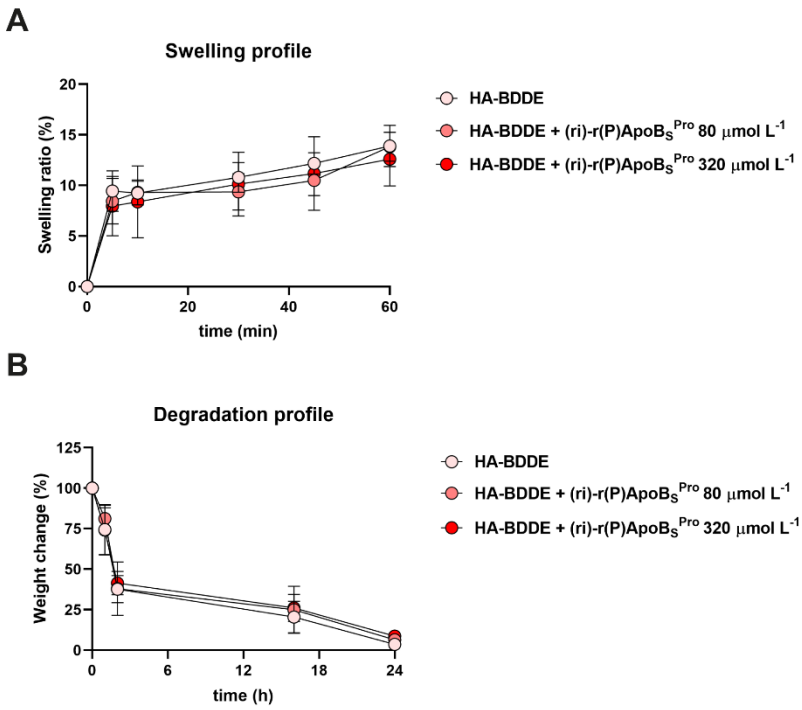

Figure 1. Swelling (A) and degradation (B) profile of HA-BDDE alone and loaded with different concentrations of (ri)-r(P)ApoB$_S^{Pro}$ peptide.

Peptide release from the hydrogel system

After peptide loading into the hydrogel, samples were analyzed to verify whether peptide is released over time. To this purpose, HA-BDDE hydrogel system loaded with 80 or 320 µmol L^{-1} (ri)-r(P)ApoB$_S^{Pro}$ were immersed in water and aliquots were collected at defined time intervals, in order to estimate the amount of the released peptide by HPLC analyses. Obtained data indicate that peptide release is proportional to the amount of initially loaded peptide, being always released 15% of the initial amount after 24 h **(Figures 2A and 2B)**.

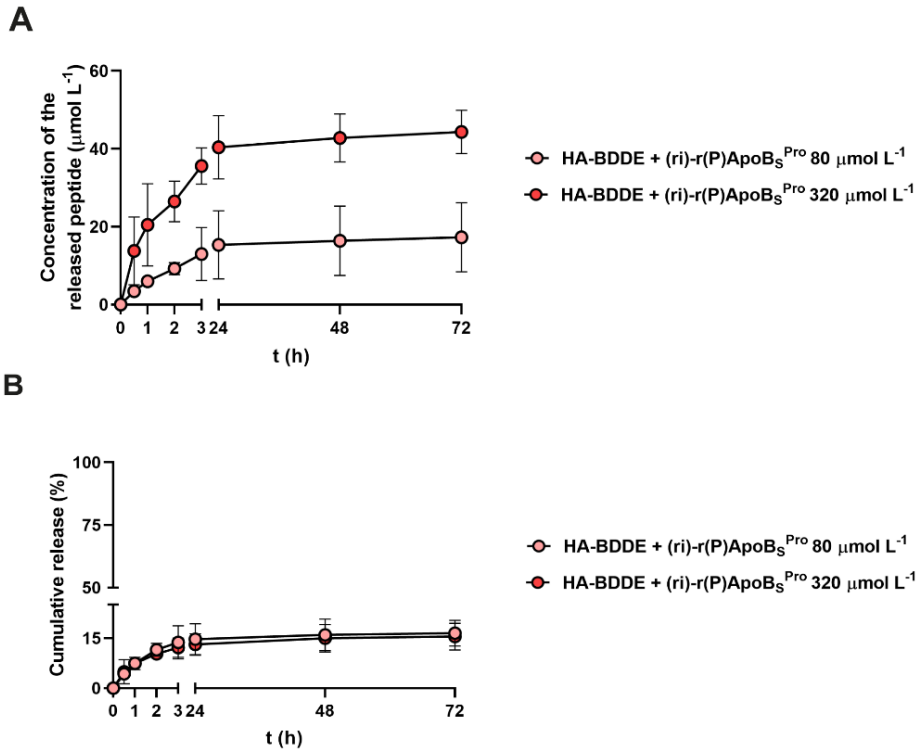

Figure 2. *In vitro* release profile. (A) Evaluation of peptide amount released from HA-BDDE loaded with two different peptide concentrations, *i.e.* 80 or 320 µmol L^{-1} **(B)** Cumulative release of (ri)-r(P)ApoB$_S^{Pro}$ expressed as percentage with respect to the total initial amount of peptide filled into gel.

Antimicrobial properties of HA-BDDE loaded with (ri)-r(P)ApoB$_S^{Pro}$
In order to evaluate whether the newly developed hydrogel-based system is able to preserve the bioactivity of (ri)-r(P)ApoB$_S^{Pro}$, we assessed the antimicrobial efficacy of HA-BDDE hydrogels loaded with synthetic peptide against methicillin-resistant *S. aureus* (MRSA WKZ-2) and *E. coli* ATCC 25922, as representatives of Gram-negative and Gram-positive bacterial strains. We determined the minimal inhibitory concentration (MIC) values by counting the number of bacterial colonies obtained after an over-night incubation in the presence or in the absence of peptide. HA-BDDE hydrogels loaded with (ri)-r(P)ApoB$_S^{Pro}$ were found to exert significant antibacterial effects against both bacterial strains tested. In detail, methicillin-resistant *S. aureus* (MRSA WKZ-2) was found to be susceptible to the hydrogel system loaded with the highest concentration of peptide (MIC_{40} = 320 µmol L^{-1}). The hydrogel-based formulations were even more active against *E. coli* ATCC 25922 with MIC_{90} value corresponding to 80 µmol L^{-1} and a complete growth inhibition (MIC_{100}) obtained at a concentration of peptide of 320 µmol L^{-1}. These data further confirm a higher susceptibility of Gram-negative bacterial strains to (ri)-r(P)ApoB$_S^{Pro}$ antimicrobial peptide **(Figure 3A)**. In order to investigate the ability of hydrogel to counteract bacterial migration across surfaces, we coated upper chambers of a transwell plate with HA-BDDE functionalized with (ri)-r(P)ApoB$_S^{Pro}$. Transwell experiments were performed to examine the ability of the hydrogel-based system to counteract bacterial migration across surfaces. Bacterial cells were plated into the upper chambers, the undersurfaces of which were coated with PBS, HA-BDDE hydrogel or HA-BDDE hydrogel functionalized with peptide under test. As shown in **Figure 3B**, the hydrogel loaded with 320 µmol L^{-1} peptide demonstrated to attenuate or prevent the migration of *S. aureus* and *E. coli* strains, respectively.

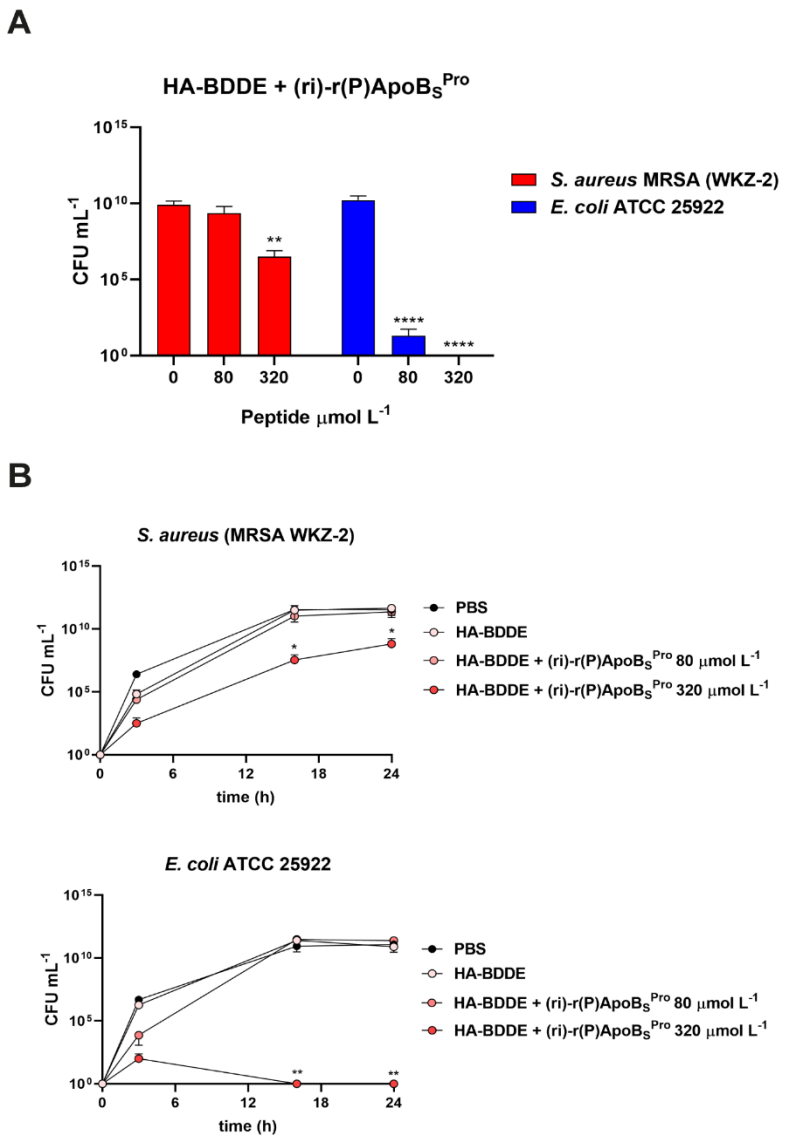

Figure 1. Antimicrobial activity of HA-BDDE hydrogel functionalized with the peptide. (A) Antimicrobial efficacy of HA-BDDE hydrogel loaded with (ri)-r(P)ApoB$_S^{Pro}$ against methicillin-resistant *S. aureus* (MRSA WKZ-2) and *E. coli* ATCC 25922 bacterial strains; reported data refer to assays performed in triplicate. **(B)** Bacterial migration across surfaces coated with HA-BDDE hydrogel functionalized with (ri)-r(P)ApoB$_S^{Pro}$. Significant differences were indicated as *($P < 0.05$), **($P < 0.01$) and ****($P < 0.0001$) for treated *versus* control samples.

Effects of HA-BDDE hydrogel loaded with (ri)-r(P)ApoB$_S^{Pro}$ on human skin cells cultures

To evaluate the biocompatibility of hyaluronic-based hydrogel loaded with (ri)-r(P)ApoB$_S^{Pro}$ peptide towards skin cell cultures, MTT assays were performed on immortalized human keratinocytes (HaCaT) and normal human fibroblasts (HDFs). HA-BDDE hydrogels loaded with 80 or 320 µmol L^{-1} of (ri)-r(P)ApoB$_S^{Pro}$ were found not to affect the viability of HaCaT and HDFs cell lines **(Figure 4).** On the contrary, HA-BDDE hydrogel system was found to significantly improve cell viability in the absence of the peptide as well as in the presence of 320 µmol L^{-1} peptide when tested on human keratinocytes **(Figure 4)**.

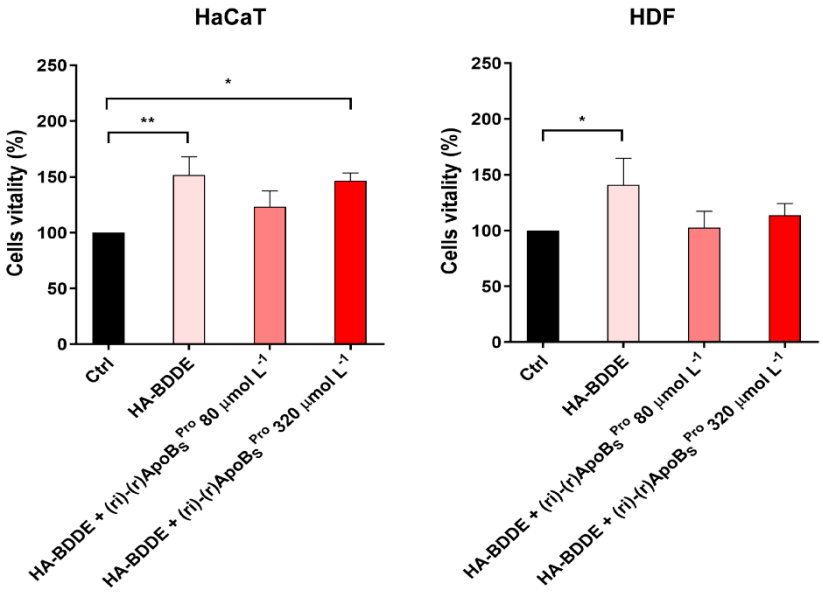

Figure 4. Effects of HA-BDDE hydrogel functionalized with the peptide on human eukaryotic cell lines (A) Cytotoxic effects of HA-BDDE hydrogel loaded with different concentrations of (ri)-r(P)ApoB$_S^{Pro}$ on HaCaT (Immortalized human keratinocytes) and HDF (human dermal fibroblasts) cells. Cell viability was assessed by MTT assays and expressed as the percentage of viable cells compared to untreated cells (control). Experiments were performed three times. Error bars represent the standard deviation of the mean. Significant differences were indicated as *($P < 0.05$) or **($P < 0.01$), for treated *versus* control samples.

4. Discussion

The incessant spreading of drug-resistant bacteria prompts to search for novel antibiotics, and for novel materials able to efficiently deliver antimicrobial agents to the target site. Several approaches were developed to release bioactive drugs into the infected sites, such as nanoparticles, hydrogels, creams, ointments, and patches [10]. Hydrogel-based systems were demonstrated to be excellent candidates as drug formulations because of their high biocompatibility, their capability to easily encapsulate hydrophilic drugs, and their swelling behavior [11]. A hyaluronic acid (HA)-based hydrogel was here selected to develop a suitable system to topically deliver a promising antimicrobial peptide. Besides contributing to viscoelasticity and lubrication of tissues, HA also plays an important role in physiological processes, such as inflammation, wound healing, and tissue development [12]. These HA properties combined with antimicrobial features of the peptide of interest might allow to produce a promising formulation to be employed in dermatological field [13]. This was the main aim of this research work that allowed to functionalize a crosslinked HA-hydrogel with the synthetic (ri)-r(P)ApoB$_S^{Pro}$ peptide derived from a sequence encrypted in human apolipoprotein B. The presence of high amounts of the peptide into the hydrogel system was found not to affect its swelling properties and degradation profile. At the same time, the anti-infective efficacy of HA-hydrogel loaded with (ri)-r(P)ApoB$_S^{Pro}$ was confirmed on both Gram-negative and Gram-positive bacterial strains, including strains characterized by resistance phenotype. The hydrogel functionalized with the peptide under test was also found to be able to counteract bacterial migration across surfaces, a property that opens interesting perspectives in the treatment of dermal and epidermal infections. Furthermore, the hydrogel-based system was found to be able to release the bioactive peptide with a fast kinetic, even if only 15% of the total initially loaded peptide was found to be released after a prolonged incubation. This could be enough to provide the therapeutic doses required to kill pathogens and preserve cell integrity. However, further analyses should be conducted to deepen this aspect. Importantly, no toxic effects were detected on human skin cell lines, and the presence of hyaluronic acid was found to increase the viability of keratinocytes, thus highlighting positive effects in wound healing. Altogether, these findings open new perspectives to the applicability of (ri)-r(P)ApoB$_S^{Pro}$ in the treatment of skin infections and injures.

5. References

[1] M. Bally *et al.*, “Risk of acute myocardial infarction with NSAIDs in real world use: bayesian meta-analysis of individual patient data.,” *BMJ*, vol. 357, p. j1909, May 2017, doi: 10.1136/bmj.j1909.

[2] M. Zasloff, “Antimicrobial peptides of multicellular organisms,” *Nature*, vol. 415, no. 6870, pp. 389–395, Jan. 2002, doi: 10.1038/415389a.

[3] P. Ghasemiyeh and S. Mohammadi-Samani, “Hydrogels as Drug Delivery Systems; Pros and Cons,” 2019. doi: 10.30476/TIPS.2019.81604.1002.

[4] L. P. da Silva, R. L. Reis, V. M. Correlo, and A. P. Marques, “Hydrogel-Based Strategies to Advance Therapies for Chronic Skin Wounds.,” *Annu. Rev. Biomed. Eng.*, vol. 21, no. 1, pp. 145–169, Jun. 2019, doi: 10.1146/annurev-bioeng-060418-052422.

[5] F. Ullah, M. B. H. Othman, F. Javed, Z. Ahmad, and H. M. Akil, “Classification, processing and application of hydrogels: A review,” *Mater. Sci. Eng. C*, vol. 57, pp. 414–433, Dec. 2015, doi: 10.1016/j.msec.2015.07.053.

[6] X. Xu, A. K. Jha, D. A. Harrington, M. C. Farach-Carson, and X. Jia, “Hyaluronic acid-based hydrogels: from a natural polysaccharide to complex networks,” *Soft Matter*, vol. 8, no. 12, p. 3280, 2012, doi: 10.1039/c2sm06463d.

[7] J. Zhu, F. Li, X. Wang, J. Yu, and D. Wu, “Hyaluronic Acid and Polyethylene Glycol Hybrid Hydrogel Encapsulating Nanogel with Hemostasis and Sustainable Antibacterial Property for Wound Healing.,” *ACS Appl. Mater. Interfaces*, vol. 10, no. 16, pp. 13304–13316, Apr. 2018, doi: 10.1021/acsami.7b18927.

[8] W. Cao *et al.*, “The preparation and biocompatible evaluation of injectable dual crosslinking hyaluronic acid hydrogels as cytoprotective agents,” *J. Mater. Chem. B*, vol. 7, no. 28, pp. 4413–4423, 2019, doi: 10.1039/C9TB00839J.

[9] X. Li *et al.*, “Effect of the hyaluronic acid-poloxamer hydrogel on skin-wound healing: in vitro and in vivo studies,” *Anim. Model. Exp. Med.*, p. ame2.12067, Apr. 2019, doi: 10.1002/ame2.12067.

[10] R. K. Thapa, D. B. Diep, and H. H. Tønnesen, “Topical

antimicrobial peptide formulations for wound healing: Current developments and future prospects," *Acta Biomater.*, vol. 103, pp. 52–67, Feb. 2020, doi: 10.1016/j.actbio.2019.12.025.

[11] J. Li and D. J. Mooney, "Designing hydrogels for controlled drug delivery," *Nat. Rev. Mater.*, vol. 1, no. 12, p. 16071, Dec. 2016, doi: 10.1038/natrevmats.2016.71.

[12] S. Trombino, C. Servidio, F. Curcio, and R. Cassano, "Strategies for Hyaluronic Acid-Based Hydrogel Design in Drug Delivery.," *Pharmaceutics*, vol. 11, no. 8, p. 407, Aug. 2019, doi: 10.3390/pharmaceutics11080407.

[13] V. Gribova *et al.*, "Polyanionic Hydrogels as Reservoirs for Polycationic Antibiotic Substitutes Providing Prolonged Antibacterial Activity," *ACS Appl. Mater. Interfaces*, vol. 12, no. 17, pp. 19258–19267, Apr. 2020, doi: 10.1021/acsami.9b23140.

CHAPTER 6.

General discussion and concluding remarks

Angela Cesaro

Department of Chemical Sciences, PhD in Biotechnology

University of Naples Federico II

General discussion and concluding remarks

The global expansion of antibiotic resistance has significantly decreased the effectiveness of conventional antibiotics [1]. Indeed, according to the Global Burden of Disease (GBD) study, skin and soft tissue infections (SSTIs) are the fourth leading cause of mortality and disability worldwide [2]. The so-called red-alert or ESKAPE pathogens (*Enterococcus faecium*, *Staphylococcus aureus*, *Klebsiella pneumoniae*, *Acinetobacter baumannii*, *Pseudomonas aeruginosa*, and *Enterobacter* species), which are resistant and recalcitrant to many front-line antimicrobials, are involved in several skin infections and diseases, such as dermatitis, *acne vulgaris*, psoriasis, pyoderma, cellulitis, and decubitus ulcers [3]. The bases of antibiotic resistance are defined by the bacterial response to the treatment. Consequently, the clinical definition of resistance depends on breakpoints of the minimal inhibitory concentrations (MICs), that determine therapeutic failure upon antibiotic treatment [4]. Antibiotics have a significant role in dermatologic field, being able to treat a wide range of diseases. Because of their excessive availability, they are susceptible to overuse within the medical practice, thus leading to the spreading of multidrug-resistant pathogens [5]. Three different types of antimicrobial resistance have been identified in the case of bacteria: intrinsic, acquired and phenotypic [1]. The activity of genes encoding antibiotic-inactivating enzymes, the lack of target, and the reduction in antibiotic permeability represent key elements mediating intrinsic resistance. This set of mechanisms diffuses among microbial populations by horizontal gene transfer and/or mutations, thus increasing the acquired resistance phenomenon. It has been also reported that bacterial strains usually susceptible may become transiently resistant upon a variation of physiological conditions, such as biofilm formation. This phenomenon has been defined as phenotypic resistant [4]. In this scenario, the design and discovery of novel antimicrobials less prone to induce the development of resistance phenotype are urgently needed. Antimicrobial peptides (AMPs) are small molecules involved in the body's first line of defense. They present evident advantages over conventional antibiotics, including a lower probability to induce resistance development, a broad-spectrum antimicrobial and antibiofilm properties, and the ability to modulate host immune response [1]. For this reason, the main aim of the present PhD thesis has been the design and the characterization of antimicrobial peptides able to counteract and treat resistant bacteria in skin and soft tissue infections.

In **Chapter 2**, the effectiveness of three AMPs, previously identified in human Apolipoprotein B100 (residues 887–922) *via* an algorithmic approach [6], has been evaluated against common skin resistant pathogens. Several mammalian proteins are reported to be a source of bioactive peptides, thus opening a new field in the research of novel antimicrobials [7]. Indeed, besides their physiological functions, lipoproteins have been hypothesized to play a key role in preventing bacterial infections, as key components of innate immunity [8]. ApoB derived peptides demonstrated significant broad-spectrum antimicrobial effects (2.5-20 μmol L^{-1}) on all the bacterial strains tested, including *K. pneumoniae*, *A. baumannii*, *P. aeruginosa* and *Staphylococci* strains. Interesting properties have been reported in the literature also for peptides derived from apolipoprotein E, such as apoEd, apoEdpL-F and $rApoE_{PM}$, that have been demonstrated to be active on *S. aureus*, *E. coli* and *P. aeruginosa* strains in concentrations ranging from 5 to 25 μmol L^{-1} [9][10]. This further reinforces the concept that AMPs encrypted in the human proteome represent an appealing source of an attractive class of molecules [11]. Moreover, as previously reported for several AMPs [12][13][14], the encrypted ApoB peptides were found to display their antimicrobial effects through depolarization of bacterial membranes, a presumed prerequisite for internalization into the cell or for cell direct lysis.

Over the past decades, several studies have demonstrated synergism between AMPs and conventional antibiotics. Indeed, renalexin was found to improve the activity of polymyxin E, doxycycline, and clarithromycin when drugs were tested in combination [1]. Similarly, the antimicrobial properties of ceftriaxone, amoxicillin–clavulanate, ceftazidime, meropenem, and piperacillin were found to increase by 4-8 times when combined with magainin 2 [1]. Interestingly, ApoB-derived peptides were found to potentiate the activity of conventional antibiotics towards common skin pathogenis. In particular, $r(P)ApoB_L^{Pro}$ and $r(P)ApoB_S^{Pro}$ were found to synergize with polymyxin B and colistin against the Gram-negative pathogen *K. pneumoniae* ATCC 70603, showing antimicrobial effects at concentrations significantly lower than those required in monotherapy. These findings suggest an interesting role of these peptides as adjuvants to be employed in the design of novel antimicrobial therapies. To date, promising combinatorial therapies have been clinically investigated in several trials involving drug-resistant infections [1]. The benefits of the design of a successful combination therapy based on AMPs and conventional antibiotics include a reduction in effective administered doses and in

hospitalization time, a shorter exposure time to antibiotics and, as a consequence, a lower probability to induce resistance phenotypes.
Importantly, it was demonstrated that the encrypted peptides under test did not select for bacterial resistance even when bacterial cells were subjected to a prolonged exposure. Indeed, while MIC_{100} values of gentamicin and colistin were found to increase by 4-10 folds, MIC_{100} values of ApoB-derived cryptides resulted unchanged in the same experimental conditions. Although no clear evidence exist about the timeframe required for a bacterial population to become resistant to AMPs [1], it has been extensively demonstrate that AMPs fast bactericidal effects and their mechanism of action based on multiple targets significantly decrease the probability to induce resistance phenotype [15]. It has also to be highlighted that the treatment of skin wounds and diseases is further complicated by the development of microbial biofilms. In recent years, several anti-biofilm approaches, such as quorum sensing antagonists, antibodies, anti-adhesion strategies, and bacteriophages, have been proposed to treat the resistance patterns of biofilm matrixes. A promising and effective strategy is also represented by the employment of anti-biofilm peptides, which act on specific targets, such as matrix components and/or highly conserved regulatory mechanisms [16]. For this reason, in **Chapter 2**, the anti-biofilm properties of ApoB-derived cryptides were investigated. The encrypted peptides were found to display significant anti-biofilm effects on the opportunistic skin pathogens *A. baumannii* ATCC 17878, *K. pneumoniae* ATCC 70603 and *S. epidermidis* ATCC 35984 by reducing biofilm biovolume, by altering matrix architecture and by inducing cell death. These effects are comparable to those described for several antibiofilm AMPs, such as the peptide P1 or human hepcidin 20 able to disrupt the architecture of *Streptococcus* and *Staphylococcus* biofilm by significantly decreasing viable bacterial cells [17][18]. In the case of ApoB-derived peptides, a strong deconstruction of biofilm matrix has been also reported. Obtained results open interesting perspectives to ApoB-derived peptides applicability in cosmeceutical field, since biofilms display increased resistance to antibiotic treatment and are associated with several human skin infections [19][20].
An important aspect to be considered in the development of a novel antimicrobial therapy is the biocompatibility of developed drug. Peptide-based therapeutics might exert cytotoxic effects by inducing allergic responses or by eliciting immunogenicity enhancement through an induction of cytokines activity [21][22]. In **Chapter 3**, multiple experimental approaches have been carried out to evaluate the

biocompatibility of ApoB-derived peptides on human skin cells and microbiome.
Slight toxic effects on human dermal fibroblasts have been detected at the highest peptide concentrations tested and only upon long exposure times, thus indicating that encrypted peptides under test are endowed with a satisfying cytotoxic profile. Interestingly, cancer cells were found to be more susceptible than normal cells to ApoB-derived peptides even if toxic effects were found not to be associated with cell membrane damage. This is in line with data reported in the literature for many anticancer AMPs [23], which exert their selective cytotoxicity towards tumoral cells through alterations of intracellular mechanisms [23]. Importantly, we also demonstrated that no increase in cytokines expression or release occurred when human macrophages were exposed to peptides, thus excluding potential immune responses induced by the treatment with peptides under test. Even more importantly, AMPs have been found to be able to modulate the immune response, a feature that makes them versatile drugs to be employed in the treatment of skin infections. Indeed, several opportunistic pathogens have been found to be able to activate the immune response of underlying skin cells at the site of injuries [24]. For this reason, we also evaluated the effects of ApoB-derived peptides on HDFs infected with *S. aureus*. Peptide r(P)ApoB$_S^{Pro}$ demonstrated to be able to decrease the expression levels of IL-8 and IL-6 pro-inflammatory cytokines in a co-culture system of human cells and bacteria, thus indicating that it is able to play an interesting role in host protection.
Side effects associated with antimicrobial therapies are also elicited by alterations in resident skin bacterial communities and by changes in host- commensals interactions [25]. Indeed, skin microbiota engages in a mutualistic relationship with the host by up- and down-regulating specific genes. Interestingly, ApoB-derived peptides have been found not to affect the activity of histone deacetylase enzymes, which play a key role in host-commensal calibration [26][27][28]. This suggests that the treatment of skin infections with peptides under study might not alter the crucial host-commensal balance. Furthermore, ApoB-derived peptides were demonstrated to display slight antimicrobial effects towards skin commensal population, thus revealing as a promising strategy to treat skin infections without significantly affecting skin microbial composition.
Despite their several advantages, antimicrobial peptides applicability has been limited by several factors including their high sensitivity to proteases present in biological systems [29]. Peptides susceptibility to proteolysis and their consequent inactivation in biological matrixes

make urgent the development of effective alternatives, such as modified synthetic peptides [30]. To improve the pharmacokinetic profile of AMPs, it is possible to design “peptidomimetics”, compounds endowed with essential elements mimicking a natural peptide, but with improved properties and stability with respect to the parental molecule [31]. To date, the retro-inverso modification of a peptide is an approach widely used to design novel and stable bioactive molecules [32]. As described in **Chapter 4**, a retro-inverso variant [(ri)-r(P)ApoB$_S^{Pro}$] of the shortest antimicrobial peptide identified in human ApoB has been here designed and characterized. The engineered peptidomimetic has been obtained by reversing the sequence of r(P)ApoB$_S^{Pro}$, in order to guarantee side-chain topology, and by replacing (L) with (D)-amino acids, in order to ensure structural stability. Similarly to RI1002, RIJK3, RIJK4 and RI10108 retro-inverso peptides [33], (ri)-r(P)ApoB$_S^{Pro}$ was found to share many of the biological features of the parental (L)-peptide while showing a higher stability in serum a stronger activity in an animal model of skin infection.

As we hypothesized, the antimicrobial activity of the retro-inverso peptidomimetic was found to be fully preserved upon exposure to serum proteases and analyses of its degradation profile confirmed a longer half-life with respect to that of the natural parental peptide. Importantly, MIC_{100} values and anti-biofilm effects of the retro-inverso peptidomimetic were found to be comparable to those of the lead natural peptide. Moreover, the presence of the enantiomeric amino acids was found not to alter peptide biocompatibility towards human skin cell lines and erythrocytes. (ri)-r(P)ApoB$_S^{Pro}$ was also found to be able to protect keratinocytes from infections, thus indicating that it has great potentialities to be employed as a novel antimicrobial drug in dermatological field. Indeed, the modifications applied to (L)-ApoB-derived peptide were found to significantly increase peptide stability both *in vitro* and *in vivo*. In experiments on a pre-clinical mouse model of skin infection, the retro-inverso peptidomimetic was found to display stronger anti-infective effects at doses significantly lower than those required to have the same effects in the case of the natural peptides. Hence, the strategy to engineer a retro-inverso variant entirely composed of D-enantiomeric amino acids was fundamental to overcome susceptibility issues, which have traditionally hindered the development of peptide and protein-based therapies [30], thus making this molecule suitable for future preclinical and clinical studies.

Skin wounds and infections affect millions of people annually worldwide. In this context, antimicrobial peptides have demonstrated great potentialities in effectively killing responsible bacteria with minimal

risks of resistance development [34]. It appears clear that the development of an optimized topical formulation guaranteeing high peptide stability and effective peptide release at the site of infection is a key step towards the development of a therapeutic strategy to be employed in dermatological field. For this purpose, in **Chapter 5**, it is described the development and characterization of a hyaluronic acid (HA)-based hydrogel functionalized with (ri)-r(P)ApoB$_S^{Pro}$. Hyaluronic acid polymer has several advantages, such as biocompatibility, biodegradability, and non-immunogenicity [35]. Furthermore, it is a component of the extracellular matrix, and plays an important role in wound healing processes and tissue repair [36]. Besides, the presence of hydrophilic groups and HA swelling ability are key elements facilitating the encapsulation of antimicrobials [37]. As described in **Chapter 5**, the hydrogel-based system demonstrated to encapsulate a high amount of peptide without losing its mechanical properties. Importantly, HA-based hydrogel loaded with (ri)-r(P)ApoB$_S^{Pro}$ was found to display antimicrobial properties on both Gram-negative and Gram-positive bacterial strains, including resistant ones. The newly developed delivery system was also found to rapidly release peptide molecules without affecting cell viability. When assayed on human skin cell lines, HA-based hydrogel functionalized with (ri)-r(P)ApoB$_S^{Pro}$ was rather found to significantly improve the viability of keratinocytes, thus suggesting that the system might exert promising positive effects in wound healing processes.

In conclusion, the results collected in the present PhD thesis demonstrated the anti-infective properties of ApoB-derived peptides against common skin pathogens. In addition to their direct antimicrobial and antibiofilm activities, the peptides were demonstrated to be able to synergize with classical antibiotics by enhancing their activity. Peptides also displayed excellent toxicity profiles while not selecting for bacterial resistance. A hyper-stable retro-inverso variant of the lead peptide was also designed and synthetized. It ensured efficacy *in vivo* and was encapsulated in a hydrogel-based system to be delivered at the target site. Altogether, these findings add an important step to the path leading to the development of a therapeutic option to be employed in dermatological field for the treatment of skin drug-resistant infections.

5. References

[1] M. Magana *et al.*, “The value of antimicrobial peptides in the age of resistance,” *Lancet Infect. Dis.*, vol. 20, no. 9, pp. e216–e230, Sep. 2020, doi: 10.1016/S1473-3099(20)30327-3.

[2] C. Karimkhani *et al.*, “Global Skin Disease Morbidity and Mortality,” *JAMA Dermatology*, vol. 153, no. 5, p. 406, May 2017, doi: 10.1001/jamadermatol.2016.5538.

[3] S. Santajit and N. Indrawattana, “Mechanisms of Antimicrobial Resistance in ESKAPE Pathogens,” *Biomed Res. Int.*, vol. 2016, pp. 1–8, 2016, doi: 10.1155/2016/2475067.

[4] J. Olivares, A. Bernardini, G. Garcia-Leon, F. Corona, M. B Sanchez, and J. L. Martinez, “The intrinsic resistome of bacterial pathogens.,” *Front. Microbiol.*, vol. 4, p. 103, 2013, doi: 10.3389/fmicb.2013.00103.

[5] S. Y. CHON, H. Q. DOAN, R. M. MAYS, S. M. SINGH, R. A. GORDON, and S. K. TYRING, “Antibiotic overuse and resistance in dermatology,” *Dermatol. Ther.*, vol. 25, no. 1, pp. 55–69, Jan. 2012, doi: 10.1111/j.1529-8019.2012.01520.x.

[6] R. Gaglione *et al.*, “Novel human bioactive peptides identified in Apolipoprotein B: Evaluation of their therapeutic potential,” *Biochem. Pharmacol.*, vol. 130, pp. 34–50, Apr. 2017, doi: 10.1016/j.bcp.2017.01.009.

[7] D. J. Autelitano, A. Rajic, A. I. Smith, M. C. Berndt, L. L. Ilag, and M. Vadas, “The cryptome: a subset of the proteome, comprising cryptic peptides with distinct bioactivities,” *Drug Discov. Today*, vol. 11, no. 7–8, pp. 306–314, Apr. 2006, doi: 10.1016/j.drudis.2006.02.003.

[8] R. Han, “Plasma lipoproteins are important components of the immune system,” *Microbiol. Immunol.*, vol. 54, no. 4, pp. 246–253, Apr. 2010, doi: 10.1111/j.1348-0421.2010.00203.x.

[9] B. A. Kelly *et al.*, “Apolipoprotein E-derived antimicrobial peptide analogues with altered membrane affinity and increased potency and breadth of activity,” *FEBS J.*, vol. 274, no. 17, pp. 4511–4525, Sep. 2007, doi: 10.1111/j.1742-4658.2007.05981.x.

[10] K. Pane *et al.*, “A new cryptic cationic antimicrobial peptide from human apolipoprotein E with antibacterial activity and

immunomodulatory effects on human cells," *FEBS J.*, vol. 283, no. 11, pp. 2115–2131, Jun. 2016, doi: 10.1111/febs.13725.

[11] A. Pfalzgraff, K. Brandenburg, and G. Weindl, "Antimicrobial Peptides and Their Therapeutic Potential for Bacterial Skin Infections and Wounds," *Front. Pharmacol.*, vol. 9, Mar. 2018, doi: 10.3389/fphar.2018.00281.

[12] G. Boix-Lemonche, M. Lekka, and B. Skerlavaj, "A Rapid Fluorescence-Based Microplate Assay to Investigate the Interaction of Membrane Active Antimicrobial Peptides with Whole Gram-Positive Bacteria," *Antibiotics*, vol. 9, no. 2, p. 92, Feb. 2020, doi: 10.3390/antibiotics9020092.

[13] R. N. Murugan *et al.*, "De Novo Design and Synthesis of Ultra-Short Peptidomimetic Antibiotics Having Dual Antimicrobial and Anti-Inflammatory Activities," *PLoS One*, vol. 8, no. 11, p. e80025, Nov. 2013, doi: 10.1371/journal.pone.0080025.

[14] W. Gao *et al.*, "Identification of a novel cathelicidin antimicrobial peptide from ducks and determination of its functional activity and antibacterial mechanism," *Sci. Rep.*, vol. 5, no. 1, p. 17260, Dec. 2015, doi: 10.1038/srep17260.

[15] R. Spohn *et al.*, "Integrated evolutionary analysis reveals antimicrobial peptides with limited resistance," *Nat. Commun.*, vol. 10, no. 1, p. 4538, Dec. 2019, doi: 10.1038/s41467-019-12364-6.

[16] R. E. W. Hancock and H.-G. Sahl, "Antimicrobial and host-defense peptides as new anti-infective therapeutic strategies," *Nat. Biotechnol.*, vol. 24, no. 12, pp. 1551–1557, Dec. 2006, doi: 10.1038/nbt1267.

[17] J. A. Perry and G. D. Wright, "Forces shaping the antibiotic resistome.," *Bioessays*, vol. 36, no. 12, pp. 1179–84, Dec. 2014, doi: 10.1002/bies.201400128.

[18] J. M. Ansari, N. M. Abraham, J. Massaro, K. Murphy, J. Smith-Carpenter, and E. Fikrig, "Anti-Biofilm Activity of a Self-Aggregating Peptide against Streptococcus mutans," *Front. Microbiol.*, vol. 8, Mar. 2017, doi: 10.3389/fmicb.2017.00488.

[19] C. de la Fuente-Núñez, F. Reffuveille, L. Fernández, and R. E. Hancock, "Bacterial biofilm development as a multicellular adaptation: antibiotic resistance and new therapeutic strategies,"

Curr. Opin. Microbiol., vol. 16, no. 5, pp. 580–589, Oct. 2013, doi: 10.1016/j.mib.2013.06.013.

[20] C. de la Fuente-Núñez, M. H. Cardoso, E. de Souza Cândido, O. L. Franco, and R. E. W. Hancock, “Synthetic antibiofilm peptides,” *Biochim. Biophys. Acta - Biomembr.*, vol. 1858, no. 5, pp. 1061–1069, May 2016, doi: 10.1016/j.bbamem.2015.12.015.

[21] M. Rahnamaeian and A. Vilcinskas, “Short antimicrobial peptides as cosmetic ingredients to deter dermatological pathogens,” *Appl. Microbiol. Biotechnol.*, vol. 99, no. 21, pp. 8847–8855, Nov. 2015, doi: 10.1007/s00253-015-6926-1.

[22] Y. Fujita and H. Taguchi, “Current status of multiple antigen-presenting peptide vaccine systems: Application of organic and inorganic nanoparticles,” *Chem. Cent. J.*, vol. 5, no. 1, p. 48, Dec. 2011, doi: 10.1186/1752-153X-5-48.

[23] C. Wang *et al.*, “Rapid Cytotoxicity of Antimicrobial Peptide Tempoprin-1CEa in Breast Cancer Cells through Membrane Destruction and Intracellular Calcium Mechanism,” *PLoS One*, vol. 8, no. 4, p. e60462, Apr. 2013, doi: 10.1371/journal.pone.0060462.

[24] E. M. Haisma, M. H. Rietveld, A. de Breij, J. T. van Dissel, A. El Ghalbzouri, and P. H. Nibbering, “Inflammatory and Antimicrobial Responses to Methicillin-Resistant Staphylococcus aureus in an In Vitro Wound Infection Model,” *PLoS One*, vol. 8, no. 12, p. e82800, Dec. 2013, doi: 10.1371/journal.pone.0082800.

[25] A. J. SanMiguel, J. S. Meisel, J. Horwinski, Q. Zheng, and E. A. Grice, “Topical Antimicrobial Treatments Can Elicit Shifts to Resident Skin Bacterial Communities and Reduce Colonization by Staphylococcus aureus Competitors.,” *Antimicrob. Agents Chemother.*, vol. 61, no. 9, Sep. 2017, doi: 10.1128/AAC.00774-17.

[26] M. Pernot, R. Vanderesse, C. Frochot, F. Guillemin, and M. Barberi-Heyob, “Stability of peptides and therapeutic success in cancer.,” *Expert Opin. Drug Metab. Toxicol.*, vol. 7, no. 7, pp. 793–802, Jul. 2011, doi: 10.1517/17425255.2011.574126.

[27] A. Schwarz, A. Bruhs, and T. Schwarz, “The Short-Chain Fatty Acid Sodium Butyrate Functions as a Regulator of the Skin Immune System,” *J. Invest. Dermatol.*, vol. 137, no. 4, pp. 855–

864, Apr. 2017, doi: 10.1016/j.jid.2016.11.014.

[28] P. Sittipo, J. Shim, and Y. Lee, “Microbial Metabolites Determine Host Health and the Status of Some Diseases,” *Int. J. Mol. Sci.*, vol. 20, no. 21, p. 5296, Oct. 2019, doi: 10.3390/ijms20215296.

[29] M. Pernot, R. Vanderesse, C. Frochot, F. Guillemin, and M. Barberi-Heyob, “Stability of peptides and therapeutic success in cancer,” *Expert Opin. Drug Metab. Toxicol.*, vol. 7, no. 7, pp. 793–802, Jul. 2011, doi: 10.1517/17425255.2011.574126.

[30] R. Serra *et al.*, “Chronic wound infections: the role of Pseudomonas aeruginosa and Staphylococcus aureus,” *Expert Rev. Anti. Infect. Ther.*, vol. 13, no. 5, pp. 605–613, May 2015, doi: 10.1586/14787210.2015.1023291.

[31] Y. A. Haggag, “Peptides as Drug Candidates: Limitations and Recent Development Perspectives,” *Biomed. J. Sci. Tech. Res.*, vol. 8, no. 4, Sep. 2018, doi: 10.26717/BJSTR.2018.08.001694.

[32] M. Chorev and M. Goodman, “A dozen years of retro-inverso peptidomimetics,” *Acc. Chem. Res.*, vol. 26, no. 5, pp. 266–273, May 1993, doi: 10.1021/ar00029a007.

[33] C. de la Fuente-Núñez *et al.*, “D-Enantiomeric Peptides that Eradicate Wild-Type and Multidrug-Resistant Biofilms and Protect against Lethal Pseudomonas aeruginosa Infections,” *Chem. Biol.*, vol. 22, no. 2, pp. 196–205, Feb. 2015, doi: 10.1016/j.chembiol.2015.01.002.

[34] R. K. Thapa, D. B. Diep, and H. H. Tønnesen, “Topical antimicrobial peptide formulations for wound healing: Current developments and future prospects,” *Acta Biomater.*, vol. 103, pp. 52–67, Feb. 2020, doi: 10.1016/j.actbio.2019.12.025.

[35] X. Xu, A. K. Jha, D. A. Harrington, M. C. Farach-Carson, and X. Jia, “Hyaluronic acid-based hydrogels: from a natural polysaccharide to complex networks,” *Soft Matter*, vol. 8, no. 12, p. 3280, 2012, doi: 10.1039/c2sm06463d.

[36] S. Trombino, C. Servidio, F. Curcio, and R. Cassano, “Strategies for Hyaluronic Acid-Based Hydrogel Design in Drug Delivery.,” *Pharmaceutics*, vol. 11, no. 8, p. 407, Aug. 2019, doi: 10.3390/pharmaceutics11080407.

[37] J. Li and D. J. Mooney, “Designing hydrogels for controlled drug

delivery," *Nat. Rev. Mater.*, vol. 1, no. 12, p. 16071, Dec. 2016, doi: 10.1038/natrevmats.2016.71.

ABBREVIATIONS

SSTIs: skin and soft tissue infections; MDR: multi-drug-resistant; **AMPs**: antimicrobial peptides; **HDPs**: host defence peptides; **IDR:** Innate Defense Regulatory; **HDL**, **LDH** and **VLDH** high-density, low-density and very low-density lipoproteins; **ApoB**: Apolipoprotein B; ATCC American Type Culture Collection; **DiSC$_3$-5** dye 3,3'-dipropylthiadicarbocyanine iodide; **IL-8**: interleukin 8, **IL-6**: interleukin 6; **MCP-1**: monocyte chemoattractant protein; **IFN-α**: interferon α; **TNF-α**: tumor necrosis factor; **LPS**: lipopolysaccharide; **LTA:** lipoteichoic acid; **MRSA:** methicillin-resistant Staphylococcus aureus; **MIC**: minimal inhibitory concentration; **TSA**: Tryptic Soy Agar; **MHB**: Muller Hinton Broth; **NB**: Nutrient Broth; **SD**: standard deviation; **SDS**: sodium dodecyl sulfate; **FIC**: fractional inhibitory concentration; **CATH-2**: cathelicidin-2; **PBS**: phosphate-buffered saline; **CFU**: colony forming unit; **CLSM**: Confocal Laser Scanning Microscopy **SEM**: Scanning Electron Microscopy; **TKC**: time killing curve; **PI**: Propidium iodide; **TFA**: trifluoroacetic acid; **MTT**: 3-(4,5-dimethylthiazol-2-yl)- 2,5-diphenyltetrazolium bromide; **HaCaT**: immortalized human keratinocytes; **A431**: human epidermoid carcinoma cells; **HDF:** human dermal fibroblasts; **DMEM**: Dulbecco's modified Eagle's medium; **FBS**: fetal bovine serum; **MOI:** multiplicity of infection; **qRT-PCR:** quantitative real-time PCR; **PMA**: phorbol 12-myristate 13-acetate; **HDAC**: histone deacetylase enzyme; **LDH:** Lactate dehydrogenase; **RP-HPLC/ESI-MS:** reverse-phase high performance liquid chromatography coupled to mass spectrometry; **CD:** circular dichroism; **TFE:** trifluoroethanol **RBCs:** human red blood cells; **HA**: hyaluronic acid; **BDDE**: butanediol diglycidyl ether; **HA-BDDE:** hyaluronic acid hydrogel crosslinked with 2.5% 1,4-butanediol diglycidyl ether; **GBD**: Global Burden of Disease.

List of Publications

1. Gaglione R.**,** Smaldone G., **Cesaro A.**, Rumolo M., De Luca M., Di Girolamo R., Oliva R., Del Vecchio P., Notomista E., Pedone E., Arciello A. **Impact of a single point mutation on the antimicrobial and fibrillogenic properties of cryptides from human apolipoprotein B.** *Pharmaceuticals* (Manuscript in preparation)

2. **Cesaro A.**, Der Torossian Torres M., Gaglione R., Dell'Olmo E., Di Girolamo R., Bosso A., Pizzo E., Haagsman H. P., Veldhuizen E.J.A., de la Fuente-Nunez C., Arciello A. **Synthetic antibiotic derived from sequences encrypted in human plasma apolipoprotein B.** Submitted to *Proceedings of the National Academy of Sciences of the United States of America (PNAS)*.

3. **Cesaro A.**, Bruno F., Nazzaro F., De Feo V., Khan H., Xiao J., Arciello A., Filosa R., **Biological effects of some mediterranean essential oils on human health: a minireview.** *Frontiers in Nutrition* (under revision)

4. Dell'Olmo E., Gaglione R., Sabbah M., Schibeci M., **Cesaro A.**, Di Girolamo R., Porta R., Arciello A. **Host defense peptides identified in human apolipoprotein B as novel food biopreservatives and active coating components.** *Food Microbiology* (under revision)

5. Dell'Olmo E., Gaglione R., **Cesaro A.**, Cafaro V., Teertstra W.R., de Cock H., Notomista E., Haagsman H.P., Veldhuizen E.J.A., Arciello A. **Host Defence Peptides identified in human Apolipoprotein B as promising antifungal agents.** *Applied Microbiology and Biotechnology*, vol. 105, no. 5, pp. 1953–1964, Mar. 2021, doi: 10.1007/s00253-021-11114-3.

6. Gaglione R., **Cesaro A.**, Dell'Olmo E., Di Girolamo R., Tartaglione L., Pizzo E., Arciello A. **Cryptides identified in human Apolipoprotein B as new weapons to fight antibiotic resistance in cystic fibrosis disease.** *International Journal of Molecular Sciences*, vol. 21, no. 6, p. 2049, Mar. 2020, doi: 10.3390/ijms21062049.

7. Gaglione R., **Cesaro A.**, Dell'Olmo E., Della Ventura B., Casillo A., Di Girolamo R., Velotta R., Notomista E., Veldhuizen E.J.A., Corsaro M.M., De Rosa C., Arciello A. **Effects of human antimicrobial cryptides identified in apolipoprotein B depend on specific features of bacterial strains.** *Scientific Report*, vol. 9, no. 1, p. 6728, Dec. 2019, doi: 10.1038/s41598-019-43063-3.

List of Communications

1. **Cesaro A.**, Der Torossian Torres M., Gaglione R., Dell'Olmo E., Di Girolamo R., Veldhuizen E.J.A., de la Fuente-Nunez C., Filosa R., Arciello A. 4th International Cosmetic Congress. Ankara, Turkey, December 4th-5th, 2020.

2. **Cesaro A.**, Gaglione R., Dell'Olmo E., Di Girolamo R., Notomista E., Veldhuizen E.J.A., Arciello A. **Novel therapeutic strategies based on cryptic HDPs to fight antibiotic resistance in skin diseases.** IMAP 2019, 9th International Meeting on Antimicrobial Peptides, Utrecht, Netherlands, August 28– 30, 2019.

3. Dell'Olmo E., Gaglione R., Giosafatto V. L. C., Di Girolamo R., **Cesaro A.**, Piccoli R., Notomista E., Veldhuizen E. J. A., Porta R., Arciello A. **Human apolipoprotein B: an unpredictable and promising source of novel food preservatives.** 2nd Workshop of Società Italiana Biochimici (SIB) 2019.

4. Gaglione R., **Cesaro A.**, Dell'Olmo E., Notomista E., Pizzo E., Arciello A. **Cryptides identified in human apolipoprotein B: new weapons to fight antibiotic-resistance in CF disease.** 13th European CF Young Investigators Meeting 2019. Paris, France, February 27th - March 1st

5. Dell'Olmo E., Gaglione R., Giosafatto C.V.L., Sabbah M., Di Girolamo R., **Cesaro A.**, Piccoli R., Notomista E., Veldhuizen E.J.A, Porta R., Arciello A. **Human Apolipoprotein B: an unpredictable and promising source of novel food preservatives.** ANTIMIC 2019, July 2-4, 2019, Lilliad, Villeneuve d'Ascq, University of Lille, FRANCE.

6. Gaglione R., Dell'Olmo E., **Cesaro A.**, Della Ventura B., Casillo A., Di Girolamo R., Notomista E., Pizzo E., Corsaro M.M., Auriemma F., Arciello A. **Novel insights into the mechanism of action of human cryptides identified in apolipoprotein B.** IMAP 2018, 8th International Meeting on Antimicrobial Peptides, Edinburgh, UK, September 2 – 4, 2018.

EXPERIENCE IN FOREIGN LABORATORIES

Visiting period at the Department of Infectious Diseases and Immunology, Division Molecular Host Defence, Faculty of Veterinary Medicine, Utrecht University, The Netherlands, from March 1st 2019 to September 1st 2019. The work was carried out in the lab of Professor Henk P. Haagsman and supervised by assistant Professor Edwin J. A. Veldhuizen.

Visiting period at AMP Biotec s.r.l, Apollosa (BN), Italy, from July 1st 2020 to January 1st 2021. The work was carried out in the lab of Dr Alberto di Crosta and supervised by Professor Rosanna Filosa.

ACKNOWLEDGEMENTS

During these three years, I imagined many times how I would write the most precious part of this thesis. I hope to find the right words to express the gratitude I feel for each of you.

Foremost, I would like to thank Prof. Angela Arciello for giving me the opportunity to work in her research group, introducing me to the world of science. Thank you for leading me and providing me the freedom to express myself, for giving me the opportunity to work on an exciting research project, and for having significantly contributed to my personal and professional growth.

Thanks to Dr. Rosa Gaglione, for the generosity with which she transmitted me all her knowledge, for her friendship and contagious positivity.

Thanks to Eliana, Maria, Shurooq, Luigi, Davide, Paola, Anna and Prof. Daria Monti, for sharing the daily life of the laboratory. Thanks for the support, the lunches, the coffee breaks, and all the fun times spent together. These three years would not have been the same without them.

Thanks to Prof. Edwin Veldhuizen, who lead me with patience and extreme sympathy in the six months I spent in the Netherlands and who, with his teachings, allowed me to acquire fundamental knowledge for my path. I would also thank Prof. Henk Haagsman for welcoming me with extreme cordiality in his laboratory, making me always feel part of his group. A special thanks go to Lianci with whom I shared moments of unforgettable and sincere friendship. I thank all the MHD group, Albert, Melanie, Hanne, Roel, Maaike, Ngoc, and Trev, for the unforgettable moments spent together in Utrecht.

Thanks to Prof. César de la Fuente, for giving me the opportunity to spend three months in his laboratory. His passion for science and the innovativeness of his ideas were, for me, a source of great inspiration. Thanks to Marcelo, for his precious teachings, for encouraging me to do my best, and for the perfect harmony with which we worked together. I would like to say Thanks also to all the members of de la Fuente Lab, Ester, Sebahat, Andreia, Adriane, and Marcelo M., for making the months spent in Philadelphia unique and unforgettable, never making me feel homesick.

Thanks to Prof. Rosanna Filosa and Dr Alberto Di Crosta, who introduced me to a completely new reality with experience and professionalism. Thank you so much for the trust placed in me, the precious advice, and teachings.

Thanks to Laurel, Hanna Pietro, and Diana, my unique housemates, without whom I would not have survived during the months I spent abroad.

Thanks to all my friends for always being encouraging, patiently listening to all my talks about science and the famous “antimicrobial peptides”.

A special thanks go to my wonderful family, for always being by my side, supporting me at all times. Thanks to my extraordinary parents for teaching me to always do my best in any situation, never betray myself and above all to always follow my passions. Thanks to my brother for being the shoulder I can always count on.

And lastly, special thanks to Francesco, for encouraging me every day, for sharing all my choices, and, above all, for always believing in me.

RINGRAZIAMENTI

Durante questi tre anni ho immaginato più volte come avrei scritto quella che probabilmente è la parte più importante di questa tesi. Spero di trovare le giuste parole per esprimere la gratitudine che provo per ognuno di voi.

Innanzitutto, vorrei ringraziare la Prof.ssa Angela Arciello, per avermi dato l'opportunità di lavorare nel suo gruppo di ricerca aprendomi le porte al mondo della scienza. Grazie per avermi fatto da guida lasciandomi sempre la libertà di esprimermi, di avermi dato la possibilità di lavorare ad un progetto di ricerca appassionante e di aver contribuito in maniera significativa alla mia crescita personale e professionale.

Grazie alla Dott.ssa Rosa Gaglione, per la generosità con cui mi ha trasmesso ogni sua conoscenza, per la sua amicizia e per la sua contagiosa positività.

Grazie ad Eliana, Maria, Shurooq, Luigi, Davide, Paola, Anna e con loro la Prof.ssa Daria Monti, per aver condiviso con me la quotidianità del laboratorio. Grazie per il supporto, i pranzi, le pause caffè e tutti i momenti divertenti trascorsi insieme. Questi tre anni non sarebbero stati gli stessi senza di loro.

Grazie al Prof. Edwin Veldhuizen, che mi ha guidato con pazienza ed estrema simpatia nei sei mesi trascorsi in Olanda e che, con i suoi insegnamenti, mi ha consentito di acquisire conoscenze fondamentali per il mio percorso. Con lui ringrazio il Prof. Henk Haagsman per avermi accolto con estrema cordialità nel suo laboratorio, facendomi sentire sempre parte del suo gruppo. Un ringraziamento speciale va a Lianci, con la quale ho condiviso momenti di indimenticabile e sincera amicizia. Ringrazio tutto il gruppo MHD, Albert, Melanie, Hanne, Roel, Maaike, Ngnoc e Treev, per gli indimenticabili momenti trascorsi insieme ad Utrecht.

Grazie al Prof. César De La Fuente, per avermi dato l'opportunità di trascorre tre mesi nel suo laboratorio. La sua passione per la scienza e l'innovatività delle sue idee sono state, per me, fonte di grande ispirazione. Grazie a Marcelo, per i suoi preziosi insegnamenti, per avermi spronata a dare il massimo e per la perfetta sintonia con cui abbiamo lavorato insieme. Vorrei dire Grazie anche a tutti i componenti del De La Fuente Lab, Ester, Sebahat, Andreia, Adriane e Marcelo M.,

per aver reso unici ed indimenticabili i mesi trascorsi a Philadelphia, non facendomi mai sentire nostalgia di casa.

Grazie alla Prof.ssa Rosanna Filosa e al Dott. Alberto Di Crosta, che, con esperienza e professionalità, mi hanno introdotto in una realtà a me completamente nuova. Grazie infinite per la fiducia riposta in me, i preziosi consigli e gli insegnamenti.

Grazie a Laurel, Hanna, Pietro e Diana, i miei unici coinquilini, senza i quali non sarei sopravvissuta durante i mesi trascorsi all'estero.

Grazie a tutti i miei amici per essere sempre stati di incoraggiamento, ascoltando pazientemente tutti i miei discorsi sulla scienza e sui famosi "peptidi antimicrobici".

Un ringraziamento speciale va alla mia splendida famiglia, per essermi sempre accanto, supportandomi in ogni momento. Grazie ai miei straordinari genitori per avermi insegnato a dare sempre il massimo in qualsiasi situazione, a non tradire mai me stessa e soprattutto a seguire sempre le mie passioni. Grazie, inoltre, a mio fratello per essere la spalla su cui posso sempre contare.

Ed infine, un grazie speciale a Francesco, per avermi incoraggiato ogni giorno, per aver condiviso tutte le mie scelte, e, soprattutto, per aver sempre creduto in me.

Applied Microbiology and Biotechnology
https://doi.org/10.1007/s00253-021-11114-3

BIOTECHNOLOGICALLY RELEVANT ENZYMES AND PROTEINS

Host defence peptides identified in human apolipoprotein B as promising antifungal agents

Eliana Dell'Olmo[1,2] · Rosa Gaglione[1,3] · Angela Cesaro[1] · Valeria Cafaro[4] · Wieke R. Teertstra[5] · Hans de Cock[5] · Eugenio Notomista[4] · Henk P. Haagsman[2] · Edwin J. A. Veldhuizen[2] · Angela Arciello[1,3]

Received: 9 July 2020 / Revised: 4 December 2020 / Accepted: 13 January 2021

Abstract

Therapeutic options to treat invasive fungal infections are still limited. This makes the development of novel antifungal agents highly desirable. Naturally occurring antifungal peptides represent valid candidates, since they are not harmful for human cells and are endowed with a wide range of activities and their mechanism of action is different from that of conventional antifungal drugs. Here, we characterized for the first time the antifungal properties of novel peptides identified in human apolipoprotein B. ApoB-derived peptides, here named r(P)ApoB$_L^{Pro}$, r(P)ApoB$_L^{Ala}$ and r(P)ApoB$_S^{Pro}$, were found to have significant fungicidal activity towards *Candida albicans* (*C. albicans*) cells. Peptides were also found to be able to slow down metabolic activity of *Aspergillus niger* (*A. niger*) spores. In addition, experiments were carried out to clarify the mechanism of fungicidal activity of ApoB-derived peptides. Peptides immediately interacted with *C. albicans* cell surfaces, as indicated by fluorescence live cell imaging analyses, and induced severe membrane damage, as indicated by propidium iodide uptake induced upon treatment of *C. albicans* cells with ApoB-derived peptides. ApoB-derived peptides were also tested on *A. niger* swollen spores, initial hyphae and branched mycelium. The effects of peptides were found to be more severe on swollen spores and initial hyphae compared to mycelium. Fluorescence live cell imaging analyses confirmed peptide internalization into swollen spores with a consequent accumulation into hyphae. Altogether, these findings open interesting perspectives to the application of ApoB-derived peptides as effective antifungal agents.

Key points

- *Human cryptides identified in ApoB are effective antifungal agents.*
- *ApoB-derived cryptides exert fungicidal effects towards C. albicans cells.*
- *ApoB-derived cryptides affect different stages of growth of A. niger.*

Keywords Antifungal peptides · Human cryptides · Fungal infections · Peptide therapeutics

Introduction

The emergence of fungal infections represents a worldwide issue with a serious economic and social impact (Ciociola et al. 2016). Since the 1980s, an increase in cases of serious invasive fungal infections is observed due to the growing number of highly susceptible people, mainly immunocompromised, elderly and transplanted subjects, cancer patients and premature infants (Brown et al. 2012). Fungal pathogens as *Candida*, *Aspergillus*, *Pneumocystis*, and *Cryptococcus* spp.

✉ Edwin J. A. Veldhuizen
e.j.a.veldhuizen@uu.nl

✉ Angela Arciello
anarciel@unina.it

[1] Department of Chemical Sciences, University of Naples Federico II, 80126 Naples, Italy

[2] Department of Biomolecular Health Sciences, Division of Infectious Diseases and Immunology, Section Molecular Host Defence, Faculty of Veterinary Medicine, Utrecht University, Utrecht, The Netherlands

[3] Istituto Nazionale di Biostrutture e Biosistemi (INBB), Rome, Italy

[4] Department of Biology, University of Naples Federico II, 80126 Naples, Italy

[5] Molecular Microbiology, Department of Biology, Faculty of Science, Utrecht University, Utrecht, The Netherlands

Published online: 12 February 2021

are responsible for 1.4 million deaths each year (Brown et al. 2012; Sanglard 2016). The situation is even more complicated because of the variety and non-specificity of symptoms (Schmiedel and Zimmerli 2016), ranging from either mild and superficial (e.g. cutaneous infections as dermatophytosis and tinea versicolor) to life-threatening, systemic illness (e.g. candidiasis, aspergillosis and mucomycosis).

Infections by *Candida* and *Aspergillus* species

Although *C. albicans* is a normal commensal for humans (Hancock and Lehrer 1998; Bennett et al. 2014), it is responsible for 75% of women vaginal candidiasis and for 90% of oropharyngeal candidiasis in HIV-infected patients with AIDS (Staab 1999; Sobel 2007). Indeed, *C. albicans* has been found to be able to invade a local site (mucocutaneous or cutaneous candidiasis, onychomycosis) or to cause systemic infections (renal, liver abscess, lung and nervous central system) (Badiee and Hashemizadeh 2014). It has also been reported that *Candida* species are the most common pathogens responsible for infections in hospitalized patients characterized by a high mortality rate (Strollo et al. 2017). Among fungal species able to colonize humans, *Aspergillus* spp. have been reported to be responsible for several types of infections and allergic bronchopulmonary aspergillosis (Anaissie et al. 2002; Alastruey-Izquierdo et al. 2013; Badiee and Hashemizadeh 2014). Indeed, *Aspergillus* ubiquitous spores are able to reach the respiratory tract by inhalation, thus causing noninvasive and invasive pulmonary aspergillosis, the latter especially in immunocompromised hosts. Along with the difficulties in the diagnosis, the narrow spectrum of available antifungals leads to the rapid rise of resistance phenotypes (Cowen et al. 2015; Fisher et al. 2018a). Indeed, the therapeutic options for invasive fungal infections are limited to only three structural classes of drugs, such as polyenes, azoles and echinocandins (Morita and Nozawa 1985; Roemer and Krysan 2014). Polyenes, including amphotericin B, exert significant toxic effects that might be overcome by developing awfully expensive formulations. For these reasons, the most tolerated azoles or echinocandins are the preferred therapeutic option (Bellmann and Smuszkiewicz 2017). Examples are represented by fluconazole to treat *Candida* infections or voriconazole to treat aspergillosis. Echinocandins are effective against several fungal strains, such as *Candida* spp., including no-*albicans* strains, and have been reported to exert fungistatic effects on *Aspergillus* spp. (Bowman et al. 2002; Bellmann and Smuszkiewicz 2017). Unfortunately, many cases of resistant fungal strains have been reported, due to the lower number of antifungal drugs available and to delays in diagnosis (Cowen et al. 2015; Fisher et al. 2018b). Hence, the discovery and development of novel alternative strategies is imperative.

Host defence peptides as antifungal peptides

Host defence peptides (HDPs), which comprise antifungal peptides (AFPs), may represent valid candidates (Sun et al. 2018; Mookherjee et al. 2020) (Zasloff 2002; Thevissen et al. 2007; Lupetti et al. 2008) because of their unique properties, such as their selectivity towards bacterial/fungal cells, their mechanism of action, which is different from that of conventional antifungal drugs and their moderate toxicity and immunogenicity (Lupetti et al. 2008; Aoki and Ueda 2013; Ciociola et al. 2016). Antifungal peptides represent a group of evolutionarily conserved molecules of the innate immune system present in all complex living organisms. They are characterized by common features, such as small size, positive net charge and high hydrophobicity (Thery et al. 2019a). Based on their mechanism of action, they can be classified into (i) membrane traversing peptides, which are able to lead membrane pore formation or to act on specific targets, such as β-glucan or chitin synthesis; and (ii) non-membrane traversing peptides, which interact with cell membrane and consequently cause cell lysis (Neelabh et al. 2016). Nowadays, more than 1200 antifungal peptides isolated from bacteria, other fungi, plants and animals have been identified and listed in databases (Essig et al. 2014; Thery et al. 2019a). Mammalian organisms release a large amount of AFPs as components of the innate immune system. Examples are α- and β-defensins, cathelicidins and histatins (Kościuczuk et al. 2012; Cuperus et al. 2013; Bondaryk et al. 2017), which have been found to be effective towards a wide range of fungal pathogens (Mookherjee et al. 2020), including *C. albicans* and *Aspergillus spp.*

ApoB-derived peptides as antifungal peptides

Here, we analysed for the first time the antifungal properties of three recombinant peptides identified in human apolipoprotein B (Gaglione et al. 2017; Gaglione et al. 2019b; Gaglione et al. 2019a), here named r(P)ApoB$_L^{Pro}$, r(P)ApoB$_L^{Ala}$ and r(P)ApoB$_S^{Pro}$, where (P) indicates the presence of an additional Pro residue at the N-terminus of the peptides released by the acidic cleavage of an Asp-Pro bond; superscripts "Pro" and "Ala" stand for the amino acid residue at position 7 (Gaglione et al. 2020), whereas subscripts "L" and "S" indicate a longer and a shorter version of the identified peptide, respectively (Gaglione et al. 2017; Gaglione et al. 2020). Peptides' sequences, lengths, isoelectric points, experimental and theoretical molecular weights and net charges at neutral pH are reported in Table 1. In the present study, we found that ApoB-derived peptides exert significant fungicidal effects towards *C. albicans* cells by affecting membrane permeability. ApoB-derived peptides have been found to inhibit *A. niger* filamentous fungus strongly also. Indeed, peptides were demonstrated to slow down the metabolic activity of *A. niger* spores, hyphae and

Table 1 Peptides' sequences, lengths, isoelectric points, experimental and theoretical molecular weights, and net charges at neutral pH

Peptide	Sequence	Length	Experimental *Mr*	Theoretical *Mr*	Isoelectric point	Net charge at neutral pH
r(P)ApoB$_L^{Pro}$	**P**HVALKPGKLKFIIPSPKRPVKLLSGGNTLHLVSTTKT	37	4076.96 Da	4074.96 Da	11.4	7.2
r(P)ApoB$_L^{Ala}$	**P**HVALKAGKLKFIIPSPKRPVKLLSGGNTLHLVSTTKT	37	4044.75 Da	4048.92 Da	11.4	7.2
r(P)ApoB$_S^{Pro}$	**P**HVALKPGKLKFIIPSPKRPVKLLSG	26	2820.85 Da	2821.54 Da	11.3	6.1
r(C)ApoB$_L^{Pro}$	**C**HVALKPGKLKFIIPSPKRPVKLLSGGNTLHLVSTTKT	37	4465.64 Da	4468.28 Da	10.69	7.1

branched mycelium by internalization into germinating spores and consequent accumulation into hyphae. Our results strongly suggest that ApoB-derived peptides represent valid candidates for the development of novel antifungal agents.

Materials and methods

Materials

All reagents were purchased from Merck (Milan, Italy), unless specified otherwise. CATH-2 peptide was obtained from CPC Scientific Inc. (Sunnyvale, USA).

Fungal strains and growth conditions

Cultures of *C. albicans* ATCC 10231 were grown on Yeast Malt (YM) agar plates. For all the experiments, yeasts were cultured at 30 °C in 10 mL yeast extract peptone dextrose broth (YPD) until mid-logarithmic phase was reached. Growth rate was monitored by measuring optical density (OD) values at 620 nm; when mid-logarithmic phase was reached, *Candida* cells were collected and diluted to 2×10^6 CFU/mL in 1/100 YM broth. To determine minimal fungicidal concentration (MFC) values, tenfold dilutions of culture were plated into YM broth. *A. niger* N402 was grown at 30 °C in 20-mL minimal medium (MM) (De Vries et al. 2004) containing 2% glucose and 1.5% agar. Conidia used to inoculate cultures were harvested from 4-day-old colonies by using a solution containing 0.8% NaCl and 0.005% Tween-80.

Expression ad isolation of recombinant ApoB-derived peptides

Expression and isolation of recombinant peptides were performed as described previously (Gaglione et al. 2017; Pane et al. 2018b; Gaglione et al. 2019b; Gaglione et al. 2020). ApoB-derived peptides' sequences are reported in Table 1.

Production of fluorescently labelled r(C)ApoB$_L^{Pro}$

r(C)ApoB$_L^{Pro}$ was obtained by chemical hydrolysis of purified ONC-DCless-H6-(C)-ApoB$_L^{Pro}$ fusion protein in 5 M guanidine-HCl containing 1 mM TCEP (tris(2-carboxyethyl)phosphine) at pH 7.4. A chimeric construct was expressed and purified as previously reported (Gaglione et al. 2017; Pane et al. 2018b; Gaglione et al. 2019b; Gaglione et al. 2020). Peptide release was monitored by reversed-phase high-performance liquid chromatography (RP-HPLC) carried out by using a Jasco LC-4000 system equipped with PU-4086 semipreparative pumps and MD-4010 photo diode array detector. A Europa Protein 300 C18 column (5 μm, 25 × 1) from Teknokroma (Barcelona, Spain) was used. Solvents were

0.05% trifluoroacetic acid (TFA) in water (solvent A) and 0.05% TFA in acetonitrile (solvent B). Elution profiles were recorded by a linear gradient as follows: from 5 to 25% solvent B in 10 min, from 25 to 35% solvent B in 30 min, from 35 to 50% solvent B in 10 min, from 50 to 100% solvent B in 10 min, and isocratic elution at 100% solvent B for 10 min. Elution was monitored at 214 nm at a flow rate of 2 mL/min. r(C)ApoB$_L^{Pro}$ peptide was then purified by a column-free procedure based on different solubilities of carrier and peptide at pH 7.0 (Pane et al. 2018b). To this purpose, the hydrolysis mixture was neutralized by adding a diluted ammonia solution for 5 min at 28 °C under nitrogen atmosphere. Insoluble fusion protein and carrier were then separated from soluble peptide by 10-min centrifugation at 18,000 g at 4 °C. The soluble fraction was analysed by RP-HPLC performed by using a Europa Protein 300 C18 column (Teknokroma, Barcelona, Spain) as previously described, in order to evaluate peptide purity. Supernatant, containing soluble peptide, was subjected to the labelling reaction.

Labelling of purified peptide

r(C)ApoB$_L^{Pro}$ N-terminal cysteine reactive residue was labelled with the thiol-reactive probe 5-iodoacetamidofluorescein (5'-IAF), in order to produce 5'-IAF-r(C)ApoB$_L^{Pro}$ labelled peptide. Purified r(C)ApoB$_L^{Pro}$ peptide (9.6 mg, 60 μM final concentration) was incubated with 5'-IAF (0.25 mM final concentration; 15 mM stock solution in dimethyl formamide) in 15 mM sodium phosphate buffer (NaP) pH 7.4 containing 2 M guanidine-HCl for 2 h at 25 °C in the dark under nitrogen atmosphere. Molar ratio of 5'-IAF over thiols was 4:1. r(C)ApoB$_L^{Pro}$ labelling reaction was monitored by RP-HPLC performed on a Europa Protein 300 C18 column as reported above (Figure S2). To simplify peptide purification by RP-HPLC, the reaction was quenched by adding L-cysteine in a molar excess of 10:1 on 5'-IAF for 1 h at 37 °C in the dark. 5'IAF-r(C)ApoB$_L^{Pro}$ was purified by RP-HPLC and lyophilized and resuspended in water. Labelled peptide concentration was determined using the molar extinction coefficient reported in the literature (5'-IAF ε492 nm = 80,000–85,000 M^{-1} cm^{-1}) and by BCA colorimetric assay. Purity of labelled peptide was evaluated by RP-HPLC performed on Europa Protein 300 C18 column.

Determination of minimal fungicidal concentration values

MFC (minimum fungicidal concentration) values were assessed by colony counting assays, as previously described (Van Dijk et al. 2007), with few modifications. Briefly, 50 μL of a 2 × 10^6 CFU/mL suspension of *C. albicans* ATCC 10231 cells in 1/100 YM broth were incubated for 3 h at 37 °C with an equal volume of peptide (0–40 μM). Tenfold dilutions in YM broth were then plated onto YPD agar plates and incubated overnight at 37 °C. Finally, colonies of surviving yeast cells were counted.

Killing kinetic studies

To kinetically analyse fungicidal activity of ApoB-derived peptides, experiments on *C. albicans* ATCC 10231 cells were performed. Yeast cells grown overnight in YM (Yeast Malt) medium were diluted in fresh YM medium and then incubated at 37 °C until logarithmic phase of growth was reached. Yeasts were then diluted to 2 × 10^6 CFU/mL in a final volume of 500 μL in 1/100 YM broth and mixed with the peptides (1:1 v/v). Increasing concentrations of peptide were analysed (ranging from 0 to 20 μM). At defined time intervals, samples (20 μL) were serially diluted (from 10- to 10,000-fold), and 100 μL of each dilution was plated on YPD Agar. Following an incubation of 16 h at 37 °C, yeast colonies were counted.

PI uptake assay

Propidium iodide uptake was monitored as previously described (Stone et al. 2003) with some modifications. Briefly, 45 μL of 1 × 10^7 CFU/mL of *C. albicans* ATCC 10231 cells were plated into 96-well plates, treated with 45 μL of peptides with increasing concentrations (0–20 μM) and incubated for 1 h at 37 °C. After that, 10 μL of PI at a final concentration of 5 μM was added. After 10 min of incubation, PI fluorescence was measured by using a microtiter plate reader (FLUOstar Omega, BMG LABTECH, Germany) at an excitation wavelength of 485 nm and an emission wavelength of 650 nm. The percentage of PI uptake was calculated as follows: [F(sample)-F(CTRL)/F(100%) − F(CTRL)] × 100, where F(CTRL) is the fluorescence of untreated sample and F(100%) is the fluorescence of heat-treated samples (15 min at 95 °C).

ATP release assay

ATP released by cells exposed to peptides was measured by using an ATP determination kit from Molecular Probes (Life Sciences, Bleiswijk, The Netherlands). Briefly, a suspension of 1 × 10^7 CFU/mL *C. albicans* ATCC 10231 cells in 1:100 YM was incubated with increasing concentrations of each peptide for 10 and 60 min at 37 °C. Samples were then centrifuged for 1 min at 1200×*g* and the supernatant was stored on ice for ATP determination, performed as described by the manufacturer. ATP concentration in control samples was found to be lower than 10 nM (data not shown).

Localization of 5′-IAF-r(C)ApoB$_L^{Pro}$ by confocal laser scanning live imaging microscopy

Experiments were performed as previously described by Jang and co-workers with some modifications (Jang et al. 2010). For all the experiments, 35-mm culture dishes (FluoroDish™, WPI, Sarasota, FL) were coated with 0.5 mg/mL Concanavalin A in water. A suspension (100 μL) of 1×10^7 CFU/mL *C. albicans* ATCC 10231 in 1:100 YM medium was then added. Fluorescently labelled peptide (50 μL) was added in the medium containing 5 μM PI. In the case of *A. niger* N402 hyphae, 100 μL of a solution of 1×10^7 spores/mL were incubated at 37 °C for 24 h in the presence of peptides. At defined time points (0, 16 and 24 h), analyses were performed. Images were acquired by using a Leica SPE-II and a 63× objective at the Centre for Cell Imaging (CCI)—Utrecht University. A 488-nm argon laser and a 561-nm DPSS laser were used for simultaneous detection of 5'-IAF-r(C)ApoB$_L^{Pro}$ and PI, respectively.

Metabolic activity analyses

The effects of ApoB-derived peptides on *A. niger* N402 metabolic activity were analysed by using cell proliferator reagent WST-1 (Roche Applied Science, Mannheim, Germany). Briefly, 45 μL of a 1×10^5 spores/mL suspension in MM were incubated for 24 h at 30 °C with an equal volume of peptide (0–40 μM). In each well, 10 μL of WST-1 10× were added. At defined time intervals, sample absorbance values were measured at 450 nm by using 650 nm as reference wavelength at a microtiter plate reader (FLUOstar Omega, BMG LABTECH, Germany). To investigate the effects of ApoB-derived peptides on *A. niger* N402 swollen spores, hyphae, and mycelium, these were incubated in MM containing 2% glucose for 6, 16 and 24 h prior to treatment with peptides, respectively.

Statistical analyses

Statistical analysis was performed using ANOVA or Student's *t* test. Significant differences were indicated as *($P < 0.05$), **($P < 0.01$), ***($P < 0.001$) or ****($P < 0.0001$).

Results

Antifungal activity of r(P)ApoB$_L^{Pro}$, r(P)ApoB$_S^{Pro}$ and r(P)ApoB$_L^{Ala}$ peptides

The antifungal properties of recombinant ApoB-derived peptides were tested. First of all, we evaluated purity and integrity of the peptides by performing SDS-PAGE and mass spectrometry analyses, as shown in Supplementary Figures S1 and S2. We firstly investigated the effects of peptides on *C. albicans* ATCC 10231. For this purpose, increasing amounts of r(P)ApoB$_L^{Pro}$, r(P)ApoB$_S^{Pro}$ or r(P)ApoB$_L^{Ala}$ were incubated with the fungal cells for 3 h and the chicken CATH-2 peptide was used as positive control. As shown in Fig. 1, ApoB-derived peptides were found to exert a strong fungicidal activity towards *C. albicans* ATCC 10231 at 10 μM of r(P)ApoB$_L^{Pro}$ and r(P)ApoB$_L^{Ala}$ and at 20 μM for the shorter version of the peptide. MFC_{100} (minimal fungicidal concentrations) values determined when peptides were tested on *C. albicans* ATCC 10231 are reported in Supplementary Table S1.

In *order* to analyse the antifungal effects of ApoB-derived HDPs over time, kinetic killing curves were obtained by treating *C. albicans* ATCC 10231 with increasing concentrations of each peptide and for different time intervals. At the highest peptide concentrations tested (5-10 μM), *C. albicans* ATCC 10231 was killed within 10 min, whereas, at lower concentrations (5 μM), the same effects were observed after 180 min (Fig. 2).

Effects of ApoB-derived peptides on yeast cell membranes

In order to determine the mechanism of fungicidal activity of ApoB-derived HDPs, propidium iodide uptake was analysed upon treatment of *C. albicans* ATCC 10231 cells with peptides. *C. albicans* ATCC 10231 cells were treated with ApoB-derived peptides at concentrations corresponding to MFC values for 1 h at 37 °C. A significant increase of propidium iodide uptake was selectively observed in the case of cells treated with ApoB-derived peptides (Fig. 3). This clearly suggests that ApoB-derived peptides' antifungal activity against

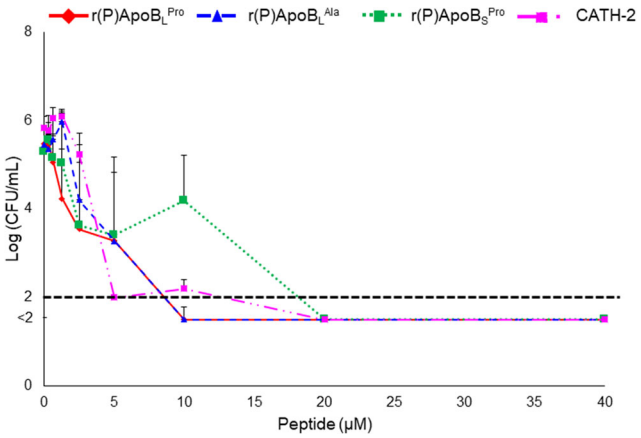

Fig. 1 Antifungal activity of r(P)ApoB$_L^{Pro}$, r(P)ApoB$_L^{Ala}$ and r(P)ApoB$_S^{Pro}$ peptides. Minimum fungicidal concentration (MFC) values were assessed by colony count assays. Data represent the mean (± SEM) of three independent experiments, each one carried out with triplicate determinations. CATH-2 peptide was used as a positive control. Point values below the black dashed line represent conditions in which 0 colonies were counted

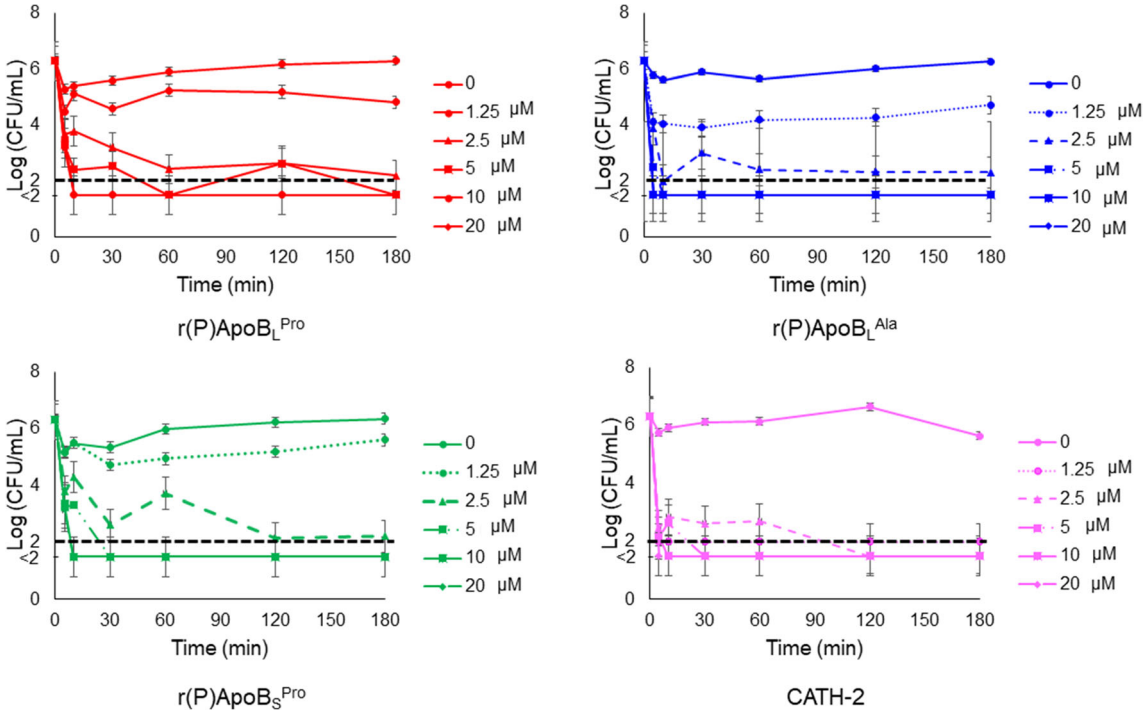

Fig. 2 Time killing curves obtained by incubating *C. albicans* ATCC 10231 with increasing concentrations of r(P)ApoB$_L^{Pro}$, r(P)ApoB$_L^{Ala}$ or r(P)ApoB$_S^{Pro}$ peptides for different time intervals. Data represent the mean (± SEM) of at least three independent experiments, each one carried out with triplicate determinations. Point values below the black dashed lines represent conditions in which 0 colonies were counted

C. albicans ATCC 10231 cells was mediated by membrane permeabilization. To support this finding, the effects of ApoB-derived peptides on ATP leakage were also evaluated. To this purpose, *C. albicans* ATCC 10231 cells were treated with ApoB-derived peptides at concentrations corresponding to MFC values for 10 and 60 min at 37 °C. Interestingly, it was observed that r(P)ApoB$_L^{Pro}$, r(P)ApoB$_L^{Ala}$ and r(P)ApoB$_S^{Pro}$ peptides induce ATP release from *C. albicans* ATCC 10231 cells after 10 min of incubation, with a slight increase after 60-min incubation only in the case of r(P)ApoB$_L^{Pro}$ (Fig. 4). These results support propidium iodide data reported in Fig. 4 and indicate that membrane permeabilization occurs upon peptide treatment. Altogether, these findings allow us to hypothesize a fast interaction between ApoB-derived peptides and *C. albicans* ATCC 10231 cell membranes.

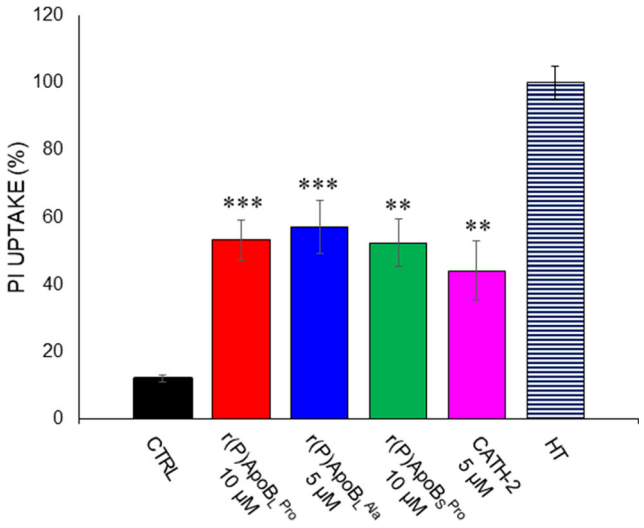

Fig. 3 Propidium iodide (PI) uptake into *C. albicans* ATCC 10231 cells upon treatment with r(P)ApoB$_L^{Pro}$, r(P)ApoB$_L^{Ala}$ or r(P)ApoB$_S^{Pro}$. PI uptake was determined by a spectrofluorometric assay. Data represent the mean (± SEM) of at least three independent experiments, each one carried out with triplicate determinations. Significant differences were found to be ****$P < 0.0001$ for treated *versus* control samples. CATH-2 peptide and the heat-treated cells were used as positive controls

Intracellular localization of ApoB-derived peptides in *C. albicans* ATCC 10231 cells

In order to further investigate the mechanism of action of ApoB-derived peptides, live imaging analyses were carried out. To this purpose, *C. albicans* ATCC 10231 cells were treated with a fluorescent version of r(P)ApoB$_L^{Pro}$ peptide, here named 5'-IAF-r(C)ApoB$_L^{Pro}$ (see the "Materials and methods" section for details) (Pane et al. 2018b; Pane et al. 2018a). The effects of 5'-IAF-r(C)ApoB$_L^{Pro}$ on *C. albicans* ATCC 10231 cells were found to be identical to those of r(C)ApoB$_L^{Pro}$, as reported in Supplementary Table S1 and in Supplementary Figure S3, thus indicating that the labelling procedure does not alter the peptide's mechanism of action.

C. albicans ATCC 10231 cells were treated with 10 μM 5'-IAF-r(C)ApoB$_L^{Pro}$ for 30 min in the presence of propidium

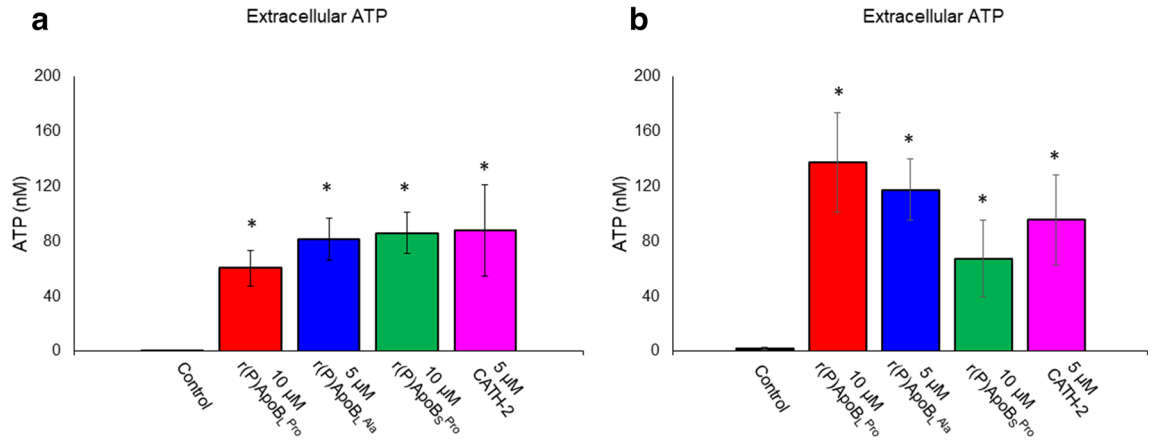

Fig. 4 ATP release from *C. albicans* ATCC 10231 cells upon treatment with r(P)ApoB$_L^{Pro}$, r(P)ApoB$_L^{Ala}$ or r(P)ApoB$_S^{Pro}$. ATP release was determined in the culture medium. Data represent the mean (± SEM) of at least three independent experiments, each one carried out in duplicate, upon an incubation of 10 (A) or 60 min (B) with each peptide. Significant differences were found to be $*P < 0.05$ for treated *versus* control samples. CATH-2 peptide was used as a positive control

iodide dye. Upon treatment, *C. albicans* ATCC 10231 cells were analysed by confocal laser scanning live imaging microscopy. Interestingly, fluorescently labelled peptide (green signal in Fig. 5) immediately appeared and localized at the fungal surface, with a progressive increase of fluorescent signal intensity over time (Fig. 5). Real tracking of 5'-IAF-r(C)ApoB$_L^{Pro}$ is provided as a supplementary movie. In agreement with this, a progressive uptake of propidium iodide in treated cells was observed over time (red signals associated to *Candida* cells). The phenomenon appears clearly evident even if red spots, probably due to aggregation of PI in culture medium, appear visible outside the cells. This suggests that peptide interaction with yeast membranes is immediately responsible for severe membrane damages (Fig. 5).

Analysis of ApoB-derived peptides effects on *A. niger* N402

The effects of ApoB-derived peptides were also tested on the filamentous fungus *A. niger* N402. To this purpose, metabolic activity of fungal spores in the absence or in the presence of increasing concentrations of peptides was evaluated by

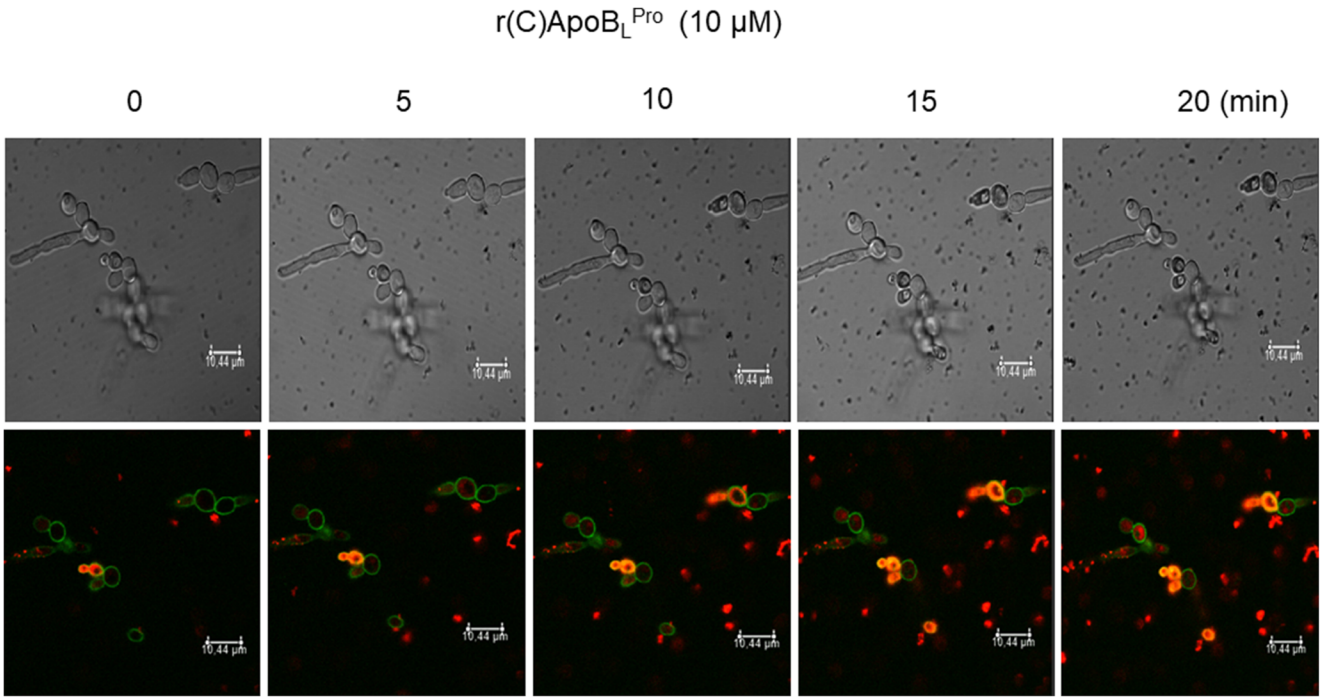

Fig. 5 Localization of 5'-IAF-r(C)ApoB$_L^{Pro}$ peptide (green signal) into *C. albicans* ATCC 10231 cells in the presence of propidium iodide (PI) dye (red signal) analysed by confocal laser scanning live imaging microscopy. Movies are provided as Supplementary material. Scale bar10 µm

performing WST-1 assays. Interestingly, r(P)ApoB$_L^{Pro}$, r(P)ApoB$_L^{Ala}$, r(P)ApoB$_S^{Pro}$ and CATH-2 peptides were found to reduce *A. niger* N402 spores' metabolic activity in a dose-dependent manner (Fig. 6). On the basis of the results of metabolic activity assays, MFC_{50} (minimal fungicidal concentrations) values were calculated for *A. niger* spores as the peptide concentration required to inhibit the metabolic activity of spores by 50%. Data are reported in Supplementary Table S1. Filamentous fungi like *A. niger* reproduce asexually and form spores (or conidia) which easily spread in the environment. Spores are metabolically dormant and germinate under favourable environmental conditions (van Leeuwen et al. 2013). The switch from dormant spores to mycelium formation is associated with a defined sequence of events. During this process, fungi go through morphological changes associated with cell wall reorganization (Wendland 2001). For this reason, the effects of ApoB-derived peptides and CATH-2 were tested on swollen spores, initial hyphae and branched mycelium. To analyse the effects of peptides on swollen spores, spores were incubated for 6 h in minimal medium (MM). Following incubation, peptides were added at different concentrations and metabolic activity was analysed after a further 24-h incubation. It was found that ApoB-derived peptides, as well as CATH-2, were able to significantly affect the metabolic activity of swollen spores (Fig. 6). The effects of the peptides on initial hyphae were also analysed. To this purpose, *A. niger* N402 spores were incubated for 16 h, in order to allow germination and hyphal outgrowth. ApoB-derived HDPs were then added for a further 24 h and, at the end of the incubation, the WST-1 assay was performed to test the metabolic activity. Interestingly, all three ApoB-derived peptides were found to significantly affect metabolic activity of newly formed hyphae, while CATH-2 was effective only at the highest concentration tested (Fig. 6). When branched mycelium was analysed, r(P)ApoB$_L^{Ala}$ and r(P)ApoB$_S^{Pro}$ were found to be the most effective peptides, whereas r(P)ApoB$_L^{Pro}$ was found to be able to significantly reduce metabolic activity only at the highest concentration tested (40 μM). CATH-2 was, instead, found to be ineffective (Fig. 6).

Analysis of fluorescently labelled r(C)ApoB$_L^{Pro}$ internalization into *A. niger* N402

In order to further characterize the effects of ApoB-derived peptides on *A. niger* N402, spores were incubated with 10-μM fluorescently labelled r(C)ApoB$_L^{Pro}$ for 24 h at 30 °C. Following incubation, confocal laser scanning microscopy analyses highlighted the ability of the 5'-IAF-r(C)ApoB$_L^{Pro}$ peptide to interact with swollen spores. Indeed, upon 16-h incubation, 5'-IAF-r(C)ApoB$_L^{Pro}$ was found to accumulate into initial

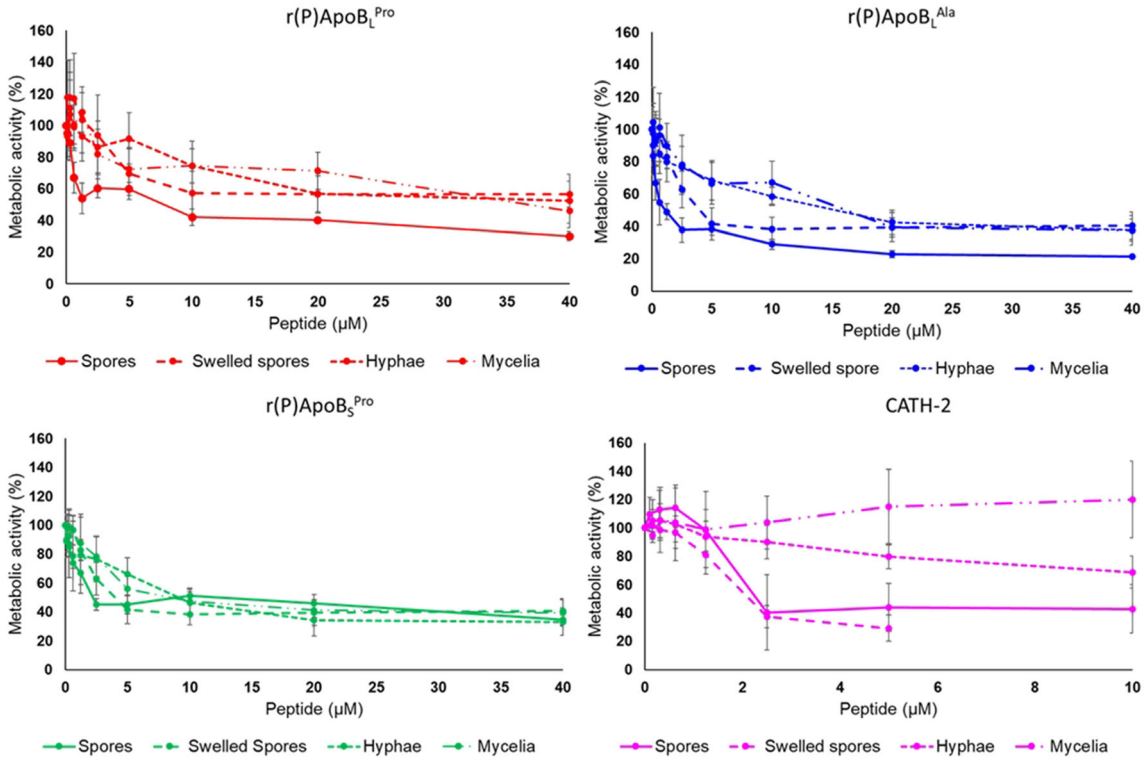

Fig. 6 Dose response curves reporting the effects of r(P)ApoB$_L^{Pro}$, r(P)ApoB$_L^{Ala}$, r(P)ApoB$_S^{Pro}$ and CATH-2 used as a positive control, on the metabolic activity of *A. niger* N402 spores, swollen spores, initial hyphae and mycelium. Data represent the mean (± SEM) of at least three independent experiments, each one carried out in triplicate. Statistical analyses revealed significant differences between treated and control samples (*$P < 0.05$, ** for $P < 0.01$, ***$P < 0.001$ and ****$P < 0.0001$)

hyphae, with a consequent accumulation into branched mycelium upon 24-h incubation (Fig. 7).

Discussion

Yeasts and fungi are widespread organisms able to grow even in harsh conditions (Gulis and Bärlocher 2017; Bahafid et al. 2017). It is increasingly acknowledged that the intensive and increasing employment of antifungals in modern medicine, agriculture, and animal production is responsible for the fast development of resistance phenotypes (Kontoyiannis 2017). Along with antifungals misuse, the restricted number of effective antifungal agents represents an urgent issue (Verweij et al. 2016). The development of novel effective antifungal strategies based on yet unexplored molecules with alternative mechanisms of action is imperative. In this scenario, HDPs have attracted great attention because of their broad spectrum of activities and peculiar mechanism of action (Hancock and Lehrer 1998; Zasloff 2002; Brogden et al. 2003).

ApoB-derived peptides exert fungicidal activity on *C. albicans* ATCC 10231

Here, the antifungal activity of ApoB-derived peptides has been evaluated for the first time on *C. albicans* ATCC 10231 and on *A. niger* N402 filamentous fungus, selected as prototypes of fungal species responsible for human infections and food spoilage, respectively. Indeed, while *Candida* species are the most common pathogens responsible for infections in hospitalized patients characterized by a high mortality rate (Strollo et al. 2017), *A. niger* is a saprophytic and filamentous fungus generally able to adapt to several habitats and to produce mycotoxins, thus representing the main contaminant of several food samples, such as fruits, vegetables, cereals and nuts leading to their discoloration, rotting and decay (Morita and Nozawa 1985; Kim and Park 2012; Roemer and Krysan 2014; Cowen et al. 2015; Prakash et al. 2015; Kumar et al. 2017). Interestingly, r(P)ApoB$_L^{Pro}$, r(P)ApoB$_L^{Ala}$ and r(P)ApoB$_S^{Pro}$ peptides were found to be able to exert significant fungicidal activity when tested on *C. albicans* ATCC 10231. In particular, peptides were found to exploit their fungicidal action towards *C. albicans* within 10 min when tested at their MFC concentration values. Accordingly, membrane permeabilization assays highlighted an almost immediate interaction between ApoB-derived peptides and *C. albicans* cells, resulting in damage and permeabilization of membranes. In all cases, similar effects were observed for all three ApoB-derived peptides.

ApoB-derived peptides immediately interact with *C. albicans* ATCC 10231 cell surface

The production of fluorescently labelled r(C)ApoB$_L^{Pro}$ peptide allowed us to analyse peptide mechanism of action by live imaging confocal laser scanning microscopy. Fluorescently

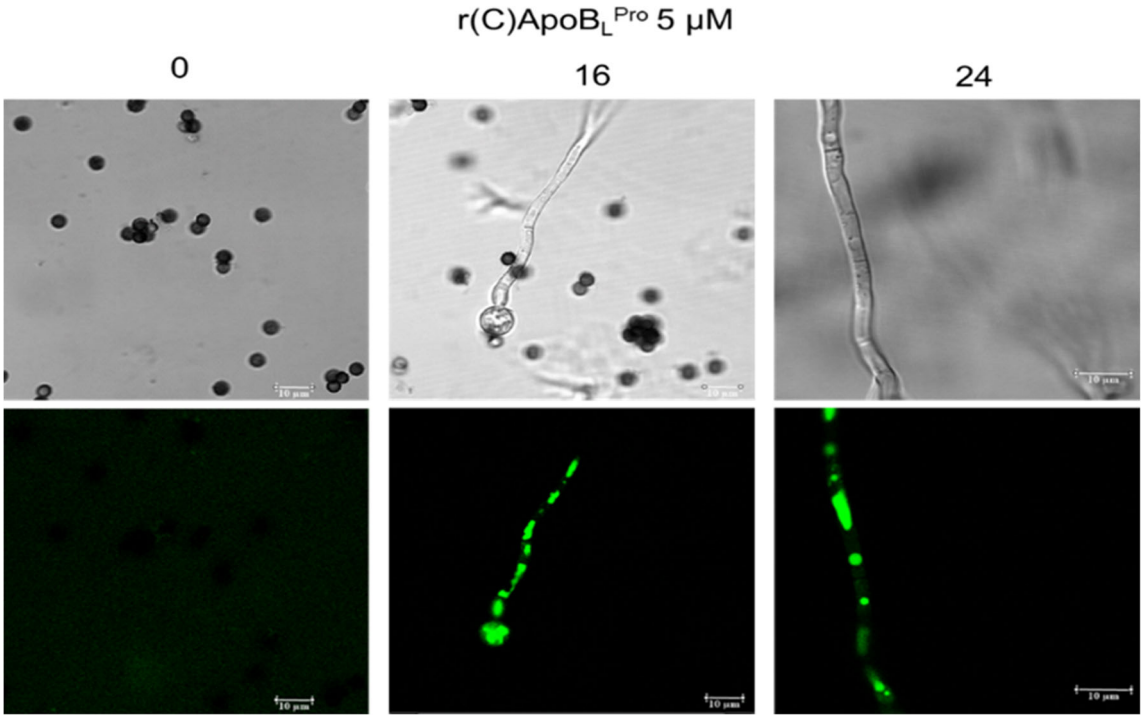

Fig. 7 Localization of 5'-IAF-r(C)ApoB$_L^{Pro}$ peptide in *A. niger* N402 initial hyphae and branched mycelium. Images were acquired upon 0, 16 and 24 h incubation of *A. niger* N402 with 5'-IAF-r(C)ApoB$_L^{Pro}$ peptide. Scale bar 10 μm

labelled r(C)ApoB$_L^{Pro}$ immediately localized on fungal cell surfaces, with an almost concomitant uptake of propidium iodide into the fungal cells. This phenomenon was found to progressively increase over time. Similar observations have been reported for different HDPs, such as astacidin 1 identified in hemocyanin of the freshwater crayfish *Pacifastacus leniusculus* (Choi and Lee 2014). This peptide was found to exert significant antifungal activity using a pore-forming mechanism on *C. albicans* cell membranes (Choi and Lee 2014). A similar mechanism of action has also been reported for HDPs CATH-2 and LL-37 (Ordonez et al. 2014). All these peptides have been reported to induce ATP leakage after 5-min incubation when tested on *C. albicans* cells. In earlier studies, fluorescence microscopy analyses revealed that CATH-2 is able to immediately interact with *C. albicans* cells, while LL-37 requires about 3-min incubation prior to interaction with membranes (Ordonez et al. 2014).

ApoB-derived peptides affect *A. niger* N402 metabolic activity

Here, we also demonstrated that ApoB-derived peptides are able to affect the metabolic activity of *A. niger* N402 filamentous fungus. Interestingly, analyses on swollen spores, initial hyphae and branched mycelium highlighted that ApoB-derived peptides are able to interact more efficiently with swollen spores and hyphae than with branched mycelium. These observations are in agreement with previous findings regarding the effects of Skh-AMP 1 peptide on *Aspergillus fumigatus* (Khani et al. 2020). Indeed, Skh-AMP 1 was found to be able to affect spores' survival rate, although at concentrations significantly higher than those required in the case of ApoB-derived peptides to exert significant effects. It has to be noticed that, differently from ApoB-derived peptides, Skh-AMP 1 was found to act on *Aspergillus* hyphae membranes more efficiently than on spores (Khani et al. 2020). In the case of KK14 de novo synthesized peptide and its analogues, a significant inhibition of the growth of *A. niger* dormant spores was demonstrated, even if all the peptide analogues were found to lost their activity when tested on the germinating conidia (Thery et al. 2019b). However, these peptides are characterized by a different mechanism of action when compared to ApoB-derived HDPs, being able to permeabilize the cell wall of *Fusarium culmorum* (Thery et al. 2019b). In the case of ApoB-derived HDPs, no significant PI uptake and ATP leakage were detected upon incubation of *A. niger* incubation with peptides (data not shown). Hence, the obtained findings suggest that, even if ApoB-derived HDPs interact with the *A. niger* cell wall, no permeabilization is induced upon interaction. Consequently, peptide uptake might occur during swelling of the spores. Indeed, during this phase, water and nutrient uptake by spores is associated with a lower rigidity of the cell wall, an event that might favour peptide uptake with a consequent inhibition of fungal metabolic activity.

ApoB-derived peptides affect different stages of growth of *A. niger* N402

Our findings highlight the huge potentiality of ApoB-derived peptides, which are able to act at low concentrations and even on different fungal stages of growth, such as spores, generally recalcitrant to the treatment with conventional antifungal agents. Interestingly, confocal laser scanning microscopy analyses, performed using fluorescently labelled r(C)ApoB$_L^{Pro}$ peptide, revealed peptide interaction with swollen spores and its subsequent accumulation into hyphae. In the case of PepBiotics CR173 and CR183, the ability to inactivate hyphae of *A. fumigatus* has been reported and correlated to a putative effect on mitochondria (van Eijk et al. 2020). In the literature, plant defensins, extracted from chopea seeds, have been reported to exert strong antifungal effects on *Fusarium culmorum* (Schmidt et al. 2019), although MFC values are higher than those here described for ApoB-derived peptides. In the case of chopea-thionin II, an initial interaction of the peptide with fungal cells was reported (Schmidt et al. 2019), with consequent membrane permeabilization and cell lysis or, as demonstrated here for ApoB-derived peptides, with subsequent internalization into fungal swollen spores or initial hyphae. Peptides isolated from *Leuconostoc mesenteroides* DU15 were, instead, found to be able to affect by 50% the growth of *A. niger* by causing significant morphological changes of branched mycelium, as evidenced by scanning electron microscopy analyses, and a reduction in the number of fungus cells (Muhialdin et al. 2015). Based on the obtained results, ApoB-derived peptides are able to exert strong effects on *A. niger* N402, and, even more importantly, they possess additional properties with respect to previously identified antifungal peptides, such as lower MFC values and the ability to affect different stages of fungal growth. Further experiments will be surely performed in the future to deepen on the molecular mechanism underlying the interesting properties demonstrated in the case of ApoB-derived peptides.

Altogether, the obtained findings indicate that ApoB-derived peptides represent novel antifungal agents suitable for the future development of effective strategies to treat fungal infections generally recalcitrant to conventional therapeutic approaches, also considering that they have been previously demonstrated to be neither toxic nor haemolytic for murine and human eukaryotic cell lines (Gaglione et al. 2017).

Supplementary Information The online version contains supplementary material available at https://doi.org/10.1007/s00253-021-11114-3.

Acknowledgements The authors would like to thank Richard Wubbolts and Esther van 't Veld from the Centre for Cell Imaging at Utrecht University for their help with the confocal imaging experiments.

Authors' contributions EDO, WRT, HdC and EJAV planned the research. HPH, EJAV and AA supervised the project. EDO, RG, AC and VC executed the experiments. EDO, WRT, HdC, HPH and EJAV analysed the data. RG, AC, VC and EN recombinantly produced peptides and fluorescently labelled r(C)ApoB$_L^{Pro}$ peptide. EDO and AA wrote the manuscript. All authors discussed the results and commented on the manuscript.

Funding Open Access funding provided by Università degli Studi di Napoli Federico II.

Data availability All data generated or analysed during this study are included in this published article and its supplementary information files.

Declarations

Conflict of interest The authors declare no conflict of interest.

Ethics statement This article does not contain any studies with human participants or animals performed by any of the authors.

References

Alastruey-Izquierdo A, Mellado E, Peláez T, Pemán J, Zapico S, Alvarez M, Rodríguez-Tudela JL, Cuenca-Estrella M (2013) Population-based survey of filamentous fungi and antifungal resistance in Spain (FILPOP study). Antimicrob Agents Chemother 57:3380–3387. https://doi.org/10.1128/AAC.00383-13

Anaissie EJ, Stratton SL, Dignani MC, Summerbell RC, Rex JH, Monson TP, Spencer T, Kasai M, Francesconi A, Walsh TJ (2002) Pathogenic *Aspergillus* species recovered from a Hospital Water System: a 3-year prospective study. Clin Infect Dis 34:780–789. https://doi.org/10.1086/338958

Aoki W, Ueda M (2013) Characterization of antimicrobial peptides toward the development of novel antibiotics. Pharmaceuticals 6:1055–1081

Badiee P, Hashemizadeh Z (2014) Opportunistic invasive fungal infections: Diagnosis & clinical management. Indian J Med Res 139:195–204

Bahafid W, Joutey NT, Asri M, Sayel H, Tirry N, El Ghachtouli N (2017) Yeast biomass: an alternative for bioremediation of heavy metals. In: Yeast - Industrial Applications. InTech

Bellmann R, Smuszkiewicz P (2017) Pharmacokinetics of antifungal drugs: practical implications for optimized treatment of patients. Infection 45:737–779. https://doi.org/10.1007/s15010-017-1042-z

Bennett JE, Dolin R, Blaser MJ (2014) Mandell, Douglas, and Bennett's Principles and Practice of Infectious Diseases. Elsevier Inc.

Bondaryk M, Staniszewska M, Zielińska P, Urbańczyk-Lipkowska Z (2017) Natural antimicrobial peptides as inspiration for design of a new generation antifungal compounds. J Fungi 3

Bowman JC, Hicks PS, Kurtz MB, Rosen H, Schmatz DM, Liberator PA, Douglas CM (2002) The antifungal echinocandin caspofungin acetate kills growing cells of *Aspergillus fumigatus* in vitro. Antimicrob Agents Chemother 46:3001–3012. https://doi.org/10.1128/aac.46.9.3001-3012.2002

Brogden KA, Ackermann M, McCray PB, Tack BF (2003) Antimicrobial peptides in animals and their role in host defences. Int J Antimicrob Agents 22:465–478. https://doi.org/10.1016/s0924-8579(03)00180-8

Brown GD, Denning DW, Gow NAR, Levitz SM, Netea MG, White TC (2012) Hidden killers: human fungal infections. Sci Transl Med 4:165rv13

Choi H, Lee DG (2014) Antifungal activity and pore-forming mechanism of astacidin 1 against *Candida albicans*. Biochimie 105:58–63. https://doi.org/10.1016/j.biochi.2014.06.014

Ciociola T, Giovati L, Conti S, Walter Magliani CS& LP (2016) Natural and synthetic peptides with antifungal activity. Future Med Chem

Cowen LE, Sanglard D, Howard SJ, Rogers PD, Perlin DS (2015) Mechanisms of antifungal drug resistance. Cold Spring Harb Perspect Med 5:1–22. https://doi.org/10.1101/cshperspect.a019752

Cuperus T, Coorens M, van Dijk A, Haagsman HP (2013) Avian host defense peptides. Dev Comp Immunol 41:352–369. https://doi.org/10.1016/j.dci.2013.04.019

De Vries RP, Burgers K, Van De Vondervoort PJI, Frisvad JC, Samson RA, Visser J (2004) A new black *Aspergillus* species, *A. vadensis*, is a promising host for homologous and heterologous protein production. Appl Environ Microbiol 70:3954–3959. https://doi.org/10.1128/AEM.70.7.3954-3959.2004

Essig A, Hofmann D, Münch D, Gayathri S, Künzler M, Kallio PT, Sahl HG, Wider G, Schneider T, Aebi M (2014) Copsin, a novel peptide-based fungal antibiotic interfering with the peptidoglycan synthesis. J Biol Chem 289:34953–34964. https://doi.org/10.1074/jbc.M114.599878

Fisher MC, Hawkins NJ, Sanglard D, Gurr SJ (2018a) Worldwide emergence of resistance to antifungal drugs challenges human health and food security. Science (80-.) 360:739–742

Fisher MC, Hawkins NJ, Sanglard D, Gurr SJ (2018b) Worldwide emergence of resistance to antifungal drugs challenges human health and food security. Science (80-.) 360:739–742

Gaglione R, Dell'Olmo E, Bosso A, Chino M, Pane K, Ascione F, Itri F, Caserta S, Amoresano A, Lombardi A, Haagsman HP, Piccoli R, Pizzo E, Veldhuizen EJA, Notomista E, Arciello A (2017) Novel human bioactive peptides identified in apolipoprotein B: evaluation of their therapeutic potential. Biochem Pharmacol 130:34–50. https://doi.org/10.1016/j.bcp.2017.01.009

Gaglione R, Cesaro A, Dell'Olmo E, Della Ventura B, Casillo A, Di Girolamo R, Velotta R, Notomista E, Veldhuizen EJA, Corsaro MM, De Rosa C, Arciello A (2019a) Effects of human antimicrobial cryptides identified in apolipoprotein B depend on specific features of bacterial strains. Sci Rep 9:9. https://doi.org/10.1038/s41598-019-43063-3

Gaglione R, Pane K, Dell'Olmo E, Cafaro V, Pizzo E, Olivieri G, Notomista E, Arciello A (2019b) Cost-effective production of recombinant peptides in *Escherichia coli*. New Biotechnol 51:39–48. https://doi.org/10.1016/j.nbt.2019.02.004

Gaglione R, Cesaro A, Dell'olmo E, Di Girolamo R, Tartaglione L, Pizzo E, Arciello A (2020) Cryptides identified in human apolipoprotein b as new weapons to fight antibiotic resistance in cystic fibrosis disease. Int J Mol Sci 21:21. https://doi.org/10.3390/ijms21062049

Gulis V, Bärlocher F (2017) Fungi: biomass, production, and community structure. In: Methods in Stream Ecology: Third Edition. Elsevier Inc., pp 177–192

Hancock REW, Lehrer R (1998) Cationic peptides: a new source of antibiotics. Trends Biotechnol 16:82–88

Jang WS, Bajwa JS, Sun JN, Edgerton M (2010) Salivary histatin 5 internalization by translocation, but not endocytosis, is required for fungicidal activity in *Candida albicans*. Mol Microbiol 77:354–370. https://doi.org/10.1111/j.1365-2958.2010.07210.x

Khani S, Seyedjavadi SS, Hosseini HM, Goudarzi M, Valadbeigi S, Khatami S, Ajdary S, Eslamifar A, Amani J, Imani Fooladi AA, Razzaghi-Abyaneh M (2020) Effects of the antifungal peptide Skh-AMP1 derived from *Satureja khuzistanica* on cell membrane permeability, ROS production, and cell morphology of conidia and hyphae of *Aspergillus fumigatus*. Peptides. 123:170195. https://doi.org/10.1016/j.peptides.2019.170195

Kim E, Park IK (2012) Fumigant antifungal activity of Myrtaceae essential oils and constituents from *Leptospermum petersonii* against three *Aspergillus* species. Molecules 17:10459–10469. https://doi.org/10.3390/molecules170910459

Kontoyiannis DP (2017) Antifungal resistance: an emerging reality and a global challenge. J Infect Dis 216:S431–S435. https://doi.org/10.1093/infdis/jix179

Kościuczuk EM, Lisowski P, Jarczak J, Strzałkowska N, Jóźwik A, Horbańczuk J, Krzyżewski J, Zwierzchowski L, Bagnicka E (2012) Cathelicidins: family of antimicrobial peptides. A review Mol Biol Rep 39:10957–10970

Kumar P, Mishra S, Kumar A, Kumar S, Prasad CS (2017) In vivo and in vitro control activity of plant essential oils against three strains of *Aspergillus niger*. Environ Sci Pollut Res 24:21948–21959. https://doi.org/10.1007/s11356-017-9730-x

Lupetti A, Van Dissel JT, Brouwer CPJM, Nibbering PH (2008) Human antimicrobial peptides' antifungal activity against *Aspergillus fumigatus*. Eur J Clin Microbiol Infect Dis 27:1125–1129. https://doi.org/10.1007/s10096-008-0553-z

Mookherjee N, Anderson MA, Haagsman HP, Davidson DJ (2020) Antimicrobial host defence peptides: functions and clinical potential. Nat Rev Drug Discov 19:311–332

Morita T, Nozawa Y (1985) Effects of antifungal agents on ergosterol biosynthesis in *Candida albicans* and *Trichophyton mentagrophytes*: differential inhibitory sites of naphthiomate and miconazole. J Invest Dermatol 85:434–437. https://doi.org/10.1111/1523-1747.ep12277141

Muhialdin BJ, Hassan Z, Abu Bakar F, Algboory HL, Saari N (2015) Novel antifungal peptides produced by *Leuconostoc mesenteroides* DU15 effectively inhibit growth of *Aspergillus niger*. J Food Sci 80: M1026–M1030. https://doi.org/10.1111/1750-3841.12844

Neelabh, Singh K, Rani J (2016) Sequential and structural aspects of antifungal peptides from animals, bacteria and fungi based on bioinformatics tools. Probiotics Antimicrob Proteins 8:85–101

Ordonez SR, Amarullah IH, Wubbolts RW, Veldhuizen EJA, Haagsman HP (2014) Fungicidal mechanisms of cathelicidins LL-37 and CATH-2 revealed by live-cell imaging. Antimicrob Agents Chemother 58:2240–2248. https://doi.org/10.1128/AAC.01670-13

Pane K, Cafaro V, Avitabile A, Torres MDT, Vollaro A, De Gregorio E, Catania MR, Di Maro A, Bosso A, Gallo G, Zanfardino A, Varcamonti M, Pizzo E, Di Donato A, Lu TK, De La Fuente-Nunez C, Notomista E (2018a) Identification of novel cryptic multifunctional antimicrobial peptides from the human stomach enabled by a computational-experimental platform. ACS Synth Biol 7: 2105–2115. https://doi.org/10.1021/acssynbio.8b00084

Pane K, Verrillo M, Avitabile A, Pizzo E, Varcamonti M, Zanfardino A, Di Maro A, Rega C, Amoresano A, Izzo V, Di Donato A, Cafaro V, Notomista E (2018b) Chemical cleavage of an Asp-Cys sequence allows efficient production of recombinant peptides with an N-terminal cysteine residue. Bioconjug Chem 29:1373–1383. https://doi.org/10.1021/acs.bioconjchem.8b00083

Prakash B, Kedia A, Mishra PK, Dubey NK (2015) Plant essential oils as food preservatives to control moulds, mycotoxin contamination and oxidative deterioration of agri-food commodities - potentials and challenges. Food Control 47:381–391

Roemer T, Krysan DJ (2014) Antifungal drug development: challenges, unmet clinical needs, and new approaches. Cold Spring Harb Perspect Med 4

Sanglard D (2016) Emerging threats in antifungal-resistant fungal pathogens. Front Med 3

Schmidt M, Arendt EK, Thery TLC (2019) Isolation and characterisation of the antifungal activity of the cowpea defensin Cp-thionin II. Food Microbiol 82:504–514. https://doi.org/10.1016/j.fm.2019.03.021

Schmiedel Y, Zimmerli S (2016) Common invasive fungal diseases: an overview of invasive candidiasis, aspergillosis, cryptococcosis, and *Pneumocystis pneumonia*. Swiss Med Wkly 146:w14281

Sobel JD (2007) Vulvovaginal candidiasis. Lancet 369:1961–1971. https://doi.org/10.1016/S0140-6736(07)60917-9

Staab JF (1999) Adhesive and mammalian transglutaminase substrate properties of *Candida albicans* Hwp1. Science (80-) 283:1535–1538. https://doi.org/10.1126/science.283.5407.1535

Stone WL, Qui M, Smith M (2003) Lipopolysaccharide enhances the cytotoxicity of 2-chloroethyl ethyl sulfide. BMC Cell Biol 4:1. https://doi.org/10.1186/1471-2121-4-1

Strollo S, Lionakis MS, Adjemian J, Steiner CA, Prevots DR (2017) Epidemiology of hospitalizations associated with invasive candidiasis, United States, 2002-2012. Emerg Infect Dis 23:7–13. https://doi.org/10.3201/eid2301.161198

Sun E, Belanger CR, Haney EF, Hancock REW (2018) Host defense (antimicrobial) peptides. In: Peptide Applications in Biomedicine, Biotechnology and Bioengineering. Elsevier Inc., pp 253–285

Thery T, Lynch KM, Arendt EK (2019a) Natural antifungal peptides/proteins as model for novel food preservatives. Compr Rev Food Sci Food Saf 18:1327–1360

Thery T, Shwaiki LN, O'Callaghan YC, O'Brien NM, Arendt EK (2019b) Antifungal activity of a de novo synthetic peptide and derivatives against fungal food contaminants. J Pept Sci 25:e3137. https://doi.org/10.1002/psc.3137

Thevissen K, Kristensen HH, Thomma BPHJ, Cammue BPA, François IEJA (2007) Therapeutic potential of antifungal plant and insect defensins. Drug Discov Today 12:966–971

Van Dijk A, Veldhuizen EJA, Kalkhove SIC, Tjeerdsma-Van Bokhoven JLM, Romijn RA, Haagsman HP (2007) The β-defensin gallinacin-6 is expressed in the chicken digestive tract and has antimicrobial activity against food-borne pathogens. Antimicrob Agents Chemother 51:912–922. https://doi.org/10.1128/AAC.00568-06

van Eijk M, Boerefijn S, Cen L, Rosa M, Morren MJH, van der Ent CK, Kraak B, Dijksterhuis J, Valdes ID (2020) Haagsman HP, de Cock H Cathelicidin-inspired antimicrobial peptides as novel antifungal compounds. Med Mycol 58:1073–1084. https://doi.org/10.1093/MMY/MYAA014

van Leeuwen MR, Krijgsheld P, Bleichrodt R, Menke H, Stam H, Stark J, Wösten HAB, Dijksterhuis J (2013) Germination of conidia of *Aspergillus niger* is accompanied by major changes in RNA profiles. Stud Mycol 74:59–70. https://doi.org/10.3114/sim0009

Verweij PE, Chowdhary A, Melchers WJG, Meis JF (2016) Azole resistance in *Aspergillus fumigatus*: can we retain the clinical use of mold-active antifungal azoles? Clin Infect Dis 62:362–368. https://doi.org/10.1093/cid/civ885

Wendland J (2001) Comparison of morphogenetic networks of filamentous fungi and yeast. Fungal Genet Biol 34:63–82

Zasloff M (2002) Antimicrobial peptides of multicellular organisms. Nature 415:389–395

International Journal of
Molecular Sciences

MDPI

Article

Cryptides Identified in Human Apolipoprotein B as New Weapons to Fight Antibiotic Resistance in Cystic Fibrosis Disease

Rosa Gaglione [1,3], Angela Cesaro [1], Eliana Dell'Olmo [1], Rocco Di Girolamo [1], Luca Tartaglione [1], Elio Pizzo [2] and Angela Arciello [1,3,*]

1 Department of Chemical Sciences, University of Naples Federico II, Via Cintia 21, I-80126 Naples, Italy; rosa.gaglione@unina.it (R.G.); angela.cesaro@unina.it (A.C.); eliana.dellolmo@unina.it (E.D.); rocco.digirolamo@unina.it (R.D.G.); luca.tartaglione.lt@gmail.com (L.T.)
2 Department of Biology, University of Naples Federico II, Via Cintia 21, I-80126 Naples, Italy; elipizzo@unina.it
3 Istituto Nazionale di Biostrutture e Biosistemi (INBB), I-00136 Rome, Italy
* Correspondence: anarciel@unina.it

Received: 29 February 2020; Accepted: 13 March 2020; Published: 17 March 2020

Abstract: Chronic respiratory infections are the main cause of morbidity and mortality in cystic fibrosis (CF) patients, and are characterized by the development of multidrug resistance (MDR) phenotype and biofilm formation, generally recalcitrant to treatment with conventional antibiotics. Hence, novel effective strategies are urgently needed. Antimicrobial peptides represent new promising therapeutic agents. Here, we analyze for the first time the efficacy of three versions of a cryptide identified in human apolipoprotein B (ApoB, residues 887-922) towards bacterial strains clinically isolated from CF patients. Antimicrobial and anti-biofilm properties of ApoB-derived cryptides have been analyzed by broth microdilution assays, crystal violet assays, confocal laser scanning microscopy and scanning electron microscopy. Cell proliferation assays have been performed to test cryptide effects on human host cells. ApoB-derived cryptides have been found to be endowed with significant antimicrobial and anti-biofilm properties towards *Pseudomonas* and *Burkholderia* strains clinically isolated from CF patients. Peptides have been also found to be able to act in combination with the antibiotic ciprofloxacin, and they are harmless when tested on human bronchial epithelial mesothelial cells. These findings open interesting perspectives to cryptide applicability in the treatment of chronic lung infections associated with CF disease.

Keywords: antibiotic resistance; cystic fibrosis; antimicrobial peptides; host defense peptides; cryptides; anti-biofilm peptides; synergistic effects

1. Introduction

Cystic fibrosis (CF) is a rare autosomal recessive disease affecting 1 in 2500 newborns in Europe [1]. More than 2000 mutations have been identified in the Cystic Fibrosis Transmembrane conductance Regulator (CFTR) gene and have been associated with the disease. CFTR gene encodes a chloride ion channel whose malfunctioning causes the production of viscous secretions coating the airway epithelia [2,3]. This phenomenon is responsible for the accumulation of trapped microbes, including *Pseudomonas aeruginosa*, with consequent deterioration of lung tissue and impairment of respiratory functions [4]. Indeed, chronic respiratory infections and inflammation are the main causes of death in CF [5]. Despite aggressive antibiotic treatments, *Pseudomonas* strains often grow in CF lungs and lead to chronic and recalcitrant infections characterized by a robust host inflammatory response [6,7]. Pulmonary infections due to the Gram-negative *P. aeruginosa* strain are the main cause of lung decline

and death in patients suffering from CF [8–10]. *P. aeruginosa* colonization of host tissues is mediated by an initial attachment of bacteria to epithelial cells [11,12], followed by internalization into cells [13–16]. This phenomenon protects bacteria from host defense mechanisms and from the killing action of conventional antibiotics that hardly enter epithelial cells [17]. This is generally responsible for systemic diffusion of bacteria and for the consequent chronic nature of *P. aeruginosa* lung infections [18]. Moreover, chronic inflammation and mucus provide an environment favorable to the development of resistance phenotype for bacteria in biofilms, thus hampering antibiotic efficacy [19]. *Burkholderia* species also cause serious challenges in CF patients, even if infections associated with these strains are relatively rare [20]. Indeed, a main post-transplant complication is represented by infections caused by multidrug resistant (MDR) bacteria, with the *Burkholderia* species recognized as significant contributors to CF morbidity and mortality associated with increased post-transplant death rate [21,22]. Conventional antibiotics generally appear ineffective and their prolonged use is responsible for the development of the MDR phenotype. The concomitant decrease in the pharmaceutical industry research pipeline for novel antimicrobial agents during the last three decades has, thus, resulted in an urgent need for the discovery of novel effective antimicrobial strategies [23]. In this scenario, naturally occurring antimicrobial peptides (AMPs), or their derivatives, represent an appealing source for the generation of new therapeutic agents able to treat chronic MDR bacterial infections [24,25]. AMPs are produced by all living organisms as the first line of defense against invading microorganisms, and the majority of them are characterized by net positive charge at neutral pH and by the tendency to form amphipathic structures in a hydrophobic environment [26,27]. So far, hundreds of naturally occurring AMPs have been isolated and characterized as highly efficacious, safe, and tolerable antimicrobials [28,29]. Being able to selectively interact with bacterial cytoplasmic membranes in a manner not dependent upon specific receptors, AMPs are generally endowed with broad-spectrum antimicrobial activity [30,31], and several of them have been reported to combat biofilms because of their potent bactericidal activity and their ability to first penetrate and then to disorganize biofilm structures [32]. Furthermore, AMPs frequently synergize with antimicrobial compounds to repress molecular pathways leading to biofilm development [32]. Here, we analyze for the first time the antimicrobial and anti-biofilm properties of two recently characterized AMPs [33] towards *Pseudomonas* and *Burkholderia* strains clinically isolated from CF patients. AMPs under test have been identified in human apolipoprotein B (ApoB) by using a bioinformatic method developed by our research group [33–41]. Indeed, it is increasingly evident that eukaryotic proteins, with functions not necessarily related to host defense, act as sources of "cryptic" bioactive peptides released upon proteolytic processing by bacterial and/or host proteases [42–44]. We previously characterized two variants of the cryptide identified in human ApoB (residues 887–922), i.e., peptides ApoB887–923 and ApoB887–911 [33]. These two host defense peptides (HDPs), recombinantly produced in bacterial cells, have been here named r(P)ApoB$_L^{Pro}$ and r(P)ApoB$_S^{Pro}$ because of the presence of a Pro residue becoming the N-terminus of the peptides released by the acidic cleavage of an Asp-Pro bond [33,36]. Here, we also characterized a further peptide, i.e., a version of the longest peptide characterized by the presence of an Ala residue instead of a Pro residue in position six of peptide sequence, here named r(P)ApoB$_L^{Ala}$. Peptides r(P)ApoB$_L^{Pro}$ and r(P)ApoB$_S^{Pro}$ have been previously found to be endowed with antimicrobial, anti-biofilm, wound healing and immunomodulatory properties, and are able to synergistically act in combination with either conventional antibiotics or EDTA [33]. On the other hand, peptides have been found to be neither toxic nor hemolytic towards mammalian cells [33]. It has been also demonstrated that electrostatic interactions between negatively charged bacterial membranes and positively charged ApoB-derived AMPs play a key role in mediating peptide toxicity, although they are strongly influenced by the composition of negatively charged bacterial surfaces and by defined extracellular microenvironments [35]. Here, we demonstrate that the three ApoB-derived cryptides exert significant antimicrobial and anti-biofilm effects towards *Pseudomonas* and *Burkholderia* strains clinically isolated from CF patients and that they are able to act in combination with the ciprofloxacin antibiotic, widely used to treat chronic lung infections in CF patients [45]. Furthermore, ApoB-derived cryptides have been found to be not toxic when tested on

human bronchial epithelial mesothelial cells. Altogether, these findings open interesting perspectives to peptide applicability, suggesting the possibility to develop in the future successful combinatorial therapeutic approaches, based on the concomitant administration of AMPs and conventional antibiotics, with a consequently very low potential to induce a resistance phenotype.

2. Results

2.1. Evaluation of ApoB-Derived Peptide Effects on Clinically Isolated Baterial Strains

In order to evaluate the ApoB-derived peptide ability to counteract microbial infections in CF, their effects were tested on six clinically isolated bacterial strains, i.e., *P. aeruginosa* RP 73, *P. aeruginosa* KK 27, *P. aeruginosa* 14, *P. aeruginosa* AA2, *Burkholderia multivorans* LMG 17582, and *Burkholderia cenocepacia* LMG 18863. To this purpose, the susceptibility of planktonic bacteria to ApoB-derived peptides was examined by using broth microdilution method [33] that allows the measurement of minimum inhibitory concentration (MIC) values. As reported in Table 1, the three ApoB-derived peptides under test were found to exert antimicrobial effects on three out of six bacterial strains tested. In particular, bacterial strains *P. aeruginosa* RP 73, *P. aeruginosa* KK 27, and *B. multivorans* LMG 17582 were found to be susceptible to ApoB-derived peptide antimicrobial activity, with MIC_{100} values ranging from 5 to 40 μM (Table 1). Peptide r(P)$ApoB_L^{Ala}$ was found to be the most active in directly killing bacterial cells (Table 1).

Table 1. Minimum inhibitory concentration (MIC) values determined for r(P)$ApoB_L^{Pro}$, r(P)$ApoB_L^{Ala}$ and r(P)$ApoB_S^{Pro}$ tested on clinically isolated bacterial strains.

	MIC_{100} (μM)		
	r(P)$ApoB_L^{Pro}$	r(P)$ApoB_L^{Ala}$	r(P)$ApoB_S^{Pro}$
P. aeruginosa RP 73	10–20	5–10	20–40
P. aeruginosa 14	>40	>40	>40
P. aeruginosa AA2	>40	>40	>40
P. aeruginosa KK 27	20–40	10–20	20–40
Burkholderia cenocepacia LMG 18863	>40	>40	>40
Burkholderia multivorans LMG 17582	10–20	10–20	20–40

2.2. Evaluation of ApoB-Derived Peptide Anti-biofilm Activity on Clinically Isolated Baterial Strains

2.2.1. Evaluation of ApoB-Derived Peptide Anti-Biofilm Activity by Microtiter Plate Assay

To evaluate whether recombinant ApoB-derived peptides are endowed with anti-biofilm activity, analyses were performed on clinically isolated bacterial strains *P. aeruginosa* RP 73, *P. aeruginosa* KK 27, *P. aeruginosa* 14, *P. aeruginosa* AA2, *B. multivorans* LMG 17582, and *B. cenocepacia* LMG 18863 in 0.5X Mueller Hinton Broth (MHB). By following different experimental approaches, peptide effects were tested on the three main stages of biofilm development, such as attachment, formation and detachment. To test peptide effects on biofilm attachment, following overnight growth, a bacterial culture was diluted into MHB medium containing increasing concentrations of the peptide under test (0–40 μM), and incubated for 4 h at 37 °C [33]. When, instead, peptide effects were tested on biofilm formation, the experimental procedure described above was followed with the only exception that bacterial cells were incubated with increasing concentrations of peptides for 24 h at 37 °C [33]. Finally, the effects of ApoB-derived peptides were tested on biofilm detachment [33]. In each case, following incubation with peptides, biofilm was analyzed by staining with crystal violet. As shown in Figure 1, ApoB-derived peptides have been found to be effective on biofilm attachment, with the greatest effects obtained in the case of *P. aeruginosa* KK 27 and *P. aeruginosa* 14 bacterial strains for all the three peptides under test. In the case of biofilm formation, the greatest effects were found to be exerted by r(P)$ApoB_L^{Ala}$ and

r(P)ApoB$_S^{Pro}$ on *P. aeruginosa* 14 (~50% inhibition) (Figure 1). Even more interestingly, about 30%–40% biofilm eradication was observed in the case of *B. cenocepacia* LMG 18863 upon treatment with 2.5 μM r(P)ApoB$_L^{Ala}$ (Figure 1). A similar effect was obtained upon treatment of *P. aeruginosa* KK 27 preformed biofilm with 2.5 μM r(P)ApoB$_S^{Pro}$ (Figure 1). Moreover, about 20% biofilm eradication was observed upon treatment of *P. aeruginosa* RP 73 with very low concentrations (1.25 μM) of r(P)ApoB$_S^{Pro}$.

Altogether, obtained data indicate that peptides exert anti-biofilm effects even on bacterial strains not sensitive to their direct antimicrobial activity. In most of the cases, significant anti-biofilm effects were detected at peptide concentrations (1.25–2.5 μM) lower than those required to directly kill planktonic cells (Table 1 and Figure 1). Data reported in Figure 1 represent the mean ± standard deviation (SD) of at least three independent experiments.

2.2.2. Evaluation of ApoB-Derived Peptides Anti-Biofilm Activity by Laser Scanning Confocal Microscopy

In order to further investigate anti-biofilm properties of ApoB-derived peptides, analyses were also performed by confocal laser scanning microscopy (CLSM). For this approach, we selected two bacterial strains not responsive to ApoB-derived peptides direct antimicrobial activity, such as *B. cenocepacia* LMG 18863 and *P. aeruginosa* 14. Peptide effects on biofilm attachment, formation and detachment were evaluated upon sample staining with LIVE/DEAD BacLight bacterial viability kit. Analyses revealed that all three peptides are able to affect biofilm attachment and formation in the case of *B. cenocepacia* LMG 18863 (Figure 2). Even more interestingly, peptides are able to affect pre-formed biofilm with the strongest effects observed in the presence of r(P)ApoB$_L^{Ala}$ (Figure 2). By staining bacterial biofilm with SYPRO® ruby dye, which is able to specifically stain biofilm extracellular matrix, the appearance of highly fluorescent aggregates is clearly evident upon treatment with peptides (Figure 2), thus indicating that peptides induce strong alterations of biofilm matrix architecture, as previously reported for different anti-biofilm agents [46]. Similar results were obtained also in the case of *P. aeruginosa* 14 (Figure 3). These findings are also supported by biofilm biovolume determinations by CLSM reported in Figure 4, that indicate a strong and significant effect of r(P)ApoB$_S^{Pro}$ peptide on biofilm eradication in the case of both bacterial strains (Figure 4c,f). Furthermore, peptides have been found to exert significant effects on biofilm biovolume when attachment is tested (Figure 4a,d), except for r(P)ApoB$_L^{Ala}$ for which no significant reduction in biovolume is observed, although a disaggregating effect is clearly evident (Figures 2 and 3). This might be due to the fact that, upon treatment with r(P)ApoB$_L^{Ala}$ peptide, planktonic cells escape from biofilm by floating, with a consequent significant contribution to biovolume. Altogether, these findings confirm that peptides are able to exert significant anti-biofilm effects even on bacterial strains not sensitive to their direct antimicrobial activity.

2.2.3. Evaluation of ApoB-Derived Peptides Anti-Biofilm Activity by Scanning Electron Microscopy

To analyze morphological modifications of bacterial biofilm upon treatment with peptides, scanning electron microscopy (SEM) analyses were also performed on bacterial strains not responsive to peptide direct antimicrobial activity, such as *B. cenocepacia* LMG 18863 and *P. aeruginosa* 14. In untreated samples, bacteria present smooth and intact surfaces and appear embedded into the extracellular biofilm matrix in the case of both bacterial strains (Figure 5). When bacteria are treated with peptides, instead, a significant decrease or disappearance of biofilm matrix is clearly evident with a concomitant decrease of cell density.

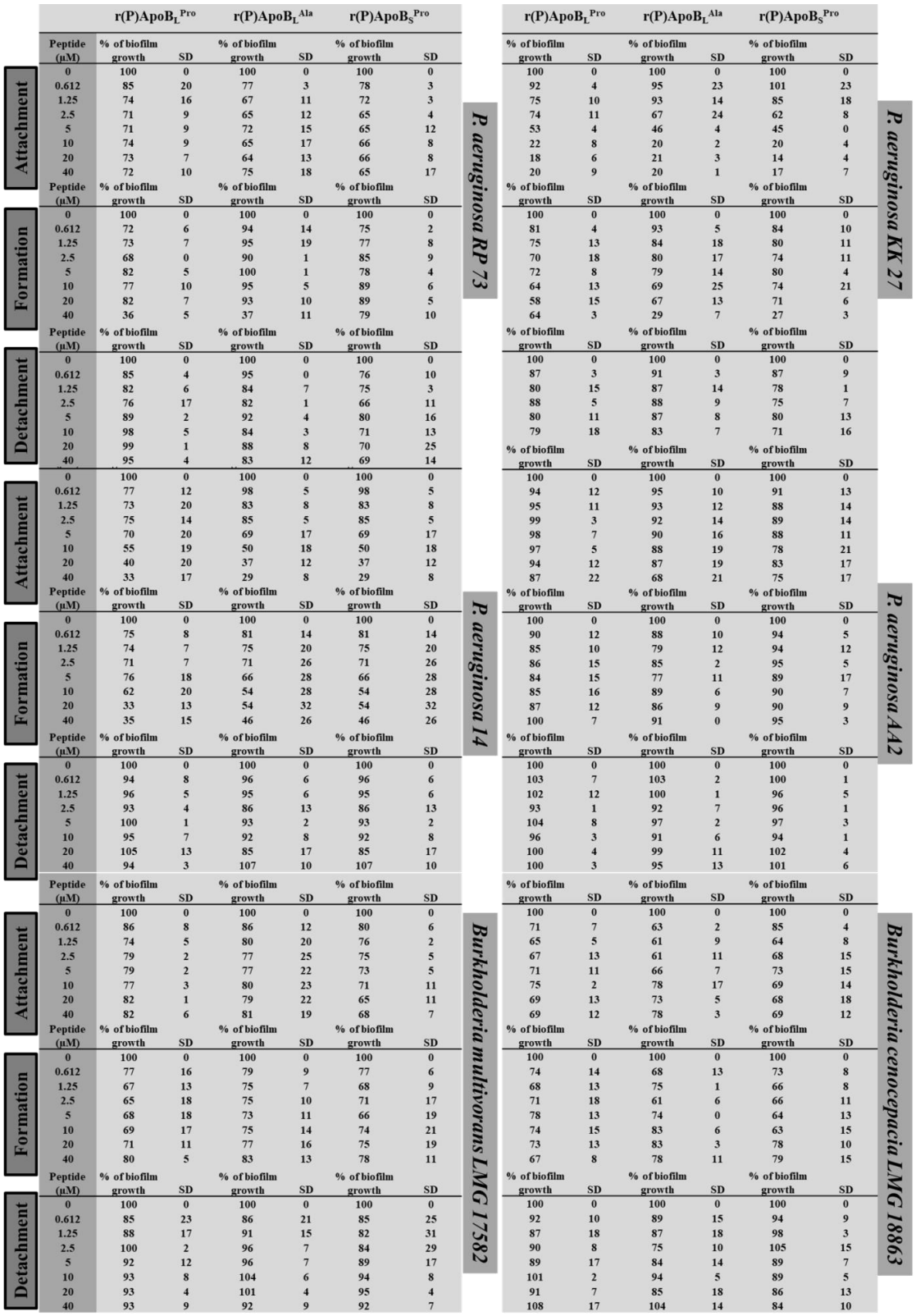

	r(P)ApoB$_L^{Pro}$		r(P)ApoB$_L^{Ala}$		r(P)ApoB$_S^{Pro}$		r(P)ApoB$_L^{Pro}$		r(P)ApoB$_L^{Ala}$		r(P)ApoB$_S^{Pro}$		
	Peptide (μM)	% of biofilm growth	SD	% of biofilm growth	SD	% of biofilm growth	SD	% of biofilm growth	SD	% of biofilm growth	SD	% of biofilm growth	SD	
Attachment	0	100	0	100	0	100	0	100	0	100	0	100	0	*P. aeruginosa* RP 73
	0.612	85	20	77	3	78	3	92	4	95	23	101	23	
	1.25	74	16	67	11	72	3	75	10	93	14	85	18	
	2.5	71	9	65	12	65	4	74	11	67	24	62	8	
	5	71	9	72	15	65	12	53	4	46	4	45	0	
	10	74	9	65	17	66	8	22	8	20	2	20	4	
	20	73	7	64	13	66	8	18	6	21	3	14	4	
	40	72	10	75	18	65	17	20	9	20	1	17	7	
Formation	Peptide (μM)	% of biofilm growth	SD	% of biofilm growth	SD	% of biofilm growth	SD	% of biofilm growth	SD	% of biofilm growth	SD	% of biofilm growth	SD	
	0	100	0	100	0	100	0	100	0	100	0	100	0	
	0.612	72	6	94	14	75	2	81	4	93	5	84	10	
	1.25	73	7	95	19	77	8	75	13	84	18	80	11	
	2.5	68	0	90	1	85	9	70	18	80	17	74	11	
	5	82	5	100	1	78	4	72	8	79	14	80	4	
	10	77	10	95	5	89	6	64	13	69	25	74	21	
	20	82	7	93	10	89	5	58	15	67	13	71	6	
	40	36	5	37	11	79	10	64	3	29	7	27	3	
Detachment	Peptide (μM)	% of biofilm growth	SD	% of biofilm growth	SD	% of biofilm growth	SD	% of biofilm growth	SD	% of biofilm growth	SD	% of biofilm growth	SD	
	0	100	0	100	0	100	0	100	0	100	0	100	0	
	0.612	85	4	95	0	76	10	87	3	91	3	87	9	
	1.25	82	6	84	7	75	3	80	15	87	14	78	1	
	2.5	76	17	82	1	66	11	88	5	88	9	75	7	
	5	89	2	92	4	80	16	80	11	87	8	80	13	
	10	98	5	84	3	71	13	79	18	83	7	71	16	
	20	99	1	88	8	70	25							
	40	95	4	83	12	69	14							
Attachment	0	100	0	100	0	100	0	100	0	100	0	100	0	*P. aeruginosa* 14
	0.612	77	12	98	5	98	5	94	12	95	10	91	13	
	1.25	73	20	83	8	83	8	95	11	93	12	88	14	
	2.5	75	14	85	5	85	5	99	3	92	14	89	14	
	5	70	20	69	17	69	17	98	7	90	16	88	11	
	10	55	19	50	18	50	18	97	5	88	19	78	21	
	20	40	20	37	12	37	12	94	12	87	19	83	17	
	40	33	17	29	8	29	8	87	22	68	21	75	17	
Formation	Peptide (μM)	% of biofilm growth	SD	% of biofilm growth	SD	% of biofilm growth	SD	% of biofilm growth	SD	% of biofilm growth	SD	% of biofilm growth	SD	
	0	100	0	100	0	100	0	100	0	100	0	100	0	
	0.612	75	8	81	14	81	14	90	12	88	10	94	5	
	1.25	74	7	75	20	75	20	85	10	79	12	94	12	
	2.5	71	7	71	26	71	26	86	15	85	2	95	5	
	5	76	18	66	28	66	28	84	15	77	11	89	17	
	10	62	20	54	28	54	28	85	16	89	6	90	7	
	20	33	13	54	32	54	32	87	12	86	9	90	9	
	40	35	15	46	26	46	26	100	7	91	0	95	3	
Detachment	Peptide (μM)	% of biofilm growth	SD	% of biofilm growth	SD	% of biofilm growth	SD	% of biofilm growth	SD	% of biofilm growth	SD	% of biofilm growth	SD	
	0	100	0	100	0	100	0	100	0	100	0	100	0	
	0.612	94	8	96	6	96	6	103	7	103	2	100	1	
	1.25	96	5	95	6	95	6	102	12	100	1	96	5	
	2.5	93	4	86	13	86	13	93	1	92	7	96	1	
	5	100	1	93	2	93	2	104	8	97	2	97	3	
	10	95	7	92	8	92	8	96	3	91	6	94	1	
	20	105	13	85	17	85	17	100	4	99	11	102	4	
	40	94	3	107	10	107	10	100	3	95	13	101	6	
Attachment	Peptide (μM)	% of biofilm growth	SD	% of biofilm growth	SD	% of biofilm growth	SD	% of biofilm growth	SD	% of biofilm growth	SD	% of biofilm growth	SD	
	0	100	0	100	0	100	0	100	0	100	0	100	0	*Burkholderia multivorans* LMG 17582
	0.612	86	8	86	12	80	6	71	7	63	2	85	4	
	1.25	74	5	80	20	76	2	65	5	61	9	64	8	
	2.5	79	2	77	25	75	5	67	13	61	11	68	15	
	5	79	2	77	22	73	5	71	11	66	7	73	15	
	10	77	3	80	23	71	11	75	2	78	17	69	14	
	20	82	1	79	22	65	11	69	13	73	5	68	18	
	40	82	6	81	19	68	7	69	12	78	3	69	12	
Formation	Peptide (μM)	% of biofilm growth	SD	% of biofilm growth	SD	% of biofilm growth	SD	% of biofilm growth	SD	% of biofilm growth	SD	% of biofilm growth	SD	
	0	100	0	100	0	100	0	100	0	100	0	100	0	
	0.612	77	16	79	9	77	6	74	14	68	13	73	8	
	1.25	67	13	75	7	68	9	68	13	75	1	66	8	
	2.5	65	18	75	10	71	17	71	18	61	6	66	11	
	5	68	18	73	11	66	19	78	13	74	0	64	13	
	10	69	17	75	14	74	21	74	15	83	6	63	15	
	20	71	11	77	16	75	19	73	13	83	3	78	10	
	40	80	5	83	13	78	11	67	8	78	11	79	15	
Detachment	Peptide (μM)	% of biofilm growth	SD	% of biofilm growth	SD	% of biofilm growth	SD	% of biofilm growth	SD	% of biofilm growth	SD	% of biofilm growth	SD	
	0	100	0	100	0	100	0	100	0	100	0	100	0	
	0.612	85	23	86	21	85	25	92	10	89	15	94	9	
	1.25	88	17	91	15	82	31	87	18	87	18	98	3	
	2.5	100	2	96	7	84	29	90	8	75	10	105	15	
	5	92	12	96	7	89	17	89	17	84	14	89	7	
	10	93	8	104	6	94	8	101	2	94	5	89	5	
	20	93	4	101	4	95	4	91	7	85	18	86	13	
	40	93	9	92	9	92	7	108	17	104	14	84	10	*Burkholderia cenocepacia* LMG 18863

Figure 1. Anti-biofilm activity of r(P)ApoB$_L^{Pro}$, r(P)ApoB$_L^{Ala}$, and r(P)ApoB$_S^{Pro}$ peptides on *P. aeruginosa* RP 73, *P. aeruginosa* KK 27, *P. aeruginosa* 14, *P. aeruginosa* AA2, *B. multivorans* LMG 17582, and *B. cenocepacia* LMG 18863 in MHB medium.

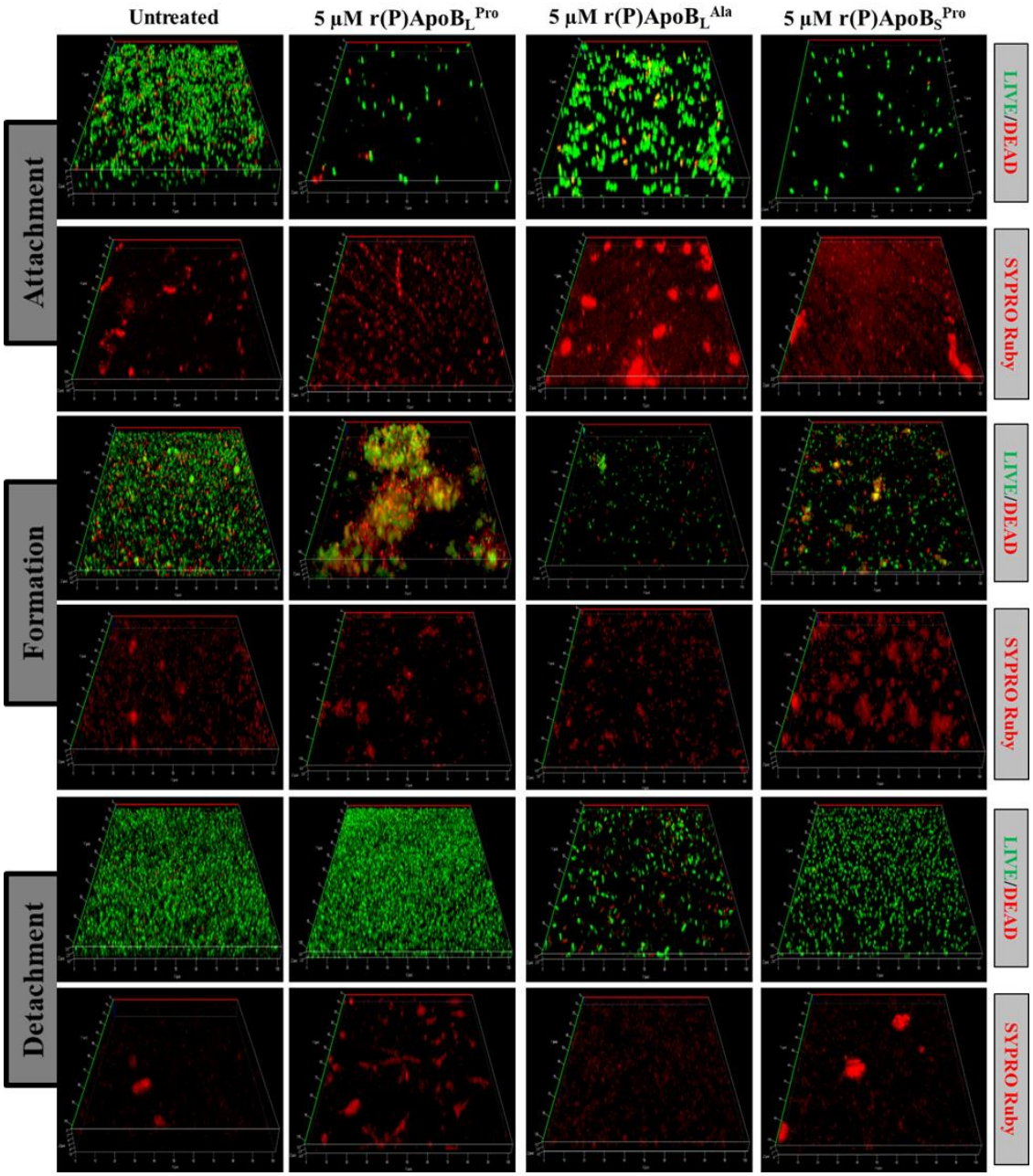

Figure 2. Effects of r(P)ApoB$_L^{Pro}$, r(P)ApoB$_L^{Ala}$, and r(P)ApoB$_S^{Pro}$ peptides on *B. cenocepacia* LMG 18863 biofilm attachment, formation and detachment. Biofilm cells were stained by using LIVE/DEAD BacLight bacterial viability kit (Molecular Probes, Eugene, OR, USA) containing 1:1 ratio of Syto-9 (green fluorescence, all cells) and propidium iodide (PI, red fluorescence, dead cells) and FilmTracer™ SYPRO® Ruby biofilm matrix staining (Invitrogen™, F10318). Images are 3D projections of biofilm structure obtained by laser scanning confocal z-stack using Zen Lite 2.3 software. All images were taken under identical conditions.

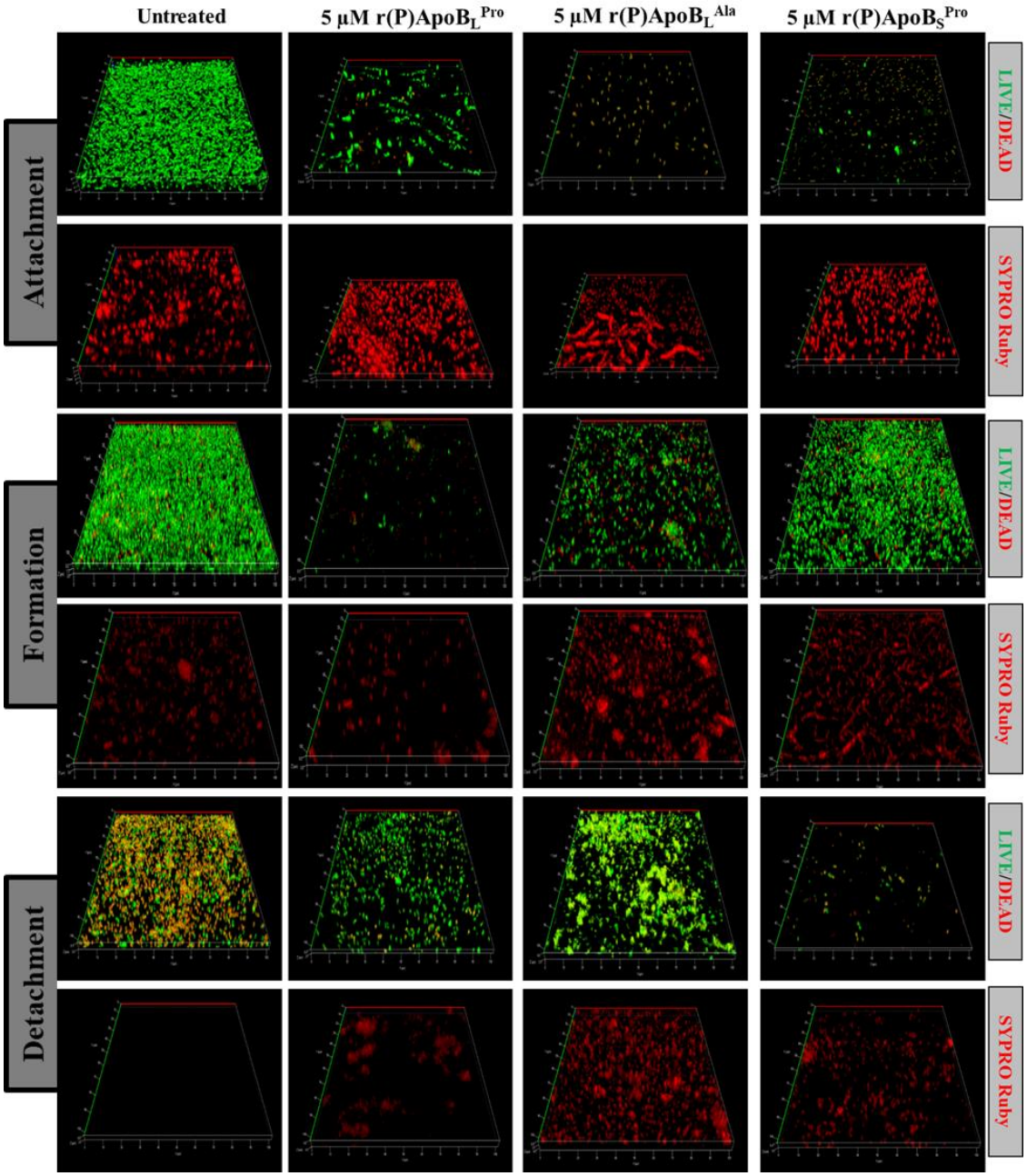

Figure 3. Effects of r(P)ApoB$_L^{Pro}$, r(P)ApoB$_L^{Ala}$ and r(P)ApoB$_S^{Pro}$ peptides on *P. aeruginosa* 14 biofilm attachment, formation and detachment. Biofilm cells were stained by using LIVE/DEAD BacLight bacterial viability kit (Molecular Probes, Eugene, OR, USA) containing 1:1 ratio of Syto-9 (green fluorescence, all cells) and propidium iodide (PI, red fluorescence, dead cells) and FilmTracer™ SYPRO® Ruby biofilm matrix staining (Invitrogen™, F10318). Images are 3D projections of biofilm structure obtained by laser scanning confocal z-stack using Zen Lite 2.3 software. All images were taken under identical conditions.

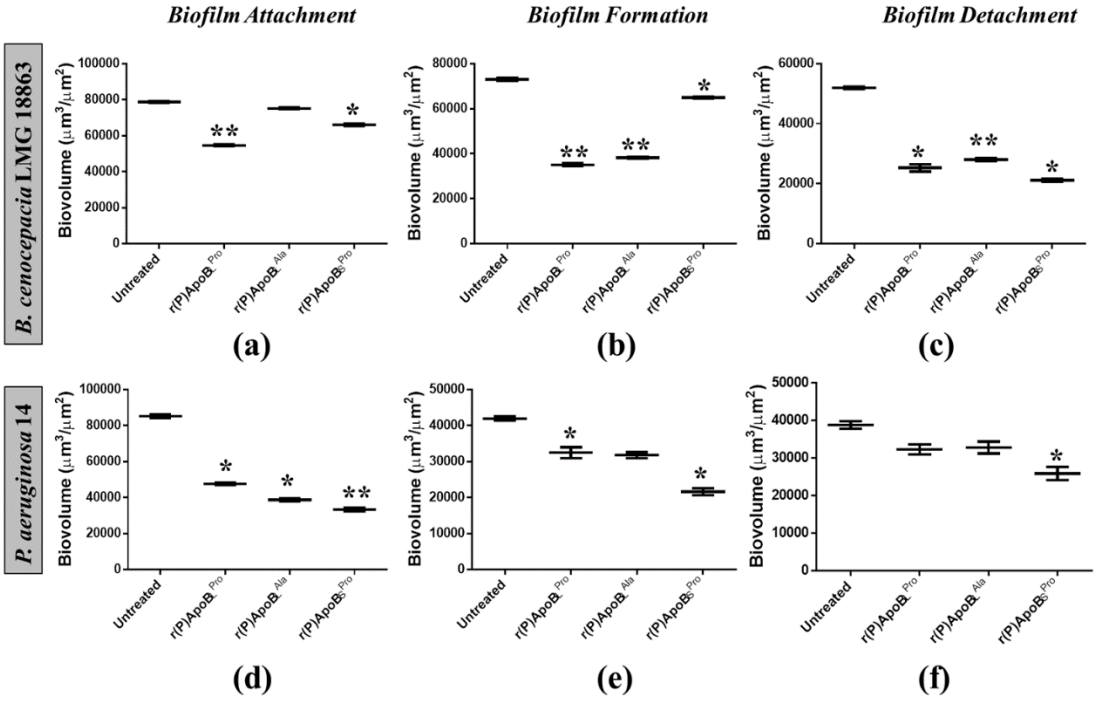

Figure 4. Analysis of the effects of r(P)ApoB$_L^{Pro}$, r(P)ApoB$_L^{Ala}$ and r(P)ApoB$_S^{Pro}$ peptides on biofilm attachment (**a**,**d**), formation (**b**,**e**) and detachment (**c**,**f**) in the case of *B. cenocepacia* LMG 18863 (**a**–**c**) and *P. aeruginosa* 14 (**d**– **f**). Biovolume ($\mu m^3/\mu m^2$) was measured by using Zen Lite 2.3 software. Significant differences were indicated as * $p < 0.05$ or ** $p < 0.01$ for treated versus control samples.

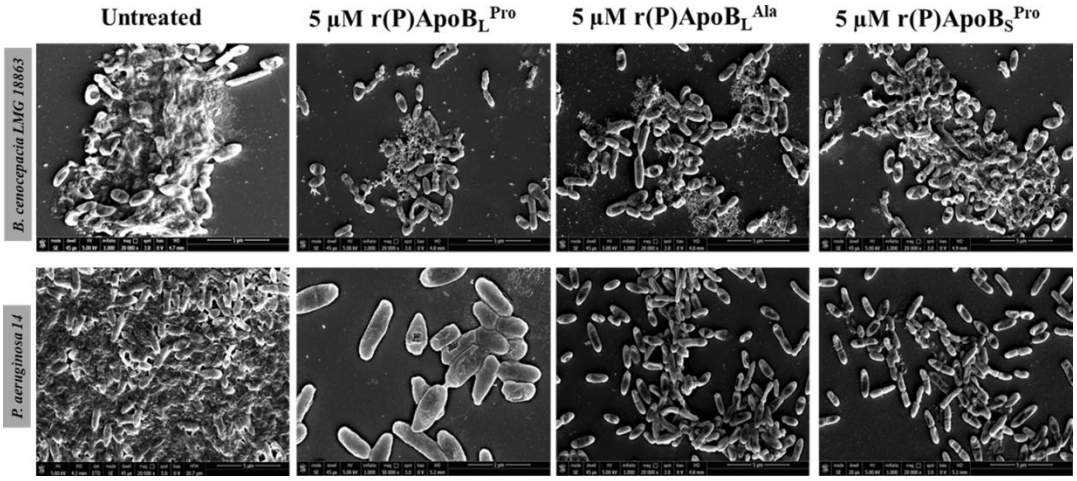

Figure 5. Morphological analyses of *B. cenocepacia* LMG 18863 (top panel) and *P. aeruginosa* 14 (lower panel) preformed biofilms by SEM. Representative images are shown upon treatment of bacterial biofilm with 5 μM r(P)ApoB$_L^{Pro}$, r(P)ApoB$_L^{Ala}$, and r(P)ApoB$_S^{Pro}$. Bars 5 μm.

2.3. Combinatorial Therapeutic Approach

To verify whether ApoB-derived peptides are able to synergistically act in combination with conventional antibiotics to counteract bacterial infections associated with biofilm in CF, CLSM analyses were performed to evaluate the effects of combinations of r(P)ApoB$_L^{Pro}$ or r(P)ApoB$_L^{Ala}$ and ciprofloxacin on preformed biofilm. Analyses were performed on *B. cenocepacia* LMG 18863 bacterial strain, since chronic lung infections associated with this strain strongly contribute to CF morbidity and mortality and are generally recalcitrant to conventional antibiotics [21,22]. Effects of r(P)ApoB$_L^{Pro}$ or

r(P)ApoB$_L$^{Ala} peptide in combination with ciprofloxacin were tested on preformed biofilm, in order to better simulate clinical conditions.

As shown in Figure 6, by comparing the effects of combinations of r(P)ApoB$_L$^{Pro} and ciprofloxacin with the effects of single agents on preformed biofilm, a significantly greater reduction of biofilm biovolume is observed in the case of the sample treated with the compound mixture together with a concomitant increase of the number of dead cells embedded into the biofilm matrix (Figure 6). Similarly, about the effects of combinations of r(P)ApoB$_L$^{Ala} and ciprofloxacin on preformed biofilm, a significantly greater reduction of biofilm biovolume is observed in the presence of compounds combination (Figure 7).

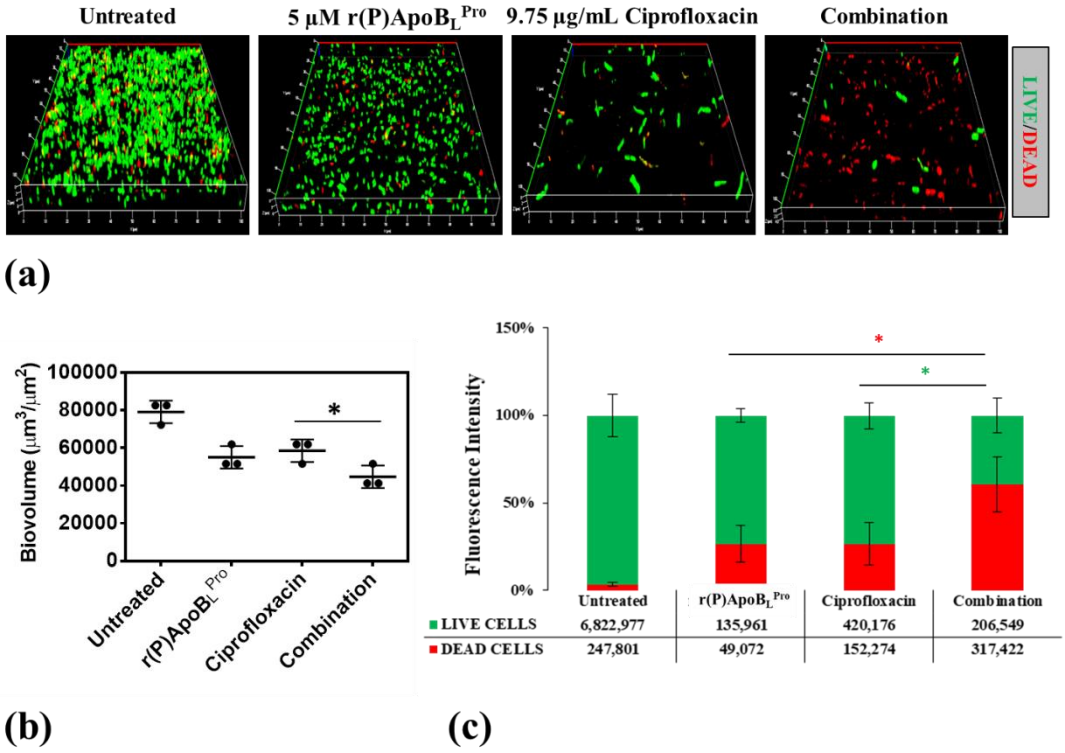

Figure 6. Effects of r(P)ApoB$_L$^{Pro}, ciprofloxacin and a combination of the two compounds on preformed biofilm (**a**). Biofilm cells were stained by using LIVE/DEAD BacLight bacterial viability kit (Molecular Probes, Eugene, OR) containing 1:1 ratio of Syto-9 (green fluorescence, all cells) and propidium iodide (PI, red fluorescence, dead cells). Images are 3D projections of biofilm structure obtained by laser scanning confocal z-stack using Zen Lite 2.3 software. All images were taken under identical conditions. Biovolume ($\mu m^3/\mu m^2$) was measured by using Zen Lite 2.3 software. Significant differences were indicated as * $p < 0.05$ for treated versus control samples (**b**). Numbers of live and dead cells were evaluated by using Zen Lite 2.3 software (**c**).

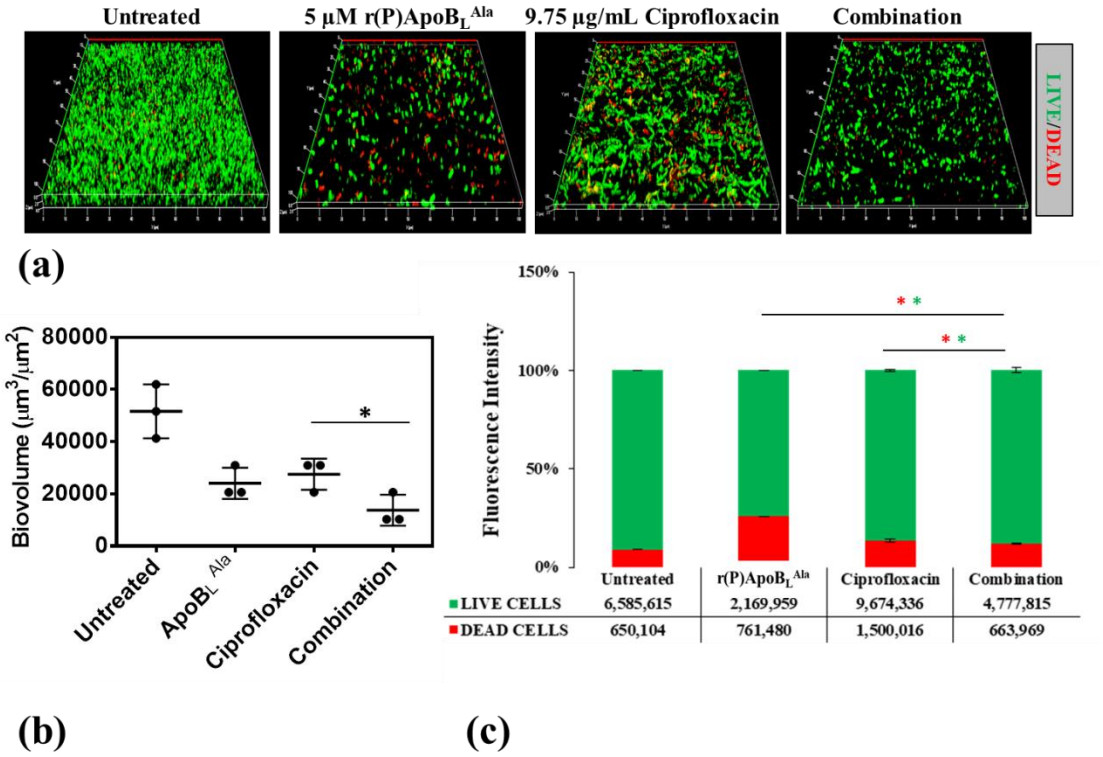

Figure 7. Effects of r(P)ApoB$_L^{Ala}$, ciprofloxacin and a combination of the two compounds on preformed biofilm (**a**). Biofilm cells were stained by using LIVE/DEAD BacLight bacterial viability kit (Molecular Probes, Eugene, OR) containing 1:1 ratio of Syto-9 (green fluorescence, all cells) and propidium iodide (PI, red fluorescence, dead cells). Images are 3D projections of biofilm structure obtained by laser scanning confocal z-stack using Zen Lite 2.3 software. All images were taken under identical conditions. Biovolume (µm^3/µm^2) was measured by using Zen Lite 2.3 software. Significant differences were indicated as * $p < 0.05$ for treated versus control samples (**b**). Numbers of live and dead cells were evaluated by using Zen Lite 2.3 software (**c**).

2.4. Evaluation of Peptide Biocompatibility

Peptide applicability in therapeutic approaches aimed at counteracting bacterial infections associated with CF is strongly dependent on the absence of any toxic effect towards host cells. For this reason, biocompatibility assays were performed to test ApoB-derived peptide effects on immortalized human bronchial epithelial mesothelial (BEAS) cells. As shown in Figure 8, only slight toxic effects were detected and the most biocompatible peptide was found to be r(P)ApoB$_L^{Ala}$. Indeed, in the presence of this peptide, only slight toxic effects were detected upon 72 h treatment and at the highest peptide concentrations tested (Figure 8).

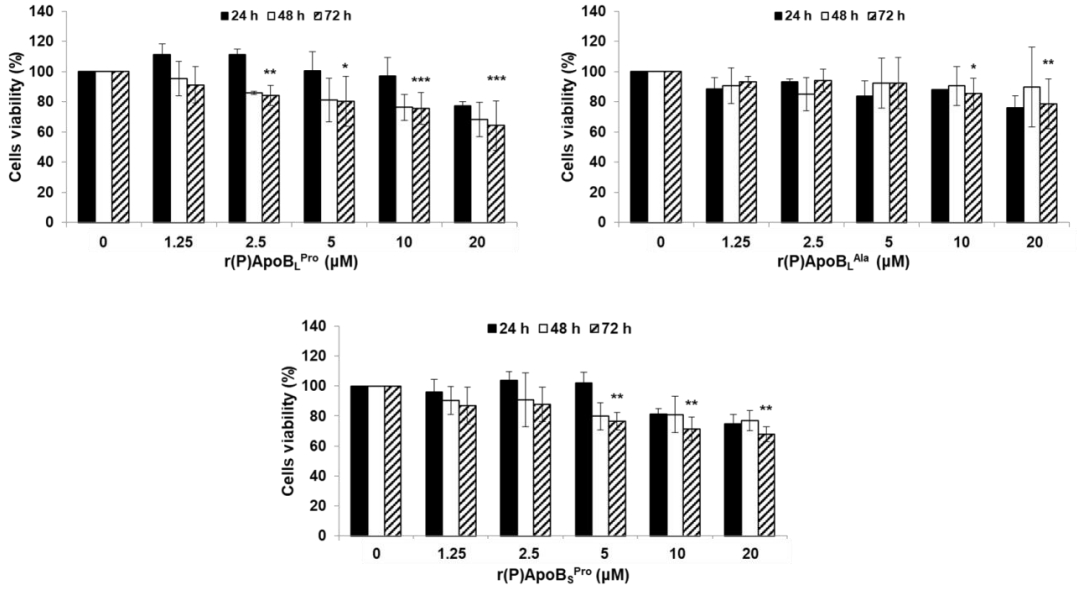

Figure 8. Effects of r(P)ApoB$_L^{Pro}$, r(P)ApoB$_L^{Ala}$ and r(P)ApoB$_S^{Pro}$ peptides on the viability of BEAS cells. Cell viability was assessed by MTT assays, and expressed as the percentage of viable cells with respect to controls (untreated cells). Error bars indicate standard deviations obtained from at least three independent experiments, each one carried out with triplicate determinations. Significant differences were indicated as * $p < 0.05$, ** $p < 0.01$ or *** $p < 0.001$ for treated versus control samples.

3. Discussion

AMPs represent novel promising effective alternative agents to counteract chronic bacterial infections affecting CF patients. Indeed, as these infections are generally recalcitrant to conventional antibiotics because of the development of the MDR phenotype and of biofilm formation, the development of novel therapeutic strategies is strongly necessary. To this purpose, three versions of a cryptide identified in human ApoB [33,35] have been here tested towards six bacterial strains clinically isolated from CF patients, such as *P. aeruginosa* RP 73, *P. aeruginosa* KK 27, *P. aeruginosa* 14, *P. aeruginosa* AA2, *B. multivorans* LMG 17582, and *B. cenocepacia* LMG 18863. ApoB-derived cryptides have been found to exert direct antimicrobial activity towards three out of six bacterial strains tested. Indeed, ApoB-derived AMPs have been found to be active on *P. aeruginosa* RP 73, *P. aeruginosa* KK 27, and *B. multivorans* LMG 17582, with MIC_{100} values ranging from 5 to 40 μM. This is in agreement with recent findings indicating that ApoB-derived cryptides direct antimicrobial activity, although mediated by electrostatic interactions between cationic peptides and negatively charged bacterial membranes, is strongly influenced by chemical composition of LPS molecules exposed on the surface of different strains of *P. aeruginosa* [35]. Indeed, although several bacterial resistance components against antimicrobial peptides have been reported [47], LPS chemical composition has been proposed to play a key role in the case of ApoB-derived cryptide antimicrobial activity [35]. It has been reported that different *Burkholderia* strains present different LPS chemotypes, such as rough, partial rough, or smooth [48]. In particular, in the case of *B. cenocepacia* LMG 18863, the LPS chemotype has been identified as smooth [48]. These differences in LPS chemotype might be responsible for the different susceptibility of *Burkholderia* strains to ApoB-derived cryptides' direct antimicrobial activity. It also has to be highlighted that several *B. cenocepacia* strains have been reported to be naturally resistant to different classes of antibiotics and even to several antimicrobial peptides [49]. This is probably due to the ability of *B. cenocepacia* strains to acquire a resistance phenotype by modifying the LPS chemical composition by substituting a phosphate group with a cationic charged residue of 4-amino-4-deoxy-L-arabinose (L-Ara4N), with a consequent reduction in membrane negative potential, that plays a key role in the interaction between bacterial membranes and antimicrobial peptides [50,51]. Based on these

observations, ApoB-derived cryptides direct antimicrobial activity towards *B. multivorans* LMG 17582 appears to be really interesting. It also has to be considered that, in the case of chronic infections affecting CF patients, the mucus phenotype favors bacterial biofilm formation [20]. Bacteria embedded into biofilm matrix are more resistant to conventional antibiotics for several reasons: i) low antibiotic diffusion rate inside biofilm matrix; ii) bacteria metabolic changes due to nutrients missing, with a consequently lower susceptibility to antibiotics; and iii) appearance of persisted cells recalcitrant to conventional antibiotics and playing a key role in long-term infections [52]. Anti-biofilm cationic amphipathic peptides represent an alternative promising approach to treat infections associated with biofilm formation, since peptides act on biofilm specific targets, such as matrix components and/or highly conserved regulatory mechanisms [53]. Here, we tested the ability of r(P)ApoB$_L^{Pro}$, r(P)ApoB$_L^{Ala}$ and r(P)ApoB$_S^{Pro}$ to affect the biofilm of bacterial strains clinically isolated from CF patients. In particular, we analyzed the ability of ApoB-derived cryptides to interfere with the three main stages of biofilm development, i.e., attachment, formation and detachment [33]. We found that all the three ApoB-derived cryptides are able to exert significant effects on biofilm attachment and formation. Even more interestingly, ApoB-derived cryptides have been found to exert significant anti-biofilm effects even on bacterial strains not sensitive to their direct antimicrobial activity. In particular, ApoB-derived AMPs have been found to affect *P. aeruginosa* 14 biofilm attachment and formation and *B. cenocepacia* LMG 18863 preformed biofilm at a very low concentration (2.5 μM). As reported for different AMPs, obtained data allow us to exclude any correlation between peptide direct antimicrobial activity and their anti-biofilm properties. Indeed, peptide IDR-1018 has been reported to be endowed with strong anti-biofilm activity towards a pool of *P. aeruginosa* and *Burkholderia* strains in the absence of any direct antimicrobial effect [54]. To deeply characterize ApoB-derived cryptides anti-biofilm activity, we also performed analyses by confocal laser scanning microscopy (CLSM) and scanning electron microscopy (SEM) on *P. aeruginosa 14* and *B. cenocepacia* LMG 18863, two strains not sensitive to ApoB-derived AMP's direct antimicrobial activity. CLSM analyses revealed the ability of ApoB-derived cryptides to alter biofilm architecture, as indicated by the appearance of highly fluorescent aggregates only in treated samples upon staining with SYPRO® Ruby, a dye able to specifically label biofilm extracellular matrix. Accordingly, a significant reduction in biofilm biovolume has been evaluated in the case of samples treated with ApoB-derived cryptides. Furthermore, scanning electron microscopy analyses clearly indicate the ability of ApoB-derived cryptides to disrupt the biofilm matrix of bacterial strains not responsive to the peptides' direct antimicrobial activity. These observations are in perfect agreement with data reported for peptide 6K-F17, which is able to strongly affect *P. aeruginosa* biofilm by disrupting the extracellular matrix, thus determining a significant decrease of biofilm biovolume [55]. However, CLSM and SEM analyses indicate only a slight increase of bacterial cells death upon treatment with 6K-F17 [55]. Based on obtained results, we also evaluated the possibility to set up effective combinatorial therapeutic approaches by concomitantly administrating ApoB-derived cryptides and conventional antibiotics to bacterial cells. To this purpose, we analyzed the anti-biofilm properties of combinations of r(P)ApoB$_L^{Pro}$ or r(P)ApoB$_L^{Ala}$ and the antibiotic ciprofloxacin, which is widely used to treat bacterial infections in CF patients [45]. The effects of compound mixtures have been tested on *P. aeruginosa 14* or *B. cenocepacia* LMG 18863 preformed biofilm. Effects of combinations of r(P)ApoB$_L^{Pro}$ or r(P)ApoB$_L^{Ala}$ and ciprofloxacin on preformed biofilm have been found to be stronger than those of single agents, with more severe effects on biofilm biovolume. It has been previously reported that, upon biofilm treatment with the ciprofloxacin antibiotic, a deep alteration of the matrix structure and a strong decrease of biofilm biovolume are immediately observed, probably associated with a high killing rate of bacterial cells embedded into the biofilm matrix [56]. However, upon a prolonged exposure to ciprofloxacin, the activation of specific mechanisms leading to a variation of biofilm phenotype makes the antibiotic ineffective [56]. This phenomenon might be overcome by the development of successful combinatorial therapeutic approaches, which present several advantages over conventional therapeutic treatments based on the administration of single agents. Indeed, several anti-biofilm peptides have been reported to be able to

act in synergism with a broad range of conventional antibiotics [57]. This allows us to significantly reduce the effective dose of antibiotics up to 64-fold, with a consequent lower possibility to induce MDR phenotype and to simultaneously reduce effective peptide concentrations [57]. In the case of CAMA peptides, synergism with the conventional antibiotics tobramycin, ciprofloxacin and colistin has been demonstrated in the treatment of *P. aeruginosa* biofilm, with the consequent possibility of reducing antibiotics doses up to 8-fold and peptide concentrations up to 10-fold [58]. Since one of the bottlenecks for the development of successful peptide-based therapies is peptide cytotoxicity, we also tested ApoB-derived cryptides effects on immortalized human bronchial epithelial mesothelial (BEAS) cells, and found that peptides are biocompatible, since slight toxic effects are detected only upon 72 h cell treatment and at the highest peptide concentrations tested. Altogether, obtained findings open interesting perspectives to the applicability of ApoB-derived cryptides in the treatment of bacterial chronic infections associated with biofilm formation and characterized by MDR phenotype, such as those affecting CF patients, and to the development in the future of successful combinatorial therapeutic approaches based on the concomitant administration of peptides and conventional antibiotics.

4. Materials and Methods

4.1. Materials

All the reagents were purchase from Sigma-Aldrich (Milan, Italy), unless differently specified.

4.2. Recombinant Production of ApoB-Derived Peptides

Expression and isolation of recombinant ApoB-derived peptides was carried out as previously described [33,35]. Pro → Ala substitution in position six of the longest peptide was obtained by QuikChange II site-directed mutagenesis performed by using the following primers: primer forward 5′-CATTTTACCCGCTTTCAGCGCAACATGCGGGTG-3′ and primer reverse 5′-GATCCGCATGTTGCGCTGAAAGCGGGTAAACTG-3′.

4.3. Bacterial Strains and Growth Conditions

Bacterial strains *P. aeruginosa* RP 73, *P. aeruginosa* KK 27, *P. aeruginosa* 14, *P. aeruginosa* AA2, *B. multivorans* LMG 17582, and *B. cenocepacia* LMG 18863 were kindly provided by Dr. Alessandra Bragonzi (Infection and CF Unit, San Raffaele Scientific Institute, Milan, Italy). Bacterial strains were grown in MHB (Becton Dickinson Difco, Franklin Lakes, NJ, USA) and on Tryptic Soy Agar (TSA; Oxoid Ltd., Hampshire, UK). In all the experiments, bacteria were inoculated and grown overnight in MHB at 37 °C.

4.4. Eukaryotic Cells and Growth Conditions

Immortalized human bronchial epithelial mesothelial cells (BEAS) were cultured in high-glucose Dulbecco's modified Eagle's medium (DMEM) supplemented with 10% fetal bovine serum and 1% penicillin-streptomycin at 37 °C in the presence of 5% carbon dioxide (CO_2).

4.5. Cell Viability Assays

Peptide effects on eukaryotic cell viability was evaluated by seeding cells in 96-well plates (100 µL/well) at a density of 3×10^3 cells/well. Upon 24 h, cells were incubated with increasing peptide concentrations (0–40 µM), for 24, 48 and 72 h. At the end of the treatment, cell viability was assessed by the 3-(4,5-dimethylthiazol-2-yl)-2,5-diphenyltetrazolium bromide (MTT) assay. MTT reagent, dissolved in DMEM without phenol red, was added to the cells (100 µL/well) at a final concentration of 0.5 mg/mL. After 4 h at 37 °C, the culture medium was removed and the resulting formazan salts were dissolved by the addition of isopropanol containing 0.1 N HCl (100 µL/well) [41]. Absorbance values of blue formazan were determined at 570 nm by using an automatic plate reader (Synergy™ H4 Hybrid Microplate Reader, BioTek Instruments, Inc., Winooski, VT, USA). Cell survival was expressed as the

percentage of viable cells in the presence of the peptide under test, with respect to control cells grown in the absence of the peptide.

4.6. Antimicrobial Activity Assays

To test the antimicrobial activity of ApoB-derived peptides, a previously described experimental procedure was used [33]. MIC_{100} values correspond to the lowest concentration of peptide associated with no detectable bacterial growth.

4.7. Anti-Biofilm Activity by Crystal Violet Assay

ApoB-derived peptides effects on biofilm attachment, formation and detachment were evaluated as previously described [33]. Optical densities at 595 nm of biofilm stained biomasses were measured by using a microtiter plate reader (Synergy™ H4 Hybrid Microplate Reader, BioTek Instruments, Inc., Winooski, VT, USA).

4.8. Anti-Biofilm Activity by CLSM Analyses

Bacterial biofilm was grown on glass cover slips in 24-well plates in 0.5X MHB in static conditions. In particular, bacterial cells from an overnight culture were diluted to about 1×10^8 CFU/mL and then seeded into wells for 4 or 24 h at 37 °C in the presence of the peptide under test, in order to evaluate biofilm attachment and formation, respectively. When effects on preformed biofilm were evaluated, bacterial biofilms were formed for 24 h at 37 °C, and then treated with peptides under test for further 24 h to evaluate their ability to eradicate preformed biofilm. Afterwards, non-adherent bacteria were removed by gently washing samples with sterile phosphate buffer and viability of cells embedded into biofilm structure was determined by sample staining with LIVE/DEAD® BacLight™ Bacterial Viability kit (Molecular Probes, Thermo Fisher Scientific, Waltham, MA, USA), while FilmTracer™ SYPRO® Ruby biofilm matrix dye has been used to stain matrices of biofilms (Invitrogen, Carlsbad, CA, USA). Staining was performed accordingly to manufacturer instructions. Biofilm images were captured by using a confocal laser scanning microscopy (Zeiss LSM 710, Zeiss, Germany) and a 63X objective oil immersion system. Biofilm architecture was analyzed by using the Zen Lite 2.3 software package (Zeiss, Germany). Each experiment was performed in triplicate. All images were taken under identical conditions.

4.9. Anti-Biofilm Activity by Scanning Electron Microscopy

To perform scanning electron microscopy (SEM) analyses, *B. cenocepacia* LMG 18863 and *P. aeruginosa 14* cells were incubated with 5 μM r(P)ApoB$_L^{Pro}$, r(P)ApoB$_L^{Ala}$ or r(P)ApoB$_S^{Pro}$ peptides for 24 h at 37 °C. Following incubation, bacterial biofilms were fixed in 2.5% glutaraldehyde. Following overnight incubation, bacterial biofilms were washed three times in distilled water and then dehydrated with a graded ethanol series: 25% ethanol (1 × 10 min); 50% ethanol (1 × 10 min); 75% ethanol (1 × 10 min); 95% ethanol (1 × 10 min); 100% anhydrous ethanol (3 × 30 min). Bacterial biofilms deposited onto glass substrate were sputter coated with a thin layer of Au-Pd (Sputter Coater Denton Vacuum DeskV) to allow subsequent morphological characterization using a FEI Nova NanoSEM 450 at an accelerating voltage of 5 kV with Everhart Thornley Detector (ETD) and Through Lens Detector (TLD) at high magnification.

4.10. Statistical Analysis

Statistical analysis was performed using a Student's t-test. Significant differences were indicated as * $p < 0.05$, ** $p < 0.01$ or *** $p < 0.001$.

Author Contributions: Conceptualization, R.G. and A.A.; methodology, R.G., A.C., E.D.O., L.T. and R.D.G.; validation, R.G.; formal analysis, R.G.; investigation, R.G., A.C., E.D.O. and R.D.G.; resources, E.P. and A.A.; data curation, R.G., A.C., L.T. and E.D.O.; writing—original draft preparation, R.G., A.C., E.D.O. and A.A.;

writing—review & editing, all authors; supervision, A.A.; project administration, A.A.; funding acquisition, E.P. and A.A. All authors have read and agreed to the published version of the manuscript.

Funding: This research was funded by the Italian Cystic Fibrosis Foundation (grant number FFC#16/2017).

Conflicts of Interest: The authors declare no conflict of interest.

Abbreviations

CF	Cystic Fibrosis
MDR	Multidrug Resistance
ApoB	Apolipoprotein B
HDPs	Host Defense Peptides
CFTR	Cystic fibrosis transmembrane conductance regulator
AMPs	Antimicrobial peptides
MIC	Minimum inhibitory concentration
MHB	Mueller Hinton Broth
CLSM	Confocal laser scanning microscopy
SEM	Scanning electron microscopy
PI	Propidium iodide
LPS	Lipopolysaccharide

References

1. Farrell, P.M. The prevalence of cystic fibrosis in the European Union. *J. Cyst. Fibros.* **2008**, *7*, 450–453. [CrossRef]
2. Evans, C.M.; Koo, J.S. Airway mucus: The good, the bad, the sticky. *Pharmacol Ther.* **2009**, *121*, 332–348. [CrossRef]
3. Chace, K.V.; Flux, M.; Sachdev, G.P. Comparison of physicochemical properties of purified mucus glycoproteins isolated from respiratory secretions of cystic fibrosis and asthmatic patients. *Biochemistry* **1985**, *24*, 7334–7341. [CrossRef] [PubMed]
4. Knowles, M.R.; Durie, P.R. What is cystic fibrosis? *N. Engl. J. Med.* **2002**, *347*, 439–442. [CrossRef] [PubMed]
5. Ciofu, O.; Hansen, C.R.; Høiby, N. Respiratory bacterial infections in cystic fibrosis. *Curr. Opin. Pulm. Med.* **2013**, *19*, 251–258. [CrossRef] [PubMed]
6. Rudkjøbing, V.B.; Thomsen, T.R.; Alhede, M.; Kragh, K.N.; Nielsen, P.H.; Johansen, U.R.; Givskov, M.; Høiby, N.; Bjarnsholt, T. The microorganisms in chronically infected end-stage and non-end-stage cystic fibrosis patients. *FEMS Immunol. Med. Microbiol.* **2012**, *65*, 236–244. [CrossRef]
7. Bjarnsholt, T.; Jensen, P.Ø.; Fiandaca, M.J.; Pedersen, J.; Hansen, C.R.; Andersen, C.B.; Pressler, T.; Givskov, M.; Høiby, N. Pseudomonas aeruginosa biofilms in the respiratory tract of cystic fibrosis patients. *Pediatr. Pulmonol.* **2009**, *44*, 547–558. [CrossRef] [PubMed]
8. Parker, D.; Ahn, D.; Cohen, T.; Prince, A. Innate Immune Signaling Activated by MDR Bacteria in the Airway. *Physio. Rev.* **2016**, *96*, 19–53. [CrossRef]
9. Blanc, D.S.; Petignat, C.; Janin, B.; Bille, J.; Francioli, P. Frequency and molecular diversity of *Pseudomonas aeruginosa* upon admission and during hospitalization: A prospective epidemiologic study. *Clin. Microbiol. Infect.* **1998**, *4*, 242–247. [CrossRef]
10. Sadikot, R.T.; Blackwell, T.S.; Christman, J.W.; Prince, A.S. Pathogen–host interactions in *Pseudomonas aeruginosa* pneumonia. *Am. J. Respir. Crit. Care Med.* **2005**, *171*, 1209–1223. [CrossRef]
11. Larrosa, M.; Truchado, P.; Espin, J.C.; Tomas-Barberan, F.A.; Allende, A.; Garcia-Conesa, M.T. Evaluation of Pseudomonas aeruginosa (PAO1) adhesion to human alveolar epithelial cells A549 using SYTO 9 dye. *Mol. Cell Probes* **2012**, *26*, 121–126. [CrossRef] [PubMed]
12. Hirakata, Y.; Izumikawa, K.; Yamaguchi, T.; Igimi, S.; Furuya, N.; Maesaki, S.; Tomono, K.; Yamada, Y.; Kohno, S.; Yamaguchi, K.; et al. Adherence to and penetration of human intestinal Caco-2 epithelial cell monolayers by Pseudomonas aeruginosa. *Infect. Immun.* **1998**, *66*, 1748–1751. [CrossRef]
13. Pier, G.B.; Grout, M.; Zaidi, T.S. Cystic fibrosis transmembrane conductance regulator is an epithelial cell receptor for clearance of Pseudomonas aeruginosa from the lung. *Proc. Natl. Acad. Sci. USA* **1997**, *94*, 12088–12093. [CrossRef] [PubMed]

14. Pier, G.B.; Grout, M.; Zaidi, T.S.; Olsen, J.C.; Johnson, L.G.; Yankaskas, J.R.; Goldberg, J.B. Role of mutant CFTR in hypersusceptibility of cystic fibrosis patients to lung infections. *Science* **1996**, *271*, 64–67. [CrossRef]
15. Esen, M.; Grassme, H.; Riethmuller, J.; Riehle, A.; Fassbender, K.; Gulbins, E. Invasion of human epithelial cells by Pseudomonas aeruginosa involves src-like tyrosine kinases p60Src and p59Fyn. *Infect. Immun.* **2001**, *69*, 281–287. [CrossRef] [PubMed]
16. Darling, K.E.; Evans, T.J. Effects of nitric oxide on Pseudomonas aeruginosa infection of epithelial cells from a human respiratory cell line derived from a patient with cystic fibrosis. *Infect. Immun.* **2003**, *71*, 2341–2349. [CrossRef]
17. Brinch, K.S.; Frimodt-Moller, N.; Hoiby, N.; Kristensen, H.H. Influence of antidrug antibodies on plectasin efficacy and pharmacokinetics. *Antimicrob. Agents Chemother.* **2009**, *53*, 4794–4800. [CrossRef]
18. Chi, E.; Mehl, T.; Nunn, D.; Lory, S. Interaction of Pseudomonas aeruginosa with A549 pneumocyte cells. *Infect. Immun.* **1991**, *59*, 822–828. [CrossRef]
19. Drenkard, E.; Ausubel, F.M. Pseudomonas biofilm formation and antibiotic resistance are linked to phenotypic variation. *Nature* **2002**, *416*, 740–743. [CrossRef]
20. Scoffone, V.C.; Chiarelli, L.R.; Trespidi, G.; Mentasti, M.; Riccardi, G.; Buroni, S. Burkholderia cenocepacia Infections in Cystic Fibrosis Patients: Drug Resistance and Therapeutic Approaches. *Front. Microbiol.* **2017**, *8*, 1592. [CrossRef]
21. Alexander, B.D.; Petzold, E.W.; Reller, L.B.; Palmer, S.M.; Davis, R.D.; Woods, C.W.; Lipuma, J.J. Survival after lung transplantation of cystic fibrosis patients infected with Burkholderia cepacia complex. *Am. J. Transplant.* **2008**, *8*, 1025–1030. [CrossRef] [PubMed]
22. Chaparro, C.; Keshavjee, S. Lung transplantation for cystic fibrosis: An update. *Expert Rev. Respir. Med.* **2016**, *10*, 1269–1280. [CrossRef] [PubMed]
23. Mercer, D.K.; O'Neil, D.A. Peptides as the next generation of anti-infectives. *Future Med. Chem.* **2013**, *5*, 315–337. [CrossRef] [PubMed]
24. Haney, E.F.; Hancock, R.B. Peptide design for antimicrobial and immunomodulatory applications. *Biopolymers* **2013**, *100*, 572–583. [CrossRef]
25. Cruz, J.; Ortiz, C.; Guzman, F.; Fernandez-Lafuente, R.; Torres, R. Antimicrobial peptides: Promising compounds against pathogenic microorganisms. *Curr. Med. Chem.* **2014**, *21*, 2299–2321. [CrossRef]
26. Epand, R.M.; Vogel, H.J. Diversity of antimicrobial peptides and their mechanisms of action. *Biochim. Biophys. Acta* **1999**, *1462*, 11–28. [CrossRef]
27. Shai, Y. Mode of action of membrane active antimicrobial peptides. *Biopolymers* **2002**, *66*, 236–248. [CrossRef]
28. Cao, H.; Ke, T.; Liu, R.; Yu, J.; Dong, C.; Cheng, M.; Huang, J.; Liu, S. Identification of a Novel Proline-Rich Antimicrobial Peptide from Brassica napus. *PLoS ONE* **2015**, *10*, e0137414. [CrossRef]
29. Fosgerau, K.; Hoffmann, T. Peptide therapeutics: Current status and future directions. *Drug Discov. Today* **2015**, *20*, 122–128. [CrossRef]
30. Yeaman, M.R.; Yount, N.Y. Mechanisms of antimicrobial peptide action and resistance. *Pharmacol. Rev.* **2003**, *55*, 27–55. [CrossRef]
31. Vineeth Kumar, T.V.; Sanil, G. A Review of the Mechanism of Action of Amphibian Antimicrobial Peptides Focusing on Peptide-Membrane Interaction and Membrane Curvature. *Curr. Protein. Pept. Sci.* **2017**, *18*, 1263–1272. [PubMed]
32. Shahrour, H.; Ferrer-Espada, R.; Dandache, I.; Bárcena-Varela, S.; Sánchez-Gómez, S.; Chokr, A.; Martinez-de-Tejada, G. AMPs as Anti-biofilm Agents for Human Therapy and Prophylaxis. *Adv. Exp. Med. Biol.* **2019**, *1117*, 257–279. [PubMed]
33. Gaglione, R.; Dell'Olmo, E.; Bosso, A.; Chino, M.; Pane, K.; Ascione, F.; Itri, F.; Caserta, S.; Amoresano, A.; Lombardi, A.; et al. Novel human bioactive peptides identified in Apolipoprotein B: Evaluation of their therapeutic potential. *Biochem. Pharmacol.* **2017**, *130*, 34–50. [CrossRef] [PubMed]
34. Pane, K.; Durante, L.; Crescenzi, O.; Cafaro, V.; Pizzo, E.; Varcamonti, M.; Zanfardino, A.; Izzo, V.; Di Donato, A.; Notomista, E. Antimicrobial potency of cationic antimicrobial peptides can be predicted from their amino acid composition: Application to the detection of "cryptic" antimicrobial peptides. *J. Theor. Biol.* **2017**, *419*, 254–265. [CrossRef]
35. Gaglione, R.; Cesaro, A.; Dell'Olmo, E.; Della Ventura, B.; Casillo, A.; Di Girolamo, R.; Velotta, R.; Notomista, E.; Veldhuizen, E.J.A.; Corsaro, M.M.; et al. Effects of human antimicrobial cryptides identified in apolipoprotein B depend on specific features of bacterial strains. *Sci. Rep.* **2019**, *9*, 6728. [CrossRef]

36. Gaglione, R.; Pane, K.; Dell'Olmo, E.; Cafaro, V.; Pizzo, E.; Olivieri, G.; Notomista, E.; Arciello, A. Cost-effective production of recombinant peptides in Escherichia coli. *N. Biotechnol.* **2019**, *51*, 39–48. [CrossRef]
37. Pane, K.; Cafaro, V.; Avitabile, A.; Torres, M.T.; Vollaro, A.; De Gregorio, E.; Catania, M.R.; Di Maro, A.; Bosso, A.; Gallo, G.; et al. Identification of Novel Cryptic Multifunctional Antimicrobial Peptides from the Human Stomach Enabled by a Computational-Experimental Platform. *ACS Synth. Biol.* **2018**, *7*, 2105–2115. [CrossRef]
38. Zanfardino, A.; Bosso, A.; Gallo, G.; Pistorio, V.; Di Napoli, M.; Gaglione, R.; Dell'Olmo, E.; Varcamonti, M.; Notomista, E.; Arciello, A.; et al. Human apolipoprotein E as a reservoir of cryptic bioactive peptides: The case of ApoE 133-167. *J. Pept. Sci.* **2018**, *24*, e3095. [CrossRef]
39. Pizzo, E.; Pane, K.; Bosso, A.; Landi, N.; Ragucci, S.; Russo, R.; Gaglione, R.; Torres, M.D.T.; de la Fuente-Nunez, C.; Arciello, A.; et al. Novel bioactive peptides from PD-L1/2, a type 1 ribosome inactivating protein from Phytolacca dioica L. Evaluation of their antimicrobial properties and anti-biofilm activities. *Biochim. Biophys. Acta Biomembr.* **2018**, *1860*, 1425–1435. [CrossRef]
40. Pizzo, E.; Cafaro, V.; Di Donato, A.; Notomista, E. Cryptic Antimicrobial Peptides: Identification Methods and Current Knowledge of their Immunomodulatory Properties. *Curr. Pharm. Des.* **2018**, *24*, 1054–1066. [CrossRef]
41. Gaglione, R.; Pirone, L.; Farina, B.; Fusco, S.; Smaldone, G.; Aulitto, M.; Dell'Olmo, E.; Roscetto, E.; Del Gatto, A.; Fattorusso, R.; et al. Insights into the anticancer properties of the first antimicrobial peptide from Archaea. *Biochim. Biophys. Acta Gen. Subj.* **2017**, *1861*, 2155–2164. [CrossRef] [PubMed]
42. Kasetty, G.; Papareddy, P.; Kalle, M.; Rydengård, V.; Walse, B.; Svensson, B.; Mörgelin, M.; Malmsten, M.; Schmidtchen, A. The C-terminal sequence of several human serine proteases encodes host defense functions. *J. Innate Immun.* **2011**, *3*, 471–482. [CrossRef] [PubMed]
43. Lee, D.Y.; Huang, C.M.; Nakatsuji, T.; Thiboutot, D.; Kang, S.A.; Monestier, M.; Gallo, R.L. Histone H4 is a major component of the antimicrobial action of human sebocytes. *J. Invest. Dermatol.* **2009**, *129*, 2489–2496. [CrossRef] [PubMed]
44. Beck, W.H.; Adams, C.P.; Biglang-Awa, I.M.; Patel, A.B.; Vincent, H.; Haas-Stapleton, E.J.; Weers, P.M. Apolipoprotein A-I binding to anionic vesicles and lipopolysaccharides: Role for lysine residues in antimicrobial properties. *Biochim. Biophys. Acta* **2013**, *1828*, 1503–1510. [CrossRef] [PubMed]
45. Langton Hewer, S.C.; Smyth, A.R. Antibiotic strategies for eradicating Pseudomonas aeruginosa in people with cystic fibrosis. *Cochrane Database Syst. Rev.* **2014**, *11*, CD004197.
46. Sanchez, Z.; Tani, A.; Kimbara, K. Extensive reduction of cell viability and enhanced matrix production in Pseudomonas aeruginosa PAO1 flow biofilms treated with a D-amino acid mixture. *Appl. Environ. Microbiol.* **2013**, *79*, 1396–1399. [CrossRef]
47. Bechinger, B.; Gorr, S.U. Antimicrobial Peptides: Mechanisms of Action and Resistance. *J. Dent. Res.* **2017**, *96*, 254–260. [CrossRef]
48. De Soyza, A.; Ellis, C.D.; Khan, C.M.A.; Corris, P.A.; Demarco De Hormaeche, R. Burkholderia cenocepacia lipopolysaccharide, lipid A, and proinflammatory activity. *Am. J. Respir. Crit. Care Med.* **2004**, *170*, 70–77. [CrossRef]
49. Mahenthiralingam, E.; Urban, T.A.; Goldberg, J.B. The multifarious, multireplicon Burkholderia cepacia complex. *Nat. Rev. Microbiol.* **2005**, *3*, 144–156. [CrossRef]
50. Raetz, C.R.H.; Reynolds, C.M.; Trent, M.S.; Bishop, R.E. Lipid A Modification Systems in Gram-Negative Bacteria. *Annu. Rev. Biochem.* **2007**, *76*, 295–329. [CrossRef]
51. Olaitan, A.O.; Morand, S.; Rolain, J.M. Mechanisms of polymyxin resistance: Acquired and intrinsic resistance in bacteria. *Front. Microbiol.* **2014**, *5*, 29–30. [CrossRef] [PubMed]
52. Mulcahy, L.R.; Burns, J.L.; Lory, S.; Lewis, K. Emergence of Pseudomonas aeruginosa strains producing high levels of persister cells in patients with cystic fibrosis. *J. Bacteriol.* **2010**, *192*, 6191–6199. [CrossRef] [PubMed]
53. Pletzer, D.; Hancock, R.E.W. Antibiofilm peptides: Potential as broadspectrum agents. *J. Bacteriol.* **2016**, *198*, 2572–2578. [CrossRef] [PubMed]
54. Mansour, S.C.; de la Fuente-Núñez, C.; Hancock, R.E. Peptide IDR-1018: Modulating the immune system and targeting bacterial biofilms to treat antibiotic-resistant bacterial infections. *J. Pept. Sci.* **2015**, *21*, 323–329. [CrossRef] [PubMed]

55. Beaudoin, T.; Stone, T.A.; Glibowicka, M.; Adams, C.; Yau, Y.; Ahmadi, S.; Bear, C.E.; Grasemann, H.; Waters, V.; Deber, C.M. Activity of a novel antimicrobial peptide against Pseudomonas aeruginosa biofilms. *Sci. Rep.* **2018**, *8*, 14728. [CrossRef] [PubMed]
56. Soares, A.; Roussel, V.; Pestel-Caron, M.; Barreau, M.; Caron, F.; Bouffartigues, E.; Chevalier, S.; Etienne, M. Understanding Ciprofloxacin Failure in *Pseudomonas aeruginosa* Biofilm: Persister Cells Survive Matrix Disruption. *Front. Microbiol.* **2019**, *10*, 2603. [CrossRef]
57. Reffuveille, F.; De La Fuente-Núñez, C.; Mansour, S.; Hancock, R.E.W. A broad-spectrum antibiofilm peptide enhances antibiotic action against bacterial biofilms. *Antimicrob. Agents Chemother.* **2014**, *58*, 5363–5371. [CrossRef]
58. Dosler, S.; Karaaslan, E. Inhibition and destruction of Pseudomonas aeruginosa biofilms by antibiotics and antimicrobial peptides. *Peptides* **2014**, *62*, 32–37. [CrossRef]

SCIENTIFIC REPORTS

OPEN

Effects of human antimicrobial cryptides identified in apolipoprotein B depend on specific features of bacterial strains

Received: 3 January 2019
Accepted: 12 April 2019
Published online: 30 April 2019

Rosa Gaglione[1], Angela Cesaro[1], Eliana Dell'Olmo[1], Bartolomeo Della Ventura[2], Angela Casillo[1], Rocco Di Girolamo[1], Raffaele Velotta[2], Eugenio Notomista[3], Edwin J. A. Veldhuizen[4], Maria Michela Corsaro[1], Claudio De Rosa[1] & Angela Arciello[1,5]

Cationic Host Defense Peptides (HDPs) are endowed with a broad variety of activities, including direct antimicrobial properties and modulatory roles in the innate immune response. Even if it has been widely demonstrated that bacterial membrane represents the main target of peptide antimicrobial activity, the molecular mechanisms underlying membrane perturbation by HDPs have not been fully clarified yet. Recently, two cryptic HDPs have been identified in human apolipoprotein B and found to be endowed with a broad-spectrum antimicrobial activity, and with anti-biofilm, wound healing and immunomodulatory properties. Moreover, ApoB derived HDPs are able to synergistically act in combination with conventional antibiotics, while being not toxic for eukaryotic cells. Here, by using a multidisciplinary approach, including time killing curves, Zeta potential measurements, membrane permeabilization assays, electron microscopy analyses, and isothermal titration calorimetry studies, the antimicrobial effects of ApoB cryptides have been analysed on bacterial strains either susceptible or resistant to peptide toxicity. Intriguingly, it emerged that even if electrostatic interactions between negatively charged bacterial membranes and positively charged HDPs play a key role in mediating peptide toxicity, they are strongly influenced by the composition of negatively charged bacterial surfaces and by defined extracellular microenvironments.

Antimicrobial peptides (AMPs) are effectors of the innate immune system in a wide variety of species from the plant and animal kingdoms, including humans[1]. Although structurally different, most of these peptides fold into amphiphilic structures due to their short size (<50 amino acid residues), net positive charge and high content of hydrophobic residues[2]. Their activity against a wide range of microorganisms combined with their unique property of displaying few to no resistance effects[3] allowed AMPs to gain great attention as promising and effective alternatives to conventional antibiotics, also against strains resistant to approved antibacterial agents[4]. Since these peptides are also able to modulate the immune response of host organisms, their efficiency is considerably enhanced. Because of this extension of functionalities, they have been more properly named "host defence peptides" (HDPs)[5,6]. The key features that make HDPs antimicrobial are their cationic nature, their ability to bind to bacterial membranes and to adopt specific secondary structures in membrane environments[7], an essential prerequisite to their attachment and insertion into bacterial membranes. HDPs have been found to kill bacteria by first associating with their negatively charged cell surfaces and subsequently disrupt their cell membranes *via* mechanisms that involve membrane thinning, formation of transient pores, or disruption of lipid matrix, which impairs barrier function of bacterial membranes[8]. Some HDPs are also able to pass through the lipid bilayer of the membrane to act on intracellular targets[8]. Furthermore, some HDPs preferentially attack septating bacterial cells where peptides have been found to be associated to the septum and the curved regions of the outer membrane[9]. Since most HDPs target the bacterial plasma membrane directly rather than through specific protein receptors[10],

[1]Department of Chemical Sciences, University of Naples Federico II, 80126, Naples, Italy. [2]Department of Physics, University of Naples Federico II, 80126, Naples, Italy. [3]Department of Biology, University of Naples Federico II, 80126, Naples, Italy. [4]Department of Infectious Diseases and Immunology, Division Molecular Host Defence, Faculty of Veterinary Medicine, Utrecht University, Utrecht, The Netherlands. [5]Istituto Nazionale di Biostrutture e Biosistemi (INBB), Rome, Italy. Correspondence and requests for materials should be addressed to A.A. (email: anarciel@unina.it)

membrane phospholipid composition and net charge also play a key role in determining peptides antimicrobial activity[11]. Indeed, these parameters vary not only from bacterium to bacterium, but also as a response to changing environments[12] and exposure to antimicrobial agents[13]. Peptide concentration also represents a further key parameter, with maximal antimicrobial activity reached only at peptide concentrations exceeding a threshold value[14]. Indeed, upon an initial electrostatic interaction between positively charged peptide molecules and negatively charged lipids, peptides reach an appropriate local concentration, allowing their penetration into the hydrophobic core of the bilayer[15,16]. Membrane bilayer thickness also appears to have an effect on the ability of a peptide to bind to the membrane and, consequently, on the ability of a lipid bilayer to induce peptide secondary structures[17,18]. However, despite decades of research, novel structural and dynamic features of membrane-associated HDPs are continuously being discovered[19] and the exact molecular mechanism underlying HDPs ability to perturb bacterial membranes still remains controversial. Here, we analyse the antimicrobial activity of two recently characterized HDPs[20], identified in human apolipoprotin B by using a bioinformatics method developed by our research group[21–25]. It has been reported that several eukaryotic proteins, with functions not necessarily related to host defence, act as sources of "cryptic" bioactive peptides released upon proteolytic processing by bacterial and/or host proteases[26–28]. The two novel bioactive peptides analysed in the present study represent two variants of the HDP identified in human apolipoprotein B (residues 887–922), *i.e.* peptides ApoB887–923 and ApoB887–911. These two HDPs, recombinantly produced in bacterial cells, have been here named r(P)ApoB$_L$ and r(P)ApoB$_S$ because of the presence of a Pro residue becoming the N-terminus of the peptides released by the acidic cleavage of an Asp-Pro bond[20]. The primary structure of the two ApoB derived HDPs is reported in Fig. S1. Both recombinant peptides have been found to be endowed with antimicrobial, anti-biofilm, wound healing and immunomodulatory properties[20]. On the other hand, they have been found to be neither toxic for mammalian cells nor hemolytic towards murine red blood cells. Interestingly, ApoB derived peptides were also found to exert significant synergistic effects in combination with either conventional antibiotics or EDTA[20]. Noteworthy, bacterial strains found to be not responsive to ApoB derived peptides, such as *S. aureus* strains and *P. aeruginosa* ATCC 27853, appeared highly susceptible to selected combinations of peptides and antibiotics or EDTA[20], thus opening interesting perspectives to the development of successful combination therapy approaches, that have a very low potential to induce resistance phenotype. Since the definition of the molecular bases of ApoB derived peptides biological activities could greatly contribute to the rational design of effective combinatorial therapeutic approaches, in the present paper, time killing curves, Zeta potential measurements, membrane permeabilization assays, isothermal titration calorimetry studies and morphological analyses by electron microscopy have been performed.

Results

Killing kinetics studies. It has been previously reported that ApoB derived peptides are effective on *B. globigii* TNO BM013 and *P. aeruginosa* PAO1 bacterial strains[20], as shown in Table S1. Here, in order to analyse the kinetic of peptides bactericidal activity, we obtained kinetic killing curves by treating bacterial cells with increasing concentrations of either r(P)ApoB$_L$ or r(P)ApoB$_S$ for different time intervals (0–180 min). The two bacterial strains have been selected as a prototype of Gram-positive (*B. globigii* TNO BM013) and Gram-negative (*P. aeruginosa* PAO1) strains susceptible to antimicrobial ApoB derived peptides. In all the experiments, chicken cathelicidin-2 (CATH-2), a known antimicrobial peptide from chicken[29], was tested as a positive control (Fig. 1E,F). To perform the analyses, following the incubation with peptides, control and treated samples were serially diluted and plated on agar, in order to count bacterial colonies[30]. As reported in Fig. 1A,C, at the highest peptide concentrations tested (10–20 μM), *B. globigii* TNO BM013 cells were killed within 10–30 min. At the lowest peptide concentrations (1.25–2.5 μM), instead, the same effect was obtained within 120 min (Fig. 1A,C). When peptides were tested on *P. aeruginosa* PAO1, bacterial cells were killed within 30 minutes at the highest peptide concentrations tested (10–20 μM), and within 120–180 minutes at lower peptide concentrations (2.5–5 μM) (Fig. 1B,D). In the case of CATH-2 control peptide, all the curves obtained appear perfectly superimposable, since all peptide concentrations tested were found to have the same effects. As a consequence, only the curves corresponding to the highest peptide concentration tested (20 μM) appear visible (Fig. 1E,F).

Zeta potential measurements of bacterial cells upon treatment with peptides. To evaluate ApoB derived peptides effects on bacterial membrane surface, Zeta potential (ζ) measurements were carried out. First of all, ζ values of control bacterial cells were determined over time (0–180 min) in NB 0.5X medium, in order to obtain the electrostatic potential at the shear plane of the bacteria in solution (Fig. S2). It was found that ζ did not vary throughout the incubation time in the case of all the strains tested, thus indicating their high stability. In detail, the average potential of untreated *B. globigii* TNO BM013, *S. aureus* MRSA WKZ-2, *P. aeruginosa* PAO1 and *P. aeruginosa* ATCC 27853 strains were found to be -33 ± 3, -28 ± 3, -23 ± 2, and -11 ± 2 mV, respectively (Fig. S2 and Table 1). The different values obtained for the various bacterial strains might be due to differences in membrane composition. Bacterial strains susceptible to antimicrobial ApoB derived peptides, *i.e. B. globigii* TNO BM013 and *P. aeruginosa* PAO1, were exposed to r(P)ApoB$_L$ or r(P)ApoB$_S$ at a concentration corresponding to their MIC values (Table S1). Upon treatment with each peptide, ζ was recorded at regular time intervals for 180 min. All the recorded ζ values are reported in Fig. S3. Values corresponding to the time point necessary to obtain complete cell death of treated bacterial cells on agar plates (30 min) have been reported for *B. globigii* TNO BM013 and *P. aeruginosa* PAO1 (both of them susceptible to antimicrobial peptides) in Fig. 2A,C, respectively. In Fig. 2B,D, instead, ζ values measured at the highest peptide concentration tested (40 μM) for *S. aureus* MRSA WKZ-2 and *P. aeruginosa* ATCC 27853 (both of them non-susceptible to antimicrobial peptides) are reported. Upon incubation of *B. globigii* TNO BM013 with r(P)ApoB$_L$ or r(P)ApoB$_S$, ζ was found to shift from -33 ± 3 mV to -11 ± 3 and -19 ± 3 mV, respectively (Fig. 2A and Table 1). This is indicative of the occurrence of electrostatic interactions between positively charged peptides and negatively charged bacterial

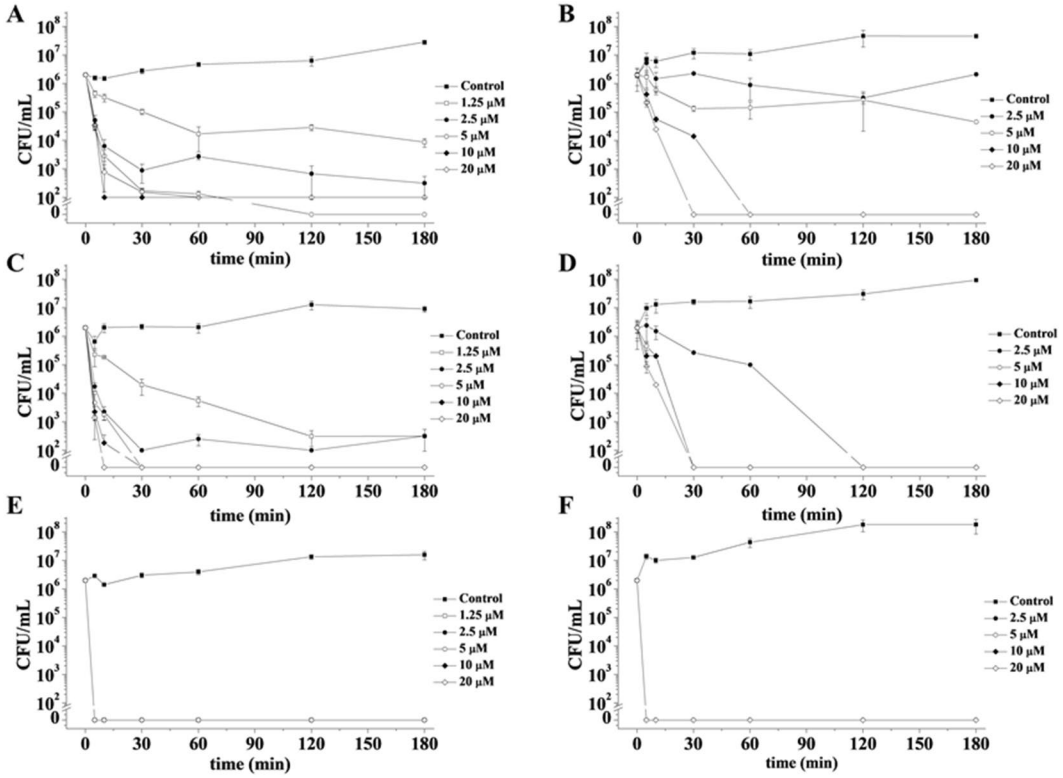

Figure 1. Time killing curves obtained by incubating *B. globigii* TNO BM013 (**A**,**C**,**E**) and *P. aeruginosa* PAO1 (**B**,**D**,**F**) strains with increasing concentrations of r(P)ApoB$_L$ (**A**,**B**), r(P)ApoB$_S$ (**C**,**D**) and CATH-2 (**E**,**F**) peptides for different lengths of time. Data represent the mean (± standard deviation, SD) of at least three independent experiments, each one carried out with triplicate determinations. For all the experimental points, $^*P < 0.05$, $^{**}P < 0.01$, or $^{***}P < 0.001$ were obtained for control *versus* treated samples.

	SAMPLE	Z-POTENTIAL ± DS (mV)
B. globigii TNO BM013	Cells t_0	−33 ± 3
	Cells $t_{30\ min}$	−29 ± 2
	Cells + r(P)ApoB$_L$ $t_{30\ min}$	−11 ± 3
	Cells + r(P)ApoB$_S$ $t_{30\ min}$	−19 ± 3
P. aeruginosa PAO1	Cells t_0	−23 ± 2
	Cells $t_{30\ min}$	−23 ± 2
	Cells + r(P)ApoB$_L$ $t_{30\ min}$	−19 ± 3
	Cells + r(P)ApoB$_S$ $t_{30\ min}$	−17 ± 3
S. aureus MRSA WKZ−2	Cells t_0	−28 ± 3
	Cells $t_{30\ min}$	−26 ± 2
	Cells + r(P)ApoB$_L$ $t_{30\ min}$	−4 ± 3
	Cells + r(P)ApoB$_S$ $t_{30\ min}$	−4 ± 3
P. aeruginosa ATCC 27853	Cells t_0	−11 ± 2
	Cells $t_{30\ min}$	−10 ± 2
	Cells + r(P)ApoB$_L$ $t_{30\ min}$	−3 ± 2
	Cells + r(P)ApoB$_S$ $t_{30\ min}$	−3 ± 2
Peptides alone	r(P)ApoB$_L$	−3 ± 1
	r(P)ApoB$_S$	−3 ± 1

Table 1. Zeta-potential values recorded for bacterial cells at time 0 and upon 30 min in the absence or in the presence of ApoB derived peptides; zeta-potential values of each peptide in solution are also reported.

surfaces, which leads to a partial neutralization of bacterial surface charge. A similar behavior was also observed in the case of Gram-negative *P. aeruginosa* PAO1 bacterial strain upon treatment with r(P)ApoB$_L$ or r(P)ApoB$_S$, since also in this case ζ shifted towards more positive values (Fig. 2C and Table 1). It is worth to highlight that,

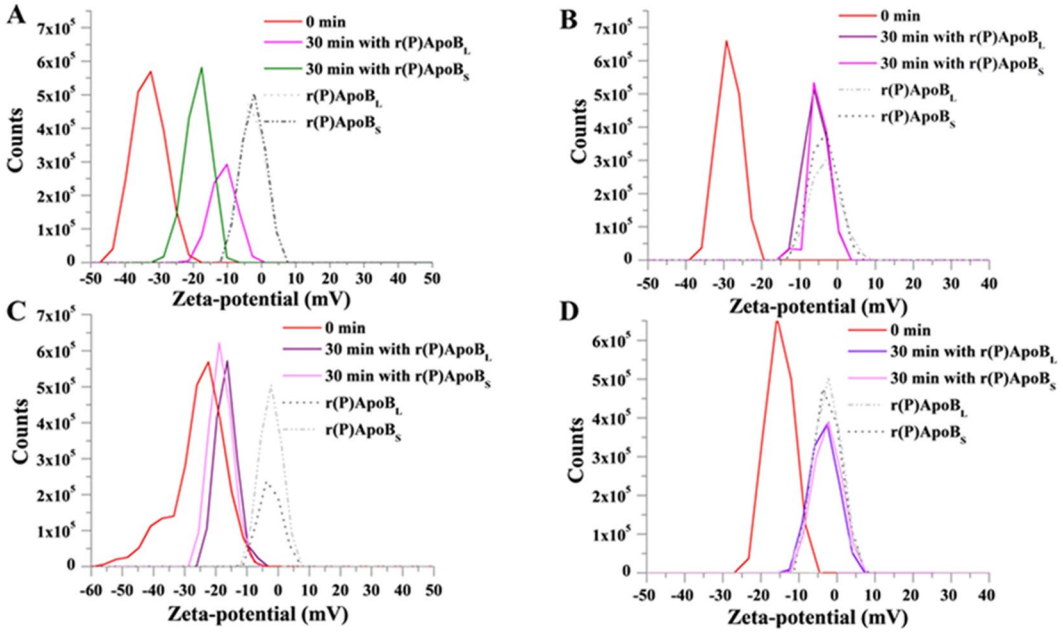

Figure 2. ApoB derived peptides effects on the Zeta potential of treated bacterial cells. Zeta potential values of *B. globigii* TNO BM013 (**A**) and *P. aeruginosa* PAO1 (**C**) bacterial strains were determined upon treatment with r(P)ApoB$_L$ or r(P)ApoB$_S$ peptides at a concentration corresponding to MIC$_{100}$ values. Zeta potential values of bacterial strains not responsive to antimicrobial ApoB derived peptides, *i.e. S. aureus* MRSA WKZ-2 (**B**) and *P. aeruginosa* ATCC 27853 (**D**), were determined upon treatment with peptides at the highest concentration tested (40 μM) for 180 min. Dashed curves represent the Zeta potential values of ApoB derived peptides alone in bacterial culture medium (NB 0.5X). In the case of *B. globigii* TNO BM013 (**A**) and *P. aeruginosa* PAO1 (**C**) bacterial strains, a positive ζ shift is indicative of an interaction between bacterial cells and peptides. On the contrary, in the case of *S. aureus* MRSA WKZ-2 (**B**) and *P. aeruginosa* ATCC 27853 (**D**) bacterial strains, signals recorded upon treatment with peptides (continuous lines) are almost completely superimposable to those recorded for free peptide in culture medium at 40 μM (dashed lines), thus indicating absence of interactions between bacterial cells and peptides. Data represent the average of at least three independent experiments.

in the case of *B. globigii* TNO BM013 bacterial strain, a larger ζ shift was observed with respect to *P. aeruginosa* PAO1, as expected on the basis of its higher sensitivity to peptide toxicity. On the contrary, in the case of bacterial strains non-responsive to antimicrobial ApoB derived peptides, obtained signals were found to be almost completely superimposable to those recorded for the free peptide in solution at the same concentration (Fig. 2B,D, dashed lines), thus clearly indicating that only the signal attributable to the free peptide in solution was measured (Fig. 2B,D, dashed lines). This indicates that, in the case of non-responsive bacterial strains, no electrostatic interactions occur between bacterial surfaces and antimicrobial peptides. It is presumable that some extracellular factors or bacterial membrane composition might interfere with electrostatic interactions between negatively charged bacterial surfaces and positively charged peptides, and this ultimately makes peptides ineffective.

Membrane permeabilization assays. To evaluate the effect of ApoB derived peptides on bacterial membrane permeability, N-Phenyl-1-naphthylamine (NPN) fluorescent probe was used. As expected, NPN uptake was found to be negligible for untreated bacterial cells, characterized by intact cell surface (Table 2 and Fig. S4A,B). The spectrofluorometric assay was also performed upon treatment of bacterial strains with ApoB derived peptides for 30 min at 37 °C. Incubation time was selected on the basis of time killing curve data (Fig. 1). *B. globigii* TNO BM013 and *P. aeruginosa* PAO1 responsive strains were treated with peptide concentrations corresponding to previously determined MIC$_{100}$ values[20], reported in Table S1, whereas not responsive *S. aureus* MRSA WKZ-2 and *P. aeruginosa* ATCC 27853 strains were treated with 40 μM peptides for 30 min at 37 °C. As shown in Table 2, NPN uptake factor was found to be 1.4 ± 0.9 for control *P. aeruginosa* PAO1 cells, and increased to 8.9 ± 1.2 and 11.1 ± 2.0 upon treatment with r(P)ApoB$_L$ and r(P)ApoB$_S$, respectively (Table 2). Similar results were obtained when responsive Gram-positive *B. globigii* TNO BM013 strain was tested. Indeed, NPN uptake factor was found to be 4.1 ± 0.9 for control cells and 7.8 ± 1.1 or 7.6 ± 1.0 for cells treated with r(P)ApoB$_L$ and r(P)ApoB$_S$, respectively (Table 2). On the other hand, no significant variation in NPN uptake was detected when not responsive bacterial cells were treated with ApoB derived peptides (Table 2). As a positive control, bacterial strains under test were treated with increasing concentrations of polycationic antibiotic colistin (0.25–4 μg/mL) or glycopeptide antibiotic vancomycin (0.00156–0.250 μg/mL). In both cases, following treatment, NPN uptake was found to increase in a concentration dependent manner (Fig. S4A,B). Indeed, both antibiotics, although with different mechanisms, have been reported to ultimately cause membrane permeabilization[31,32]. Altogether, obtained results confirm the crucial role played by bacterial membrane as main target of ApoB derived peptides antimicrobial activity.

	Samples	NPN uptake factor ± SD
B. globigii TNO BM013	Cells	4.1 ± 0.9
	Cells + r(P)ApoB$_L$ $t_{30\ min}$	7.8 ± 1.1
	Cells + r(P)ApoB$_S$ $t_{30\ min}$	7.6 ± 1.0
P. aeruginosa PAO1	Cells t_0	1.4 ± 0.9
	Cells + r(P)ApoB$_L$ $t_{30\ min}$	8.9 ± 1.2
	Cells + r(P)ApoB$_S$ $t_{30\ min}$	11.1 ± 2.0
S. aureus MRSA WKZ-2	Cells t_0	1.6 ± 0.5
	Cells + r(P)ApoB$_L$ $t_{30\ min}$	0.7 ± 0.1
	Cells + r(P)ApoB$_S$ $t_{30\ min}$	1.2 ± 0.1
P. aeruginosa ATCC 27853	Cells t_0	0.2 ± 0.1
	Cells + r(P)ApoB$_L$ $t_{30\ min}$	0.3 ± 0.1
	Cells + r(P)ApoB$_S$ $t_{30\ min}$	0.5 ± 0.1

Table 2. NPN uptake factors determined upon incubation of bacterial cells in the presence or in the absence of ApoB derived peptides. Data represent the average of at least three independent experiments.

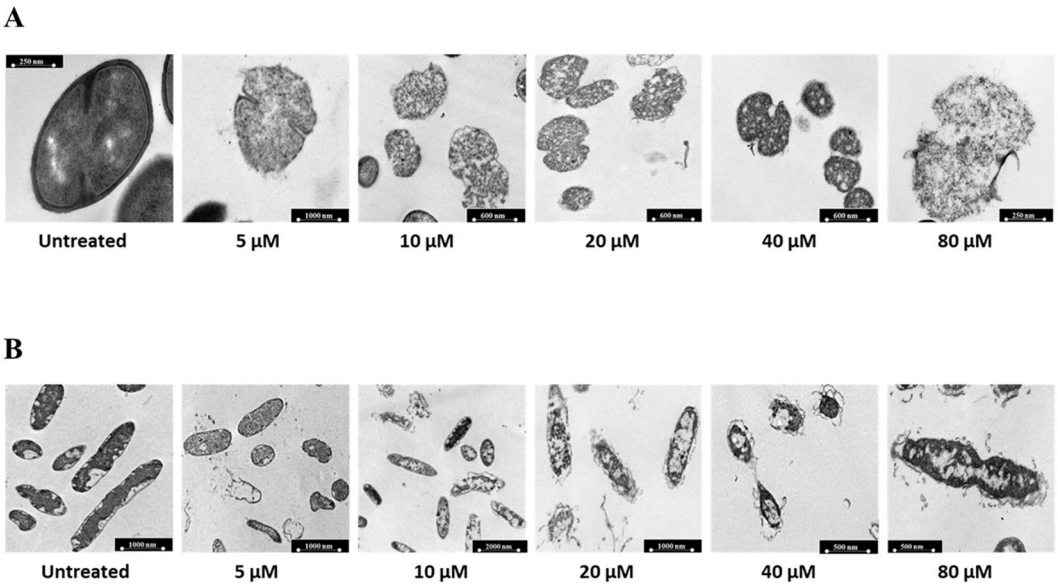

Figure 3. Morphological analyses of *B. globigii* TNO BM013 (**A**) and *P. aeruginosa* PAO1 (**B**) cells by TEM. Representative images are shown upon treatment of bacterial cells with increasing concentrations (0–80 μM) of r(P)ApoB$_L$ peptide. A total of 60 cells were analysed for each peptide concentration in two independent experiments. Bars 250, 500 or 1,000 nm.

Morphological alterations induced by ApoB derived peptides. To evaluate morphological alterations of bacterial strains susceptible to antimicrobial ApoB derived peptides, transmission electron microscopy (TEM) analyses were performed. In the case of control bacterial cells, intact membranes, a homogeneous intracellular distribution of DNA and ribosomes rich areas were observed (dark areas in Fig. 3). When bacterial cells were, instead, treated with increasing concentrations of r(P)ApoB$_L$ peptide, a progressive detachment of cell wall and cell lysis was observed in the case of Gram-positive *B. globigii* TNO BM013 (Fig. 3A). Similarly, in the case of Gram-negative *P. aeruginosa* PAO1, a progressive wrinkling of outer membrane, dissociation of membrane fragments, permeabilization of outer and inner membranes and the leakage of electron dense material was detected (Fig. 3B). Moreover, in both cases, a complete alteration of intracellular morphology, with a decrease of cytoplasm density, was evaluated at the highest peptide concentrations tested (Fig. 3). Similar results were obtained when *B. globigii* TNO BM013 and *P. aeruginosa* PAO1 strains were treated with r(P)ApoB$_S$ peptide at a concentration of 5 and 20 μM, respectively (Fig. 4A,B). It is noteworthy that significant morphological alterations were already detected when peptides were tested at sub-MIC concentrations.

Furthermore, to analyse the surface of responsive bacterial cells upon treatment with antimicrobial ApoB derived peptides, scanning electron microscopy (SEM) analyses were also performed. In the absence of peptides, bacterial cells displayed smooth and intact surfaces (Figs 5 and 6). Preliminary occurrence of biofilm extracellular matrix formation was also detected in the case of control *P. aeruginosa* PAO1 cells (Figs 5B and 6B). When bacterial cells were, instead, treated with peptides, bacterial surfaces appeared corrugated with some dimples,

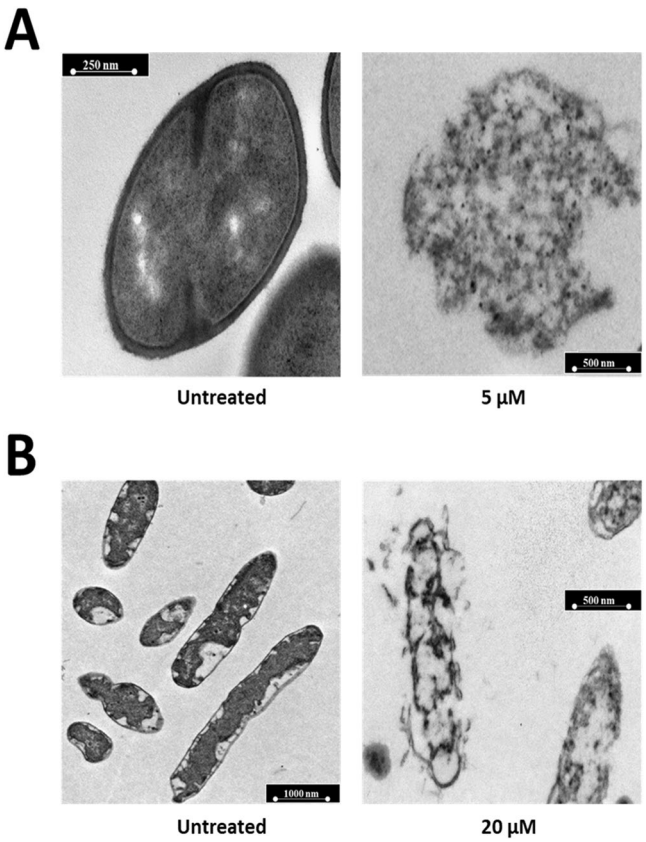

Figure 4. Morphological analyses of *B. globigii* TNO BM013 (**A**) and *P. aeruginosa* PAO1 (**B**) cells by TEM. Representative images are shown upon treatment of bacterial cells with r(P)ApoB$_S$ concentrations corresponding to sub-MIC values (5 µM and 20 µM for *B. globigii* TNO BM013 and *P. aeruginosa* PAO1 cells, respectively). A total of 60 cells were analysed for each sample in two independent experiments. Bars 250, 500 or 1,000 nm.

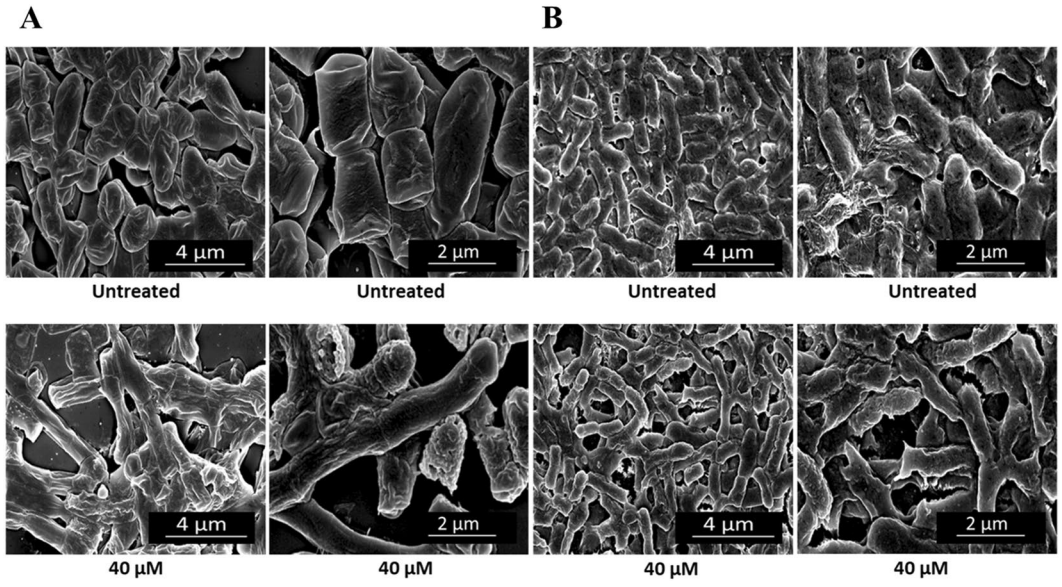

Figure 5. Morphological analyses of *B. globigii* TNO BM013 (**A**) and *P. aeruginosa* PAO1 (**B**) cells by SEM. Representative images are shown upon treatment of bacterial cells with 40 µM r(P)ApoB$_L$. A total of 60 cells were analysed for each sample in two independent experiments. Bars 2 or 4 µm.

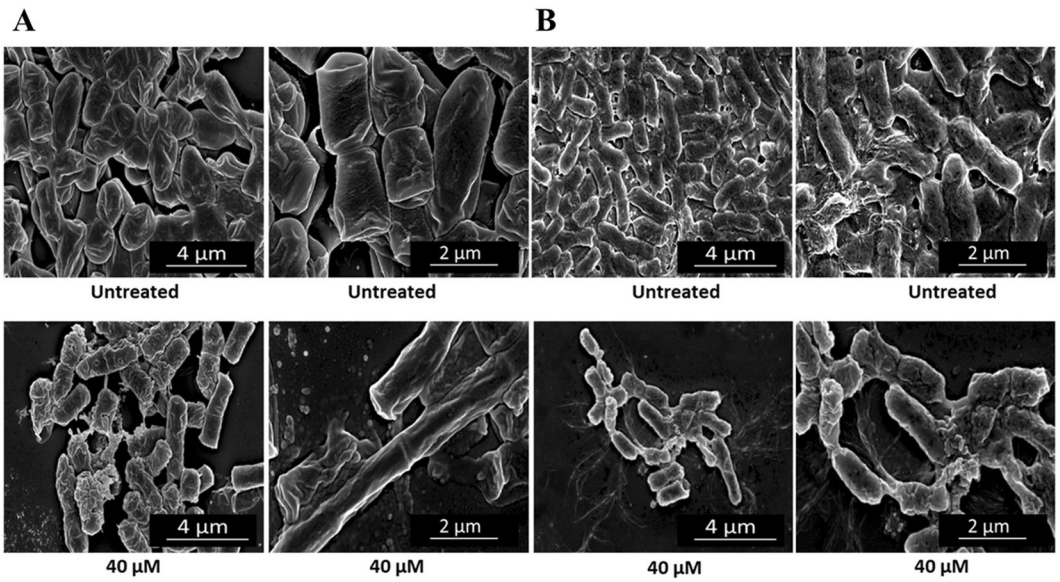

Figure 6. Morphological analyses of *B. globigii* TNO BM013 (**A**) and *P. aeruginosa* PAO1 (**B**) cells by SEM. Representative images are shown upon treatment of bacterial cells with 40 µM r(P)ApoB$_S$. A total of 60 cells were analysed for each sample in two independent experiments. Bars 2 or 4 µm.

both in the case of *B. globigii* TNO BM013 and *P. aeruginosa* PAO1 strains (Figs 5 and 6). Even more interesting is the evidence that the treatment of *B. globigii* TNO BM013 cells with ApoB derived peptides induces cells to grow as long filaments (Figs 5A and 6A), probably as a consequence of septation block, thus strongly suggesting that these peptides act by ultimately inhibiting cell division. To monitor this phenomenon, experiments were also performed by incubating *B. globigii* TNO BM013 cells with increasing concentrations of either r(P)ApoB$_L$ or r(P)ApoB$_S$ peptide. Obtained results, reported in Figs S5 and S6, clearly indicate that both peptides induce a septation block even at concentrations significantly lower than MIC$_{100}$ value. Moreover, obtained results support the evidence that peptides effects strongly depend on the features of bacterial strains under test. Indeed, when *P. aeruginosa* PAO1 cells were treated with 40 µM r(P)ApoB$_L$ (Fig. 5B) or 40 µM r(P)ApoB$_S$ peptide (Fig. 6B), no evidence of cell division block was detected. However, in both cases, a significantly lower cell density, indicative of a massive cell death, was revealed (Figs 5B and 6B). Moreover, in the case of all the treated samples, cell surfaces appeared irregular, corrugated, and withered (Figs 5 and 6), with some dimples and signs of cytoplasm leakage especially in the case of *P. aeruginosa* PAO1strain (Figs 5B and 6B).

Analysis of lipopolysaccharides (LPSs) isolated from *P. aeruginosa* ATCC 27853 and *P. aeruginosa* PAO1 bacterial strains. We previously demonstrated, by Far UV-CD analyses, that r(P)ApoB$_L$ peptide gradually assumes a defined structure in the presence of increasing concentrations of LPS, what suggests a direct binding of this peptide to LPS[20]. Here, to investigate the role played by LPS molecules in the efficacy or the inefficacy of ApoB derived peptides on Gram-negative bacterial strains, we extracted LPS molecules from *P. aeruginosa* ATCC 27853 and *P. aeruginosa* PAO1 bacteria. Afterwards, we analysed the interaction between ApoB derived peptides and the two purified LPS fractions by isothermal titration calorimetry (ITC) experiments. As shown in Fig. 7A, r(P)ApoB$_L$ and r(P)ApoB$_S$ peptides appear to bind to LPS molecules extracted from the two bacterial strains in a very similar fashion. Binding reactions were found to be all endothermic, thus indicating that they are driven by entropy rather than enthalpy. In the case of the binding of r(P)ApoB$_L$ peptide to the LPS extracted from *P. aeruginosa* PAO1, a dissociation constant (Kd) of 3.6×10^{-6} M was determined, with an entropy (ΔS) of 269 J/mol and a positive enthalpy (ΔH) of 51.1 KJ/mol (Table S2). Similar spectra and binding parameters were also obtained in the case of the interaction of r(P)ApoB$_S$ peptide with LPS molecules extracted from *P. aeruginosa* PA01 bacterial strain (Fig. 7A and Table S2). No significant differences were detected when the binding of both ApoB derived peptides to LPS molecules extracted from *P. aeruginosa* ATCC 27853 strain was analysed (Fig. 7A and Table S2). Altogether, obtained data indicate that both ApoB derived peptides are able to directly interact with LPS molecules extracted from the two bacterial strains, with no major differences in the binding of peptides to LPS molecules extracted from *P. aeruginosa* susceptible and not responsive bacterial strains (Fig. 7A and Table S2), at least in *in vitro* experiments and in the experimental conditions tested. To deepen on the role that LPS molecules might play in determining the different susceptibility of Gram-negative bacterial strains to ApoB derived peptides toxicity, we also performed a preliminary characterization of LPS molecules extracted from *P. aeruginosa* ATCC 27853 and *P. aeruginosa* PAO1 bacterial strains. To this purpose, LPSs extracted from dried bacterial cells by the PCP method were analysed by 14% DOC-PAGE electrophoresis and visualized by silver nitrate staining, that revealed a smooth LPS for both strains. Smooth LPS extracted from *E. coli* O55:B5 was used as a standard (data not shown). To define the glycosyl compositions of the intact LPSs, acetylated methyl glycosides were analysed by GC-MS. The monosaccharides were identified from their EI mass spectra and from

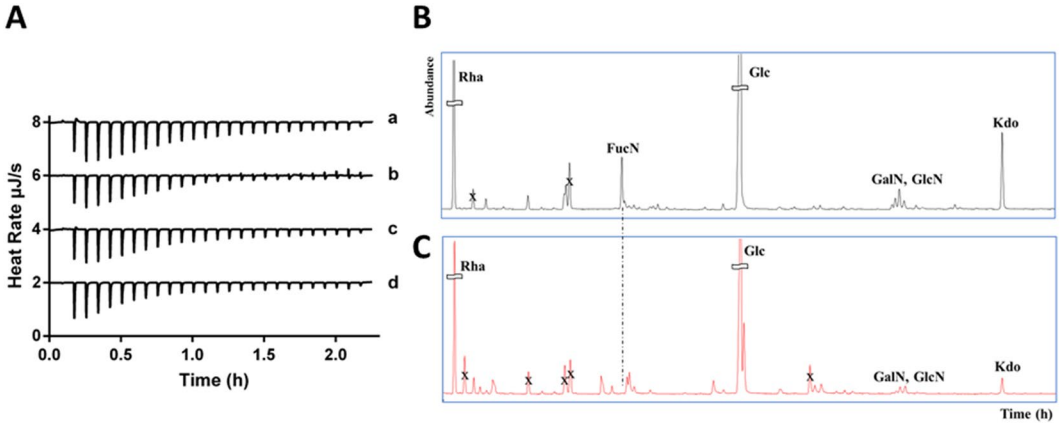

Figure 7. Analysis of the binding between ApoB derived peptides and LPSs extracted from *P. aeruginosa* PAO1 and *P. aeruginosa* ATCC 27853 bacterial strains by isothermal titration calorimetry (ITC) (**A**). The negative peaks indicate heat requirement for binding (endothermic), and are indicative of an entropy-driven binding reaction. (a) Binding of r(P)ApoB$_L$ peptide to LPS from *P. aeruginosa* PAO1; (b) binding of r(P)ApoB$_L$ peptide to LPS from *P. aeruginosa* ATCC 27853; (c) binding of r(P)ApoB$_S$ peptide to LPS from *P. aeruginosa* PAO1; (d) binding of r(P)ApoB$_S$ peptide to LPS from *P. aeruginosa* ATCC 27853. Chromatograms of acetylated methyl glycosides of LPSs extracted from *P. aeruginosa* PAO1 (**B**), and from *P. aeruginosa* ATCC 27853 (**C**).

their GC column retention time by comparison with authentic standards. For both LPSs, rhamnose (Rha), glucose (Glc), 2-amino-2-deoxy-D-galactopyranose (GalN), 2-amino-2-deoxy-D-glucopyranose (GlcN), and 3-deoxy-D-manno-oct-2-ulosonic acid (Kdo) were found to be present (Fig. 7B,C). The occurrence of heptoses in both LPSs was displayed only upon a de-phosphorylation reaction obtained by HF treatment (data not shown). It is important to highlight the selective presence of 2-amino-2,6-dideoxy-D-galactopyranose (FucN) in *P. aeruginosa* PAO1 LPS, as indicated by the chromatogram (Fig. 7B). It is noteworthy that the majority of *P. aeruginosa* strains have been reported to co-express two chemically and distinct forms of LPS O-antigens: (i) a serotype containing the O-antigen B-band and (ii) a common antigen referred to as O-antigen A-band. The chemical structure of the A-band from most of the sero-types was shown to be a linear α-D-rhamnan[33]; instead, the chemical structure of the B-band was reported to contain two derivatives of the 2,3-diamino-2,3-dideoxy-D-mannuronic acid (Man2N3NA) and FucN[34]. Our results suggest the absence of the B-band in the case of *P. aeruginosa* ATCC 27853 strain. This feature might be responsible for the different response of the two Gram-negative strains under test to ApoB derived peptides.

Discussion

The healthcare burden associated to the increasing emergence of microorganisms resistant to multiple antimicrobial compounds has accelerated in recent years, and alternative weapons are urgently needed. However, despite huge efforts, the discovery, development, manufacture and marketing of new antibiotics has significantly slowed down in the past 30 years, whereas the clinical and economic impact of resistance is alarmingly rising. Although the scientific difficulty in identifying novel antibiotics may be increasing, as microbes become resistant to an ever-increasing array of treatments and, concomitantly, the identification of novel targets is challenging, the main explanation is that investments made by large pharmaceutical companies did not lead to profitable products[35]. In this scenario, naturally occurring Host Defense Peptides (HDPs) are gaining great attention. Indeed, being essential constituents of innate immunity, they represent promising lead structures to develop antibiotics against Gram-negative and Gram-positive bacteria, including strains resistant to approved antibacterial agents[4]. We recently characterized novel human HDPs identified by a bioinformatics approach in human ApoB[20,21], and demonstrated that the two recombinant ApoB derived HDPs are endowed with a broad-spectrum anti-microbial activity, and with anti-biofilm, wound healing and immunomodulatory properties[20]. On the other hand, they have been found to be neither toxic nor hemolytic towards eukaryotic cells, what opens interesting perspectives to their therapeutic applicability[20]. However, it should be emphasized that ApoB derived AMPs were found to be antimicrobial towards four out of eight strains tested, *i.e. E. coli* ATCC 25922, *P. aeruginosa* PAO1, *B. globigii* TNO BM013, and *B. licheniformis* ATCC 21424, with MIC$_{100}$ values comprised between 1.25 and 20 µM, indicating that they are effective on both Gram-negative and Gram-positive bacterial strains[20]. On the other hand, they were found to be ineffective towards *P. aeruginosa* ATCC 27853, methicillin-resistant *S. aureus* (MRSA WKZ-2), and *S. aureus* ATCC 29213[20]. However, when peptides were tested in combination with conventional antibiotics or EDTA, remarkable synergistic effects were detected[20]. Indeed, bacterial strains found to be not responsive to ApoB derived AMPs toxicity, such as *S. aureus* strains and *P. aeruginosa* ATCC 27853, were found to be highly susceptible to combinations of ApoB derived peptides with antibiotics or EDTA[20]. This paves the way to the development of successful combination therapy approaches, that have a very low potential to induce resistance phenotype. Since the definition of the molecular bases of ApoB derived peptides antimicrobial activity could be crucial for the design of effective combinatorial therapeutic approaches, the mechanism of action of the two ApoB derived AMPs has been here investigated by selecting four bacterial strains as prototypes of Gram-positive and

Gram-negative strains susceptible or resistant to antimicrobial ApoB derived peptides. First of all, we analysed the kinetic of peptides bactericidal activity, and demonstrated that, at the highest peptide concentrations tested (10–20 μM), susceptible bacterial cells (*B. globigii* TNO BM013 and *P. aeruginosa* PAO1cells) were killed within a very short time interval, *i.e.* 30 min. This evidence is in perfect agreement with data collected by measuring Zeta potential values upon incubation of susceptible bacterial cells with ApoB derived peptides tested at concentrations corresponding to previously determined MIC_{100} values. Indeed, in all the cases, a significant increase of Zeta potential values was detected, what is indicative of the occurrence of electrostatic interactions between positively charged peptides and negatively charged bacterial surfaces, with a consequent neutralization of bacterial surface. Interestingly, a greater variation in Zeta potential values was detected in the case of the strain characterized by the highest sensitivity to peptide toxicity, *i.e. B. globigii* TNO BM013. This might be indicative of a higher electrostatic affinity between cationic peptides and negatively charged bacterial surface. Indeed, it has been reported that bacterial membrane surface neutralization is a key event mediating the anti-microbial activity of several peptides[36], with Zeta potential alteration generally preceding membrane permeabilization leading to cell death[36]. In perfect agreement with this finding, a significant increase of NPN uptake factor was selectively detected upon treatment of susceptible bacterial strains with ApoB derived peptides, thus strongly supporting the evidence that Zeta potential increase precedes membrane permeabilization, and confirming the crucial role played by bacterial membrane as main target of ApoB derived peptides antimicrobial activity. Moreover, in the case of *B. globigii* TNO BM013 susceptible bacterial strain, Zeta potential increase and membrane permeabilization is also accompanied by a septation block, as indicated by electron microscopy analyses performed at different time intervals and upon treatment with increasing ApoB derived peptides concentrations. These findings are in perfect agreement with a recent report indicating that *E. coli* treatment with antimicrobial peptides causes cells to filament through a division block controlled by the PhoQ/PhoP signaling pathway[37]. Bacterial cell filamentation, here observed by electron microscopy analyses, might be a result of DNA replication inhibition, SOS induction, chromosome segregation, or failure of septation process[38]. It has been previously reported that treatment of *E. coli* with the antimicrobial peptide microcin J25 causes cells to filament, with a consequent inhibition of cell division processes through a non-SOS-dependent mechanism mediating a bacteriostatic mode of action[39]. Similarly, *E. coli* cells treated with diptericin showed a significantly elongated morphology, indicating that this peptide may affect cell targets involved in cell division to induce cell death, as suggested by its selective activity on actively growing *E. coli* cells[40]. Also human defensin 5 (HD5) was found to induce extensive cell elongation, with a consequent disruption of cell division events[41]. Interestingly, in agreement with our findings, such treatment outcomes were observed only upon treatment of Gram-negative bacteria with HD5, thus suggesting a common inhibitory activity depending on specific features of bacterial strains under test. Also in the case of ApoB derived peptides, effects appear to strongly depend on specific properties of analysed bacterial strains. Indeed, in the case of Gram-negative *P. aeruginosa* PAO1 strain, no signs of cell division block were detected upon treatment with ApoB derived peptides, although significant alterations of cell morphology, with irregular and corrugated cell surfaces, signs of cytoplasm leakage and cell death, were detected. It has also to be emphasized that two out of four bacterial strains selected in the present study appear resistant to ApoB derived peptides antimicrobial activity, although they are characterized by negatively charged surfaces, as indicated by Zeta potential values determinations. In particular, in the case of Gram-positive *B. globigii* TNO BM013 and *S. aureus* MRSA WKZ-2 bacterial strains, Zeta potential values have been found to be -33 ± 3 and -28 ± 3, respectively, but only *B. globigii* TNO BM013 cells were found to be susceptible to ApoB derived peptides antimicrobial activity. In the case of Gram-negative *P. aeruginosa* PAO1 and *P. aeruginosa* ATCC 27853 strains, instead, Zeta potential values were found to be very different, *i.e.* -23 ± 2 and -11 ± 2 mV, respectively. It is plausible that this dissimilarity reflects differences in bacterial membrane composition ultimately affecting peptide ability to interfere with bacterial cell viability. Since no significant effects on Zeta potential values were detected in the case of resistant bacterial cells treated with ApoB derived peptides, it has been hypothesized a failure of electrostatic interactions between negatively charged bacterial surfaces and positively charged peptides, with a consequent counteraction of ApoB derived peptides antimicrobial activity. Indeed, it has been extensively reported that electrostatic interactions play a pivotal role in the cell killing process mediated by antimicrobial peptides[42]. Based on obtained results, it has been hypothesized that some extracellular factors or bacterial membrane composition might interfere with electrostatic interactions between peptides and bacterial surfaces in the case of resistant bacterial cells. Since previous analyses by Far UV-CD suggested a direct binding of $r(P)ApoB_L$ peptide to bacterial LPS[20], experiments were here performed to verify whether ApoB derived peptides are able to directly interact with LPS molecules extracted from *P. aeruginosa* PAO1 and *P. aeruginosa* ATCC 27853 bacterial strains. Analyses, performed by isothermal titration calorimetry (ITC), indicated that both ApoB derived peptides are able to directly interact with LPS molecules extracted from the two bacterial strains, with no significant differences, at least when peptide binding to LPS molecules is tested in *in vitro* experiments. However, it has to be considered that, in physiological conditions, where up to 100,000 molecules of LPS are located at the surface of one single Gram-negative bacterium[43], several factors, such as membrane composition or extracellular microenvironment, might interfere with peptide binding to exposed LPS molecules. Based on this, we also performed a preliminary characterization of LPS molecules extracted from *P. aeruginosa* PAO1 and *P. aeruginosa* ATCC 27853 bacterial strains, in order to evaluate whether differences in LPS structures might be responsible for the efficacy or the inefficacy of ApoB derived peptides on Gram-negative bacterial strains. Performed analyses indicated the selective presence of 2-amino-2,6-dideoxy-D-galactopyranose (FucN) in the LPS of susceptible *P. aeruginosa* PAO1 bacterial strain, whereas LPS B-band was found to be absent in the case of resistant *P. aeruginosa* ATCC 27853 strain. Since the B-band is reported to display negative charges, such as those of the Man2N3NA residues[34], electrostatic interactions between positively charged ApoB derived peptides and LPS molecules exposed on *P. aeruginosa* PAO1 bacteria might involve these monosaccharides. Instead, the sole presence of the hydrophobic rhamnan chain (A-band) in the LPS of resistant *P. aeruginosa* ATCC 27853 strain could be responsible for the failure of the electrostatic interactions between peptides and bacterial

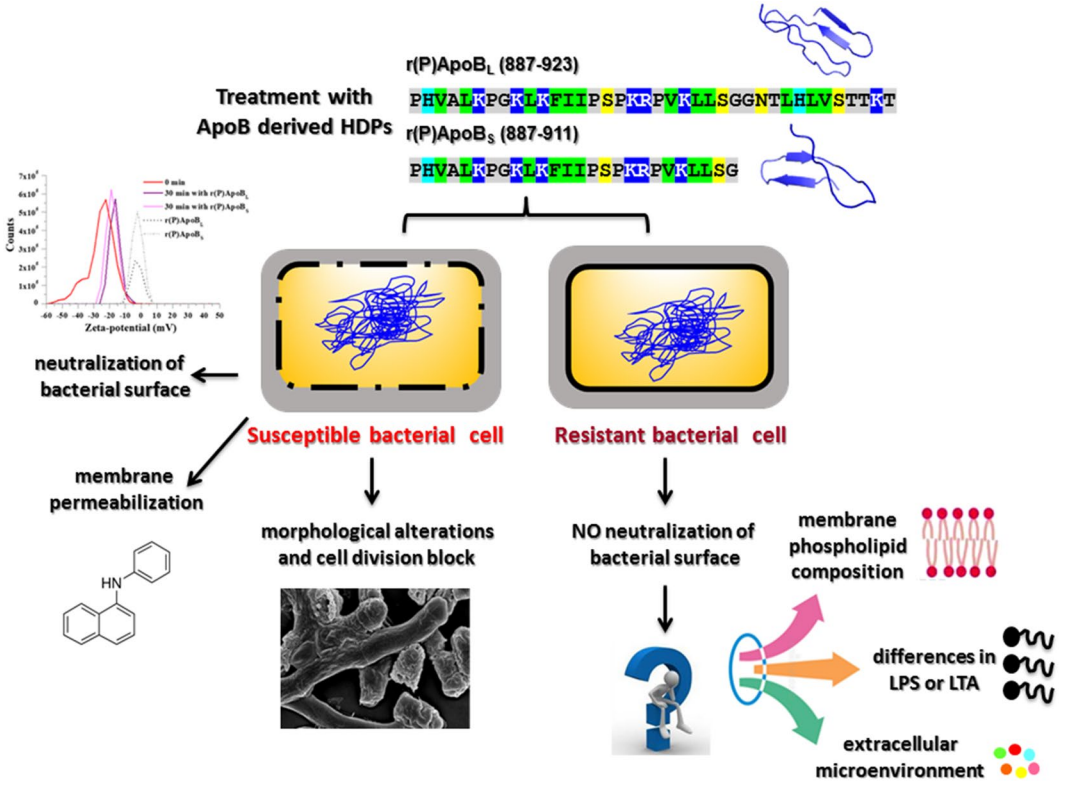

Figure 8. Schematic representation of the main experimental evidence herein collected.

surfaces. This might be one of the key factors responsible for the different response of the two Gram-negative bacterial strains to ApoB derived peptides toxicity.

Altogether, collected results indicate that ApoB derived peptides exert their antimicrobial activity by mainly targeting bacterial membrane and subsequently affecting intracellular molecules and/or processes, such as cell division (Fig. 8). Obtained findings also strongly indicate that an interference with electrostatic interactions between negatively charged bacterial surfaces and positively charged peptides, probably due to extracellular microenvironment or bacterial membrane composition, might counteract ApoB derived peptides antimicrobial activity (Fig. 8).

Materials and Methods

Materials. All the reagents were purchase from Sigma-Aldrich (Milan, Italy), unless differently specified. Chicken cathelicidin-2 (CATH-2) peptide was obtained from CPC Scientific Inc. (Sunnyvale, USA).

Recombinant production of ApoB derived peptides. Expression and isolation of recombinant peptides was carried out as previously described[20] with the only exception of a final gel-filtration step, that was added in order to remove salts used along the purification process and that tend to attach to the peptides, as previously reported[44,45].

Bacterial strains and growth conditions. Methicillin-resistant *Staphylococcus aureus* (MRSA WKZ-2), *Bacillus globigii* TNO BM013, *Pseudomonas aeruginosa* ATCC 27853, and *Pseudomonas aeruginosa* PAO1 bacterial strains were grown as previously described[20].

Anti-microbial activity assay. To test the anti-microbial activity of ApoB derived peptides, previously described experimental procedure was used[20]. MIC_{100} values correspond to the lowest concentration of peptide associated to no detectable bacterial growth.

Killing kinetic studies. To kinetically analyse bacterial killing by ApoB derived peptides, experiments were performed on *B. globigii* TNO BM013 and *P. aeruginosa* PAO1 strains as previously described[20].

Zeta potential measurements of bacterial cells in the presence of ApoB derived peptides. To perform analyses, bacteria were grown over-night in MHB medium, then diluted in fresh MHB, and incubated at 37 °C until logarithmic phase of growth was reached. Bacteria were then diluted to 4×10^6 CFU/mL in a final volume of 5 mL of NB 0.5X, and mixed with the peptide under test (1:1 v/v). In the case of bacterial strains susceptible to antimicrobial ApoB derived peptides, r(P)ApoB$_L$ and r(P)ApoB$_S$ were tested at concentrations corresponding to MIC_{100} values. In the case of not responsive strains, instead, only the highest peptide concentration was tested (40 μM). At defined time intervals (0–180 min), Zeta potential values were determined. Zeta potential

measurements of control samples were carried out in NB 0.5X pH 7.4. To test different peptide concentrations, serial dilutions were performed, in order to mix bacteria and peptides at a ratio of 1:1 v/v. The Zeta potential of bacterial cells was determined at 25 °C from the mean of 3 independent measurements (30 runs each), in the absence and in the presence of different peptide concentrations. Zeta potential values were obtained by phase analysis light scattering (PALS) in a Zetasizer Nano ZS 90 device (Malvern, Worcestershire, UK), equipped with Helium–Neon laser (633 nm) as a source of light, with the detection at 173 degree scattering angle at room temperature (25 °C), using disposable Zeta cells with gold electrodes. Values of viscosity and refractive index were set to 0.8872 cP and 1.330, respectively.

NPN uptake assay. NPN uptake assays were carried out by following the previously described experimental procedure[46]. To do this, 1-N-phenylnaphthylamine (NPN) was diluted to 1 mM in 5 mM HEPES buffer pH 7.2. Control wells were prepared as follows: (i) buffer alone (1 mL); (ii) buffer (1 mL) and NPN (2 µL); (iii) bacteria in buffer (1 mL); (iv) bacteria in buffer (1 mL), NPN (2 µL). Antibiotics or peptides were mixed with bacterial suspension in Eppendorf tubes for 2 and 30 min, respectively, and then transferred into cuvettes. NPN was added immediately before the measurement of fluorescence; the values were recorded within 3 min. Fluorescence emission was detected at 420 nm upon excitation at 340 nm by using a PerkinElmer LS-55 luminescence spectrometer (Waltham, MA, USA). Each assay was performed at least three times. The results are expressed as NPN uptake factors, calculated by subtracting background, *i.e.* the value obtained in the absence of NPN.

Transmission electron microscopy. Bactericidal effects of ApoB derived peptides were also investigated by transmission electron microscopy (TEM) analyses, which required higher bacterial cell densities (2×10^8 CFU/mL). For this reason, additional colony count assays were performed to determine ApoB derived peptides MIC_{100} values at this bacterial cell density. In the case of both peptides, a MIC_{100} value of about 80 µM was determined. To perform analyses, *B. globigii* TNO BM013 and *P. aeruginosa* PAO1 strains were incubated with increasing concentrations of peptides (0–80 µM) for 3 hrs at 37 °C. Samples were then fixed with 2% glutaraldehyde (Polysciences, Eppelheim, Germany) in 5 mM $CaCl_2$, 10 mM $MgCl_2$ (both Merck, Darmstadt, Germany) in 0.1 M sodium cacodylate buffer pH 7.4 over-night at 4 °C. Bacteria treatment with peptides was stopped by adding the fixative and keeping the cells over-night at 4 °C. Cells were then washed 3 times by incubation in sodium cacodylate buffer for 10 min and embedded in 2% low-melting point agarose v/v. Cells were then post-fixed with 4% osmium tetroxide (Electron Microscopy Sciences, EMS, Hatfield, USA) and 1.5% $K_4Fe(CN)_6$–$3H_2O$ (Merck, Darmstadt, Germany) in distilled water for 2 hrs at 4 °C. Upon cell washing with distilled water (5 times for 10 min), cells were incubated in 0.5% uranylacetate (EMS, Hatfield, USA) for 1 hr at 4 °C. After further washing with distilled water (3 times for 10 min), samples were embedded in Epon resin and ultrathin sections (50 nm) of each block were prepared by using a Leica UCT ultramicrotome (Leica, Vienna, Austria). Obtained sections were stained with uranyl acetate and lead citrate by using the Leica AC20 system (Leica, Vienna, Austria). TEM images have been acquired in bright field mode using a Philips EM 208 S transmission electron microscope with an accelerating voltage of 80 kV.

Scanning electron microscopy. Bacterial cells in exponential growth phase were grown for 3 hrs in NB 0.5X in microfuge tubes in the absence or in the presence of ApoB derived peptides. Also in this case, high bacterial cell densities were required (2×10^8 CFU/mL) for the analysis, and it should be underlined that, in these experimental conditions, peptides MIC_{100} value was found to be about 80 µM. To perform scanning electron microscopy (SEM) analyses, *B. globigii* TNO BM013 and *P. aeruginosa* PAO1 strains were incubated with 40 µM peptides for 3 hrs at 37 °C. Following incubation, bacterial cells were centrifuged at 10,000 rpm at 4 °C and fixed in 2.5% glutaraldehyde. Following over-night incubation, bacterial cells were washed three times in distilled water (dH2O) and then dehydrated with a graded ethanol series: 25% ethanol (1×10 min); 50% ethanol (1×10 min); 75% ethanol (1×10 min); 95% ethanol (1×10 min); 100% anhydrous ethanol (3×30 min). Bacterial cells deposited onto glass substrate were first sputter coated with a thin layer of Au-Pd (Sputter Coater Denton Vacuum Desk V) to allow subsequent morphological characterization using a FEI Nova NanoSEM 450 at an accelerating voltage of 5 kV with Everhart Thornley Detector (ETD) and Through Lens Detector (TLD) at high magnification.

Lipopolysaccharide (LPS) isolation, purification and characterization. Dried cells from *P. aeruginosa* PAO1 (1 g) and *P. aeruginosa* ATCC 27853 (0.9 g) were extracted by PCP method, *i.e.* by using phenol/chloroform/petroleum ether (2:5:8 v:v:v)[47]. The yields of extracted LPS was found to be 9% and 5% for *P. aeruginosa* PAO 1 and *P. aeruginosa* ATCC 27853, respectively. Both extracts were analysed by 14% DOC-PAGE, that was performed by using Laemmli procedure[48,49] and sodium deoxycholate (DOC) as detergent. LPS bands were visualized by silver staining as described previously[50]. The glycosyl analysis was performed as previously reported[51]. Briefly, LPS samples (0.5 mg) were mixed with 1 mL of HCl/CH_3OH, subjected to methanolysis for 16 hrs at 80 °C, and then acetylated. Simultaneously, another sample of both native LPSs (0.5 mg) was firstly treated with HF (48%; 100 µL) and then subjected to methanolysis and acetylation. Finally, all the acetylated methyl glycosides (MGA) were analysed on an Agilent 7820 A GC System-5977B MSD spectrometer equipped with the automatic injector 7693A and a Zebron ZB-5 capillary column (Phenomenex, Toornace, CA, USA; fow rate 1 mL/min; He as carrier gas). MGA were analysed using the following temperature program: 140 °C for 3 min, 140 °C → 240 °C at 3 °C/min.

Isothermal titration calorimetry. Interaction between ApoB derived peptides and LPS molecules extracted from *P. aeruginosa* PAO1 or *P. aeruginosa* ATCC 27853 bacterial strains was tested by isothermal titration calorimetry (ITC) experiments, which were carried out on a Low Volume NanoITC (TA instruments, Waters LLC, New Castle, USA) at 37 °C. To this purpose, LPS molecules were diluted to 0.5 mg/mL in 50% phosphate buffer (PBS), and vortexed for 5 min. Afterwards 190 µL of LPS suspension were added to the cell chamber. The

syringe was then filled with 50 µL of 266 µM peptide solutions in 50% PBS. Titrations were incremental with 2 µL injections at 300 seconds intervals. Control spectra, obtained by injection of the same amount of each peptide in buffer solution, were subtracted to correct for heat production upon peptide dilution. Collected data were analyzed by using Nano Analyze software (TA instruments, Waters LLC, New Castle, USA).

Statistical analysis. Statistical analysis was performed using a Student's t-Test. Significant differences were indicated as *($P < 0.05$), **($P < 0.01$) or ***($P < 0.001$).

Data Availability

All the data supporting the conclusions have been included within the article.

References

1. Agerberth, B. *et al*. FALL-39, a putative human peptide antibiotic, is cysteine-free and expressed in bone marrow and testis. *Proc. Natl. Acad. Sci. USA* **92**, 195–199 (1995).
2. Hancock, R. E. W. & Sahl, H. G. Antimicrobial and host-defense peptides as new anti-infective therapeutic strategies. *Nat. Biotechnol.* **24**, 1551–1557 (2006).
3. Hancock, R. E. W. Mechanisms of action of newer antibiotics for Gram-positive pathogens. *Lancet Infect. Dis.* **95**, 209–218 (2005).
4. Ostorhazi, E., Nemes-Nikodem, É., Knappe, D. & Hoffmann, R. *In vivo* activity of optimized apidaecin and oncocin peptides against a multiresistant, KPC-producing Klebsiella pneumoniae strain. *Protein Pept. Lett.* **21**, 368–373 (2014).
5. Steinstraesser, L., Kraneburg, U., Jacobsen, F. & Al-Benna, S. Host defense peptides and their antimicrobial-immunomodulatory duality. *Immunobiology* **216**, 322–333 (2011).
6. Holzl, M. A., Hofer, J., Steinberger, P., Pfistershammer, K. & Zlabinger, G. J. Host antimicrobial proteins as endogenous immunomodulators. *Immunol. Lett.* **119**, 4–11 (2008).
7. Hancock, R. E. W. & Chapple, D. S. Peptide antibiotics. *Antimicrob. Agents Chemother.* **43**, 1317–1323 (1999).
8. Papo, N. & Shai, Y. Host defense peptides as new weapons in cancer treatment. *Cell. Mol. Life Sci.* **62**, 784–790 (2005).
9. Barns, K. J. & Weisshaar, J. C. Real-time attack of LL-37 on single Bacillus subtilis cells. *Biochim Biophys Acta* **1828**, 1511–1520 (2013).
10. Zhang, L., Rozek, A. & Hancock, R. E. W. Interaction of cationic antimicrobial peptides with model membranes. *J. Biol. Chem.* **276**, 35714–35722 (2001).
11. Yeamen, M. R. & Yount, N. Y. Mechanisms of antimicrobial peptide action and resistance. *Pharmacol. Rev.* **55**, 27–54 (2003).
12. Joyce, G. H., Hammond, R. K. & White, D. C. Changes in membrane lipid composition in exponentially growing Staphylococcus aureus during the shift from 37 to 25 °C. *J. Bacteriol.* **104**, 323–330 (1970).
13. Bozdogan, B., Esel, D., Whitener, C., Browne, F. A. & Appelbaum, P. C. Antibacterial susceptibility of a vancomycin-resistant Staphylococcus aureus strain isolated at the Hershey Medical Center. *J. Antimicrob. Chemother.* **52**, 864–868 (2003).
14. Lee, M. T., Hung, W. C., Chen, F. Y. & Huang, H. W. Mechanism and kinetics of pore formation in membranes by water soluble amphipathic peptides. *Proc. Natl. Acad. Sci. USA* **105**, 5087–5092 (2008).
15. Biaggi, M. H., Riske, K. A. & Lamy-Freund, M. T. Melanotropic peptides-lipid bilayer interaction. Comparison of the hormone alpha-MSH to a biologically more potent analog. *Biophys. Chem.* **67**, 139–149 (1997).
16. Biaggi, M. H., Pinheiro, T. J., Watts, A. & Lamy-Freund, M. T. Spin label and 2H-NMR studies on the interaction of melanotropic peptides with lipid bilayers. *Eur. Biophys. J.* **24**, 251–259 (1996).
17. Ramamoorthy, A., Thennarasu, S., Lee, D. K., Tan, A. & Maloy, L. Solid-state NMR investigation of the membrane-disrupting mechanism of antimicrobial peptides MSI-78 and MSI-594 derived from magainin 2 and melittin. *Biophys. J.* **91**, 206–216 (2006).
18. Henzler Wildman, K. A., Lee, D. K. & Ramamoorthy, A. Mechanism of lipid bilayer disruption by the human antimicrobial peptide, LL-37. *Biochemistry* **42**, 6545–6558 (2003).
19. Hong, M. & Su, Y. Structure and dynamics of cationic membrane peptides and proteins: Insights from solid-state NMR. *Protein Sci.* **20**, 641–655 (2011).
20. Gaglione, R. *et al*. Novel human bioactive peptides identified in Apolipoprotein B: Evaluation of their therapeutic potential. *Biochem. Pharmacol.* **130**, 34–50 (2017).
21. Pane, K. *et al*. Antimicrobial potency of cationic antimicrobial peptides can be predicted from their amino acid composition: Application to the detection of "cryptic" antimicrobial peptides. *J. Theor. Biol.* **419**, 254–265 (2017).
22. Gaglione, R. *et al*. Insights into the anticancer properties of the first antimicrobial peptide from Archaea. *Biochim Biophys Acta Gen Subj* **1861**, 2155–2164 (2017).
23. Bosso, A. *et al*. A new cryptic host defense peptide identified in human 11-hydroxysteroid dehydrogenase-1 β-like: from in silico identification to experimental evidence. *Biochim Biophys Acta Gen Subj* **1861**, 2342–2353 (2017).
24. Zanfardino, A. *et al*. Human apolipoprotein E as a reservoir of cryptic bioactive peptides: The case of ApoE 133-167. *J. Pept. Sci.* **24**, e3095 (2018).
25. Pizzo, E. *et al*. Novel bioactive peptides from PD-L1/2, a type 1 ribosome inactivating protein from Phytolacca dioica L. Evaluation of their antimicrobial properties and anti-biofilm activities. *Biochim Biophys Acta Biomembr* **1860**, 1425–1435.
26. Kasetty, G. *et al*. The C-terminal sequence of several human serine proteases encodes host defense functions. *J. Innate Immun.* **3**, 471–482 (2011).
27. Lee, D. Y. *et al*. Histone H4 is a major component of the antimicrobial action of human sebocytes. *J. Invest. Dermatol.* **129**, 2489–2496 (2009).
28. Beck, W. H. *et al*. Apolipoprotein A-I binding to anionic vesicles and lipopolysaccharides: role for lysine residues in antimicrobial properties. *Biochim Biophys Acta* **1828**, 1503–1510 (2013).
29. van Dijk, A. *et al*. Chicken heterophils are recruited to the site of Salmonella infection and release antibacterial mature Cathelicidin-2 upon stimulation with LPS. *Mol. Immunol.* **46**, 1517–1526 (2009).
30. MacGowan, A. P. *et al*. A new time-kill method of assessing the relative efficacy of antimicrobial agents alone and in combination developed using a representative beta-lactam, aminoglycoside and fluoroquinolone. *J. Antimicrob. Chemother.* **38**, 193–203 (1996).
31. Dhariwal, A. K. & Tullu, M. S. Colistin: re-emergence of the 'forgotten' antimicrobial agent. *J. Postgrad. Med.* **59**, 208–215 (2013).
32. González, C., Rubio, M., Romero-Vivas, J., González, M. & Picazo, J. J. Bacteremic pneumonia due to Staphylococcus aureus: A comparison of disease caused by methicillin-resistant and methicillin-susceptible organisms. *Clin. Infect. Dis.* **29**, 1171–1177 (1999).
33. Arsenault, T. L. *et al*. Structural studies on the polysaccharide portion of A-band lipopolysaccharide from a mutant (AK1401) of Pseudomonas aeruginosa strain PAO1. *Can J Chem* **69**, 1273–1280 (1991).
34. Sadovskaya, I. *et al*. Structural characterization of the outer core and the O-chain linkage region of lipopolysaccharide from Pseudomonas aeruginosa serotype O5. *Eur. J. Biochem.* **267**, 1640–1650 (2000).
35. Fernandes, P. & Martens, E. Antibiotics in late clinical development. *Biochem. Pharmacol.* **133**, 152–163 (2017).
36. Halder, S. *et al*. Alteration of Zeta potential and membrane permeability in bacteria: a study with cationic agents. *Springerplus* **4**, 672 (2015).

37. Yadavalli, S. S. *et al*. Antimicrobial peptides trigger a division block in Escherichia coli through stimulation of a signalling system. *Nat Commun* **7**, 12340 (2016).
38. Lutkenhaus, J. Regulation of cell division in E. coli. *Trends Genet.* **6**, 22–25 (1990).
39. Salomón, R. A. & Farías, R. N. Microcin 25, a novel antimicrobial peptide produced by Escherichia coli. *J. Bacteriol.* **174**, 7428–7435 (1992).
40. Ishikawa, M., Kubo, T. & Natori, S. Purification and characterization of a diptericin homologue from Sarcophaga peregrina (flesh fly). *Biochem. J.* **287**, 573–578 (1992).
41. Chileveru, H. R. *et al*. Visualizing attack of Escherichia coli by the antimicrobial peptide human defensin 5. *Biochemistry* **54**, 1767–1777 (2015).
42. Gaspar, D., Veiga, A. S., Sinthuvanich, C., Schneider, J. P. & Castanho, M. A. Anticancer peptide SVS-1: efficacy precedes membrane neutralization. *Biochemistry* **51**, 6263–6265 (2012).
43. Vincent, J. L., Opal, S. M., Marshall, J. C. & Tracey, K. J. Sepsis definitions: time for change. *Lancet* **381**, 774–775 (2013).
44. Bommarius, B. *et al*. Cost-effective expression and purification of antimicrobial and host defense peptides in Escherichia coli. *Peptides* **31**, 1957–1965 (2010).
45. Gaglione, R. *et al*. Cost-effective production of recombinant peptides in Escherichia coli. *N. Biotechnol.* **51**, 39–48 (2019).
46. Helander, I. M. & Mattila-Sandholm, T. Fluorometric assessment of gram-negative bacterial permeabilization. *J. Appl. Microbiol.* **88**, 213–219 (2000).
47. Galanos, C., Lüderitz, O. & Westphal, O. A new method for the extraction of R lipopolysaccharides. *Eur. J. Biochem.* **9**, 245–249 (1969).
48. Laemmli, U. K. Most commonly used discontinuous buffer system for SDS electrophoresis. *Nature* **227**, 680–685 (1970).
49. Carillo, S. *et al*. Structural investigation of the antagonist LPS from the cyanobacterium Oscillatoria planktothrix FP1. *Carbohydr. Res.* **388**, 73–80 (2014).
50. Tsai, C. M. & Frasch, C. E. A sensitive silver stain for detecting lipopolysaccharides in polyacrylamide gels. *Anal. Biochem.* **119**, 115–119 (1982).
51. Pieretti, G. *et al*. The complete structure of the core of the LPS from Plesiomonas shigelloides 302-73 and the identification of its O-antigen biological repeating unit. *Carbohydr. Res.* **345**, 2523–2528 (2010).

Acknowledgements

This research received no specific grant from any funding agency in the public, commercial, or not-for-profit sectors.

Author Contributions

R.G. conceived and performed most of the experiments; A.C., E.D.O., B.D.V., A.C. and R.D.G. performed the experiments and analysed the data; E.J.A.V. preformed isothermal titration calorimetry studies and analysed the data; R.V., E.N., M.M.C. and C.D.R. conceived the experiments and discussed the results; A.A. conceived the experiments, analysed the data, discussed the results, and wrote the manuscript with the contribution of all the authors.

Additional Information

Supplementary information accompanies this paper at https://doi.org/10.1038/s41598-019-43063-3.

Competing Interests: The authors declare no competing interests.

Publisher's note: Springer Nature remains neutral with regard to jurisdictional claims in published maps and institutional affiliations.

La borsa di dottorato è stata cofinanziata con risorse del
Programma Operativo Nazionale Ricerca e Innovazione 2014-2020 (CCI 2014IT16M2OP005),
Fondo Sociale Europeo, Azione I.1 "Dottorati Innovativi con caratterizzazione Industriale"

UNIONE EUROPEA
Fondo Sociale Europeo

Ministero dell'Istruzione, dell'Università e della Ricerca